April 2022

Empirical and Modeled **δ**13C and **δ**15N Isoscapes in the Gulf of Mexico and their Application to Fish Eye Lens Migration Studies

Brianna Michaud
University of South Florida

Follow this and additional works at: https://digitalcommons.usf.edu/etd

Part of the Geochemistry Commons, and the Other Oceanography and Atmospheric Sciences and Meteorology Commons

Empirical and Modeled δ^{13}C and δ^{15}N Isoscapes in the Gulf of Mexico and their Application to

Fish Eye Lens Migration Studies

by

Brianna Michaud

A dissertation submitted in partial fulfillment
of the requirements for the degree of
Doctor of Philosophy in Marine Science
with a concentration in Marine Resource Assessment
College of Marine Science
University of South Florida

Major Professor: Ernst B. Peebles, Ph.D.
Brad Rosenheim, Ph.D.
Chris Stallings, Ph.D.
Hannah Vander Zanden, Ph.D.
Kelton McMahon, Ph.D.

Date of Approval:
March 29, 2022

Keywords: stable isotope ecology, carbon isotopes, nitrogen isotopes, spatial variability

Dedication

This work is first and foremost dedicated to my friends and family. I am fortunate enough

to have an incredibly loving and supportive family. Growing up, I was frequently surrounded by

people who were vocally curious about the world and constantly modeled how to treat others

with kindness and respect as well as how to play and enjoy life. I am certain that experience was

a huge influence on who I am today. Thank you to my grandparents, Kevin and Maxine, who

hosted me for so many Thanksgivings in Pennsylvania while I've been on this side of the

country. Thank you to my stepfather, Toby who has been a wonderful addition to our family.

Thank you to my sister, Adeline who is such a smart and thoughtful person and always makes

me feel like I can do anything. Thank you, most of all, to my mother, Denise, who raised me by

herself for much of my childhood. She has been an incredible role model in her compassion, her

integrity. I feel so lucky to be her daughter. Additional contributors to my mental health include

my friends, some of whom supported me from afar (Sarah Black, Diana Lloyd) and some of

whom were a bit closer to the action (Kate Dubickas, Imogen Browne, Kara Vadman, Bea

Combs Hintze, Emily Chancellor, Mike and Stacey Schram, Theresa King, Ryan Venturelli,

Katelyn Schockman, Cara Estes, and Alex Illich). I'm also grateful for my lab mates, past and

present, particularly Jen Granneman and Julie Vecchio who frequently helped refine my ideas

and helped me become a better researcher. I also want to mention SCUBAnauts International,

Katie Shoultz-Cooper, and all the amazing kids I've gotten to work with, through which I've had

some amazing experiences in teaching and SCUBA diving. I want to dedicate this dissertation in

part to Zack Morris who was an incredibly talented and compassionate young man and was taken

from us far too young. Lastly, I'm grateful for Weedon Island and Sawgrass Lake boardwalks,

Postcard Inn piña coladas, Bodega tofu Cuban sandwiches, and the view from the Canopy.

Acknowledgements

The research contained herein could not have happened without the help of many talented people. First, my major advisor Dr. Ernst Peebles who has given me invaluable support and advice. He has been instrumental in outlining this project, guiding me in ecological interpretations, giving knowledge of Gulf of Mexico dynamics, and providing funds for isotopic analysis. I am grateful he gave me enough freedom to branch out and conduct the pilot studies that became appendices for this dissertation. He has truly been wonderful to work with. The other members of my committee, Dr. Chris Stallings, Dr. Brad Rosenheim, Dr. Hannah Vander Zanden, and Dr. Kelton McMahon, have also provided vital feedback and have made the process of getting my Ph.D. a perfect balance of challenging and rewarding. I am particularly grateful for their kind words after my dissertation defense.

Several alumnae of the Peebles lab were critical to this research being completed. Dr. Kara Radabaugh, Dr. Amy Wallace, Dr. Jen Granneman, and Dr. Julie Vecchio all conducted isoscape and eye lens stable isotope research that set the stage for my own work. In particular, Dr. Julie Vecchio taught me the technique for peeling eye lenses and our discussions of eye lens stable isotope interpretation inspired a lot of the work in the Chapter 4 of this dissertation.

Other members of the CMS community that have been important to the completion of the Ph.D. include Sami Francis and Dr. David Naar, who provided important administrative support and were always available to answer my last-minute questions. Howard Rutherford helped secure funding for fellowships that provided financial support for my Ph.D. and facilitated meetings with donors which allowed me to meet some interesting and influential people. Dr.

Table of Contents

List of Tables

List of Figures

Abstract

Isoscapes are depictions of the spatial patterns of isotopic values in a given area. Isoscapes can be created using measurements form samples (empirical isoscapes) or using statistical models of spatial isotopic variation (modeled isoscapes). Isoscapes have a wide variety of potential applications though, in the realm of marine ecology, they are most often used infer ecological processes, food web linkages, the origin of samples, and the movements of marine organisms.

However, to use isoscapes for these applications, it is necessary to have isoscapes at spatial scales relevant to the application in question. It is also necessary to have isoscapes that are based on a material that allows them to be applied to the organism or process in question. To address these necessities, the following dissertation created regional Gulf of Mexico isoscapes using the $\delta^{13}C$ and $\delta^{15}N$ values of reef-associated mesopredators, so the isoscapes could be directly applicable to many fisheries species as well as other mesopredators of interest.

The objectives of this dissertation were (1) to create empirical $\delta^{13}C$ and $\delta^{15}N$ isoscapes for the Gulf of Mexico using fish muscle, (2) to create a statistical models for those $\delta^{13}C$ and $\delta^{15}N$ values using readily available remote sensing data, (3) to use those models to evaluate predicted temporal variability in those isoscapes, (4) to use the isoscapes and models to elucidate influential ecological processes for $\delta^{13}C$ and $\delta^{15}N$ baselines, and (5) to demonstrate one application of the isoscapes using Red Snapper eye lens stable isotopes to infer movement histories of individual fish. Care was taken that the methods and products presented here could

be used in future studies, and important considerations and caveats for these methods and products are listed at the end of each chapter.

First, muscle samples from Red Snapper (*Lutjanus campechanus*) and Yellowedge Grouper (*Epinephelus flavolimbatus*) were collected from longlining research cruises in the Gulf of Mexico and analyzed for δ^{13}C and δ^{15}N values. Regressions were performed between each isotope and fish standard length to assess if there was a significant effect of trophic growth (increase in trophic position with fish size). All regressions were significant and, to prevent spatial differences in fish trophic position from overwhelming spatial differences in baseline isotopic values, residuals from the regressions were used to create isoscapes instead of the original data. Isoscapes were created for δ^{13}C and δ^{15}N values on the continental shelf of the Gulf of Mexico in areas reflecting the capture locations of each species. The Red Snapper δ^{13}C isoscape depicted a depth gradient, wherein δ^{13}C decreased with depth. This pattern was attributed to higher productivity and/or higher benthic basal resource availability inshore. The Yellowedge Grouper isoscape did not depict a depth gradient because Yellowedge Grouper were only captured close to the shelf edge. The δ^{15}N isoscapes of both species depicted a pattern of higher δ^{15}N values in areas near freshwater input with more eutrophic conditions and lower δ^{15}N values in areas with more oligotrophic conditions. This pattern was attributed to differences in the sources of bioavailable nitrogen. In areas near freshwater input, it appeared rivers were delivering organic waste (sewage or livestock effluent) that tends to have higher δ^{15}N values, whereas, in oligotrophic areas, most bioavailable nitrogen came from diazotrophic nitrogen fixation that tends to have lower δ^{15}N values.

Next, statistical models were created for the spatial patterns in δ^{13}C and δ^{15}N values to evaluate temporal variability and further elucidate influential ecological processes. Potential

predictor variables included satellite remote sensing products [CDOM, Chl, K_d (PAR), surface PAR, PAR(z), PIC, POC, and SST] and static variables (latitude, longitude, and depth) collected with each longlining deployment. Optional transformations (x^2, Ln(x), 1/x, and √x) were applied to predictor variables, and predictor variables were standardized. Potential predictor variables were used in linear multiple regression analysis, wherein variables were selected using forward selection and AIC. All models were significant and explained at least a moderate amount of spatial isotopic variation. Overall, the $\delta^{15}N$ models had higher R^2 values and performed better when the model created with one species was used to predict the $\delta^{15}N$ values of the other species. The selected variables and coefficients of the models suggested that the ecological explanations applied to the empirical isoscapes were correct with a few additions. The Red Snapper $\delta^{13}C$ model included SST with a negative coefficient, which was attributed to SST being an influence on or a proxy for phytoplankton species composition. The selected variables and coefficients of the Yellowedge Grouper $\delta^{13}C$ model suggest productivity is highly influential, and, in areas where productivity is lower and more spatially uniform, light environment is influential. Temporal variability of these isoscapes was assessed by gathering satellite products from all four seasons within an El Niño and La Niña year and using the statistical models to predict isoscapes for those time periods. Overall, the predicted isoscapes depicted very little temporal variation.

Finally, the $\delta^{13}C$ and $\delta^{15}N$ isoscapes were used in conjunction with Red Snapper eye lens stable isotopes to infer movement histories of individual fish. Fish eye lenses are proteinaceous spherical structures used to focus light within the eyes of fish. As the fish grows, the eye lens grows with it by adding successive layers (laminae) to the outside of the lens. After each layer is laid down, it undergoes attenuated apoptosis and becomes metabolically inert. Therefore, the eye lens is a conserved isotopic record of the isotopic conditions encountered by the fish, wherein the

center is the oldest material, and the outermost layer is the newest material. Individual laminae were peeled off the eye lens and analyzed for $\delta^{13}C$ and $\delta^{15}N$ values. Linear regressions between the isotopic values of laminae and eye lens diameter indicated that Red Snapper underwent trophic growth, and the equation from that regression was used to create a predicted isotopic life history (IHL) plot for a hypothetical stationary fish. Deviation scores were calculated for each fish as the summed absolute values of the differences between the measured isotopic values within the fish's eye lens and the predicted isotopic values for the hypothetical stationary fish. Deviation scores were evaluated along with the *rho* values from Spearman rank correlations of the $\delta^{13}C$ and $\delta^{15}N$ values within the eye lens of each fish to infer if a fish had undergone movement or remained relatively stationary throughout its life. If a fish had a low deviation score and a high *rho* value, it was inferred to have remained relatively stationary. Overall, this analysis and evaluation depicted a high level of individual variability in Red Snapper movement histories.

The major conclusions of this dissertation are (1) that spatial $\delta^{13}C$ variation in the Gulf of Mexico is consistent with productivity and/or basal resource dependence, and $\delta^{15}N$ spatial variation is consistent with bioavailable nitrogen sources, (2) that, based on the statistical models, there is very little temporal variability in $\delta^{13}C$ and $\delta^{15}N$ isoscapes, (3) that fish eye lens stable isotopes can be used in conjunction with isoscapes to infer possible movement histories, and (4) that Red Snapper generally undergo trophic growth with a high level of individual variability in movement histories. This dissertation provides isoscapes and isoscape models that have potentially broad applications, but applications relating to fisheries management and fish ecology are probably the most apt. The results from the Red Snapper movement histories have implications for fisheries management including the need for large sample sizes for Red Snapper studies to capture the full range of behaviors.

Chapter 1: Introduction

1.1. Stable isotope chemistry

Isotopes are forms of an element with different numbers of neutrons. Generally speaking, isotopes that have the same, or slightly more neutrons than protons have long-term stability. It was just over 100 years ago that the first machine that was able to detect isotopes was built by Fracis W. Aston. Today, there are over 3100 known isotopes of 120 elements, but only 283 of those are stable isotopes (Fry 2006). The stable isotopes that are of primary concern for this dissertation are carbon-13 (^{13}C) and nitrogen-15 (^{15}N). So called "stable isotopes" do have a very slight probability of spontaneous decay, but it is negligible for most purposes (Sharp 2017). Most isotopes have skewed distributions with one isotope being far more common than others. For example, the light isotope accounts for over 98% of all carbon and nitrogen atoms (Fry 2006).

Isotopic ratios are commonly described using δ notation. This notation is essentially a ratio of ratios describing how much a sample's isotopic ratio differs from that of a known standard. The standard for carbon is PeeDee belemnite limestone, and the standard for nitrogen is atmospheric air. The calculation for δ notation is as follows:

$$\delta^j X = \left(\frac{(\,^j X /\,^i X)_{sample}}{(\,^j X /\,^i X)_{standard}} - 1 \right) * 1000$$

where X is the element, j is the rarer, heavier isotope of X, and i is a more common, lighter isotope of X. The final multiplication by 1000 puts samples on the parts-per-thousand scale (i.e., a 1% difference becomes 10 ‰). The "natural abundance range" for most elements is -100 to 50

‰. The δ notation is useful because it allows for simple algebraic mixing and fractionation calculations with accurate results for the purposes of most studies. Small errors can arise in these calculations if samples have a δ value well outside the natural abundance range. If δ values are very high, fractionation may be underestimated, and if δ values are very low, fractionation may be overestimated (Fry 2006).

1.1.1 Fractionation

The extra neutron(s) in heavier isotopes of an element causes a slight difference in how different isotopes undergo physical and chemical processes. The differential effect of physical and chemical processes on changing the ratio of heavy-to-light isotopes in a given pool of an element is called fractionation. Fractionation is normally mass dependent, meaning isotopes with a greater relative mass differential will experience greater fractionation. There are two main types of mass-dependent fractionation: kinetic fractionation and equilibrium fractionation. Kinetic fractionation is associated with fast, incomplete, or unidirectional processes like evaporation, diffusion, and dissociation reactions as well as many biological processes (i.e., photosynthesis). In general, lighter isotopes will have higher velocity at the same temperature as heavier isotopes and lighter isotopes and will accumulate on the products side of the reaction as a result. Equilibrium fractionation is associated with equilibrium reactions (reactions that proceed in both directions at equal rates). The energy required to break a bond with a heavier isotope is slightly higher than it is for a lighter isotope. This results in heavier isotopes concentrating where bonds are strongest. The magnitude of equilibrium fractionation will depend on the bonding environment of the phases in question, including the temperature. Generally, equilibrium fractionation decreases with increasing temperature in the proportion $1/T^2$ (Sharp 2017). It

should be noted that, if any kinetic reaction goes to completion (all substrate converted to products), there is no opportunity for fractionation to occur (Peterson and Fry 1987). As a reaction grows close to completion, the magnitude of fractionation will decrease, and the substrate and products will be closer in $\delta^{13}C$ value. This process is often referred to as Raleigh distillation or Raleigh fractionation.

Carbon in the oceans is fractionated by a few key processes. First, there is equilibrium fractionation between the CO_2 in the air and the carbon species (mostly bicarbonate) in the water. The heavier ^{13}C is concentrated in the bicarbonate where bonds are stronger and, as a result, dissolved inorganic carbon in the surface oceans is around 0-1 ‰ whereas atmospheric CO_2 is around -8 ‰ (Mook et al. 1974; Fry 2006). As an equilibrium fractionation process, the fractionation of ^{13}C in surface ocean dissolved inorganic carbon is mediated by temperature (Epstein et al. 1953).

Oceanic carbon isotopes are also kinematically fractionated by photosynthesis. The difference between the $\delta^{13}C$ values of primary producers and ambient CO_2 includes both the diffusion fractionation that occurs as CO_2 enters primary-producer cells and the enzymatic fractionation (via the enzyme Rubisco) that takes place within the cells of primary producers. The net effect of these two processes is photosynthetic fractionation. Most commonly, the net effect of photosynthetic fractionation is that primary producers preferentially fix the lighter ^{12}C isotope, which results in cellular $\delta^{13}C$ values that are around 20 ‰ lower than the ambient CO_2 (Fry 2006). The magnitude of photosynthetic fractionation is influenced by the type or species of plant or algae performing photosynthesis, the concentration of ambient CO_2, the rate of productivity, and light availability (Gearing et al. 1984; Cifuentes 1987; Cooper and Deniro 1989; Rau et al. 1996; Hofmann et al. 2000). In general, macroscopic marine plants have higher

δ^{13}C values than phytoplankton (Clementz and Koch 2001), and terrestrial C4 plants have higher δ^{13}C values than C3 plants (Fry 2006). The concentration of CO_2 affects photosynthetic fractionation through Raleigh fractionation, wherein the primary producer δ^{13}C values will be closer to that of the ambient CO_2 as a greater proportion of the ambient CO_2 is consumed. This effect of the concentration of CO_2 results in lower photosynthetic fractionation when CO_2 demand is high and/or when CO_2 supply is low. These conditions can occur when there is high productivity rates/ high light availability (Popp et al. 1998; Hofmann et al. 2000; Radabaugh et al. 2014). This same process occurring at the scale of cell diffusion layers and within-cell transport results in larger algal cells generally having higher δ^{13}C values than smaller algal cells (Cooper and DeNiro 1989; Muscatine et al. 1989). The environmental factors affecting photosynthetic fractionation can also covary wherein in one factor may affect relationships with others (Rau et al. 1996). For an example, see the effect of temperature on δ^{13}C values discussed in section 4.1.

Nitrogen is fractionated by a variety of processes that convert nitrogen to various forms within the nitrogen cycle including assimilation, nitrogen fixation, denitrification, remineralization, and nitrification. Most of these processes are metabolically driven and therefore induce kinetic fractionation processes (Sharp 2017). Assimilation is the process by which inorganic nitrogen is incorporated into living tissue, and has a fractionation effect between -27 and 0 ‰. The wide range of values are controlled by the availability of nitrogen, what enzymes are responsible for NH_3 fixation, and diffusion of NH_3 through the cell walls (Fogel and Cifuentes 1993; Sharp 2017). In the oceans, nitrogen is often the limiting factor for phytoplankton growth, and therefore all bioavailable nitrogen is often consumed resulting in no fractionation effect (Lohrenz et al. 1997; Dagg and Breed 2003; Capone et al. 2008). Nitrogen

fixation is the process by which nitrogen gas is converted to organic nitrogen by bacteria, and has a fractionation effect close to 0 ‰ (Carpenter et al. 1997; Montoya et al. 2002; Montoya 2007; Sharp 2017). A compilation of nitrogen fractionation values by Fogel and Cifuentes 1993 ranged from -3 to 1 ‰. Denitrification is the process by which nitrate is converted to nitrite and nitrite is converted to nitrogen gas. Because this process is primarily performed by anaerobic bacteria, it usually occurs under hypoxic or anoxic conditions (Sharp 2017). Fractionation due to denitrification can range from -40 to 11 ‰ (Cline and Kaplan 1975; Mariotti et al. 1982). The large range of fractionation is due in part to the potential removal of produced nitrogen gas by diffusion into the atmosphere which results in Rayleigh fractionation and can produce more extreme fractionation effects (Sharp 2017). Remineralization is the process by which organic nitrogen is converted into ammonia, usually by bacterial decomposition. The fractionation effect of remineralization is close to 0 ‰ (Sharp 2017). However, because more labile, organic material with lower $\delta^{15}N$ values is preferentially broken down via remineralization, inorganic nitrogen below the euphotic zone will often have lower $\delta^{15}N$ values than residual particulate organic matter (Williams and Gordon 1970; Altabet, 1988; Smith et al., 1992; Mullerniklas et al. 1994; Kiorboe, 2001; Lee et al., 2004). Nitrification is the process by which ammonia is converted to nitrite and nitrite is converted to nitrate by nitrifying bacteria. Fractionation from nitrification ranges from -12 to 20 ‰, with nitrate ultimately having a lower $\delta^{15}N$ value than the ammonium precursor (Kendall 1998; Sharp 2017). The wide range is due to differing fractionations at each reaction step based on ambient conditions.

1.2. Stable isotopes in the environment

     Stable isotopes in the environment are a result of the isotopic sources and fractionation processes present in an area (Fry 2006; West et al. 2010). Environmental stable isotope ratios can be used in a wide variety of ecological applications including predator-prey dynamics, competition, physiology, nutrient transport, landscape ecology, and movement history (Fry 2006; Post 2002; Bearhop et al. 2004; West et al. 2010). The focus of this dissertation is using the spatial patterns of carbon and nitrogen stable isotopes in the environment (isoscapes) to infer the movement history of organisms. In order to achieve this application, it is necessary to understand the ecological causes and implications of the $\delta^{13}C$ and $\delta^{15}N$ values in the environment and in consumer species.

     One concept that is necessary for the evaluation of environmental isotopic values is that of basal resources. Basal resources are the species, groups of species, or functional groups found at the base of the food web (i.e., trees, grasses, phytoplankton, benthic algae, seagrass etc.). Different basal resources will support different food chains, though consumers increasingly integrate multiple basal resources higher up in the food web (Rooney and McCann 2012). Identifying and assessing the contribution of basal resources to food webs is important for determining trophic connections and energy pathways. Stable isotopes are useful tools for this purpose since different basal resources often have distinct isotopic ratios that are preserved in higher trophic levels (i.e., Haines and Montague 1979; France 1995; Fry and Ewel 2003). The $\delta^{13}C$ value of a consumer is assumed to largely reflect its basal resource dependence (Cherel and Hobson 2007; Grippo et al. 2011), whereas $\delta^{15}N$ values are highly fractionated as material is passed through a food web (see section 1.3.1). On marine continental shelves, basal resources supporting consumers are often grouped as phytoplankton with a $\delta^{13}C$ value around -22 ‰

(Moncreiff, and Sullivan 2001) and benthic algae which are around 5 ‰ higher (France 1995; Doi et al. 2010; Rooney et al. 2006).

1.3. Stable isotopes in consumers

Whereas the stable isotopes found in consumers reflect those found in the environment, the environmental conditions and basal resource isotopic ratios will be filtered and modified by prey choice, movement, and fractionation processes that take place within a consumer. In essence, the isotopic ratios of consumers represent a combination of the isotopic composition of prey species, the assimilated proportion of each prey, the isotopic fractionation occurring during tissue production, and the foraging location (Fry 2006; Bearhop et al. 2004; West et al. 2010). It is important to consider the influence of all these processes when interpreting consumer stable isotopes or creating consumer isoscapes.

Consumer tissues provide an isotopic signal that is averaged over the turnover time of the sampled tissue (Vander Zanden et al. 2015). Consumer tissues are considered to be at equilibrium with their diet after 4-5 half-lives of the tissue (Hobson and Clark 1992). More metabolically active tissues (i.e., blood, skin) have shorter turnover times than less metabolically active tissues (i.e., bone, scales; Vander Zanden et al. 2015). Fast growing organisms also have shorter turnover times than slower growing organisms (Fry and Arnold 1982; Hesslein et al. 1993). When conducting isotopic studies using fish muscle, many researchers use a turnover time of three months (McIntyre and Flecker 2006; Buchheister and Latour 2010; Nelson et al. 2011; Radabaugh and Peebles 2014).

One of the factors that determines the isotopic value of consumer tissue is their basal resource dependence. Consumer $\delta^{13}C$ values are often used as an indicator of basal resource use

(Hobson et al. 1994; Cherel and Hobson 2005; Radabaugh and Peebles 2014), although $\delta^{15}N$

values can also sometimes respond to a change in basal resource dependence (i.e., switching to

or from a cyanobacteria-dominated food chain; Fry and Sherr 1984; Montoya 2007). In general,

species or individuals that feed lower in the food web tend to be primarily supported by a single

basal resource (i.e., phytoplankton or benthic algae), whereas species or individuals that occur

higher up in the food web tend to integrate multiple basal resources (Vander Zanden and

Rasmussen 1999; Vander Zanden and Vadeboncoeur 2002; Rooney et al. 2006,).

1.3.1 Trophic fractionation

Whereas the primary purpose of this dissertation to infer migration through stable isotope

analysis, consumer stable isotopes are also widely used in food web studies due to the isotopic

fractionation associated with movement up the food web (Minagawa and Wada 1984; Post

2002). The study of food webs includes concept of trophic levels, which are a discrete

representation of how many steps up the food chain an animal was from a primary producer

(Lindeman 1942). However, representation of trophic levels as discrete integers betrays the fact

that most species feed on a number of food sources, each with their own different respective

places in the food web. For this reason, most modern ecologists use the term "trophic position", a

quantitative, continuous measure of the hierarchical position of a given species in the food web,

rather than "trophic level" (Vander Zanden and Rasmussen 1996).

Trophic discrimination factors (TDFs), sometimes referred to as trophic enrichment

factors, are a quantity reflecting the isotopic enrichment accompanying an increase in trophic

level ($\Delta^{13}C$ and $\Delta^{15}N$ for carbon and nitrogen, respectively; DeNiro and Epstein 1981; Minagawa

and Wada 1984; Post 2002; Chikaraishi et al. 2007). Trophic fractionation of nitrogen is

8

generally attributed to either fractionation during amino acid deamination and transamination, whereby ^{14}N amine groups are preferentially removed leaving relatively enriched nitrogen behind (metabolic fractionation; Gannes et al. 1997; Vander Zanden and Rasmussen 2001), or to isotopic discrimination during nitrogen assimilation (assimilative fractionation; Vander Zanden and Rasmussen 2001). The TDFs that are used for most trophic studies are around 1.0 ‰ per trophic level for bulk δ^{13}C values and 3.4‰ per trophic level for bulk δ^{15}N values (Minagawa and Wada 1984; Post 2002). However, reported TDFs range from -8.79 to 6.1 ‰ for carbon, and -3.22 to 9.2 ‰ for nitrogen (Caut et al. 2009), and TDFs have been shown to vary based on a variety of factors including consumer physiology, consumer type, diet quality, and trophic level (Vanderklift and Ponsard 2003; Caut et al. 2009; Canseco et al. 2021). For a pilot study exploring the relationship between TDF and growth rate, see Appendix A.

Whereas TDFs may be highly variable, and change based on a variety of factors, it is generally assumed that both δ^{13}C and δ^{15}N values increase (albeit to a minor degree in the case of δ^{13}C) as the trophic position of a consumer increases (Post 2002; Fry 2006). In order to infer how a consumer's stable isotopes reflect their environment (a pre-requisite for migration studies), the effect of trophic fractionation must be addressed. Some methods to address trophic fractionation include using compound specific isotope analysis to explicitly determine the basal resource isotopic value within a consumer and the consumer's trophic position (Bradley et al. 2015; Wallace 2019) and using the relationships between isotopes and consumer size to infer trophic contribution (Vecchio et al. 2021; Vecchio and Peebles 2022; discussed in section 6.3).

1.4. Isoscapes

An isoscape is a map of measured or predicted spatial variation in the isotopic ratios of a given element. The term first came into widespread use around 2005, but documentation of spatial variation in isotopic ratios dates back at least as far as 1954 (Dansgaard 1954; Bowen 2010). The basic premise behind the creation of isoscapes is that of spatial autocorrelation wherein, due to underlying spatial patterns of environmental factors that determine isotopic ratios, samples that were collected closer together are more likely to be similar isotopically than those collected father apart (Bowen 2010). The biogeochemical processes that influence the spatial variation in isotopic ratios include geology, climatology, biology, and hydrology (Bowen 2010). Isoscapes are used in a variety of scientific fields, including geology (West et al. 2010), archaeology (Kootker et al. 2016), and ecology (Boecklen et al. 2011). Within the realm of marine ecology, isoscapes have applications relating to basal resource dependence, food-web interactions, and the origins and movements of animals (Graham et al. 2010; Hobson et al. 2010; Olson et al. 2010).

There are two primary methods for creating isoscapes: spatially interpolating between the measured values of samples (empirical isoscapes) and creating a statistical model to predict the spatial patterns of isotopic values based on measured variables (modeled isoscapes; Bowen and Revenaugh 2003; Graham et al. 2010; West et al. 2010). Directly measured, empirical isoscapes can be very useful for individual studies however, they do not capture any potential temporal variation in the isotopic baselines of an area. If the environmental processes that influence isotopic ratios change over time, it is unlikely that an isoscape is temporally static (Bowen and Revenaugh, 2003). The temporal variation in isotopic values can be at seasonal (Mariotti et al. 1984; Kline 1999; Kürten et al. 2013; Magozzi et al. 2017), annual (Kline 1999; Hannides et al.

2009; Rooker et al. 2010), or decadal (Schloesser et al. 2009) time scales. When it comes to applying isoscapes to many studies, modeled isoscapes allow for the inference of what isotopic spatial patterns would look like at time of data collection.

Both empirical and modeled isoscapes can be created using abiotic sources (i.e., Dutton et al. 2005), basal resources (i.e., Hofmann et al. 2000), or consumers (i.e., Radabaugh et al. 2014). Isoscapes created using basal resources provide a more accurate picture of environmental factors controlling isotopic values in the food web; however many basal resources display a high level of temporal isotopic variation and so an isoscape created for any one time period may not be a good estimation of average conditions (Post 2002; McMahon et al. 2013a, b). The isotopic values of basal resources may change temporally due to a variety of factors including species composition, availability and sources of nutrients, light conditions, and temperature (Cloern and Jassby 2010; McMahon et al. 2013 a, b). Conversely, isoscapes created using consumer tissue provide a more time averaged, but trophically modified depiction of isotopic spatial patterns (Cabana and Rasmussen 1996; Vander Zanden and Rasmussen 1999; Post 2002; Fry 2006).

1.4.1 Spatial patterns in $\delta^{13}C$ values

Spatial patterns in $\delta^{13}C$ values have been shown to correlate to aqueous carbon dioxide concentrations, depth, temperature, productivity rates, and, in consumers, basal resource dependence (Fry, 1988; Cooper and DeNiro, 1989; Rau et al. 1997; Hofmann et al., 2000; Liu et al., 2007; Barnes et al. 2009; Radabaugh et al. 2013;). The very first carbon isoscape was based around a model of the variable fraction of carbon by photosynthesis (Lloyd & Farquhar, 1994). This fractionation effect is less extreme under low CO_2 concentrations or during times of high growth rates, which results in marine photosynthetic organisms from areas with high

productivity having higher δ^{13}C values (Popp et al., 1998; Hofmann et al., 2000). For example, there is a general trend in which the δ^{13}C values of benthic plants is higher in shallow water and lower in deeper waters, which is attributed to increased light availability in shallow waters leading to higher growth rates and less extreme fractionation (Wefer and Killingley, 1986; Cooper and DeNiro, 1989; Muscatine et al., 1989). Seasonal differences in light environment can also affect basal resource δ^{13}C values, particularly if light, rather than nutrients, is limiting growth in the winter months (Mariotti et al. 1984; Kline 1999). Fractionation also varies with species composition. Phytoplankton with a smaller cell size tend to be isotopically lighter than phytoplankton with a larger cell size and benthic plants tend to be 5 ‰ heavier than phytoplankton (Fry 1981; France 1995; Laws et al. 1995; Radabaugh and Peebles 2014). Subsequently, consumers that rely on a benthic basal resource have higher δ^{13}C values than consumers that rely on planktonic resources (Hobson et al. 1994; Cherel and Hobson 2007). The combination these trends often result in a pattern of consumers increasing in δ^{13}C values from offshore (where benthic producers are not readily available and productivity is lower) to nearshore (Graham et al. 2010; Radabaugh et al. 2013; Quillfeldt et al. 2015; Ceia et al. 2018). In highly stagnated areas, carbon recycling can occur wherein photosynthetic fractionation occurs, that carbon is respired/remineralized, and the same carbon is fractionated a second time resulting in algae with δ^{13}C values as low as -45 ‰ (Fry 2006). Whereas consumers that spend time in these areas may retain the very low δ^{13}C value (i.e., Kurth et al. 2019), the algae from this area are not often transported away from the area and therefore, the effect is very limited spatially.

The effect of temperature on δ^{13}C values is somewhat complex. Higher temperatures allow for higher maximum phytoplankton growth rates (Eppley 1972) which is often associated with lower fractionation as described above. Lower temperatures result in higher gas solubility in

12

water which allows for higher carbon dioxide concentrations. Higher carbon dioxide increases photosynthetic fractionation and so phytoplankton $\delta^{13}C$ values are often lower in colder waters (Rau et al. 1997). It should be noted that the magnitude of temperature effects on photosynthetic fractionation is dependent on cell-wall permeability and the ability of primary producers to actively transport carbon into cells (Rau et al. 1996; Radabaugh et al. 2014). For all these reasons, $\delta^{13}C$ values are often strongly correlated with temperature and/or latitude at both global (Goericke and Fry 1994; Hinga et al. 1994; Trueman et al. 2012; McMahon et al. 2013; Magozzi et al. 2017) and regional (Barnes et al. 2009; Radabaugh and Peebles 2014) scales. Conversely, higher temperatures result in increased ocean stratification which reduces vertical mixing and nutrient availability. These conditions favor smaller-celled phytoplankton which tend to have lower $\delta^{13}C$ values (Fry 1981; France 1995; Laws et al. 1995). Therefore, in some cases, it is possible for temperature and $\delta^{13}C$ values to have an inverse relationship.

1.4.2 Spatial patterns in $\delta^{15}N$ values

Because nitrogen is commonly a limiting nutrient for primary-producer growth in the marine environment (Lohrenz et al. 1997; Dagg and Breed 2003; Capone et al. 2008), all the available nitrogen is usually consumed and therefore nitrogen is not fractionated by photosynthesis. Exceptions to this include areas where nitrogen is not the limiting nutrient (i.e., equatorial Pacific; Altabet 2001) and time periods or locations when light limits photosynthesis rather than nutrients, which may occur during winter months (Mariotti et al. 1984; Kline 1999). Given those considerations, baseline marine nitrogen isotopic ratios are primarily a function of the $\delta^{15}N$ values of the sources of bioavailable nitrogen present (i.e., fixed nitrogen). The processes determining the $\delta^{15}N$ values of bioavailable nitrogen include the input and mixing of

13

different nitrogen sources and a variety of chemical and microbial processes all of which are variable spatially and temporally. However, a commonly observed pattern is higher $\delta^{15}N$ values in eutrophic waters and lower $\delta^{15}N$ values in oligotrophic waters (Alt-Epping et al. 2007; Nerot et al. 2012; Radabaugh et al. 2013). In oligotrophic areas, a major source of bioavailable nitrogen is diazotrophic cyanobacteria that fix nitrogen at or near 0‰, the same value as atmospheric nitrogen (Carpenter et al. 1997; Montoya et al. 2002; Montoya 2007). In the more eutrophic waters near river outflows, particulate organic matter (POM) nitrogen has been observed to be closer to 5–9‰ due to the isotopic dominance of sewage and manure relative to manufactured fertilizers in the watershed (Hansson et al. 1997; Kendall et al. 2001). The relative contribution and spatial distribution of nutrient sources is influenced by precipitation (riverine inputs) and advection of water masses (Mariotti et al. 1984; Kürten et al. 2013). Under hypoxic and anoxic conditions, denitrifying bacteria in water and sediments reduce NO_3^- and NO_2^- to gaseous N_2O and N_2. This denitrification process results in strong, positive fractionation (20–30‰), producing higher $\delta^{15}N$ values for the residual nitrate (Altabet et al. 1999; Granger et al. 2008). This process often occurs in water column oxygen minimum zones at rates high enough to affect the average isotopic ratio of nitrate (Brandes et al, 1998) but, in the Gulf of Mexico, there is also a large seasonal hypoxic area between the Mississippi River outflow and Texas where denitrification has been observed in the sediments (Gardner et al. 1993; Childs et al. 2002; Childs 2004). Temperature can have an indirect influence on $\delta^{15}N$ values because of its affect on ocean stratification which can influence the relative importance of nitrogen fixation (Montoya 2007) and the development of bottom hypoxia and anoxia (Altabet et al. 1999). In the winter to spring, there is a lower level of stratification and vertical mixing promotes entrainment of nitrate with a $\delta^{15}N$ value around 5-7 ‰ into the euphotic zone, promoting the growth of larger phytoplankton

(Sigman and Casciotti 2001). In summer to early fall, stratification increases and nitrogen

fixation becomes more influential (Montoya 2007).

1.4.3 Gulf of Mexico isoscapes

The influences on spatial patterns in $\delta^{13}C$ and $\delta^{15}N$ values mentioned above occur around

the world, however the focus of this dissertation is the $\delta^{13}C$ and $\delta^{15}N$ patterns within the Gulf of

Mexico. There have been five other studies that created coastal isoscapes for the Gulf of Mexico

(Radabaugh et al. 2013; Radabaugh and Peebles 2014; Vander Zanden et al. 2015; Cuddy 2018;

Le-Alvarado et al. 2021). These studies are summarized in Table 1.1. For more detail and

synthesis, see section 3.4.3.

Table 1.1
A table summarizing studies that include the creation of Gulf of Mexico isoscapes.

Citation	Region	Type	Material	$\delta^{13}C$ patterns	$\delta^{15}N$ patterns
Radabaugh et al. 2013	West Florida Shelf	Empirical	Fish muscle	Decrease in $\delta^{13}C$ values with depth	Higher $\delta^{15}N$ values near freshwater input, lower $\delta^{15}N$ values in oligotrophic regions
Radabaugh and Peebles 2014	West Florida Shelf	Modeled	Fish muscle	Decrease in $\delta^{13}C$ values with depth	Higher $\delta^{15}N$ values near freshwater input, lower $\delta^{15}N$ values in oligotrophic regions

Table 1.1 (Continued)

Citation	Region	Type	Material	$\delta^{13}C$ patterns	$\delta^{15}N$ patterns
Vander Zanden et al. 2015	Eastern Gulf of Mexico, Yucatan peninsula, Caribbean and the east Florida shelf	Empirical	Loggerhead sea turtle scutes	Higher $\delta^{13}C$ values towards the Caribbean	Higher $\delta^{15}N$ values near freshwater input, lower $\delta^{15}N$ values in oligotrophic regions
Cuddy 2018	Texas estuarine systems	Empirical	Seagrass leaf tissue	Lower $\delta^{13}C$ values with higher freshwater inflow and near urban areas	Higher $\delta^{15}N$ values near urban areas
Le-Alvarado et al. 2021	Whole Gulf of Mexico	Empirical	Zooplankton	Low $\delta^{13}C$ values in northwest Gulf of Mexico and high $\delta^{13}C$ values near Florida Keys	Higher $\delta^{15}N$ values near freshwater input, lower $\delta^{15}N$ values in oligotrophic regions

1.5. Migration studies and isoscapes

Animals may migrate in order to pursue optimal combinations of higher food availability and lower mortality risk (Dingle and Drake, 2007). Migration within a species can be regular and fixed (i.e., Schofield et al. 2010) or highly differentiated among individuals (i.e., Diamond et al. 2007; Patterson 2007). The particulars of how migration occurs has implications for fisheries management (Cowen et al. 2000; Hobson et al., 2019) as well as nutrient and energy dynamics within and among ecosystems (Deegan, 1993). Fisheries managers require life-history data, including migration data, to properly understand habitat use, food web structures, habitat connectivity, population structure, and energy pathways through food webs (Hyslop 1980; Fisk et al 2001; Sheppard 2010; Hobson and Norris 2008; Kell et al. 2009; Ramos and Gonzalez-Solis 2012; McMahon and McCarthy 2016).

For years, fish migration studies were primarily performed using artificial tags such as anchor tags, spaghetti tags, transmitters, satellite data loggers, and others. Whereas artificial tags certainly yield useful data, there are certain drawbacks intrinsic to the methods, including cost in terms of time and money and low rates of recapture (West et al. 2009). Most of these tagging studies are also conducted on a time scale much shorter than the potential decades-long lifespan of fish. Stable isotopes, in contrast, represent a set of natural tags require only one capture (rather than the tagging capture and subsequent recapture required by many artificial tags) and can provide large datasets of complete lifetime movement histories at a relatively low cost.

The stable isotopic values recorded in the tissues of consumers can provide information about foraging and movement along isotopically distinct habitats (Peterson and Fry, 1987; Hobson, 1999). Stable isotope data from tissues within an organism can be evaluated in conjunction with an isoscape to compare measured stable isotopic ratios to ratios that would be expected in different areas. Early marine stable isotope migration studies used $\delta^{18}O$ values of commensal organisms growing on long-lived organisms such as whales and sea turtles (Killingley 1980; Killingley and Lutcavage 1983). The use of $\delta^{13}C$ values to track migration was first demonstrated by Fry (1981) using brown shrimp. **rewrite He recorded a shift in $\delta^{13}C$ values as the shrimp moved from inshore seagrass beds to offshore plankton-based food webs. Since then, stable isotopes have been used to track migration in a variety of organisms (Hobson, 1999).

There are two primary methods used for stable isotope migration studies. First, a comparison can be made between two tissues with different turnover times. If the two tissues have the same isotopic value, it can be presumed that the consumer did not migrate during the turnover time period. If the two tissues have different isotopic values, it can be presumed that the

17

consumer migrated at some point within the shorter of the two turnover times (Tieszen et al. 1983; Hobson 1999). Second, a longer isotopic history can be obtained using sequentially synthesized, metabolically stable tissues (Vander Zanden et al. 2015; Tzadik et al. 2017). Metabolically inert tissues provide a conserved record of the isotopic environment the consumer was exposed to at the time the tissue was created and, in the case of sequentially synthesized tissues, provide a biochemical record of an individual's trophic geography across long periods of time up to the entire lifespan of individual organisms (Campana and Neilson 1985; Campana 1999; Trueman et al. 2012). Stable isotope analysis of sequentially synthesized tissues has the potential to provide trophic and geographic records for life stages (i.e., postlarval or juvenile stages) that are often under-sampled by fisheries gear (Bell-Tilcock et al. 2021; Simpson et al. 2019; Vecchio and Peebles 2020). For fish, these tissues include scales, fin rays and spines, otoliths, vertebrae, and eye lenses (Tzadik et al. 2017).

Otoliths are primarily composed of calcium carbonate and are secreted in concentric rings over the course of a fish's life, providing a full life history of the carbon and oxygen stable isotopes encountered by that fish. In the Gulf of Mexico, otoliths stable isotopes have been used to determine the nursery habitat of Red Snapper (Sluis et al. 2012; Sluis et al. 2015). First, age-0 Red Snapper were sampled from six regions around the Gulf of Mexico in order to chemically distinguish the six regions (Sluis et al. 2012). However, the use of otoliths of subadult and adult Red Snapper to assess the population connectivity between US and Mexican waters was inconclusive (Sluis et al. 2015). A similar study was conducted using the otoliths of Red Drum (Rooker et al. 2010). The $\delta^{13}C$ and $\delta^{18}O$ values of Red Drum from different nursery estuaries in the Western Gulf of Mexico were measured and then those values were compared to values found near the core of otoliths from young of the year Red Drum to determine connectivity

18

between early life and adult habitats. They found southern estuaries had higher $\delta^{13}C$ and $\delta^{18}O$ values and lower rate of movement between regions than the northern estuaries.

1.6. Fish eye lenses

1.6.1 Eye lens structure

Whereas otoliths are excellent recorders of isotopic life histories in $\delta^{13}C$ and $\delta^{18}O$ values, they often do not contain adequate nitrogen for $\delta^{15}N$ analysis which prevents the acquisition of potentially useful information about diet and movement along $\delta^{15}N$ gradients (Pinnegar and Polunin 1999). Rather than being mineral, eye lenses are largely composed of crystallin protein which contains ample N for isotopic analysis. Fish eye lenses are spherical and layers (laminae) are laid down at the outer lens as the animal grows (Nicol 1989; Horwitz 2003). They are composed of two cell types; fiber cells and lens epithelial cells (Dahm et al. 2007; Wride 2011). Epithelial cells form a one-cell-thick layer around the lens and secrete new fiber cells as the fish grows. Each new layer of fiber cells undergoes attenuated apoptosis, wherein cells remove their cytoplasmic organelles to establish and maintain optical transparency of the lens (Nicol 1989; Horwitz 2003; Dahm et al. 2007; Vihtelic, 2008; Wride 2011). Protein synthesis stops in the lens layer once attenuated apoptosis is complete, making the eye lens a metabolically inert record of biochemical life history (Nicol 1989; Dahm et al. 2007; Vihtelic 2008; Wallace et al. 2014). The nucleus of the lens is the oldest material (Grainger et al. 1992) and the outermost layer of the lens is the newest material (Nicol 1989). Eye lenses grow isometrically with the fish which has allowed for eye lens weight at age and eye lens diameter at standard length equations to be developed though these equations may vary by species (Wallace et al. 2014; Quaeck-Davies et al. 2018). These relationships allow for an approximation of fish size and/or age for a given eye

lens weight or diameter or for a given eye lens lamina (i.e., Quaeck-Davies et al. 2018; Vecchio et al. 2021).

1.6.2 Stable isotopes in eye lenses

Several studies have been conducted to assess how $\delta^{13}C$ and $\delta^{15}N$ values are recorded in eye lenses. Tests to assess the magnitude and temporal resolution of variation of $\delta^{13}C$ and $\delta^{15}N$ values within fish eye lenses found that variation among laminae was far higher than that within laminae, and that there was a high degree of agreement between the isotopic records of the left and right eye lenses of the same fish (Wallace et al. 2014). The intra-laminar variation was comparable to the nominal differences between left and right eye lenses which indicated intra-laminar variation was due to measurement precision. Both these findings suggested isotopic variation across laminae within an eye lens was not an artifact. General lifetime patterns were the same when analyzing fewer laminae (lower temporal resolution) and when analyzing more laminae (higher temporal resolution), but certain early life history details were not captured at the lower temporal resolution. A step-change feeding experiment, wherein captive fish were fed a low $\delta^{15}N$ value diet and then switched to a relatively high $\delta^{15}N$ value diet, found that the dietary change was first recorded in the eye lens an average of 15.7 days after the diet switch, and that 90% assimilation of the new diet occurred 38.5 days after the diet shift (Granneman 2018). The same experiment found the TDF between food $\delta^{15}N$ values and lens $\delta^{15}N$ values was 3.15 ± 0.06‰. A review of the state of knowledge regarding the use of eye lenses for retrospective isotopic analysis found that eye lens diameter has a strong linear relationship with body size, but the equations governing that relationship differ among species (Quaeck-Davies et al. 2018). The review also found that eye lens $\delta^{15}N$ and $\delta^{13}C$ values are generally lower

compared to that muscle tissue, but mean $\delta^{15}N$ values and $\delta^{13}C$ values did not differ significantly between tissues, and the isotopic differences are low enough that they are likely to be obscured by between-individual variation and analytical error.

1.6.3 Eye lens stable isotope studies

Eye lenses are a relatively new but increasingly used source of consumer isotopic histories. Several studies have shown the utility of eye lens stable isotopes for the elucidation of life history traits in squid (Parry 2003; Hunsicker et al. 2010; Onthank 2013; Meath 2019; Xu et al. 2019) and fish (Wallace et al. 2014; Kurth et al. 2019; Quaeck-Davies et al. 2018; Simpson et al. 2019; Curtis et al. 2020; Vecchio et al. 2021; Vecchio and Peebles 2022). Eye lens stable isotopes have the potential to record ontogenetic shifts in location (Wallace et al. 2014; Kurth et al. 2019; Vecchio et al. 2021) and diet/basal resource usage (Curtis et al. 2020; Vecchio and Peebles 2022).

One trend that is commonly observed in eye lens stable isotope studies is trophic growth (Parry 2003; Hunsicker et al. 2010; Onthank 2013; Curtis et al. 2020; Vecchio et al. 2021; Vecchio and Peebles 2022). Trophic growth is an ontogenetic increase in trophic position with size (Curtis et al. 2020; Vecchio et al. 2021). As fish increase in size, their mouth gape increases (Karpouzi and Stergiou 2003), which allows them to consume larger (usually higher trophic position) prey. Because both $\delta^{13}C$ and $\delta^{15}N$ values tend to increase with trophic position (Post 2002; McMahon et al. 2013b), trophic growth can be documented as a strong correlation between body size and either $\delta^{13}C$ or $\delta^{15}N$ values or as a strong correlation between $\delta^{13}C$ and $\delta^{15}N$ values (Curtis et al. 2020; Vecchio and Peebles 2020). There is stronger trophic fractionation for nitrogen (Minagawa and Wada 1984; Post 2002), so it is likely that under

conditions of trophic growth, $\delta^{15}N$ values would have a stronger correlation with size whereas

$\delta^{13}C$ values will also respond to shifts in basal resource which may or may not be accompanied

by a shift in trophic position (Hobson et al. 1994; Cherel and Hobson 2005; Radabaugh and

Peebles 2014).

One shortcoming of bulk stable isotope analysis is that temporal patterns observed in eye

lens $\delta^{13}C$ and $\delta^{15}N$ values could be due to movement and/or changes in diet, and it can be

difficult to determine which processes is/are responsible for temporal patterns. In order to

address this problem, stable isotope data can be combined with diet or artificial tag data (i.e.,

Vecchio and Peebles 2022) or compound specific isotope analysis can be performed in addition

to bulk analysis in order to refine or confirm the interpretation of results (Wallace 2019).

Another potential interpretation method is to infer what an isotopic life history (IHL) for a

consumer would look like if the consumer had remained stationary, only undergoing trophic

growth, and compare the stationary IHL to measured IHLs. One way to achieve this process is to

compare the IHL of a species that is known to be stationary throughout life to the IHLs of the

consumer of interest (Vecchio and Peebles 2020). Another method is to create a statistical model

of a stationary ILH by using the average relationship between $\delta^{13}C$ and $\delta^{15}N$ values and eye lens

diameter to model stationary trophic growth. Then, deviations from that model can be used to

infer movement (Vecchio and Peebles 2022).

Eye lens stable isotope studies seem to be particularly well-suited to documenting inter-

individual variation in diet and/or movement within a species (Hunsicker et al. 2010; Wallace et

al. 2014; Simpson et al. 2019; Xu et al. 2019; Curtis et al. 2020; Vecchio and Peebles 2022). In a

study that combined eye lens and muscle stable isotope analysis with stomach content analysis to

determine the feeding ecology of Commander Squid (*Berryteuthis magister*), it was noted that

the eye lens analysis indicated feeding variability that was not captured using more traditional

methods (Hunsicker et al. 2010). High inter-individual feed strategy variation was also noted in a

study featuring Humbolt Squid (*Dosidicus gigas*; Xu et al. 2019). In a study using fish, it was

found that variability within individual fish had no obvious, consistent trends that could be

attributed to environmental or temporal covariates, which suggests that the inter-individual

variation was behavioral rather than environmental (Curtis et al. 2020). The same study noted

that one species (lionfish; *Pterois* spp.) exhibited measurably less inter-individual variation than

the other (graysby; *Cephalopholis cruentata*), which suggests that eye lens stable isotopes may

be used as an indication of differences in behavioral plasticity between species. A study on

Atlantic Tarpon eye lens stable isotopes found Atlantic Tarpon had low inter-individual variation

in their early life histories and then demonstrated more individual variation once they moved to a

coastal environment around 10 years of age (Kurth et al. 2019). Documenting the inter-

individual variation of a species or life stage is useful for both ecology and fisheries management

(Wallace 2019) and could be an indication of which species or life stages may be more adaptable

to environmental changes (Hunsicker et al. 2010).

1.7. Objectives

The objectives of this dissertation were to: (1) create empirical shelf δ^{13}C and δ^{15}N

isoscapes of the Gulf of Mexico based on the muscle of two reef fish species [Red Snapper

(*Lutjanus campechanus*) and Yellowedge Grouper (*Epinephelus flavolimbatus*)], (2) use readily

available satellite data products to create a statistical model of the Gulf of Mexico isoscapes in

order to create a temporally dynamic product, (3) evaluate the overall temporal variability

predicted by the model by comparing seasonal and interannual differences between predicted

isoscapes, (4) use the empirical isoscapes and their models to infer which ecological processes are influential to spatial isotopic patterns, and (5) demonstrate how stable isotope eye lenses can be used in conjunction with isoscapes to infer movement histories in a Red Snapper. All the Gulf of Mexico isoscapes from section 1.4.3 either did not cover the entirety of the Gulf of Mexico continental shelf and/or did depict spatial isotopic patterns found in a reef-associated mesopredator fish species. The isoscapes in this dissertation were created using tissue from two reef-associated mesopredator fish species, and, because many exploited Gulf of Mexico fish species are reef-associated mesopredators, my isoscapes have potential to be useful for fisheries management. Most eye lens studies to date have primarily used eye lens stable isotopes to describe trophic patterns within and among individuals. Some studies have demonstrated that eye lens stable isotopes can also be used to infer movement but many of those studies have been limited by the spatial extent of isoscapes. Furthermore, methods for the interpretation of eye lens stable isotopes are still being developed and refined. The methods presented in this dissertation represent another step in the process of creating robust methods for the use of eye lens isotopes to infer movement histories.

It is my hope these products and techniques can be used in future ecological and fisheries applications. The modeled isoscapes were created in such a way that it can be easily used in a variety of studies by simply downloading satellite data products from a time period and location relevant to the study and applying them to the statistical models to predict $\delta^{13}C$ and $\delta^{15}N$ values in any location on the continental shelf of the Gulf of Mexico. The methods used in this dissertation for eye lens analysis can easily be applied to individuals of any species to determine the likelihood that they changed location over any particular time period.

1.8 Citations

Aberle, N., and Malzahn, A. M. 2007. Interspecific and nutrient-dependent variations in stable isotope fractionation: experimental studies simulating pelagic multitrophic systems. *Oecologia* 154(2): 291-303.

Aguilar, A., Giménez, J., Gómez–Campos, E., Cardona, L., and Borrell, A. 2014. δ^{15}N value does not reflect fasting in mysticetes. *PLoS One* 9(3): e92288.

Altabet, M. A. 1988. Variations in nitrogen isotopic composition between sinking and suspended particles: Implications for nitrogen cycling and particle transformation in the open ocean. *Deep Sea Research Part A. Oceanographic Research Papers* 35(4): 535-554.

Altabet, M. A. 2001. Nitrogen isotopic evidence for micronutrient control of fractional NO3− utilization in the equatorial Pacific. *Limnology and Oceanography* 46(2): 368-380.

Altabet, M. A., Pilskaln, C., Thunell, R., Pride, C., Sigman, D., Chavez, F., and Francois, R. 1999. The nitrogen isotope biogeochemistry of sinking particles from the margin of the Eastern North Pacific. *Deep Sea Research Part I: Oceanographic Research Papers* 46(4) 655-679.

Alt-Epping, U., Mil-Homens, M., Hebbeln, D., Abrantes, F., Schneider, R.R. 2007. Provenance of organic matter and nutrient conditions on a river- and upwelling influenced shelf: a case study from the Portuguese Margin. *Marine Geology* 243, 169–179.

Barnes, C., Jennings, S., and Barry, J. T. 2009. Environmental correlates of large-scale spatial variation in the $\delta^{13}C$ of marine animals. *Estuarine, Coastal and Shelf Science* 81(3): 368-374.

Bascompte, J., Melián, C. J., and Sala, E. 2005. Interaction strength combinations and the overfishing of a marine food web. *Proceedings of the National Academy of Sciences* 102(15): 5443-5447.

Bearhop, S., Adams, C. E., Waldron, S., Fuller, R. A., and MacLeod, H. 2004. Determining trophic niche width: a novel approach using stable isotope analysis. *Journal of Animal Ecology* 73(5): 1007-1012.

Bell-Tilcock, M., Jeffres, C. A., Rypel, A. L., Sommer, T. R., Katz, J. V., Whitman, G., and Johnson, R. C. 2021. Advancing diet reconstruction in fish eye lenses. *Methods in Ecology and Evolution* 12(3): 449-457.

Boecklen, W. J., Yarnes, C. T., Cook, B. A., and James, A. C. 2011. On the use of stable isotopes in trophic ecology. *Annual Review of Ecology, Evolution, and Systematics* 42: 411-440.

Bowen, G. J. 2010. Isoscapes: Spatial Pattern in Isotopic Biogeochemistry. *Annual Review of Earth and Planetary Sciences* 38(1): 161-187.

Bowen, G. J. and Revenaugh, J. 2003. Interpolating the isotopic composition of modern meteoric precipitation. *Water Resources Research* 39(10).

Bowes, R. E., Lafferty, M. H., and Thorp, J. H. 2014. Less means more: nutrient stress leads to higher δ^{15}N ratios in fish. *Freshwater Biology* 59(9): 1926-1931.

Bradley, C. J., Wallsgrove, N. J., Choy, C. A., Drazen, J. C., Hetherington, E. D., Hoen, D. K., and Popp, B. N. 2015. Trophic position estimates of marine teleosts using amino acid compound specific isotopic analysis. *Limnology and Oceanography: Methods* 13(9): 476-493.

Branch, T. A., Watson, R., Fulton, E. A., Jennings, S., McGilliard, C. R., Pablico, G. T., ... & Tracey, S. R. 2010. The trophic fingerprint of marine fisheries. *Nature* 468(7322): 431-435.

Brandes, J. A., Devol, A. H., Yoshinari, T., Jayakumar, D. A., and Naqvi, S. W. A. 1998. Isotopic composition of nitrate in the central Arabian Sea and eastern tropical North Pacific: A tracer for mixing and nitrogen cycles. *Limnology and Oceanography* 43(7): 1680-1689.

Buchheister, A., and Latour, R. J. 2010. Turnover and fractionation of carbon and nitrogen stable isotopes in tissues of a migratory coastal predator, summer flounder (*Paralichthys dentatus*). *Canadian Journal of Fisheries and Aquatic Sciences* 67(3): 445-461.

Cabana, G. and J. B. Rasmussen. 1996. Comparison of aquatic food chains using nitrogen isotopes. *Proceedings of the National Academy of Sciences* 93(20): 10844.

Campana, S. E. 1999. Chemistry and composition of fish otoliths: pathways, mechanisms and applications. *Marine Ecology Progress Series* 188: 263-297.

Campana, S. E., and Neilson, J. D. 1985. Microstructure of fish otoliths. *Canadian Journal of Fisheries and Aquatic Sciences* 42(5): 1014-1032.

Canseco, J. A., Niklitschek, E. J., and Harrod, C. 2021. Variability in $\delta^{13}C$ and $\delta^{15}N$ trophic discrimination factors for teleost fishes: a meta-analysis of temperature and dietary effects. *Reviews in Fish Biology and Fisheries* 1-17.

Capone, D. G., Bronk, D. A., Mulholland, M. R., and Carpenter, E. J. (Eds.). 2008. Nitrogen in the marine environment. Elsevier.

Carpenter, E.J., Harvey, H.R., Fry, B., Capone, D.G., 1997. Biogeochemical tracers of the marine cyanobacterium Trichodesmium. *Deep Sea Research Part A: Oceanographic Research Papers* 44: 27–38.

Castellini, M. A., and Rea, L. D. 1992. The biochemistry of natural fasting at its limits. *Experientia* 48(6): 575-582.

Caut, S., Angulo, E., and Courchamp, F. 2008. Discrimination factors ($\Delta^{15}N$ and $\Delta^{13}C$) in an omnivorous consumer: effect of diet isotopic ratio. *Functional Ecology* 22(2): 255-263.

Caut, S., Angulo, E. and Courchamp, F. 2009. Variation in discrimination factors (Δ^{15}N and Δ^{13}C): the effect of diet isotopic values and applications for diet reconstruction. *Journal of Applied Ecology* 46: 443-453. doi:10.1111/j.1365-2664.2009.01620.x

Ceia, F. R., Cherel, Y., Paiva, V. H., and Ramos, J. A. 2018. Stable isotope dynamics (δ^{13}C and δ^{15}N) in neritic and oceanic waters of the North Atlantic inferred from GPS-tracked Cory's shearwaters. *Frontiers in Marine Science* 5: 377.

Cherel, Y. and Hobson, K. A. 2005. Stable isotopes, beaks and predators: a new tool to study the trophic ecology of cephalopods, including giant and colossal squids. *Proceedings of the Royal Society B: Biological Sciences* 272(1572): 1601-1607.

Cherel, Y. and Hobson, K. A. 2007. Geographical variation in carbon stable isotope signatures of marine predators: a tool to investigate their foraging areas in the Southern Ocean. *Marine Ecology Progress Series* 329: 281-287.

Cherel, Y., Robin, J. P., and Maho, Y. L. 1988. Physiology and biochemistry of long-term fasting in birds. *Canadian Journal of Zoology* 66(1): 159-166.

Chikaraishi, Y., Kashiyama, Y., Ogawa, N. O., Kitazato, H., and Ohkouchi, N. 2007. Metabolic control of nitrogen isotope composition of amino acids in macroalgae and gastropods: implications for aquatic food web studies. *Marine Ecology Progress Series* 342: 85-90.

Childs, C. R. 2004. A Spatial and Temporal Assessment of Factors Controlling Denitrification in

Coastal and Continental Shelf Sediments of the Gulf of Mexico. (Doctoral dissertation, The

Florida State University) Retrieved from http://purl.flvc.org/fsu/fd/FSU_migr_etd-3816

Childs, C. R., Rabalais, N. N., Turner, R. E., and Proctor, L. M. 2002. Sediment denitrification in

the Gulf of Mexico zone of hypoxia. *Marine Ecology Progress Series* 240: 285-290.

Cifuentes, L. A. 1987. Sources and biogeochemistry of organic matter in the Delaware estuary

(Doctoral dissertation, University of Delaware).

Clementz, M. T. and Koch, P. L. 2001. Differentiating aquatic mammal habitat and foraging

ecology with stable isotopes in tooth enamel. *Oecologia* 129(3): 461-472.

Cline, J. D., and Kaplan, I. R. 1975. Isotopic fractionation of dissolved nitrate during

denitrification in the eastern tropical North Pacific Ocean. *Marine Chemistry* 3(4): 271-299.

Cloern, J. E. and Jassby, A. D. 2010. Patterns and scales of phytoplankton variability in

estuarine–coastal ecosystems. *Estuaries and Coasts* 33(2): 230-241.

Cooper, L.W., DeNiro, M.J. 1989. Stable carbon isotope variability in the seagrass *Posidonia

oceanica*: evidence for light intensity effects. *Marine Ecology Progress Series* 50: 225–229.

Cowen, R. K., Lwiza, K. M., Sponaugle, S., Paris, C. B., and Olson, D. B. 2000. Connectivity of marine populations: open or closed? *Science* 287(5454): 857-859.

Cuddy, M. R. 2018. Patterns in iscoscapes and N: P stoichioscapes of the dominant seagrasses (*Halodule wrightii* and *Thalassia testudinum*) in the western Gulf of Mexico. (Doctoral dissertation). Retrieved from: https://repositories.lib.utexas.edu/handle/2152/65703

Curtis, J. S., Albins, M. A., Peebles, E. B., and Stallings, C. D. 2020. Stable isotope analysis of eye lenses from invasive lionfish yields record of resource use. *Marine Ecology Progress Series* 637: 181-194.

Dagg, M. J. and Breed, G. A. 2003. Biological effects of Mississippi River nitrogen on the northern Gulf of Mexico—a review and synthesis. *Journal of Marine Systems* 43(3-4): 133-152.

Dahm, R., Schonthaler, H. B., Soehn, A. S., Van Marle, J., and Vrensen, G. F. 2007. Development and adult morphology of the eye lens in the zebrafish. *Experimental Eye Research* 85(1): 74-89.

Dansgaard W. 1954. The O18-abundance in fresh water. *Geochimica et Cosmochimica Acta* 6:241–60.

Deegan, L. A. 1993. Nutrient and energy transport between estuaries and coastal marine ecosystems by fish migration. *Canadian Journal of Fisheries and Aquatic Sciences* 50: 74-79.

DeNiro, M. J. and Epstein, S. 1978. Influence of diet on the distribution of carbon isotopes in animals. *Geochimica et Cosmochimica Acta* 42(5): 495-506.

Diamond, S.L., Campbell, M., Olson, D., Panto, L., Wang, Y., Zeplin, J. and Qualia, S. 2007. M overs and stayers: Individual variability in site fidelity and movements of red snapper off Texas. In: Red Snapper Ecology and Fisheries in the U.S. Gulf of Mexico (W. F. Patterson, J. H. Cowan, Jr., G. R. Fitzhugh, and D. L. Nieland, Eds.). *American Fisheries Sciences Symposium*. 60: 163–188.

Dingle, H. and Drake, V.A. 2007. What is migration? *BioScience* 57(2):113-121. doi:10.1641/B570206.

Doi, H., Kikuchi, E., Shikano, S., and Takagi, S. 2010. Differences in nitrogen and carbon stable isotopes between planktonic and benthic microalgae. *Limnology* 11(2): 185-192.

Dutton, A., Wilkinson, B. H., Welker, J. M., Bowen, G. J., and Lohmann, K. C. 2005. Spatial distribution and seasonal variation in $^{18}O/^{16}O$ of modern precipitation and river water across the conterminous United States. *Hydrological Processes: An International Journal* 19: 4121–46.

Eppley, R. W. 1972. Temperature and phytoplankton growth in the sea. *Fishery Bulletin* 70(4): 1063-1085.

Epstein, S., Buchsbaum, R., Lowenstam, H. A., and Urey, H. C. 1953. Revised carbonate-water isotopic temperature scale. *Geological Society of America Bulletin* 64(11) 1315-1326.

Fisk, A. T., Hobson, K. A., and Norstrom, R. J. 2001. Influence of chemical and biological factors on trophic transfer of persistent organic pollutants in the Northwater Polynya marine food web. *Environmental Science & Technology* 35(4): 732-738.

Fogel, M. L. and Cifuentes, L. A. 1993. Isotope fractionation during primary production. In Organic geochemistry (pp. 73-98). Springer, Boston, MA.

France, R. L. 1995. Carbon-13 enrichment in benthic compared to planktonic algae: foodweb implications. *Marine Ecology Progress Series* 124: 307-312.

Fry, B. 1981. Natural stable carbon isotope tag traces Texas shrimp migrations. *Fishery Bulletin* 79 (2): 337–345.

Fry, B., 1988. Food web structure on Georges Bank from stable C, N, and S isotopic compositions. *Limnology and Oceanography* 33:1182–1190.

Fry, B. 2006. Stable isotope ecology. New York, MY, Springer Science+Business Media.

Fry, B. and Arnold, C. 1982. Rapid $^{13}C/^{12}C$ turnover during growth of brown shrimp (*Penaeus aztecus*). *Oecologia* 54(2): 200-204.

Fry, B. and Ewel, K. C. 2003. Using stable isotopes in mangrove fisheries research—a review and outlook. *Isotopes in Environmental and Health Studies* 39(3): 191-196.

Fry, B., and E. B. Sherr. 1984. $\delta^{13}C$ measurements as indicators of carbon flow in marine and freshwater ecosystems. *Contributions in Marine Science* 27: 13–47.

Gannes, L. Z., O'Brien, D. M., and Del Rio, C. M. 1997. Stable isotopes in animal ecology: assumptions, caveats, and a call for more laboratory experiments. *Ecology* 78(4): 1271-1276.

Gardner, W. S., Briones, E. E., Kaegi, E. C., and Rowe, G. T. 1993. Ammonium excretion by benthic invertebrates and sediment-water nitrogen flux in the Gulf of Mexico near the Mississippi River outflow. *Estuaries* 16(4): 799-808.

Gearing, J. N., Gearing, P. J., Rudnick, D. T., Requejo, A. G., and Hutchins, M. J. 1984. Isotopic variability of organic carbon in a phytoplankton-based, temperate estuary. *Geochimica et Cosmochimica Acta* 48(5): 1089-1098.

Germain, L. R., Koch, P. L., Harvey, J., and McCarthy, M. D. 2013. Nitrogen isotope fractionation in amino acids from harbor seals: implications for compound-specific trophic position calculations. *Marine Ecology Progress Series* 482: 265-277.

Goericke, R., and B. Fry. 1994. Variations of marine plankton $\delta^{13}C$ with latitude, temperature, and dissolved CO^2 in the world ocean. *Global Biogeochemical Cycles* 8: 85–90.

Graham, B.S., Koch, P.L., Newsome, S.D., McMahon, K.W., Aurioles, D., 2010. Using isoscapes to trace the movements and foraging behavior of top predators in oceanic ecosystems. In: West, J.B., Bowen, G.J., Dawson, T.E., Tu, K.P. (Eds.), Isoscapes: Understanding Movement, Pattern, and Process on Earth through Isotope Mapping. Springer, New York, pp. 299–318.

Grainger, R. M., Henry, J. J., Saha, M. S., and Servetnick, M. 1992. Recent progress on the mechanisms of embryonic lens formation. *Eye* 6(2): 117-122.

Granger, J., Sigman, D. M., Lehmann, M. F., and Tortell, P. D. 2008. Nitrogen and oxygen isotope fractionation during dissimilatory nitrate reduction by denitrifying bacteria. *Limnology and Oceanography* 53(6): 2533-2545.

Granneman, J. E. 2018. Evaluation of trace-metal and isotopic records as techniques for tracking lifetime movement patterns in fishes. University of South Florida. Graduate Theses and Dissertations. Retrieved from: https://scholarcommons.usf.edu/etd/7675

Grippo, M. A., Fleeger, J. W., Dubois, S. F., and Condrey, R. 2011. Spatial variation in basal resources supporting benthic food webs revealed for the inner continental shelf. *Limnology and Oceanography* 56(3): 841-856.

Haines, E. B. and Montague, C. L. 1979. Food sources of estuarine invertebrates analyzed using $^{13}C/^{12}C$ ratios. *Ecology* 60(1): 48-56.

Hannides, C. C. S., Popp, B. N., Landry, M. R., and Graham, B. S. 2009. Quantitative determination of zooplankton trophic position using amino acid-specific stable nitrogen isotope analysis. *Limnology and Oceanography* 54: 50-61.

Hansson, S., Hobbie, J.E., Elmgren, R., Larsson, U., Fry, B., Johansson, S., 1997. The stable nitrogen isotope ratio as a marker of food-web interactions and fish migration. *Ecology* 78: 2249–2257.

Hesslein, R. H., Hallard, K. A., and Ramlal, P. 1993. Replacement of sulfur, carbon, and nitrogen in tissue of growing broad whitefish (*Coregonus nasus*) in response to a change in diet traced by $\delta^{34}S$, $\delta^{13}C$, and $\delta^{15}N$. *Canadian Journal of Fisheries and Aquatic Sciences* 50(10): 2071-2076.

Hinga, K. R., Arthur, M. A., Pilson, M. E., and Whitaker, D. 1994. Carbon isotope fractionation by marine phytoplankton in culture: the effects of CO2 concentration, pH, temperature, and species. *Global Biogeochemical Cycles* 8(1): 91-102.

Hobson, K. A. 1999. Tracing origins and migration of wildlife using stable isotopes:a review. *Oecologia* 120: 314−326.

Hobson, K. A. and Clark, R. G. 1992. Assessing avian diets using stable isotopes I: turnover of ^{13}C in tissues. *The Condor* 94(1): 181-188.

Hobson, K. A., Piatt, J. F., and Pitocchelli, J. 1994. Using stable isotopes to determine seabird trophic relationships. *Journal of Animal Ecology* 786-798.

Hobson, K. A. and Norris, D. R. 2008. Animal migration: a context for using new techniques and approaches. *Terrestrial Ecology* 2: 1-19.

Hobson, K.A., Barnett-Johnson, R., and Cerling, T., 2010. Using isoscapes to track animal migration. In: West, J.B., Bowen, G.J., Dawson, T.E., Tu, K.P. (Eds.), Isoscapes: Understanding Movement, Pattern, and Process on Earth through Isotope Mapping. Springer, New York, pp. 273–298.

Hobson, K. A., Norris, D. R., Kardynal, K. J., and Yohannes, E. 2019. Animal migration: a context for using new techniques and approaches. In Tracking animal migration with stable isotopes (pp. 1-23). Academic Press, London.

Hofmann, M., Wolf-Gladrow, D. A., Takahashi, T., Sutherland, S. C., Six, K. D., and MaierReimer, E. 2000. Stable carbon isotope distribution of particulate organic matter in the ocean: a model study. *Marine Chemist*ry 72: 131–150.

Horwitz, J. 2003. Alpha-crystallin. *Experimental Eye Research* 76(2): 145-153.

Hunsicker, M. E., Essington, T. E., Aydin, K. Y., and Ishida, B. 2010. Predatory role of the commander squid Berryteuthis magister in the eastern Bering Sea: insights from stable isotopes and food habits. *Marine Ecology Progress Series* 415: 91-108.

Hussey, N. E., MacNeil, M. A., McMeans, B. C., Olin, J. A., Dudley, S. F., Cliff, G., Wintner, S. P., Fennessy, S. T. and Fisk, A. T. 2014. Rescaling the trophic structure of marine food webs. *Ecology Letters* 17(2): 239-250.

Hyslop, E. J. 1980. Stomach contents analysis-a review of methods and their application. *Journal of Fish Biology* 17: 411-429.

Karpouzi, V. S. and Stergiou, K. I. 2003. The relationships between mouth size and shape and body length for 18 species of marine fishes and their trophic implications. *Journal of Fish Biology* 62: 1353-1365.

Kell, L. T., Dickey-Collas, M., Hintzen, N. T., Nash, R. D., Pilling, G. M., and Roel, B. A. 2009. Lumpers or splitters? Evaluating recovery and management plans for metapopulations of herring. *ICES Journal of Marine Science* 66(8): 1776-1783.

Kendall, C. 1998. Tracing nitrogen sources and cycling in catchments. In <u>Isotope tracers in catchment hydrology</u> pp. 519-576. Elsevier, Amsterdam.

Kendall, C., Silva, S.R., Kelly, V.J., 2001. Carbon and nitrogen isotopic compositions of particulate organic matter in four large river systems across the United States. *Hydrological Processes* 15: 1301–1346.

Killingley, J. S. 1980. Migrations of California gray whales tracked by oxygen-18 variations in their epizoic barnacles. *Science* 207(4432): 759-760.

Killingley, J. S. and Lutcavage, M. 1983. Loggerhead turtle movements reconstructed from ^{18}O and ^{13}C profiles from commensal barnacle shells. *Estuarine, Coastal and Shelf Science* 16(3): 345-349.

Kline, Jr, T. C. 1999. Temporal and spatial variability of ^{13}C/^{12}C and ^{15}N/^{14}N in pelagic biota of Prince William Sound, Alaska. *Canadian Journal of Fisheries and Aquatic Sciences* 56(S1): 94-117.

Kootker, L. M., van Lanen, R. J., Kars, H., and Davies, G. R. 2016. Strontium isoscapes in The Netherlands. Spatial variations in ^{87}Sr/^{86}Sr as a proxy for palaeomobility. *Journal of Archaeological Science: Reports* 6: 1-13.

Kürten, B., Frutos, I., Struck, U., Painting, S. J., Polunin, N. V., and Middelburg, J. J. 2013. Trophodynamics and functional feeding groups of North Sea fauna: a combined stable isotope and fatty acid approach. *Biogeochemistry* 113(1-3): 189-212.

Kurth, B. Neal. 2016. Trophic Ecology and Habitat Use of Atlantic Tarpon (*Megalops atlanticus*). Masters Thesis. University of South Florida. Retrieved from: https://scholarcommons.usf.edu/etd/6531

Laws, E.A., Popp, B.N., Bidigare, R.R., Kennicutt, M.C., Macko, S.A.,1995. Dependence of phytoplankton carbon isotopic composition on growth rate and $[CO_2]aq$: Theoretical considerations and experimental results. *Geochimica et Cosmochimica Acta* 59: 1131–1138.

Lee, C., Wakeham, S., and Arnosti, C. 2004. Particulate organic matter in the sea: the composition conundrum. *AMBIO: A Journal of the Human Environment* 33(8): 565-575.

Lindeman, R. L. 1942. The trophic-dynamic aspect of ecology. *Ecology* 23(4): 399-417.

Liu, K. K., Kao, S. J., Hu, H. C., Chou, W. C., Hung, G. W., and Tseng, C. M. 2007. Carbon isotopic composition of suspended and sinking particulate organic matter in the northern South China Sea—from production to deposition. *Deep Sea Research Part II: Topical Studies in Oceanography* 54: 1504–1527.

Lloyd, J. and Farquhar, G. D. 1994. $\delta^{13}C$ discrimination during CO_2 assimilation by the terrestrial biosphere. *Oecologia* 99:201–15.

Lohrenz, S. E., Fahnenstiel, G. L., Redalje, D. G., Lang, G. A., Chen, X., and Dagg, M. J. 1997. Variations in primary production of northern Gulf of Mexico continental shelf waters linked to nutrient inputs from the Mississippi River. *Marine Ecology Progress Series* 155: 45-54.

Magozzi, S., Yool, A., Vander Zanden, H. B., Wunder, M. B., and Trueman, C. N. 2017. Using ocean models to predict spatial and temporal variation in marine carbon isotopes. *Ecosphere* 8(5): e01763.

Mariotti, A., Germon, J.C., Leclerc, A., Catroux, G. and Létolle, R. 1982. Experimental determination of kinetic isotope fractionation of nitrogen isotopes during denitrification, in: Schmidt, H.-L., Förstel, H., Heinzinger, K. (Eds.), *Stable Isotopes*, Proceedings of the 4th International Conference. Elsevier, Jülich, pp. 459- 464.

Mariotti, A., Lancelot, C., and Billen, G. 1984. Natural isotopic composition of nitrogen as a tracer of origin for suspended organic matter in the Scheldt estuary. *Geochimica et Cosmochimica Acta* 48(3): 549-555.

McIntyre, P. B., and Flecker, A. S. 2006. Rapid turnover of tissue nitrogen of primary consumers in tropical freshwaters. *Oecologia* 148(1): 12-21.

McMahon, K. W., and McCarthy, M. D. 2016. Embracing variability in amino acid $\delta^{15}N$ fractionation: mechanisms, implications, and applications for trophic ecology. *Ecosphere* 7(12): e01511.

McMahon, K. W., Hamady, L. L., and Thorrold, S. R. 2013a. Ocean ecogeochemitry – a review. *Oceanography and Marine Biology: An Annual Review* 51: 327-374.

McMahon, K. W., Hamady, L. L., and Thorrold, S. R. 2013a. A review of ecogeochemistry approaches to estimating movements of marine animals. *Limnology and Oceanography* 58: 697-714.

Meath, B., Peebles, E. B., Seibel, B. A., and Judkins, H. 2019. Stable isotopes in the eye lenses of *Doryteuthis plei* (Blainville 1823): Exploring natal origins and migratory patterns in the eastern Gulf of Mexico. *Continental Shelf Research* 174: 76-84.

Menge, B. A., and Sutherland, J. P. 1976. Species diversity gradients: synthesis of the roles of predation, competition, and temporal heterogeneity. *The American Naturalist* 110(973): 351-369.

Minagawa, M. and E. Wada. 1984. Stepwise enrichment of δ^{15}N along food chains: Further evidence and the relation between δ^{15}N and animal age. *Geochimica et Cosmochimica Acta* 48(5): 1135-1140.

Moncreiff, C. A., and Sullivan, M. J. 2001. Trophic importance of epiphytic algae in subtropical seagrass beds: evidence from multiple stable isotope analyses. *Marine Ecology Progress Series* 215: 93-106.

Montoya, J.P. 2007. Natural abundance of $\delta^{15}N$ in marine planktonic ecosystems. In: Michener, R., Lajtha, K. (Eds.), Stable Isotopes in Ecology and Environmental Science, second ed. Blackwell Publishing, Malden, Massachusetts, pp. 176–201.

Montoya, J.P., Carpenter, E.J., and Capone, D.G. 2002. Nitrogen fixation and nitrogen isotope abundances in zooplankton of the oligotrophic North Atlantic. *Limnology and Oceanography* 47: 1617–1628.

Mook, W. G., Bommerson, J. C., and Staverman, W. H. 1974. Carbon isotope fractionation between dissolved bicarbonate and gaseous carbon dioxide. *Earth and Planetary Science Letters* 22(2): 169-176.

Muscatine, L., Porter, J.W., and Kaplan, I.R., 1989. Resource partitioning by reef corals as determined from stable isotope composition. 1. $\delta^{13}C$ of zooxanthellae and animal tissue vs depth. *Marine Biology* 100: 185–193.

Myers, R. A., Baum, J. K., Shepherd, T. D., Powers, S. P., and Peterson, C. H. 2007. Cascading effects of the loss of apex predatory sharks from a coastal ocean. *Science* 315(5820): 1846-1850.

Nelson, J., Chanton, J., Coleman, F., and Koenig, C. 2011. Patterns of stable carbon isotope turnover in gag, Mycteroperca microlepis, an economically important marine piscivore determined with a non-lethal surgical biopsy procedure. *Environmental Biology of Fishes* 90(3): 243-252.

Nerot, C., Lorrain, A., Grall, J., Gillikin, D.P., Munaron, J.M., Le Bris, H., and Paulet, Y.M., 2012. Stable isotope variations in benthic filter feeders across a large depth gradient on the continental shelf. *Estuarine, Coastal and Shelf Science* 96: 228–235.

Nicol, J. A. C. 1989. <u>The eyes of fishes</u>. Oxford University Press, Oxford. 308pp.

Oelbermann, K., and Scheu, S. 2002. Stable isotope enrichment (δ^{15}N and δ^{13}C) in a generalist predator (*Pardosa lugubris*, Araneae: Lycosidae): effects of prey quality. *Oecologia* 130(3): 337-344.

Olson, R.J., Popp, B.N., Graham, B.S., Lopez-Ibarra, G.A., Galvan-Magana, F., LennertCody, C.E., Bocanegra-Castillo, N., Wallsgrove, N.J., Gier, E., Alatorre-Ramirez, V., Balance, L.T., Fry, B. 2010. Food-web inferences of stable isotope spatial patterns in copepods and yellowfin tuna in the pelagic eastern Pacific Ocean. *Progress in Oceanography* 86: 124–138.

Onthank, K. L. 2013. Exploring the life histories of Cephalopods using stable isotope analysis of an archival tissue. [Order No. 3587152] PhD Dissertation, School of Biological Sciences, Washington State University. Retrieved from: https://www.proquest.com/docview/1425317087?pq-origsite=gscholar&fromopenview=true

Parry, M. 2003. The trophic ecology of two Ommastrephid squid species, *Ommastrephes bartramii* and *Shenotheuthis oualaniensis*, in the North Pacific sub-tropical gyre. PhD

Dissertation, Oceanography (Marine Biology), University of Hawaii-Manoa. Retrieved from:

https://scholarspace.manoa.hawaii.edu/handle/10125/3068

Patterson, W. F. 2007. A review of movement in Gulf of Mexico red snapper: implications for population structure pp. 221-235. In *Red snapper ecology and fisheries in the US Gulf of Mexico. American Fisheries Society, Symposium* (Vol. 60).

Pauly, D., Christensen, V., Dalsgaard, J., Froese, R., and Torres, F. 1998. Fishing down marine food webs. *Science* 279(5352): 860-863.

Peterson, B. J. and Fry, B. 1987. Stable isotopes in ecosystem studies. *Annual Review of Ecology and Systematics* 18(1): 293-320.

Pinnegar, J. K. and N. V. C. Polunin. 1999. Differential fractionation of delta C-13 and delta N-15 among fish tissues: implications for the study of trophic interactions. *Functional Ecology* 13(2): 225-231.

Popp, B. N., Laws, E. A., Bidigare, R. R., Dore, J. E., Hanson, K. L., and Wakeham, S. G. 1998. Effect of phytoplankton cell geometry on carbon isotopic fractionation. *Geochimica et Cosmochimica Acta* 62(1): 69-77.

Post, D. M. 2002. Using stable isotopes to estimate trophic position: Models, methods, and assumptions. *Ecology* 83(3): 703-718.

Quillfeldt, P., Ekschmitt, K., Brickle, P., McGill, R. A., Wolters, V., Dehnhard, N., and Masello, J. F. 2015. Variability of higher trophic level stable isotope data in space and time – a case study in a marine ecosystem. *Rapid Communications in Mass Spectrometry* 29(7): 667-674.

Quaeck-Davies, K., Bendall, V. A., MacKenzie, K. M., Hetherington, S., Newton, J., and Trueman, C. N. 2018. Teleost and elasmobranch eye lenses as a target for life-history stable isotope analyses. *PeerJ* 6: e4883.

Radabaugh, K. R., Hollander, D. J., and Peebles, E. B. 2013. Seasonal δ^{13}C and δ^{15}N isoscapes of fish populations along a continental shelf trophic gradient. *Continental Shelf Research* 68: 112-122.

Radabaugh, K. R. and Peebles, E. B. 2014. Multiple regression models of δ^{13}C and δ^{15}N for fish populations in the eastern Gulf of Mexico. *Continental Shelf Research* 84: 158-168.

Radabaugh, K. R., Malkin, E. M., Hollander, D. J., and Peebles, E. B. 2014. Evidence for light-environment control of carbon isotope fractionation by benthic microalgal communities. *Marine Ecology Progress Series* 495: 77-90.

Rau, G. H., Riebesell, U., and Wolf-Gladrow, D. 1996. A model of photosynthetic ^{13}C fractionation by marine phytoplankton based on diffusive molecular CO_2 uptake. *Marine Ecology Progress Series* 133: 275-285.

Rau, G. H., Riebesell, U., and Wolf-Gladrow, D. 1997. CO_2aq-dependent photosynthetic ^{13}C fractionation in the ocean: A model versus measurements. *Global Biogeochemical Cycles* 11(2): 267-278.

Rieutord, M. 1999. <u>Physiologie animale, vol 2.</u> Les grandes fonctions. Masson, Paris.

Robbins, C. T., Felicetti, L. A., and Sponheimer, M. 2005. The effect of dietary protein quality on nitrogen isotope discrimination in mammals and birds. *Oecologia* 144(4): 534-540.

Rooker, J. R., Stunz, G. W., Holt, S. A., and Minello, T. J. 2010. Population connectivity of red drum in the northern Gulf of Mexico. *Marine Ecology Progress Series* 407: 187-196.

Rooney, N. and McCann, K. S. 2012. Integrating food web diversity, structure and stability. *Trends in Ecology and Evolution* 27(1): 40-46.

Rooney, N., McCann, K., Gellner, G., and Moore, J. C. 2006. Structural asymmetry and the stability of diverse food webs. *Nature* 442(7100): 265-269.

Schloesser, R. W., Rooker, J. R., Louchuoarn, P., Neilson, J. D., and Secord, D. H. 2009. Interdecadal variation in seawater δ^{13}C and δ^{18}O recorded in fish otoliths. *Limnology and Oceanography* 54(5): 1665-1668.

Schofield, G., Hobson, V. J., Fossette, S., Lilley, M. K., Katselidis, K. A., and Hays, G. C. 2010. Biodiversity Research: fidelity to foraging sites, consistency of migration routes and habitat modulation of home range by sea turtles. *Diversity and Distributions* 16(5): 840-853.

Scrimgeour, C. M., Gordon, S. C., Handley, L. L., and Woodford, J. A. T. 1995. Trophic levels and anomalous $\delta^{15}N$ of insects on raspberry (*Rubus idaeus L.*). *Isotopes in Environmental and Health Studies* 31(1): 107-115.

Sharp, Z. 2017. Principles of Stable Isotope Geochemistry, 2nd Edition. doi: https://doi.org/10.25844/h9q1-0p82

Shepard, K. E., Patterson, W. F., DeVries, D. A., and Ortiz, M. 2010. Contemporary versus historical estimates of king mackerel (*Scomberomorus cavalla*) age and growth in the US Atlantic Ocean and Gulf of Mexico. *Bulletin of Marine Science* 86(3): 515-532.

Sigman, D. M. and Fripiat, F. 2019. Nitrogen isotopes in the ocean. Steele JH, Turekian KK, Thorpe SA (eds) Encyclopedia of ocean sciences 1, Academic, London, 263-278.

Simpson, S. J., Sims, D. W., and Trueman, C. N. 2019. Ontogenetic trends in resource partitioning and trophic geography of sympatric skates (Rajidae) inferred from stable isotope composition across eye lenses. *Marine Ecology Progress Series* 624: 103-116.

Sluis, M. Z., Barnett, B. K., Patterson, W. F., III, Cowan, J. H., Jr. and Shiller, A. M. 2012. Discrimination of Juvenile Red Snapper Otolith Chemical Signatures from Gulf of Mexico Nursery Regions. *Marine and Coastal Fisheries* 4: 587-598. doi:10.1080/19425120.2012.703163

Sluis, M. Z., Barnett, B. K., Patterson, W. F., III, Cowan, J. H., Jr. and Shiller, A. M. 2015. Application of Otolith Chemical Signatures to Estimate Population Connectivity of Red Snapper in the Western Gulf of Mexico. *Marine and Coastal Fisheries* 7: 483-496. doi:10.1080/19425120.2015.1088492

Smith, D. C., Simon, M., Alldredge, A. L., and Azam, F. 1992. Intense hydrolytic enzyme activity on marine aggregates and implications for rapid particle dissolution. *Nature* 359(6391): 139-142.

Tamelander, T., Søreide, J. E., Hop, H., and Carroll, M. L. 2006. Fractionation of stable isotopes in the Arctic marine copepod Calanus glacialis: Effects on the isotopic composition of marine particulate organic matter. *Journal of Experimental Marine Biology and Ecology* 333(2): 231-240.

Thompson, R. M., Hemberg, M., Starzomski, B. M., and Shurin, J. B. 2007. Trophic levels and trophic tangles: the prevalence of omnivory in real food webs. *Ecology* 88(3): 612-617

Tieszen, L. L., Boutton, T. W., Tesdahl, K. G., and Slade, N. A. 1983. Fractionation and turnover of stable carbon isotopes in animal tissues: implications for $\delta^{13}C$ analysis of diet. *Oecologia* 57(1-2): 32-37.

Trochine, C., Villanueva, V. D., Balseiro, E., and Modenutti, B. 2019. Nutritional stress by means of high C: N ratios in the diet and starvation affects nitrogen isotope ratios and trophic fractionation of omnivorous copepods. *Oecologia* 190(3): 547-557.

Trueman, C. N., MacKenzie, K. M., and Palmer, M. R. 2012. Identifying migrations in marine fishes through stable-isotope analysis. *Journal of Fish Biology* 81(2): 826-847.

Tzadik, O. E., Curtis, J. S., Granneman, J. E., Kurth, B. N., Pusack, T. J., Wallace, A. A., ... and Stallings, C. D. 2017. Chemical archives in fishes beyond otoliths: A review on the use of other body parts as chronological recorders of microchemical constituents for expanding interpretations of environmental, ecological, and life-history changes. *Limnology and Oceanography: Methods* 15(3): 238-263.

Vanderklift, M. A., and Ponsard, S. 2003. Sources of variation in consumer-diet δ 15 N enrichment: a meta-analysis. *Oecologia* 136(2): 169-182.

Vander Zanden, M. J. and Rasmussen, J. B. 1996. A trophic position model of pelagic food webs: impact on contaminant bioaccumulation in lake trout. *Ecological Monographs* 66(4): 451-477.

Vander Zanden, M. J. and J. B. Rasmussen. 1999. Primary consumer $\delta^{15}N$ and $\delta^{13}C$ and the trophic position of aquatic consumers. *Ecology* 80: 1395–1404

Vander Zanden, M.J. and Rasmussen, J.B. 2001. Variation in $\delta^{15}N$ and $\delta^{13}C$ trophic fractionation: implications for aquatic food web studies. *Limnology and Oceanography* 46: 2061–2066.

Vander Zanden M. J. and Vadeboncoeur, Y. 2002. Fishes as integrators of benthic and pelagic food webs in lakes. *Ecology* 83(8):2152-2161.

Vander Zanden, M. J., Shuter, B. J., Lester, N., and Rasmussen, J. B. 1999a. Patterns of food chain length in lakes: a stable isotope study. *The American Naturalist* 154(4): 406-416.

Vander Zanden, M. J., Casselman, J. M., and Rasmussen, J. B. 1999b. Stable isotope evidence for the food web consequences of species invasions in lakes. *Nature* 401(6752): 464-467.

Vander Zanden, M. J., Clayton, M. K., Moody, E. K., Solomon, C. T., and Weidel, B. C. 2015. Stable isotope turnover and half-life in animal tissues: a literature synthesis. *PloS One* 10(1): e0116182.

Vecchio, J. L., and Peebles, E. B. 2020. Spawning origins and ontogenetic movements for demersal fishes: An approach using eye-lens stable isotopes. *Estuarine, Coastal and Shelf Science* 246: 107047.

Vecchio, J. L. and Peebles, E. B. 2022. Lifetime-scale ontogenetic movement and diets of red grouper inferred using a combination of instantaneous and archival methods. *Environmental Biology of Fishes* 1-20.

Vecchio, J. L., Ostroff, J. L., and Peebles, E. B. 2021. Isotopic characterization of lifetime movement by two demersal fishes from the northeastern Gulf of Mexico. *Marine Ecology Progress Series* 657: 161-172.

Vihtelic, T. S. 2008. Teleost lens development and degeneration. *International Review of Cell and Molecular Biology* 269: 341-373.

Wallace, A. A. 2019. Reconstructing Geographic and Trophic Histories of Fish Using Bulk and Compound-Specific Stable Isotopes from Eye Lenses. University of South Florida. Graduate Theses and Dissertations. Retrieved from https://www.proquest.com/dissertations-theses/reconstructing-geographic-trophic-histories-fish/docview/2343285720/se-2?accountid=14745

Wallace, A. A., Hollander, D. J., and Peebles, E. B. 2014. Stable isotopes in fish eye lenses as potential recorders of trophic and geographic history. *PloS One* 9(10): e108935.

West, J. B., Bowen, G. J., Dawson, T. E., and Tu, K. P. (eds) (2010). <u>Isoscapes: Understanding movement, pattern, and process on Earth through isotope mapping</u>. New York, NY, Springer.

Williams, P. M., and Gordon, L. I. 1970. Carbon-13: carbon-12 ratios in dissolved and particulate organic matter in the sea. In *Deep Sea Research and Oceanographic Abstracts* 17(1): 19-27. Elsevier.

Wride, M. A. 2011. Lens fibre cell differentiation and organelle loss: many paths lead to clarity. *Philosophical Transactions of the Royal Society B: Biological Sciences* 366(1568): 1219-1233.

Xu, W., Chen, X., Liu, B., Chen, Y., Huan, M., Liu, N., and Lin, J. 2019. Inter-individual variation in trophic history of *Dosidicus gigas*, as indicated by stable isotopes in eye lenses. *Aquaculture and Fisheries* 4(6): 261-267.

Chapter 2: Fish-based δ^{13}C and δ^{15}N isoscapes for the continental shelf of the Gulf of Mexico

2.1 Chapter Summary

Isotope maps (isoscapes) are used to spatially depict ecological processes, to determine the energetic foundations of food webs, and to trace the origin and movement of animals. Isoscapes of δ^{13}C and δ^{15}N values were created for the continental shelf of the Gulf of Mexico using muscle samples from Red Snapper *(Lutjanus campechanus)* and Yellowedge Grouper (*Epinephelus flavolimbatus*). Red Snapper and Yellowedge Grouper had significant, positive relationships between both δ^{13}C and δ^{15}N values and fish length. Residuals from those regressions were used in the creation of the isoscapes in order to remove the effect of potential spatial differences in trophic position. Some influence from trophic growth could be seen in the isotopic data from each species. The δ^{13}C isoscape had a pattern of decreasing δ^{13}C values with increasing depth and, to a lesser extent, increased δ^{13}C values near areas of freshwater input. The δ^{15}N isoscape had a pattern of high δ^{15}N values near areas of freshwater input and low δ^{15}N values near oligotrophic Caribbean waters where production is dominated by diazotrophs. Red Snapper and Yellowedge Grouper isoscapes had similar overall patterns, with differences appearing to be related to differences among the locations where each species was collected.

2.2 Background

An isoscape is a map of the spatial patterns of isotopic values, either measured (empirical) or predicted via statistical models. Spatial variation in isotopic ratios is determined by a variety of biogeochemical processes that involve geology, climatology, biology, and hydrology (Bowen 2010). Within the realm of marine ecology, isoscapes have been used to determine the primary-producer types at the base of food webs (i.e., basal resources), food-web interactions, and the origins and movements of animals (Graham et al. 2010; Hobson et al. 2010; Olson et al. 2010). Isoscapes can also provide information on ecological processes that affect isotopic baselines. Two elements that are often used in these types of studies are carbon and nitrogen.

2.2.1 Causes of spatial variation in isotopic baselines

Photosynthetic fractionation by primary producers is a key factor that affects $\delta^{13}C$ variation in aquatic ecosystems. Primary producers preferentially fix the lighter ^{12}C isotope, which results in cellular $\delta^{13}C$ values that are lower than the ambient CO_2. The factors affecting photosynthetic fractionation can covary, wherein in one factor may affect relationships with others (Rau et al. 1996). For example, at the global scale, the $\delta^{13}C$ values of phytoplankton has been demonstrated to covary with latitude/temperature (Goericke and Fry 1994; McMahon et al. 2013; Magozzi et al. 2017). Increases in temperature decrease the solubility of CO_2 in seawater and increase maximum phytoplankton growth rate (Eppley 1972). However, the magnitude of those effects on photosynthetic fractionation is dependent on cell-wall permeability and the ability of primary producers to actively transport carbon into cells (Rau et al. 1996; Radabaugh et

al. 2014). Therefore, factors that influence spatial patterns of $\delta^{13}C$ values should not be considered in isolation.

Photosynthetic fractionation is generally less extreme under low CO_2 concentrations, low light intensity, fast growth rates, and for cells with higher surface-area-to-volume ratios (Gearing et al. 1984; Cifuentes 1987; Cooper and Deniro 1989; Rau et al. 1996; Hofmann et al. 2000). In each of these cases, a reduction in extracellular $[CO_2]$ results in Raleigh fractionation. Under Raleigh fractionation, the primary producer $\delta^{13}C$ values will be closer to that of the aqueous CO_2 as a greater proportion of the aqueous CO_2 is consumed. This phenomenon leads to (1) marine primary producers from high-productivity areas generally having higher $\delta^{13}C$ values than those from low-productivity areas (Popp et al. 1998; Hofmann et al. 2000), (2) benthic primary producers in shallow waters having higher $\delta^{13}C$ values than benthic primary producers in deeper waters (Cooper and DeNiro 1989; Muscatine et al. 1989; Radabaugh et al. 2014), (3) benthic algae under lower-light conditions having $\delta^{13}C$ values around 5‰ higher than overlying phytoplankton under higher-light conditions (France 1995; Radabaugh et al. 2014), and (4) phytoplankton with a larger cell size having higher $\delta^{13}C$ values than phytoplankton with a smaller cell size (Fry 1981; Gearing et al. 1984; France 1995; Laws et al. 1995). The net effect of these factors is a trend of decreasing $\delta^{13}C$ values in both benthic and planktonic primary producers with increasing water depth (Fry 1988; Cooper and Deniro 1989), and this trend being passed on to consumers (Radabaugh et al. 2013; Quillfeldt et al. 2015; Ceia et al. 2018).

Nitrogen is also fractionated during photosynthesis (Needoba et al. 2003), but because nitrogen is commonly a limiting nutrient for primary-producer growth (Lohrenz et al. 1997; Dagg and Breed 2003; Capone et al. 2008), all the available nitrogen is consumed. There is therefore no net fractionation from photosynthesis. Instead, baseline nitrogen isotopic ratios are

often a function of the δ^{15}N values of the sources of bioavailable nitrogen present (i.e., fixed nitrogen). Whereas the processes determining the availability of bioavailable nitrogen are variably influential, δ^{15}N values are generally higher in eutrophic waters and lower in oligotrophic waters (Alt-Epping et al. 2007; Nerot et al. 2012; Radabaugh et al. 2013). In the oligotrophic waters of the Gulf of Mexico, the main source of bioavailable nitrogen is diazotrophic nitrogen fixation which creates nitrate at or near 0‰ (Carpenter et al. 1997; Montoya et al. 2002; Montoya 2007). In the more eutrophic waters near river outflows, particulate organic matter (POM) tends to have higher δ^{15}N values due to the isotopic dominance of organic waste (sewage and manure) relative to other nitrogen sources (Hansson et al. 1997; Kendall et al. 2001). Under anoxic conditions, certain bacteria in water and sediments perform denitrification, preferentially removing bioavailable ^{14}N and producing higher δ^{15}N values for the residual nitrate and nitrite (Altabet et al. 1999; Granger et al. 2008).

The δ^{15}N baselines that result from interactions among the above processes are then transferred into the food web where they are further modified by trophic fractionation (Minagawa and Wada 1984). Tissue δ^{15}N values increase by roughly 3.4‰ per trophic level, although there are multiple studies that suggest this type of fractionation is not numerically consistent (Minagawa and Wada 1984; Pinnegar and Polunin 1999; Vander Zanden and Rasmussen 2001; Hussey et al. 2014). Carbon within food webs also undergoes trophic fractionation, but to a lesser extent (an increase of around 0-1‰ per trophic level), so δ^{15}N values are generally preferred as an indicator of the trophic position of an individual consumer (Fry and Sherr 1989; Peterson and Fry 1987; Cabana and Rasmussen 1996; Vander Zanden and Rasmussen 1999).

2.2.2 Objectives

The principal objective of this chapter was to establish general spatial patterns of δ^{13}C and δ^{15}N values on the continental shelf of the Gulf of Mexico to facilitate future stable isotope ecology studies and to reveal ecological processes influential to baseline isotopic composition in the Gulf of Mexico. Two reef-fish species were compared to determine whether general spatial trends in the resulting isoscapes were consistent between species. The methods used here are similar to those of Radabaugh et al. (2013), which created δ^{13}C and δ^{15}N isoscapes using POM, the stomach linings and stomach contents of the sea urchin *Lytechinus variegatus*, and the muscle of three fish species from locations throughout the West Florida Shelf (WFS) of the northeastern Gulf of Mexico. The δ^{15}N isoscapes they generated depicted spatial trends with higher δ^{15}N values in the northwest region of the WFS and lower values near the southwestern Florida peninsula, which is in concordance with the presumed sources of bioavailable nitrogen (riverine input and diazotrophic nitrogen fixation, respectively). The δ^{13}C isoscapes depicted a spatial trend with higher δ^{13}C values inshore and lower δ^{13}C values offshore, which is in concordance with the changes in benthic algal fractionation with light availability, primary productivity rates, and the availability of a benthic basal resource to consumers. Both the δ^{15}N and δ^{13}C isoscapes remained relatively consistent over seasons and years and among fish species. The present study expands the Radabaugh et al. (2013) isoscapes to the remainder of continental-shelf waters of the United States and Mexico.

2.3 Methods

2.3.1 Target species

Reef-fish muscle from two species, Red Snapper *(Lutjanus campechanus)* and

Yellowedge Grouper (*Epinephelus flavolimbatus*), was used to create the isoscapes instead of

POM in order to obtain more time-space-averaged isotopic patterns than those expected from

phytoplankton (Vander Zanden and Rasmussen 2001; O'Reilly et al. 2002; Post 2002; Bump et

al. 2007; Radabaugh et al. 2013). Red Snapper is a member of the family Lutjanidae (snappers),

and is found throughout the Gulf of Mexico in 10-190 m waters (Allen 1985; Smith 1997).

Adults are reef-associated and feed mainly on fishes, shrimps, crabs, worms, cephalopods, and

some planktonic items, including urochordates and gastropods (Allen 1985; Frimodt 1995).

Yellowedge Grouper is a member of the family Serranidae (groupers) found throughout

the Gulf of Mexico in 90-360 m waters. Adults are demersal and are associated with both hard-

and soft-bottom habitats near the edge of the continental shelf. They feed primarily upon crabs

and fishes (Craig and Hastings 2007; Craig et al. 2011).

2.3.2 Muscle collection

Dorsal muscle samples from Red Snapper (n = 127) and Yellowedge Grouper (n = 99)

were obtained from freshly caught fish aboard chartered, commercial fishing vessels (2011) and

the R/V *Weatherbird II* (2014, 2015, and 2016; Table 2.1). Fishes were collected using demersal

longline gear deployed in a transect survey design that extended throughout the Gulf of Mexico

continental shelf, excluding Cuba (Figure 2.1). Station placement was in continental shelf waters

from 40 to 300 m deep. Longline sets were generally deployed at six stations along predefined

transects that extended from relatively shallow to deep continental shelf areas (Murawski et al.

2018). The nominal water depths sampled along each transect were 37, 73, 110, 146, 183, and 274 m. Along several transects, the bathymetric slope was so steep that six unique stations could not be effectively sampled; depth control at those stations was difficult because the shallowest and deepest stations were <8 km apart.

Table 2.1
Metadata for the research cruises from which the fish muscle samples were obtained. The regions include the West Florida Shelf (WFS), the northern Gulf of Mexico (NG), the western Gulf of Mexico (WG), Campeche Bay, Mexico (CB), and the Yucatan Peninsula, Mexico (YP). The numbers of Red Snapper (n RS) and Yellowedge Grouper (n YEG) refer to the number caught during each cruise. The numbers of Red Snapper (Used RS) and Yellowedge Grouper (Used YEG) refer to how many of the fish caught on each cruise were used in the present study.

Year	Vessel	Region	n RS	n YEG	Used RS	Used YEG
2011	F/V *Sea Fox*	WFS	16	12	5	0
2011	F/V *Brandy*	WFS	86	42	23	10
2011	F/V *Pisces*	WFS, NG	475	55	35	33
2014	R/V *Weatherbird II*	WFS, NG	90	17	3	0
2015	R/V *Weatherbird II*	WFS, NG, CB, YP	133	40	23	19
2016	R/V *Weatherbird II*	NG, WG, CB, YP	347	56	38	37

At each station, 8 km of 3.2 mm galvanized steel (2011) or 544 kg-test monofilament (2014, 2015, and 2016) main line was deployed, with a mean of 446 baited hooks per longline set. Monofilament leaders (gangions) of 136 kg-test and 2.4 m length were clipped to the main line and attached to size-13/0 circle hooks. Bait was cut fish (Atlantic Mackerel, *Scomber scombrus*) and cut squid (primarily Humboldt Squid, *Dosidicus gigas* wings). The type of bait was switched haphazardly from hook to hook during deployments. Fishing was conducted only during daylight hours and during summer.

Upon longline retrieval, collected species were identified, and their standard lengths (SL) and total lengths (TL) were recorded in cm. Each specimen was weighed to the nearest gram on a

Marel motion-compensated scale; large fish (> 6 kg) were weighed with a hand scale (nearest 0.1

kg). At each station, a subsample of the catch (10 or fewer, depending on total number caught)

was selected to be sexed and sampled for dorsal muscle. Muscle samples were either

immediately frozen (*Weatherbird II* samples) or placed on ice (all other samples).
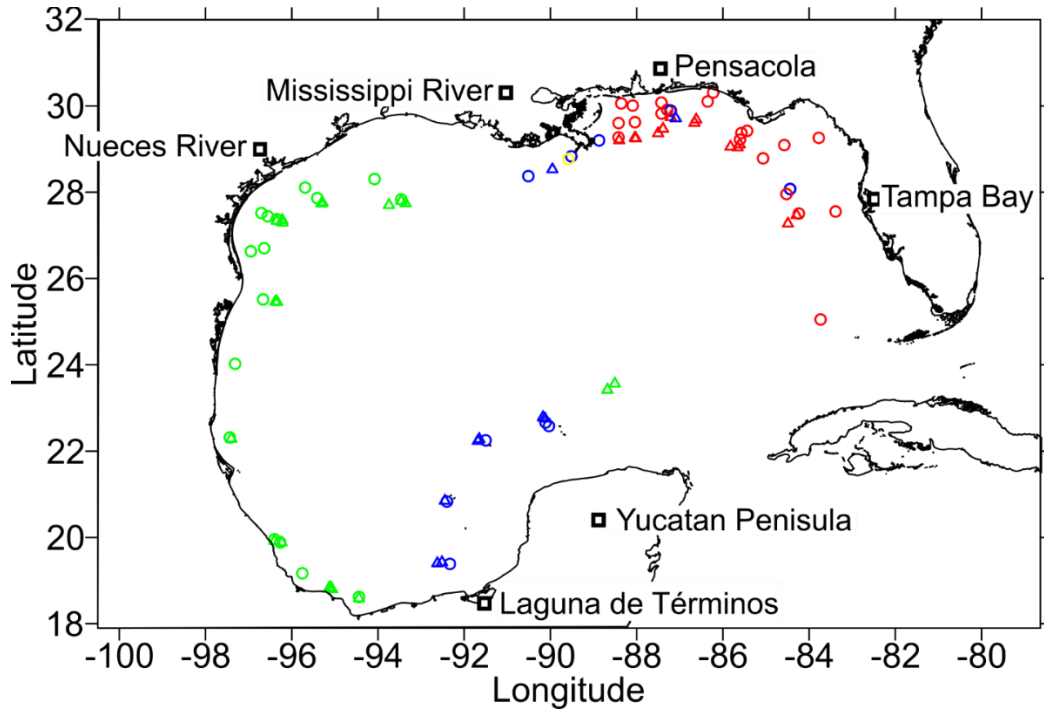
Figure 2.1
Locations (stations) where fish were collected. Stations where Red Snapper were caught have
circular symbols and stations where Yellowedge Grouper were caught have triangular symbols.
Stations are colored by the year in which they were sampled; 2011 in red, 2014 in yellow, 2015
in blue, and 2016 in green.

2.3.3 Isotope analysis

In the lab, muscle samples were dried in an oven for a minimum of 48 hours. The muscle

samples were then powdered and homogenized using a dental amalgamator. A dry weight of

300–600 µg of powdered muscle was placed in tin capsules for combustion and isotopic analysis.

$^{13}C/^{12}C$, $^{15}N/^{14}N$, and C:N were measured in replicate using a Carlo-Ebra NA2500 Series II

elemental analyzer coupled to a continuous-flow ThermoFinnigan Delta Plus XL isotope ratio

mass spectrometer at the University of South Florida College of Marine Science in St.

Petersburg, Florida. The lower limit of quantification was 12 µg C or N. Calibration standards

were NIST 8573 (δ^{13}C values = -26.39 ± 0.09 and δ^{15}N values = -4.52 ± 0.12) and NIST 8574 L-

glutamic acid (δ^{13}C values = 37.63 ± 0.1 and δ^{15}N values = 47.57 ± 0.22) reference materials. All

the muscle samples from 2011 were analyzed, whereas for 2014, 2015, and 2016, a maximum of

three haphazardly chosen muscle samples for each species at each station were analyzed. Results

are presented in standard notation (δ, in ‰) relative to international standards Pee Dee Belemnite

(PDB) and air for C and N, respectively:

$$\delta^j X = \left(\frac{(\,^j X /\,^i X)_{sample}}{(\,^j X /\,^i X)_{standard}} - 1 \right) * 1000$$

where X is the element and j and i are each an isotope of X.

2.3.4 Data analysis and isoscape generation

Before the isoscapes were created, the data were explored and modified. First,

regressions between both isotopes and standard length were performed to determine whether

there was a significant trophic effect. Because both species had significant relationships between

both δ^{13}C and δ^{15}N values and standard length, residuals from isotope-length regressions (length-

corrected δ^{13}C and δ^{15}N values) were used in place of unaltered isotopic values. This was done to

prevent spatial differences in species' diet/trophic position from interfering with the spatial

differences in baseline isotopic levels. Second, regressions were performed between δ^{13}C and

δ^{15}N values in their unaltered and length-corrected forms to assess the collinearity of the two

isotopes. Third, a Mann-Whitney U-Test was used to determine if there was a significant

difference between the average capture depths and/or isotopic values of the two species. The above analyses were performed in R (version 4.0.5, R Core Team 2020). Lastly, length-corrected $\delta^{13}C$ and $\delta^{15}N$ values (regression residuals) were averaged for each species by station to prevent stations with more individuals from arithmetically overwhelming the stations with fewer individuals. Data from up to eight muscle samples were averaged per station; at most stations, data from three samples were averaged.

Isoscapes were spatially interpolated using point kriging with a linear variogram model with no drift and no nugget effect (Surfer version 19.1.189). Isoscapes were limited to depths of 5-200 m for Red Snapper and 70-200 m for Yellowedge Grouper to reflect the depth distributions of each species, with 200 m representing the nominal outer edge of the continental shelf.

2.4 Results

In total, 1,147 Red Snapper and 222 Yellowedge Grouper were caught across all research cruises. Of these, 127 Red Snapper and 99 Yellowedge Grouper were analyzed for stable isotopes (Table 2.2). Red Snapper were caught at 49 stations, and Yellowedge Grouper were caught at 41 stations (Figure 2.1). The two species co-occurred at four stations.

The following summary statistics characterize the unaltered isotope data rather than the length-corrected data (i.e., regression residuals). Red Snapper $\delta^{13}C$ values ranged from -18.32 to -15.97‰, and Yellowedge Grouper $\delta^{13}C$ values ranged from -18.45 to –16.53‰ for (Table 2.2). Red Snapper $\delta^{15}N$ values ranged from 10.16 to 16.41‰, and Yellowedge Grouper $\delta^{15}N$ values ranged from 10.74 to 16.09‰. The sample standard deviation was 0.56‰ for $\delta^{13}C$ values and 1.51‰ for $\delta^{15}N$ values for Red Snapper and 0.41‰ for $\delta^{13}C$ values and 1.29‰ for $\delta^{15}N$ values

for Yellowedge Grouper. The only variables that had a significant difference between Red

Snapper and Yellowedge Grouper were water depth and $\delta^{13}C$ values.

Table 2.2
Summary statistics comparing Red Snapper and Yellowedge Grouper muscle isotopes. Values for depth, $\delta^{13}C$, and $\delta^{15}N$ were first averaged by station before creating the means and standard deviations (std. dev.) below. Mean depth refers to the mean starting depth of all deployments where the species was collected. Length-corrected $\delta^{13}C$ and $\delta^{15}N$ values refer to the residuals of the regressions of stable isotopes on standard length (see Figure 2.2). An asterisk (*) indicates that there was significant ($p < 0.05$) difference between Red Snapper and Yellowedge Grouper as determined by a Mann-Whitney U-Test.

	Red Snapper	Yellowedge Grouper
n	127	99
Number of stations	49	41
Mean depth (m)	66.24*	173.99*
Mean $\delta^{13}C$ value	-17.07*	-17.47*
$\delta^{13}C$ std. dev.	0.46	0.39
$\delta^{13}C$ value on standard length	$\delta^{13}C = -17.90 + 0.016(SL)$	$\delta^{13}C = -18.08 + 0.011(SL)$
Mean length-corrected $\delta^{13}C$	0.043	-0.017
Length-corrected $\delta^{13}C$ std. dev.	0.43	0.36
Mean $\delta^{15}N$ value	13.52	13.38
$\delta^{15}N$ std. dev.	1.43	1.36
$\delta^{15}N$ value on standard length	$\delta^{15}N = 11.63 + 0.038(SL)$	$\delta^{15}N = 10.94 + 0.043(SL)$
Mean length-corrected $\delta^{15}N$	-0.034	0.043
Length-corrected $\delta^{15}N$ std. dev.	1.39	1.07

There was a significant relationship between fish length and $\delta^{13}C$ and $\delta^{15}N$ values for

both Red Snapper and Yellowedge Grouper (Figure 2.2). The regressions had higher nominal R^2

values for Yellowedge Grouper for both $\delta^{13}C$ and $\delta^{15}N$ values. The R^2 values were relatively low

overall (all $R^2 < 0.3$), which indicates there was substantial variation in muscle isotopes that was

not explained by fish length.
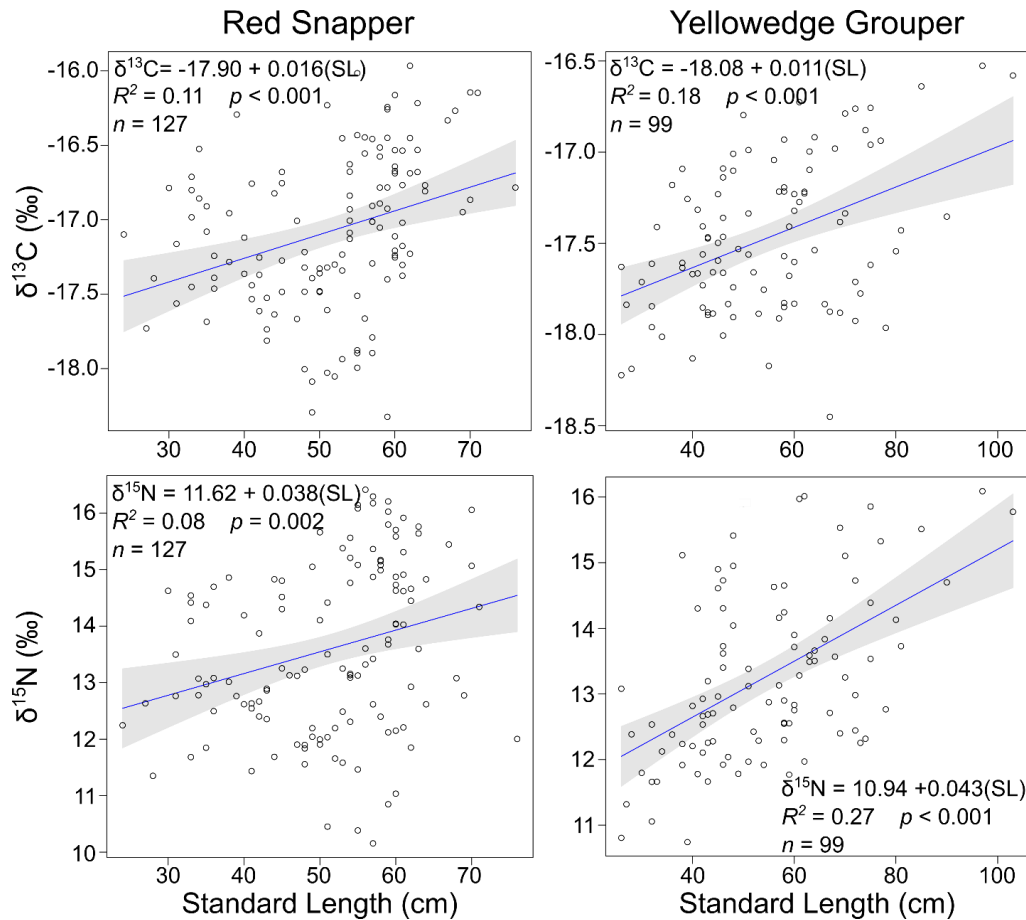
Figure 2.2
Linear, least-squares regressions of stable–isotope values (δ^{13}C or δ^{15}N) values on standard length for Red Snapper and Yellowedge Grouper, wherein each symbol represents an individual fish. Regression equations, R^2 values, p-values, and sample size (n) are presented on the graphs. Shaded areas depict 95% confidence limits for predicted means.

There was a significant relationship between δ^{13}C and δ^{15}N values in both the unaltered and length-corrected data for both Red Snapper and Yellowedge Grouper (Figure 2.3). For both species, the R^2 values of the regressions were lower for the length-corrected δ^{13}C and δ^{15}N values than for the unaltered data. Yellowedge Grouper had nominally higher R^2 values than Red Snapper in both cases.

65

2.4.1 Isoscapes

In general, the isoscapes created using the length-corrected values of Red Snapper muscle presented clearer patterns than those created using Yellowedge Grouper muscle (Figure 2.4). Both δ^{13}C isoscapes produced a general pattern of higher δ^{13}C values near areas of freshwater input (Tampa Bay, Mississippi River, Nueces River, and Laguna de Términos) and lower δ^{13}C values near the edge of the continental shelf, although the pattern is barely evident in the Yellowedge Grouper isoscape (Figure 2.4). The highest Red Snapper δ^{13}C value was at the station nearest Laguna de Términos. The station's average was based on the muscle of two fish, both of which had length-corrected δ^{13}C values greater than 0.95‰. The lowest Red Snapper δ^{13}C value was at a station towards the southern edge of the West Florida Shelf. The station's average was based on five fish, three of which had length-corrected δ^{13}C values less than -0.8‰. The highest Yellowedge Grouper δ^{13}C value was located off Pensacola, Florida; this station average was based on two fish, one of which had a very high δ^{13}C value, and one of which had a moderately high δ^{13}C value.
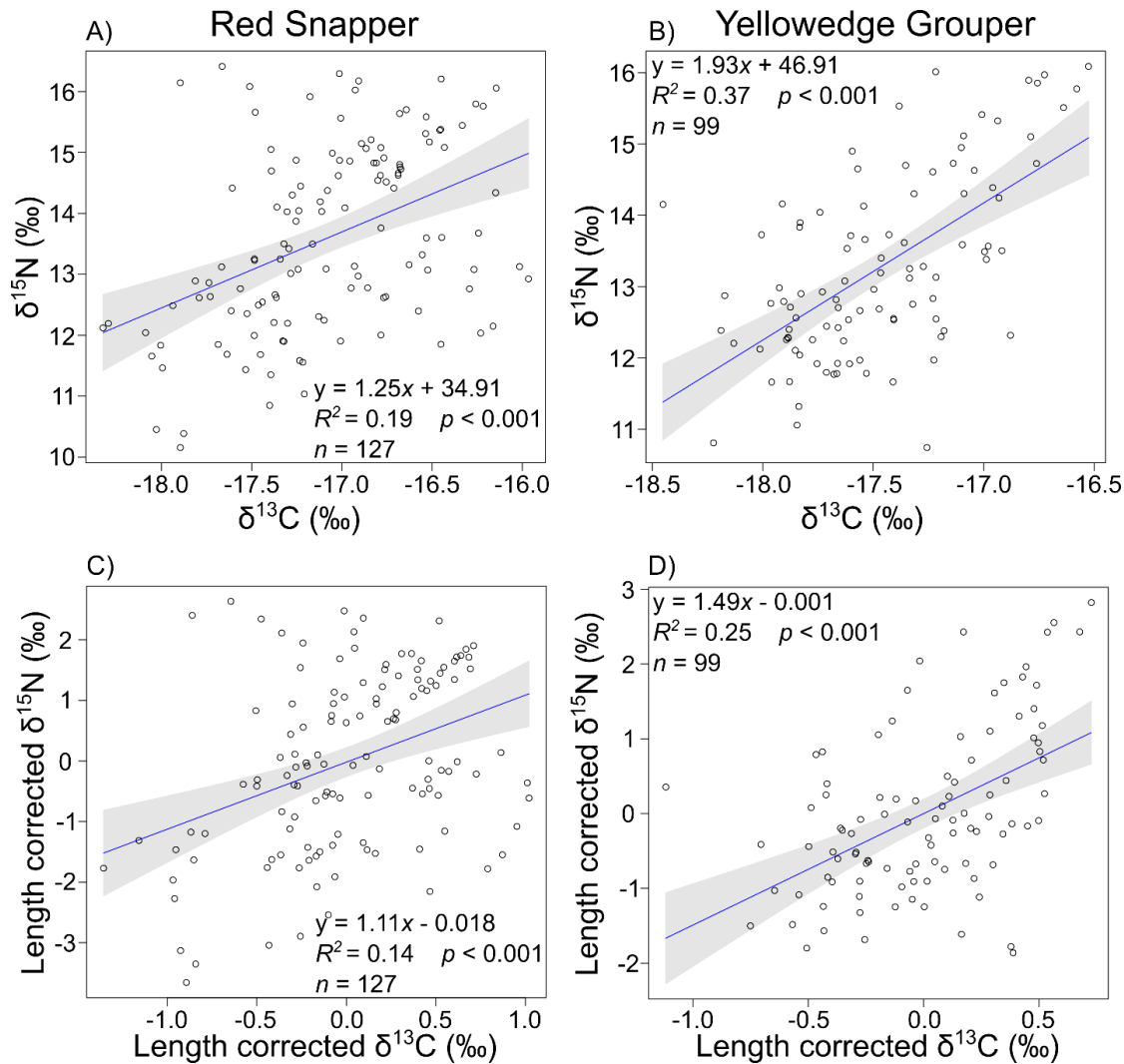
Figure 2.3
Linear, least-square regressions of $\delta^{15}N$ on $\delta^{13}C$, wherein each symbol represents an individual fish. Uncorrected data are presented in panels A and B, and length-corrected data are used in panels C and D. Regression equations, R^2 values, p-values, and sample size (n) are presented on the graphs. Shaded areas depict 95% confidence limits for predicted means.

Both species had the lowest $\delta^{15}N$ value at the station closest to the Caribbean. In the case of Red Snapper, that was at the southernmost station on the West Florida Shelf. The average value at that station was based on five fish, four of which had length-corrected $\delta^{15}N$ values less than -3‰. Yellowedge Grouper had the lowest $\delta^{15}N$ value at the easternmost station on the Yucatan Peninsula. The average value at that station was based on one fish with a length-

corrected $\delta^{15}N$ value of -1.86‰. This value does not appear to be an error or outlier since fish at nearby stations had similarly low length-corrected $\delta^{15}N$ values. The highest $\delta^{15}N$ value for Red Snapper was located at a station near the mouth of the Mississippi River. The average value at that station was based on three fish, all of which had length-corrected $\delta^{15}N$ values greater than 2.3‰. The highest $\delta^{15}N$ value for Yellowedge Grouper was located off Pensacola. The average value at that station was based on two fish, both of which had length-corrected $\delta^{15}N$ values over 1.9‰.
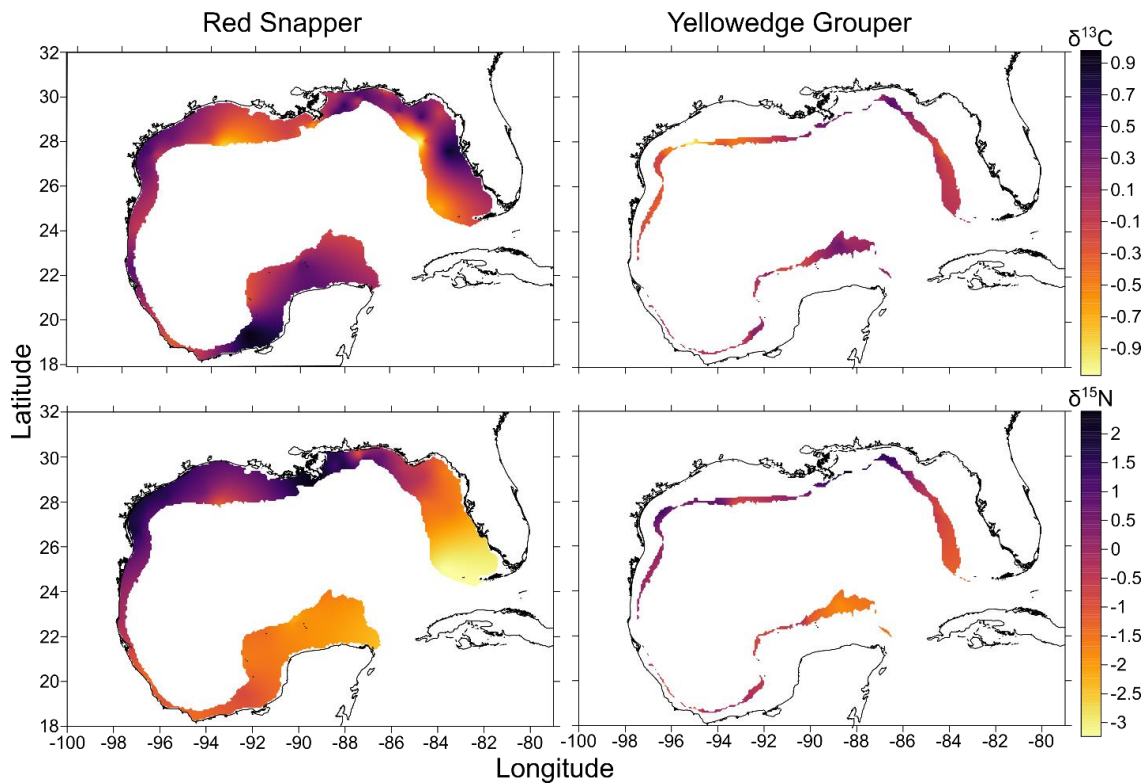
Figure 2.4
Isoscapes of length-corrected $\delta^{13}C$ and $\delta^{15}N$ values for Red Snapper and Yellowedge Grouper. The spatial extent of the isoscape was limited beyond the nominal edge of the continental shelf (the 200 m isobaths) and landward of the 5 m and 70 m isobaths respectively for Red Snapper and Yellowedge Grouper to reflect the distributions of each species.

2.5 Discussion

2.5.1 Isoscape patterns

The isoscapes created by this project depicted general spatial trends in δ^{13}C and δ^{15}N values around the Gulf of Mexico that appear to reflect aspects of the region's ecological processes. The trends in the δ^{13}C isoscapes were not as consistent as those in the δ^{15}N isoscapes and may merit further investigation, particularly investigations at increased spatial resolutions. In the Red Snapper isoscape, there was a decrease in δ^{13}C values with depth on the West Florida Shelf and in the northwest Gulf of Mexico. This pattern agrees with the isoscapes generated by Radabaugh et al. (2013), which also depicted a δ^{13}C value depth gradient. The depth gradient observed in most areas could be attributed to a decrease in the importance of benthic primary producers with depth as a result of decreased light availability at depth (Cooper and DeNiro 1989; Muscatine et al. 1989; Radabaugh et al. 2014). If Red Snapper became less dependent on benthic primary producers in deeper waters (i.e., as a basal resource rather than a direct food source), then their δ^{13}C values would have reflected this trend, as benthic algae generally contain δ^{13}C values that are about 5‰ higher than that of overlying phytoplankton (France 1995; Radabaugh et al. 2014). In ocean waters beyond the continental shelf, local contribution of benthic algae to food webs disappears altogether due to light limitation at depth. In addition to this general trend, there are river-influenced areas of the continental shelf where benthic algae are less important because they are shaded by phytoplankton or turbidity. A second, non-exclusive explanation for the δ^{13}C value depth gradient is that productivity tends to be higher in shallower, nearshore environments, and higher productivity is associated with decreased fractionation (Popp et al. 1998; Hofmann et al. 2000) and consequently higher δ^{13}C values in primary producers. Productivity rates are also a likely explanation for the spatial trend of higher

69

δ^{13}C values near areas of high freshwater input that was observable in both the Red Snapper and (to a lesser extent) Yellowedge Grouper isoscapes. The major exception to this pattern is the stations near the Nueces River outflow in the Yellowedge Grouper isoscape. These stations depict very low δ^{13}C values despite being near an area of freshwater outflow. It is possible that the lighter values seen in Yellowedge Grouper near the Nueces River are due to the area of higher productivity near that river not extending all the way out to the edge of the continental shelf where Yellowedge Grouper were caught.

The relationship between δ^{13}C values and depth is further supported by the differences between the two species. Red Snapper and Yellowedge Grouper had significant differences in depth of collection and δ^{13}C values. On average, Red Snapper had higher δ^{13}C values than Yellowedge Grouper and were caught at shallower depths. It is likely the significant difference in δ^{13}C values between species was a result of the difference in depth of collection, for the reasons stated above.

In general, lower δ^{15}N values were observed near the tropical, oligotrophic Caribbean, where nitrate input is most likely dominated by diazotrophs, and higher δ^{15}N values were observed near areas of freshwater input. This pattern of low δ^{15}N values in the Caribbean Sea is consistent with other Gulf of Mexico isoscapes (Radabaugh et al. 2013; Vander Zanden et al. 2015; Le-Alvarado et al. 2021) and a global, plankton-based δ^{15}N isoscape (McMahon et al. 2013). In tropical areas, diazotrophs convert N_2 into bioavailable nitrogen that retains δ^{15}N values near the atmospheric (air) standard of 0‰, which is passed on to consumers in the area (Carpenter et al. 1997; Montoya et al. 2002; Montoya 2007). The highest δ^{15}N values were observed near the Mississippi River outflow and near the Nueces River outflow, where several rivers flow into the Gulf of Mexico. One likely reason for the high δ^{15}N values at these locations

was riverine inputs of livestock waste or human sewage, which have relatively high δ^{15}N values (Hansson et al. 1997; Kendall et al. 2001). Another, non-exclusive possible explanation for the high δ^{15}N values in the northern Gulf of Mexico was seasonal hypoxia and anoxia allowing for denitrification which leaves behind high δ^{15}N nitrate (Altabet et al. 1999; Childs et al. 2002; Granger et al. 2008).

2.5.2 Effects of trophic growth

Further information can be gained about the trophic ecology of both species and how that ecology affects the isoscapes by looking at the relationships of each isotope with standard length and the relationships of the isotopes with each other. Red Snapper and Yellowedge Grouper both had significant relationships between standard length and both isotopes. One likely explanation for this relationship is that both species increase their trophic position as they increase in size (trophic growth; Minegawa and Wada 1984; Post 2002; Wallace et al. 2014). The relationships were stronger (based on R^2 value) for Yellowedge Grouper, which suggests one or both of these effects are stronger for this species.

Another possible reason Yellowedge Grouper had stronger relationships between standard length and isotopic values, is Yellowedge Grouper exhibit less overall spatial isotopic variability because they were collected from a smaller spatial area that was closer to the open waters of the deep Gulf of Mexico. This is supported by the standard deviations of the two species. Yellowedge Grouper had a lower standard deviation than Red Snapper in all four isotopic categories (δ^{13}C, δ^{15}N, length-corrected δ^{13}C, and length-corrected δ^{15}N values). If the Yellowedge Grouper samples had less overall spatial variation, then a greater proportion of the total variation could be explained by standard length. This is supported by the regressions

71

between standard length and each isotope,wherein Yellowedge Grouper had higher R^2 values than Red Snapper, and by the regressions between $\delta^{13}C$ and $\delta^{15}N$ values, wherein Yellowedge Grouper had a larger proportional change in R^2 after length correction. Both of these relationships suggest a greater proportion of the isotopic variation in Yellowedge Grouper was explained by trophic growth than was for Red Snapper.

There was a significant relationship between $\delta^{13}C$ and $\delta^{15}N$ values for both species both before and after length correction, but the R^2 values for the regressions were lower after length correction. One reason for the decrease in R^2 is that the relationship between $\delta^{13}C$ and $\delta^{15}N$ values both increase with increases trophic position (DeNiro and Epstein 1978; Minagawa and Wada 1984; Vander Zanden and Rasmussen 2001). The length correction was intended to largely remove the effect of trophic position on $\delta^{13}C$ and $\delta^{15}N$ values, and thus it follows that the relationship between $\delta^{13}C$ and $\delta^{15}N$ values would be weaker after length correction. However, the regressions between $\delta^{13}C$ and $\delta^{15}N$ values were still significant after length correction. Two non-exclusive explanations for this are (1) the length-correction did not fully remove the trophic-position effect on $\delta^{13}C$ and $\delta^{15}N$ values, or (2) $\delta^{13}C$ and $\delta^{15}N$ values were spatially correlated. A visual inspection of the $\delta^{13}C$ and $\delta^{15}N$ isoscapes for both species suggests the second explanation is likely at least a contributor to the observed results.

2.5.3 Isoscape utility

There are a few considerations when using these or other consumer-based isoscapes. First, the spatial variation depicted here could be a result of differences in baseline isotopes or in the diet of the consumers (i.e., eating different proportions of prey that depend on different basal resources). While the length-correction was meant to remove the effects of spatial differences in

trophic position, it is possible to have shifts in basal resource dependence without an accompanying shift in trophic position. A second consideration is that the methods used here have the implicit assumption that each fish sampled had reasonable spatial stationarity (i.e., that the fish has not recently moved to the collection location from an area with differing baseline values). Similarly, even if the fish from this study remained stationary, it is possible their prey recently moved to the collection location from an area with differing baseline values. This may be of particular concern with regards to the seasonal movement of species from nearshore habitats, which have distinct isotopic baselines, to offshore reef habitats (Nelson et al. 2012). A final consideration is that there is likely temporal variation in baseline $\delta^{13}C$ and $\delta^{15}N$ values, and the isoscapes would likely change season to season and year to year. For example, changes in the size and location of the Mississippi River plume would likely change the location and shape of the area of high $\delta^{13}C$ and $\delta^{15}N$ values in the northern Gulf of Mexico.

2.6 Citations

Allen, G. R. 1985. FAO Species Catalogue. Vol. 6. Snappers of the world. An annotated and illustrated catalogue of lutjanid species known to date. *FAO Fisheries Symposium* 125(6):208

Alt-Epping, U., Mil-Homens, M., Hebbeln, D., Abrantes, F., and Schneider, R. R. 2007. Provenance of organic matter and nutrient conditions on a river- and upwelling influenced shelf: a case study from the Portuguese Margin. *Marine Geology* 243, 169–179.

Boecklen, W. J., Yarnes, C. T., Cook, B. A., and James, A. C. 2011. On the Use of Stable Isotopes in Trophic Ecology. *Annual Review of Ecology, Evolution, and Systematics* 42(1): 411-440.

Bowen, G. J. 2010. Isoscapes: Spatial Pattern in Isotopic Biogeochemistry. *Annual Review of Earth and Planetary Sciences* 38(1): 161-187.

Bump, J. K., Fox-Dobbs, K., Bada, J. L., Koch, P. L., Peterson, R. O., and Vucetich, J. A. 2007. Stable isotopes, ecological integration, and environmental change: wolves record atmospheric carbon isotope trend better than tree rings. *Proceedings of the Royal Society B: Biological Sciences* 274: 2471–2480.

Cabana, G. and J. B. Rasmussen. 1996. Comparison of aquatic food chains using nitrogen isotopes. *Proceedings of the National Academy of Sciences* 93(20): 10844.

Capone, D. G., Bronk, D. A., Mulholland, M. R., and Carpenter, E. J. (Eds.). 2008. Nitrogen in the Marine Environment. Elsevier.

Carpenter, E. J., Harvey, H. R., Fry, B., and Capone, D. G., 1997. Biogeochemical tracers of the marine cyanobacterium Trichodesmium. *Deep Sea Research Part A: Oceanographic Research Papers* 44: 27–38.

Childs, C. R., Rabalais, N. N., Turner, R. E., and Proctor, L. M. 2002. Sediment denitrification in the Gulf of Mexico zone of hypoxia. *Marine Ecology Progress Series* 240: 285-290.

Cifuentes, L. A. 1987. Sources and biogeochemistry of organic matter in the Delaware estuary (Order No. 8719522, University of Delaware). ProQuest Dissertations and Theses, 243. Retrieved from https://www.proquest.com/dissertations-theses/sources-biogeochemistry-organic-matter-delaware/docview/303473515/se-2?accountid=14745

Ceia, F. R., Cherel, Y., Paiva, V. H., and Ramos, J. A. 2018. Stable Isotope Dynamics (δ^{13}C and δ^{15}N) in Neritic and Oceanic Waters of the North Atlantic Inferred From GPS-Tracked Cory's Shearwaters. *Frontiers in Marine Science* 5: 377.

Cooper, L. W. and DeNiro, M. J. 1989. Stable carbon isotope variability in the seagrass *Posidonia oceanica*: evidence for light intensity effects. *Marine Ecology Progress Series* 50: 225–229.

Craig, M. T. and P. A. Hastings. 2007. A molecular phylogeny of the groupers of the subfamily Epinephelinae (Serranidae) with revised classification of the epinephelini. *Ichthyological Research* 54:1-17.

Craig, M. T., Sadovy de Mitcheson, Y. J., and Heemstra, P. C. 2011. Groupers of the world: a field and market guide. North America: CRC Press/Taylor and Francis Group. 356 p. ISBN 9781466506022

Dagg, M. J. and Breed, G. A. 2003. Biological effects of Mississippi River nitrogen on the northern Gulf of Mexico—a review and synthesis. *Journal of Marine Systems* 43(3-4): 133-152.

Dansgaard, W. 1954. The O18-abundance in fresh water. *Geochimica et Cosmochimica Acta* 6:241–60

DeNiro, M. J. and Epstein, S. 1978. Influence of diet on the distribution of carbon isotopes in animals. *Geochimica et Cosmochimica Acta* 42(5): 495-506.

Eppley, R. W. 1972. Temperature and phytoplankton growth in the sea. *Fishery Bulletin* 70(4): 1063-1085.

France, R. L. 1995. Carbon-13 enrichment in benthic compared to planktonic algae: foodweb implications. *Marine Ecology Progress Series* 124: 307-312.

Frimodt, C. 1995. Multilingual illustrated guide to the world's commercial coldwater fish. Fishing News Books, Osney Mead, Oxford, England. 215 p.

Fry, B. 1988. Food web structure on Georges Bank from stable C, N, and S isotopic compositions. *Limnology and Oceanography* 33: 1182–1190.

Fry, B. and Sherr, E. B. 1989. $\delta^{13}C$ measurements as indicators of carbon flow in marine and freshwater ecosystems. *Stable Isotopes in Ecological Research* 196-229.

Gearing, J. N., Gearing, P. J., Rudnick, D. T., Requejo, A. G., and Hutchins, M. J. 1984. Isotopic variability of organic carbon in a phytoplankton-based, temperate estuary. *Geochimica et Cosmochimica Acta* 48(5): 1089-1098.

Germain, L. R., Koch, P. L., Harvey, J., and McCarthy, M. D. 2013. Nitrogen isotope fractionation in amino acids from harbor seals: implications for compound-specific trophic position calculations. *Marine Ecology Progress Series* 482: 265-277.

Goericke, R., and B. Fry. 1994. Variations of marine plankton $\delta^{13}C$ with latitude, temperature, and dissolved CO^2 in the world ocean. *Global Biogeochemical Cycles* 8: 85–90.

Graham, B.S., Koch, P.L., Newsome, S.D., McMahon, K.W., Aurioles, D., 2010. Using isoscapes to trace the movements and foraging behavior of top predators in oceanic ecosystems. In: West, J.B., Bowen, G.J., Dawson, T.E., Tu, K.P. (Eds.), Isoscapes: Understanding Movement, Pattern, and Process on Earth through Isotope Mapping. Springer, New York, pp. 299–318.

Granger, J., Sigman, D. M., Lehmann, M. F., and Tortell, P. D. 2008. Nitrogen and oxygen isotope fractionation during dissimilatory nitrate reduction by denitrifying bacteria. *Limnology and Oceanography* 53(6): 2533-2545.

Hannides, C. C., Popp, B. N., Choy, C. A., and Drazen, J. C. 2013. Midwater zooplankton and suspended particle dynamics in the North Pacific Subtropical Gyre: A stable isotope perspective. *Limnology and Oceanography* 58(6): 1931-1946.

Hansson, S., Hobbie, J. E., Elmgren, R., Larsson, U., Fry, B., and Johansson, S. 1997. The stable nitrogen isotope ratio as a marker of food-web interactions and fish migration. *Ecology* 78: 2249–2257.

Hobson, K. A., Barnett-Johnson, R., and Cerling, T. 2010. Using isoscapes to track animal migration. In: West, J.B., Bowen, G.J., Dawson, T.E., Tu, K.P. (Eds.), Isoscapes: Understanding Movement, Pattern, and Process on Earth through Isotope Mapping. Springer, New York, pp. 273–298.

Hofmann, M., Wolf-Gladrow, D. A., Takahashi, T., Sutherland, S. C., Six, K. D., and MaierReimer, E. 2000. Stable carbon isotope distribution of particulate organic matter in the ocean: a model study. *Marine Chemistry* 72: 131–150.

Hussey, N. E., MacNeil, M. A., McMeans, B. C., Olin, J. A., Dudley, S. F., Cliff, G., Wintner, S. P., Fennessy, S. T. and Fisk, A. T. 2014. Rescaling the trophic structure of marine food webs. *Ecology Letters* 17(2): 239-250.

Kendall, C., Silva, S. R., and Kelly, V. J., 2001. Carbon and nitrogen isotopic compositions of particulate organic matter in four large river systems across the United States. *Hydrological Processes* 15: 1301–1346.

Kline, Jr, T. C. 1999. Temporal and spatial variability of $^{13}C/^{12}C$ and $^{15}N/^{14}N$ in pelagic biota of Prince William Sound, Alaska. *Canadian Journal of Fisheries and Aquatic Sciences* 56(S1): 94-117.

Kootker, L. M., van Lanen, R. J., Kars, H., and Davies, G. R. 2016. Strontium isoscapes in The Netherlands. Spatial variations in 87Sr/86Sr as a proxy for palaeomobility. *Journal of Archaeological Science: Reports* 6: 1-13.

Kürten, B., Frutos, I., Struck, U., Painting, S. J., Polunin, N. V., and Middelburg, J. J. 2013. Trophodynamics and functional feeding groups of North Sea fauna: a combined stable isotope and fatty acid approach. *Biogeochemistry* 113(1-3): 189-212.

Laws, E. A., Popp, B. N., Bidigare, R. R., Kennicutt, M. C., and Macko, S. A.,1995. Dependence of phytoplankton carbon isotopic composition on growth rate and $[CO_2]aq$: Theoretical considerations and experimental results. *Geochimica et Cosmochimica Acta* 59: 1131–1138.

Le-Alvarado, M., Romo-Curiel, A. E., Sosa-Nishizaki, O., Hernández-Sánchez, O., Barbero, L., and Herzka, S. Z. 2021. Yellowfin tuna (*Thunnus albacares*) foraging habitat and trophic position in the Gulf of Mexico based on intrinsic isotope tracers. *PloS One* 16(2): e0246082.

Lohrenz, S. E., Fahnenstiel, G. L., Redalje, D. G., Lang, G. A., Chen, X., and Dagg, M. J. 1997. Variations in primary production of northern Gulf of Mexico continental shelf waters linked to nutrient inputs from the Mississippi River. *Marine Ecology Progress Series* 155: 45-54.

Magozzi, S., Yool, A., Vander Zanden, H. B., Wunder, M. B., and Trueman, C. N. 2017. Using ocean models to predict spatial and temporal variation in marine carbon isotopes. *Ecosphere* 8(5): e01763.

Mariotti, A., Lancelot, C., and Billen, G. 1984. Natural isotopic composition of nitrogen as a tracer of origin for suspended organic matter in the Scheldt estuary. *Geochimica et Cosmochimica Acta* 48(3): 549-555.

McMahon, K.W., Hamady, L.L., and Thorrold, S.R. 2013. A review of ecogeochemistry approaches to estimating movements of marine animals. *Limnology and Oceanography* 58(2): 697–714.

Minagawa, M. and Wada, E. 1984. Stepwise enrichment of δ^{15}N along food chains: Further evidence and the relation between δ^{15}N and animal age. *Geochimica et Cosmochimica Acta* 48(5): 1135-1140.

Montoya, J.P. 2007. Natural abundance of δ^{15}N in marine planktonic ecosystems. In: Michener, R. and Lajtha, K. (Eds.), Stable Isotopes in Ecology and Environmental Science, second ed. Blackwell Publishing, Malden, Massachusetts, pp. 176–201.

Montoya, J.P., Carpenter, E.J., and Capone, D.G. 2002. Nitrogen fixation and nitrogen isotope abundances in zooplankton of the oligotrophic North Atlantic. *Limnology and Oceanography* 47: 1617–1628.

Murawski, S. A., Peebles, E. B., Gracia, A., Tunnell, J. W., and Armenteros, M. 2018. Comparative abundance, species composition, and demographics of continental shelf fish assemblages throughout the Gulf of Mexico. *Marine and Coastal Fisheries* 10(3): 325-346.

Muscatine, L., Porter, J.W., and Kaplan, I.R. 1989. Resource partitioning by reef corals as determined from stable isotope composition. 1. δ^{13}C of zooxanthellae and animal tissue vs depth. *Marine Biolog*y 100: 185–193.

Needoba, J. A., Waser, N. A., Harrison, P. J., and Calvert, S. E. 2003. Nitrogen isotope fractionation in 12 species of marine phytoplankton during growth on nitrate. *Marine Ecology Progress Series* 255: 81-91.

Nelson, J., Wilson, R., Coleman, F., Koenig, C., DeVries, D., Gardner, C., and Chanton, J. 2012. Flux by fin: fish-mediated carbon and nutrient flux in the northeastern Gulf of Mexico. *Marine Biology* 159(2): 365-372.

Nerot, C., Lorrain, A., Grall, J., Gillikin, D. P., Munaron, J. M., Le Bris, H., and Paulet, Y. M. 2012. Stable isotope variations in benthic filter feeders across a large depth gradient on the continental shelf. *Estuarine, Coastal and Shelf Science* 96: 228–235.

Olson, R. J., Popp, B. N., Graham, B. S., Lopez-Ibarra, G. A., Galvan-Magana, F., LennertCody, C. E., Bocanegra-Castillo, N., Wallsgrove, N. J., Gier, E., Alatorre-Ramirez, V., Balance, L.T., Fry, B. 2010. Food-web inferences of stable isotope spatial patterns in copepods and yellowfin tuna in the pelagic eastern Pacific Ocean. *Progress in Oceanography* 86: 124–138.

O'Reilly, C. M., Hecky, R. E., Cohen, A. S., and Plisnier, P. D. 2002. Interpreting stable isotopes in food webs: recognizing the role of time averaging at different trophic levels. *Limnology and Oceanography* 47: 306–309.

Peterson, B. J. and B. Fry. 1987. Stable isotopes in ecosystem studies. *Annual Review of Ecology and Systematics* 18: 293–320.

Pinnegar, J. K. and Polunin, N. V. C. 1999. Differential fractionation of delta C-13 and delta N-15 among fish tissues: implications for the study of trophic interactions. *Functional Ecology* 13(2): 225-231.

Popp, B. N., Laws, E. A., Bidigare, R. R., Dore, J. E., Hanson, K. L., and Wakeham, S. G. 1998. Effect of phytoplankton cell geometry on carbon isotopic fractionation. *Geochimica et Cosmochimica Acta* 62(1): 69-77.

Post, D. M. 2002. Using stable isotopes to estimate trophic position: Models, methods, and assumptions. *Ecology* 83(3): 703-718.

Quillfeldt, P., Ekschmitt, K., Brickle, P., McGill, R. A., Wolters, V., Dehnhard, N., and Masello, J. F. 2015. Variability of higher trophic level stable isotope data in space and time – a case study in a marine ecosystem. *Rapid Communications in Mass Spectrometry* 29(7): 667-674.

R Core Team. 2020. R: A language and environment for statistical computing. R Foundation for Statistical Computing, Vienna, Austria. URL https://www.R-project.org/

Radabaugh, K. R., Hollander, D. J. and Peebles, E. B. 2013. Seasonal $\delta^{13}C$ and $\delta^{15}N$ isoscapes of fish populations along a continental shelf trophic gradient. *Continental Shelf Research* 68: 112-122.

Radabaugh, K. R. and Peebles, E. B. 2014. Multiple regression models of $\delta^{13}C$ and $\delta^{15}N$ for fish populations in the eastern Gulf of Mexico. *Continental Shelf Research* 84:158-168.

Radabaugh, K. R., Malkin, E. M., Hollander, D. J., and Peebles, E. B. 2014. Evidence for light-environment control of carbon isotope fractionation by benthic microalgal communities. *Marine Ecology Progress Series* 495: 77-90.

Rau, G. H., Riebesell, U., and Wolf-Gladrow, D. 1996. A model of photosynthetic ^{13}C fractionation by marine phytoplankton based on diffusive molecular CO_2 uptake. *Marine Ecology Progress Series* 133: 275-285.

Rooker, J. R., Stunz, G. W., Holt, S. A., and Minello, T. J. 2010. Population connectivity of red drum in the northern Gulf of Mexico. *Marine Ecology Progress Series* 407: 187-196.

Schloesser, R. W., Rooker, J. R., Louchuoarn, P., Neilson, J. D., and Secord, D. H. 2009. Interdecadal variation in seawater δ^{13}C and δ ^{18}O recorded in fish otoliths. *Limnology and Oceanography* 54(5): 1665-1668.

Smith, C. L. 1997. <u>National Audubon Society field guide to tropical marine fishes of the Caribbean, the Gulf of Mexico, Florida, the Bahamas, and Bermuda.</u> Alfred A. Knopf, Inc., New York. 720 p.

Vander Zanden, M. J. and J. B. Rasmussen. 1999. Primary consumer δ^{15}N and δ^{13}C and the trophic position of aquatic consumers. *Ecology*. 80: 1395–1404

Vander Zanden, M. J. and Rasmussen, J. B. 2001. Variation in $\delta^{15}N$ and $\delta^{13}C$ trophic fractionation: implications for aquatic food web studies. *Limnology and Oceanography* 46, 2061–2066.

Vander Zanden, H. B., Tucker, A. D., Hart, K. M., Lamont, M. M., Fujisaki, I., Addison, D. S., Mansfield, K. L., Phillips, K. F. Wunder, M. B., Bowen, G. J., Pajuelo, M., Bolten, A. B., and Bjorndal, K. A. 2015. Determining origin in a migratory marine vertebrate: a novel method to integrate stable isotopes and satellite tracking. *Ecological Applications* 25(2): 320-335.

Wallace, A. A., Hollander, D. J. and Peebles, E. B. 2014. Stable isotopes in fish eye lenses as potential recorders of trophic and geographic history. *PLOS One* 9(10): e108935 DOI: 10.1371/journal.pone.0108935

West, J. B., Bowen, G. J., Dawson, T. E., and Tu, K. P. (eds) (2010). <u>Isoscapes: Understanding movement, pattern, and process on Earth through isotope mapping</u>. New York, NY, Springer.

Chapter 3: Multiple regression models for Gulf of Mexico $\delta^{13}C$ and $\delta^{15}N$ isoscapes using satellite data

3.1 Chapter Summary

Modeled $\delta^{13}C$ and $\delta^{15}N$ isoscapes for the Gulf of Mexico (GOM) were created using the muscle tissue of Red Snapper (*Lutjanus campechanus*) and Yellowedge Grouper (*Epinephelus flavolimbatus*). The models were created using static (latitude, longitude, depth) and dynamic (satellite remote sensing products) predictor variables and length-corrected $\delta^{13}C$ and $\delta^{15}N$ values as response variables in multiple regression. The resulting models were used to create isoscapes reflecting the conditions from when samples were collected and seasonal isoscapes in an El Niño (2015) and a La Niña (2011) year to assess temporal variability. The Red Snapper $\delta^{13}C$ isoscapes depicted a trend of decreasing $\delta^{13}C$ values with depth everywhere except the southwestern GOM, where there was overall low spatial variability with a slight decrease in $\delta^{13}C$ values towards the Caribbean. The Yellowedge Grouper $\delta^{13}C$ isoscape depicted a trend of lower $\delta^{13}C$ values in the northwest GOM, higher $\delta^{13}C$ values in the southeast GOM, and the highest $\delta^{13}C$ values near the Mississippi River outflow and Laguna de Términos. The $\delta^{15}N$ isoscapes of both species depicted a trend of higher $\delta^{15}N$ values in areas of high productivity and lower $\delta^{15}N$ values in oligotrophic areas, most likely following a gradient of nitrogen derived from human and livestock waste to nitrogen derived from diazotrophic nitrogen fixation. Compared to the $\delta^{15}N$ models, the $\delta^{13}C$ models had lower predictive capability and performed more poorly when the model created using one species was used to predict the isotopic values of the other species. The predicted

models for $\delta^{13}C$ and $\delta^{15}N$ values showed very little seasonal or interannual temporal variation suggesting general spatial isotopic patterns are relatively consistent. These models of spatial and temporal isotopic variability may be useful for future stable isotope investigations of trophic level, basal resource dependence, and animal migration.

3.2 Background

For background on isoscapes and spatial $\delta^{13}C$ and $\delta^{15}N$ variation, see Chapter 2.

3.2.1 Temporal variation in isotopic baselines

Isotopic baselines may vary temporally as well as spatially if the underlying environmental processes that control inputs and fractionation change over time (Bowen and Revenaugh 2003). Temporal variation in $\delta^{13}C$ and $\delta^{15}N$ values has been observed at seasonal (Mariotti et al. 1984; Kline 1999; Kürten et al. 2013; Magozzi et al. 2017), annual (Kline 1999; Hannides et al. 2009; Rooker et al. 2010), and decadal (Schloesser et al. 2009) scales. Temperature, sunlight levels, and precipitation are the primary environmental factors that have the potential to change the spatial patterns or levels of isotopic baselines over time. Temperature can influence isotopic baselines in relation to growth rate and $[CO_2]$ as explained in Chapter 2, or through the degree of ocean stratification. Ocean stratification can influence the relative importance of nitrogen fixation (Montoya, 2007), and the degree of seasonal hypoxia and anoxia which allow for denitrification (Altabet et al. 1999). Interannual and, more often, seasonal differences in temperature and light environment can change the species composition and community structure of primary producers, which contribute the isotopic baselines (Magozzi et al. 2017). Seasonal differences in temperature and light environment can also affect isotopic

baselines through growth rate, particularly if light, rather than nutrients, limits growth in the winter months (Mariotti et al. 1984; Kline 1999). Precipitation location and intensity affects fluvial input to the Gulf of Mexico which will affect both δ^{13}C and δ^{15}N values through the input of nutrients and advection of particulate organic matter (Mariotti et al. 1984; Kürten et al. 2013). For all these reasons, it is potentially useful to create modeled isoscapes that are temporally dynamic.

Statistically modeled isoscapes have been created for terrestrial plant δ^{13}C values (Suits et al. 2005), phytoplankton δ^{13}C values (Hofmann et al. 2000, Magozzi et al. 2017), scallop δ^{15}N values (Jennings and Warr 2003), scallop δ^{13}C values (Barnes et al. 2009), and fish δ^{13}C and δ^{15}N values (Radabaugh and Peebles 2014) using various environmental parameters that commonly include latitude, longitude, and temperature. One study that used fish muscle from the West Florida Shelf in the Gulf of Mexico to create a statistically modeled isoscape found that spatial variation in δ^{13}C values was primarily driven by photosynthetic fractionation, primary producer species composition, and consumer reliance on benthic algae vs. phytoplankton as basal resources. The same study found spatial variation in δ^{15}N values was primarily driven by variation in nitrogen fixation and fluvial input (Radabaugh and Peebles 2014). This and other studies have demonstrated that models created using empirical data from one species can be used to predict isotopic values in other species with moderate accuracy (Jennings and Warr 2003; Barnes et al. 2009; Radabaugh and Peebles 2014), which suggests modeled isoscapes have the potential to be useful across multiple studies.

3.2.2 Objectives

One objective of the present study was to create temporally dynamic isoscapes of the continental shelf of the Gulf of Mexico using the $\delta^{13}C$ and $\delta^{15}N$ values of muscle from two reef fish species as response variables and a combination of temporally static (latitude, longitude, and depth) and temporally dynamic remote sensing parameters as predictors. Fish muscle has been chosen for this study using consumer tissue for an isoscape smooths out the small-scale spatial and temporal variation of primary producers (Vander Zanden and Rasmussen 2001; O'Reilly et al. 2002; Post 2002; Bump et al. 2007; Radabaugh et al. 2013). By modeling isotopic values using readily available environmental parameters, these can easily be applied to other studies in the region. A second objective of the present study was to evaluate potential interannual and seasonal variability predicted by the modeled isoscapes and whether the general spatial patterns in $\delta^{13}C$ and $\delta^{15}N$ values changed substantially over time.

3.3 Methods

The muscle samples used in this chapter are the same as those used in Chapter 2. Methods regarding muscle sample collection and isotopic analysis can be found in Chapter 2.

3.3.1 Remote sensing data collection

Data used in this paper were produced with the Giovanni online data system, which is developed and maintained by the National Aeronautics and Space Administration Goddard Earth Sciences Data and Information Services Center (NASA GES DISC; http://giovanni.gsfc.nasa.gov). Three-month averages of colored dissolved organic matter (CDOM; m^{-1}), chlorophyll a (Chl; mg/m^3), particulate organic carbon (POC; mg/m^3), particulate

inorganic carbon (PIC; mol/m^3), sea surface temperature (SST; °C), surface photosynthetically active radiation (PAR; Einstein/m^{2}day), and light attenuation at 490 nm [K_d(490); m^{-1}] data were obtained from MODIS-Aqua at 4 km resolution. NASA GES DISC defines particulate matter as particles that are caught by a filter with a 0.7 μm pore size, whereas dissolved matter passes through this filter. POC primarily consists of phytoplankton and organic detritus, whereas PIC primarily consists of biogenic calcium carbonate. Both are determined from remote sensing data through backscatter algorithms. The light attenuation coefficient of photosynthetically active radiation, K_d(PAR), was calculated from MODIS-Aqua derived light attenuation at 490 nm, K_d(490), using Equation 9 from Morel et al. 2007. PAR at depth, PAR(z), was calculated using water depth (z), K_d(PAR), and PAR (Kirk 1994).

$$PAR(z) = PAR * e^{-K_d*PAR*z}.$$

The value of each satellite product was assigned to each individual collection station from the pixel of satellite data closest to the latitude and longitude coordinates for the collection station. If the collection date of a station fell on the 15th of the month or later, the month of collection was included in the three-month average as well as the preceding two months. If the collection date of a station fell before the 15th of the month, the three-month average included the preceding three months and not the month of collection. The three-month time frame was selected to reflect muscle turnover time, which varies with fish species, growth, and metabolism. For muscle tissue in adult fish, isotopic half lives in diet-switch studies are generally on the order of 1.5 months to over half a year (McIntyre and Flecker 2006; Buchheister and Latour 2010; Nelson et al. 2011).

3.3.2 Data analysis and isoscape generation

Before the isoscape models were created, the data were modified in a few ways. First, regressions between both isotopes and standard length were performed to determine whether there was a significant trophic effect. Because both species had significant relationships between $\delta^{13}C$ and $\delta^{15}N$ values and standard length, residuals from isotope-length regressions (length-corrected $\delta^{13}C$ and $\delta^{15}N$ values) were used in place of unaltered isotopic values (hereafter referred to as $\delta^{13}C$ and $\delta^{15}N$ values). This was done to prevent spatial differences in species diet/trophic position from interfering with the spatial differences in baseline isotopic levels. Then, $\delta^{13}C$ and $\delta^{15}N$ values were averaged for each species by station to prevent stations with more individuals from arithmetically overwhelming the stations with fewer individuals. For stations with more than one sample, data from between two and eight muscle samples were averaged per station; at most stations, data from three samples were averaged. Shapiro-Wilk tests indicated that $\delta^{13}C$ and $\delta^{15}N$ values were normally distributed in both the original and length-corrected forms which allowed for the use of standard linear regression.

Remote sensing data were combined with static spatial data (latitude, longitude, water depth) collected at the time of the corresponding biological collections to be used as potential predictor variables for the multiple regression models of $\delta^{13}C$ and $\delta^{15}N$ values. Several transformations were evaluated to account for non-linear relationships between the datasets. Possible transformations were x^2, $Ln(x)$, $1/x$, and $\sqrt{x}$. Data were converted into absolute values for the purposes of the $Ln(x)$ and $\sqrt{x}$ transformations. After possible transformations were applied, the transformed or untransformed predictor variables were standardized by conversion into z-scores. Linear regression was performed between each predictor variable with each transformation and the $\delta^{13}C$ and $\delta^{15}N$ data (Appendix B). If a transformation increased the linear

model R^2_{adj} by 0.01 or greater, the transformed variable was used instead of the original.

Variables for the multiple regression models were chosen using stepwise selection and AIC. If a

model containing an additional variable did not decrease the AIC by at least 2, it was considered

no better than the previous model. If a variable had a coefficient that was not significantly

different from zero ($p > 0.1$), it was excluded from the dataset and the multiple regression was

re-run. Variance inflation factors (VIFs; Fox and Monette 1992) and Cook's distance (Cook and

Weisberg 1982; Fox 1997) were calculated for each model to evaluate the multicollinearity of

variables included in the model and outlier stations respectively. Based on Cook's distance, two

stations were excluded from the Red Snapper dataset and one station was excluded from the

Yellowedge Grouper dataset (Fox and Weisberg 2011). If variables within a model had VIFs

higher than five (James et al. 2013), the variable with the highest individual correlation with the

isotope in question (Appendix B) was retained, other high VIF variables were excluded, and the

multiple regression was re-run. This process was repeated until all variables included in the

model had coefficients significantly different from zero and VIFs lower than five. All the above

analyses were performed in R (version 4.0.5, R Core Team 2020). Residuals from the resulting

models were plotted spatially to evaluate if the models performed particularly well or poorly for

any regions of the Gulf of Mexico.

3.3.3 Temporal variability

     Isoscapes were created based on predicted $\delta^{13}C$ and $\delta^{15}N$ values from the multiple

regression models described above. Isoscapes were spatially interpolated using point kriging

with a linear variogram model with no drift and no nugget effect (Surfer version 19.1.189).

Isoscapes were limited to depths of 5-200 m for Red Snapper and 70-200 m for Yellowedge

Grouper to reflect the depth distributions of each species, with 200 m representing the nominal outer edge of the continental shelf. First, four isoscapes were created using remote sensing data from the collection dates of the original muscle samples (hereafter referred to as 'catchdate isoscapes'). Then, temporal variability in the isoscapes was assessed by obtaining remote sensing products from each season in a La Niña year (2011) and an El Niño year (2015) and using that data to predict $\delta^{13}C$ and $\delta^{15}N$ isoscapes in each of those seasons. The remote sensing data was gathered at the same locations as the original collection locations. Seasons within a year were defined as three consecutive month intervals starting in January of the year.

3.4 Results

A total of 1057 Red Snapper and 208 Yellowedge Grouper were caught on the research cruises in 2011, 2015, and 2016. Of these, 124 Red Snapper and 98 Yellowedge Grouper were analyzed for stable isotopes (Table 2.1). Red Snapper were caught at 48 stations around the Gulf of Mexico and Yellowedge Grouper were caught at 47 stations (Figure 2.1). Both species were captured throughout the Gulf of Mexico, excepting the southern West Florida Shelf where only Red Snapper was captured and only at a single station. Red Snapper were captured between 15 m and 140 m depth and Yellowedge Grouper were captured between 40 m and 345 m depth (10 stations at > 200m). There was only a single Yellowedge Grouper captured in water shallower than 85 m and the species is generally considered a deep-water species and therefore, despite a single fish being captured in shallower waters, the isoscapes were limited to a depth of 70 m to 200 m to reflect the general distribution of the species.

93

3.4.1 Isoscape models

All four multiple regression models created using remote sensing data were statistically significant (p-value < 0.05; Table 3.1). The model with the highest R^2_{adj} value was the Red Snapper δ^{15}N model ($R^2_{adj} = 0.875$). The model with the lowest R^2_{adj} value was the Red Snapper δ^{13}C model ($R^2_{adj} = 0.346$). The model that performed best when used to predict isotopic values for the other species was the Red Snapper δ^{15}N model ($R^2_{adj} = 0.568$). The model that performed the poorest when used to predict isotopic values for the other species was the Red Snapper δ^{13}C model ($R^2_{adj} = 0.052$). Because the predictor variables were standardized, the magnitude of the coefficients indicate the strength of the relationship between each predictor variable and the response variable, and the average predicted values were always the same for the same model. The δ^{13}C model for Red Snapper included *Depth^2*, *Long*, *1/PIC*, and *SST*. The coefficient with the greatest magnitude was *Depth^2*, which was also the best individual predictor of δ^{13}C values (Appendix B). The predicted values for the time and location of capture ranged from -0.70 to 0.49 with a standard deviation of 0.28 (Table 3.2). The δ^{13}C model for Yellowedge Grouper included *Ln(Chl)*, *Long*, *Lat^2*, and *Ln(PAR(z))*. The coefficient with the greatest magnitude was *Ln(Chl)*, which was the third-best individual predictor of δ^{13}C values after *Long* and *POC*. The predicted values time and location of capture ranged from -0.54 to 0.53 with a standard deviation of 0.25. The δ^{15}N model for Red Snapper included *Long*, *Ln(Chl)*, *Lat*, and *PAR*. The coefficient with the greatest magnitude was *Long*, which was a relatively poor individual predictor of δ^{15}N values ($R^2_{adj} = 0.064$). The predicted values time and location of capture ranged from -2.88 to 1.81 with a standard deviation of 1.28. The Yellowedge Grouper δ^{15}N model only included *Ln(CDOM)*, which was also the best individual predictor of δ^{15}N values. The predicted values time and location of capture ranged from -1.40 to 1.97 with a standard deviation of 0.95. When

the model created for one species was used to predict the length-corrected isotopic values for the

other species, the δ^{13}C models performed very poorly (both $R^2_{adj} < 0.1$), and the δ^{15}N models

performed moderately well (both $R^2_{adj} > 0.5$).

Table 3.1
A table of results from the δ^{13}C and δ^{15}N multiple regression models. Response variables were
length-corrected Red Snapper and Yellowedge Grouper muscle isotopic values, and predictor
variables were environmental parameters from remote sensing. Predictor variables were
transformed as indicated and standardized before model creation. Predictor variables are
presented in order of descending coefficient magnitude. The R^2_{adj} for the other species refers to
the model from the above species being used to predict isotopic values for the other species.

	Red Snapper	Yellowedge Grouper
δ^{13}C Model equation	LC_ δ^{13}C = -0.198*Depth^2 - 0.178*Long - 0.157*1/PIC - 0.130*SST + 0.015	LC_ δ^{13}C = 0.333*Ln(Chl) + 0.194*Long - 0.162*Lat^2 + 0.157*Ln(PAR(z)) - 0.002
R^2_{adj}	0.346	0.597
p-value	<0.001	<0.001
R^2_{adj} for other species	0.052	0.068
δ^{15}N Model equation	LC_ δ^{15}N = -0.991*Long + 0.746*Ln(Chl) + 0.724*Lat + 0.272*PAR - 0.016	LC_ δ^{15}N = 0.950*Ln(CDOM) + 0.036
R^2_{adj}	0.875	0.761
p-value	<0.001	<0.001
R^2_{adj} for other species	0.568	0.554

3.4.2 Catchdate isoscapes

The multiple regression models were used to predict δ^{13}C and δ^{15}N values at the original

capture locations at the original time of capture, and these predicted values were used to create

isoscapes (catchdate isoscapes; Figure 3.1). Patterns seen in the catchdate isoscapes were similar

to those seen in the empirical isoscapes created in Chapter 2 (Figure 3.2) though the models had

a smoothing effect on the overall patterns. The Red Snapper δ^{13}C isoscape depicted a general

pattern of decrease with depth in the northern Gulf of Mexico, the West Florida Shelf, and the

Yucatan Peninsula, but that pattern ended towards the western Gulf of Mexico and Campeche

Bay. Instead, there appears there was a slight relative high near Laguna de Términos in

Campeche Bay and consistent medium-high values in the western Gulf of Mexico. The highest

overall values were seen near the Nueces River outflow and near the northern West Florida

Shelf, and the lowest value was seen at the outer mid-West Florida Shelf. The Yellowedge

Grouper δ^{13}C isoscape did not depict a depth gradient, likely because the catch locations of

Yellowedge Grouper did include shallower regions of the shelf. Instead, the Yellowedge Grouper

δ^{13}C isoscape had its highest values near Laguna de Términos and medium high values in the

eastern Gulf of Mexico with a slight relative high near the Mississippi River outflow. The lowest

values in the Yellowedge Grouper δ^{13}C isoscape were found in the northwest Gulf of Mexico.

Table 3.2
A table of the maxima (Max), minima (Min), means, and standard deviations (Stdev) of length-corrected δ^{13}C and δ^{15}N values predicted for El Niño and La Niña years. Values were predicted using the statistical models created in this study (Table 3.1). The values from the "catchdate" rows were predicted for the time period each respective station was sampled. The El Niño isoscapes rows were calculated using every value from the four seasonal isoscapes within the El Niño year (2015) and the La Niña isoscape rows were calculated using every value from the four seasonal isoscapes within the La Niña year (2011). The El Niño – La Niña rows were calculated using the differences between El Niño and La Niña values for each station in each seasonal isoscape (i.e., Station 1240 El Niño Jan-March δ^{13}C – Station 1240 La Niña Jan-March δ^{13}C).

	Red Snapper				Yellowedge Grouper			
Length-corrected δ^{13}C values	**Max**	**Min**	**Mean**	**Stdev**	**Max**	**Min**	**Mean**	**Stdev**
Catchdate Isoscape	0.49	-0.70	0.01	0.28	0.53	-0.54	<0.01	0.25
La Niña Isoscapes	0.78	-0.87	0.01	0.35	0.92	-0.84	<0.01	0.32
El Niño Isoscapes	0.83	-0.98	0.01	0.36	0.87	-0.67	<0.01	0.29
El Niño - La Niña	0.48	-0.53	<0.01	0.18	0.39	-0.39	<0.01	0.13
Length-corrected δ^{15}N values	**Max**	**Min**	**Mean**	**Stdev**	**Max**	**Min**	**Mean**	**Stdev**
Catchdate Isoscape	1.81	-2.88	-0.02	1.28	1.97	-1.40	0.04	0.95
La Niña Isoscapes	2.58	-3.11	-0.02	1.17	2.95	-1.83	0.04	0.94
El Niño Isoscapes	2.52	-2.54	-0.02	1.14	2.43	-1.42	0.04	0.94
El Niño - La Niña	1.05	-1.10	<0.01	0.39	1.60	-1.57	<0.01	0.58
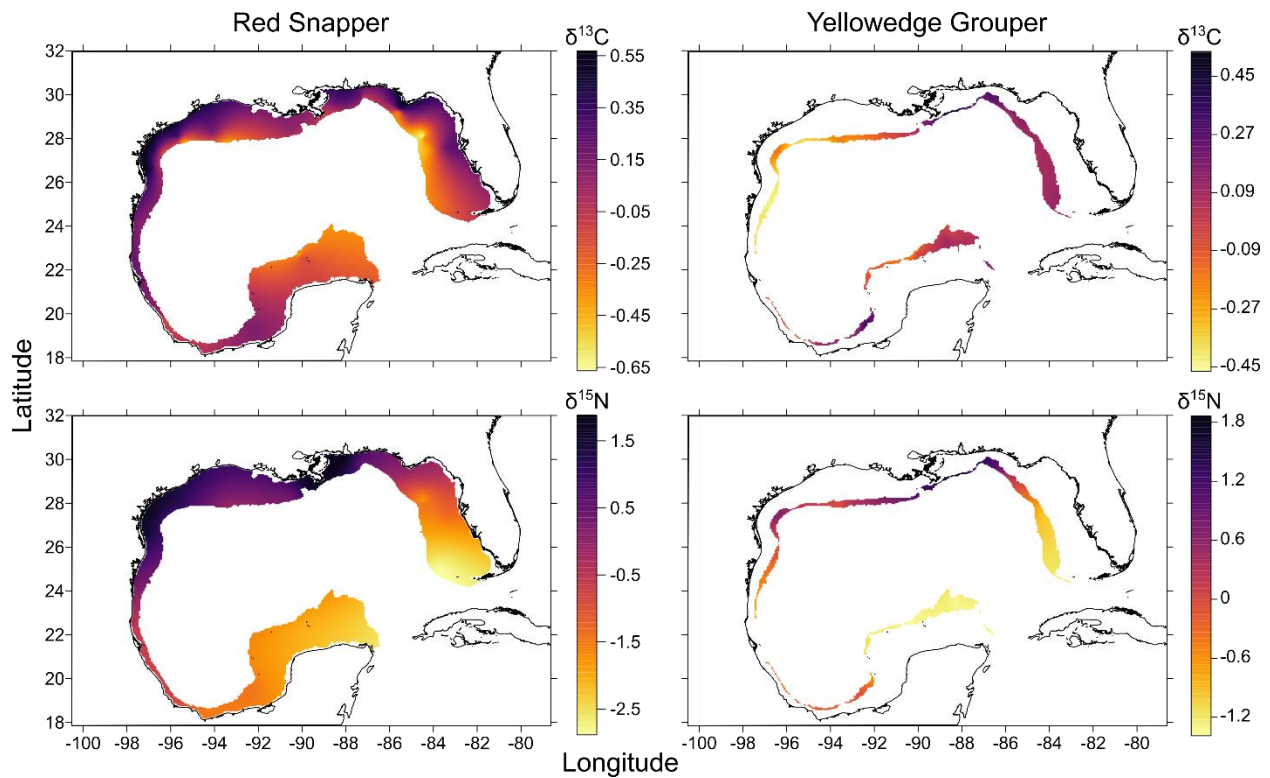
Figure 3.1
Isoscapes created for length-corrected $\delta^{13}C$ (top) and $\delta^{15}N$ (bottom) values using the predicted isotopic values from the statistical models (Table 3.1). Isotopic values were predicted using satellite products from the three months prior to the catch date as described in the methods section.

Both species' $\delta^{15}N$ isoscapes depicted higher values in the northwest Gulf of Mexico and lower values near the Caribbean. The Red Snapper $\delta^{15}N$ isoscape had its highest predicted values near the outflows of the Nueces River and Mississippi River. The lowest value was predicted on the southwest Florida Shelf near the Florida Keys. The Yellowedge Grouper $\delta^{15}N$ isoscape also had its highest values near the Mississippi River outflow, but the predicted values were lower near the Nueces River outflow. The lowest predicted values for Yellowedge Grouper were off the Yucatan Peninsula. Both species had relative highs near river outflows excepting Laguna de Términos, where neither isoscape depicted high values. Both isoscapes had their lowest values at the station closest to the Caribbean.

97
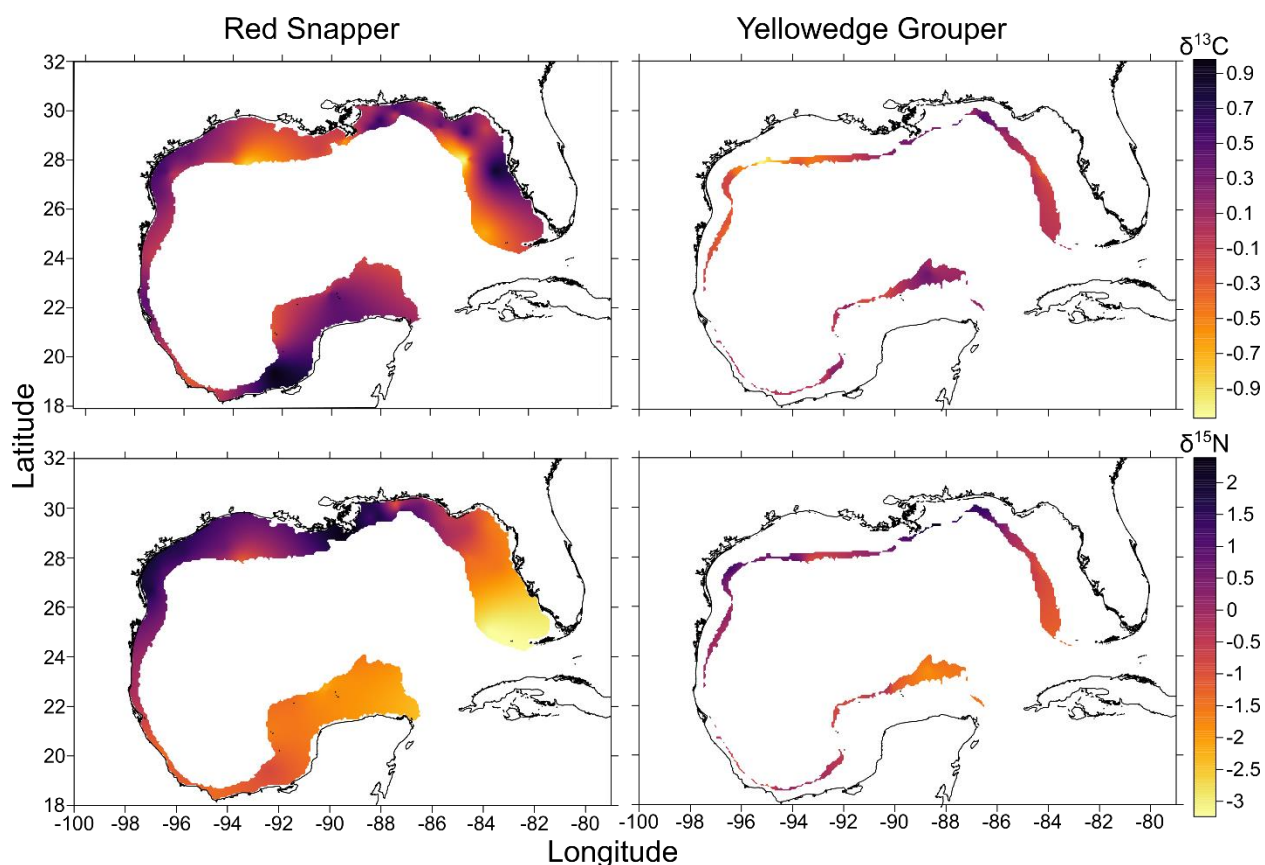
Figure 3.2
Empirical isoscapes of length-corrected $\delta^{13}C$ and $\delta^{15}N$ values for Red Snapper and Yellowedge Grouper (same as those in Chapter 2). Kriging was removed beyond the nominal edge of the continental shelf (the 200 m isobaths) and landward of the 5 m and 70 m isobaths respectively for Red Snapper and Yellowedge Grouper to reflect the distributions of each species.

Residuals (predicted - measured) of each model were plotted spatially to determine if the models did particularly well or poorly in any area (Figure 3.3). The Red Snapper model had a particularly low $\delta^{13}C$ residual (predicted value was too low) near Laguna de Términos. This station's measured value was based on two fish that had similar, non-anomalous $\delta^{13}C$ values, so this station does not appear to be an outlier. The Yellowedge Grouper model had a cluster of low $\delta^{13}C$ residuals near the Mississippi River outflow but there are also several stations in the area with high $\delta^{13}C$ residuals which suggests that area may have spatial or temporal (since one of the

98

stations with a high $\delta^{13}C$ residual was from 2015 whereas the rest were from 2011) variability that was not captured by the model. It appears the Red Snapper $\delta^{15}N$ model generally predicted lower values than the measured values. The Yellowedge Grouper $\delta^{15}N$ model residuals are generally closer to zero with a few scattered stations where the model performed more poorly.
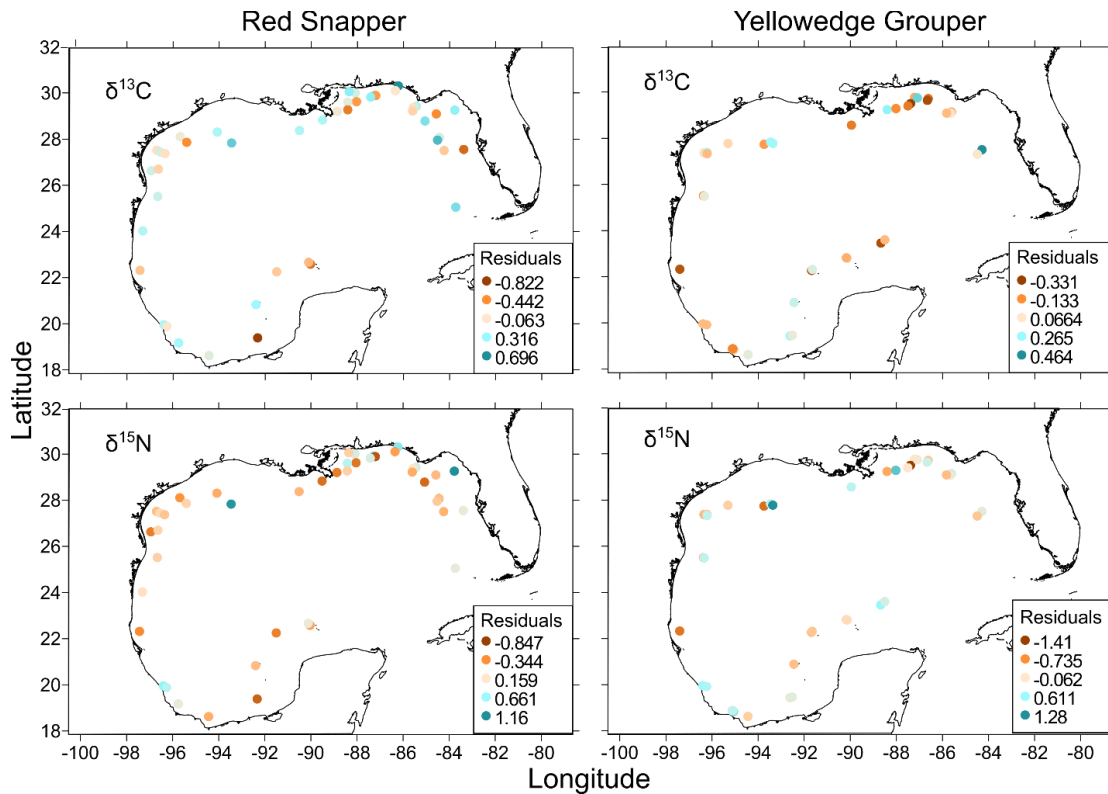
Figure 3.3
Spatially plotted residuals (predicted - measured) from the length-corrected $\delta^{13}C$ (top) and $\delta^{15}N$ (bottom) values predicted by multiple regression models for the times and locations of data collection. Residuals are plotted on a continuous color scale wherein darker orange colors represent stations where predicted length-corrected $\delta^{13}C$ or $\delta^{15}N$ values were lower than the measured length-corrected $\delta^{13}C$ or $\delta^{15}N$ values and darker blue colors represent stations where predicted values were higher than measured values.

3.4.3. Temporal variability

The models created for each species and isotope were also used to predict isotopic values at the sampling stations in different seasons and years. Those predicted values were used to

create isoscapes to assess if the general patterns seen in the catchdate isoscapes were stable at seasonal and interannual scales (Figures 3.4-3.7). The average predicted values for each species for each isotope were the same as those in the catchdate isoscapes due to the predictor variables being standardized (Table 3.2). Generally, the spatial patterns described in the above section for the catchdate isoscapes persisted regardless of season or year. The isoscapes created in El Niño (2015) and La Niña (2011) years had very similar maximum and minimum predicted values and the standard deviations of those values were also very similar. The δ^{15}N isoscapes in the La Niña year had higher maximum and lower minimum predicted values for both Red Snapper and Yellowedge Grouper than in the El Niño year. The maxima and minima for the predicted δ^{13}C values were not consistently higher or lower in the El Niño isoscapes or the La Niña isoscapes. The average difference between the predicted values at each station in the El Niño year and the La Niña year were less than 0.01 for each isotope and species. The greatest difference in values calculated for δ^{13}C was at a station off the Yucatan Peninsula where the La Niña value predicted by the Red Snapper model was 0.53 higher than the value predicted in the El Niño year. The greatest difference calculated for δ^{15}N values was at a station in the central west Gulf of Mexico where the value predicted by the Yellowedge Grouper model in the El Niño year was 1.60 higher than the value predicted in the La Niña year. The δ^{13}C modeled isoscape with the highest spatial variability (based on maximum, minimum, and standard deviation) was for Yellowedge Grouper in the September-December season of the La Niña year though its variability was still lower than that of the measured Red Snapper δ^{13}C values (Appendix C). The δ^{15}N modeled isoscape with the highest spatial variability based on standard deviation was for Red Snapper isoscape in the April-June season of the La Niña year and the δ^{15}N modeled isoscape with the highest maximum

100

and lowest minimum predicted values was for Red Snapper in the October-December season of the La Niña year.

The Red Snapper δ^{13}C model (Figure 3.4) appears to have had more seasonal and interannual variability than the Yellowedge Grouper δ^{13}C model. In both the El Niño year (2015) and the La Niña year (2011), the Campeche Bay region of the Gulf of Mexico had higher δ^{13}C values in the July-September season than in other seasons. During the same season, the Northern Gulf of Mexico had lighter δ^{13}C values than in other seasons. The highest overall δ^{13}C values were seen in the northwest Gulf of Mexico though those values were overall slightly lighter in the Oct-Dec season. There is also an area of low δ^{13}C values near the edge of the shelf in that region in the Jan-March season thought the nearshore δ^{13}C values remain high, similar to other seasons. In general, there was a gradient on the West Florida Shelf with higher δ^{13}C values in the northeast and lower values in the southwest. In the La Niña year (2011), the gradient covered the largest difference in values in the October-December season and the January-March season, whereas in the El Niño year (2015), the gradient did not cover as wide a range of values in general and is weakest in the January-March season. In the La Niña year, the Yucatan Peninsula had the lightest δ^{13}C values in the October-December season, whereas in the El Niño year, it had the lightest values in the January-March season.
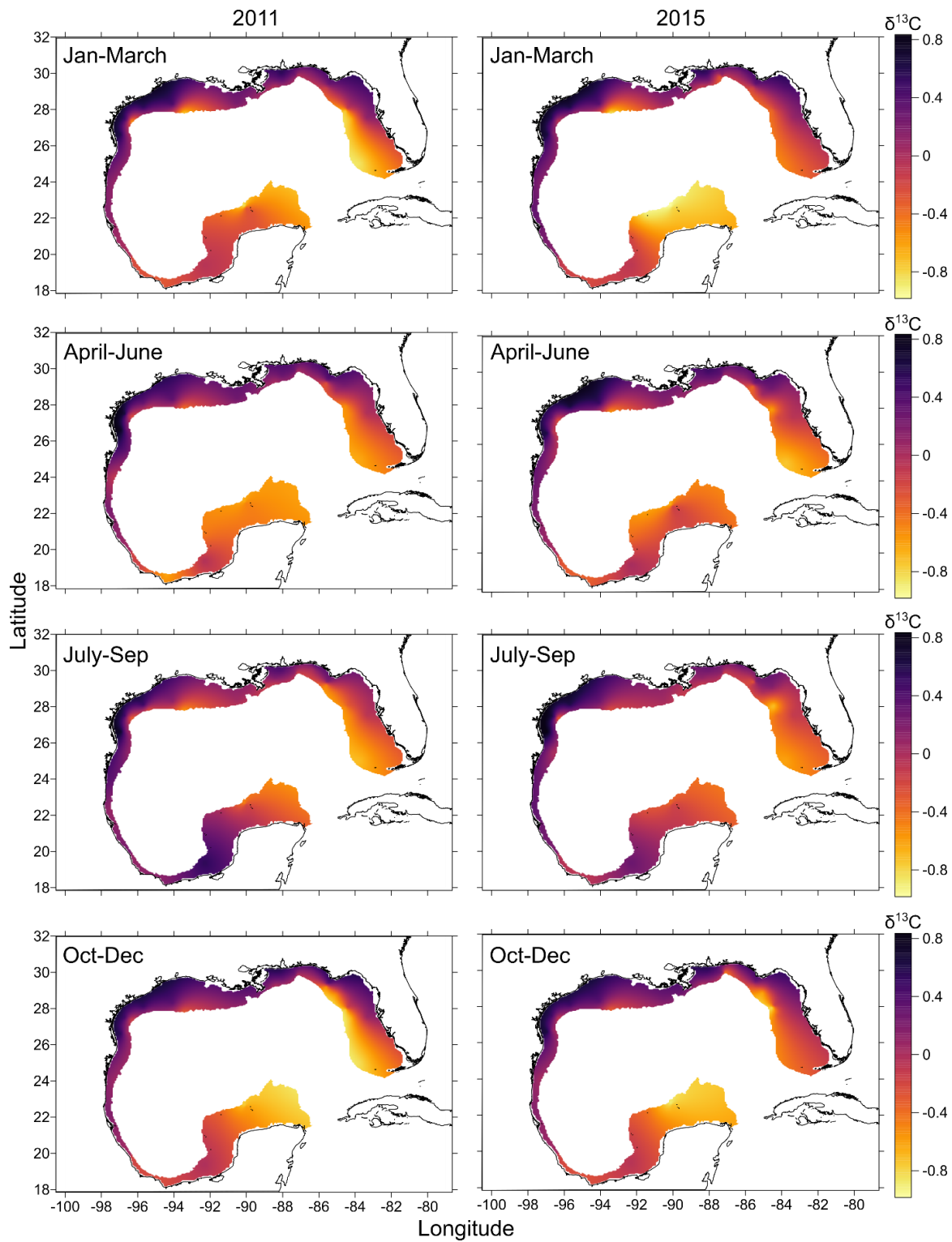
Figure 3.4
Isoscapes created for length-corrected $\delta^{13}C$ values using the model developed with Red Snapper (Table 3.1) for seasons within a La Niña year (2011) and an El Niño year (2015).
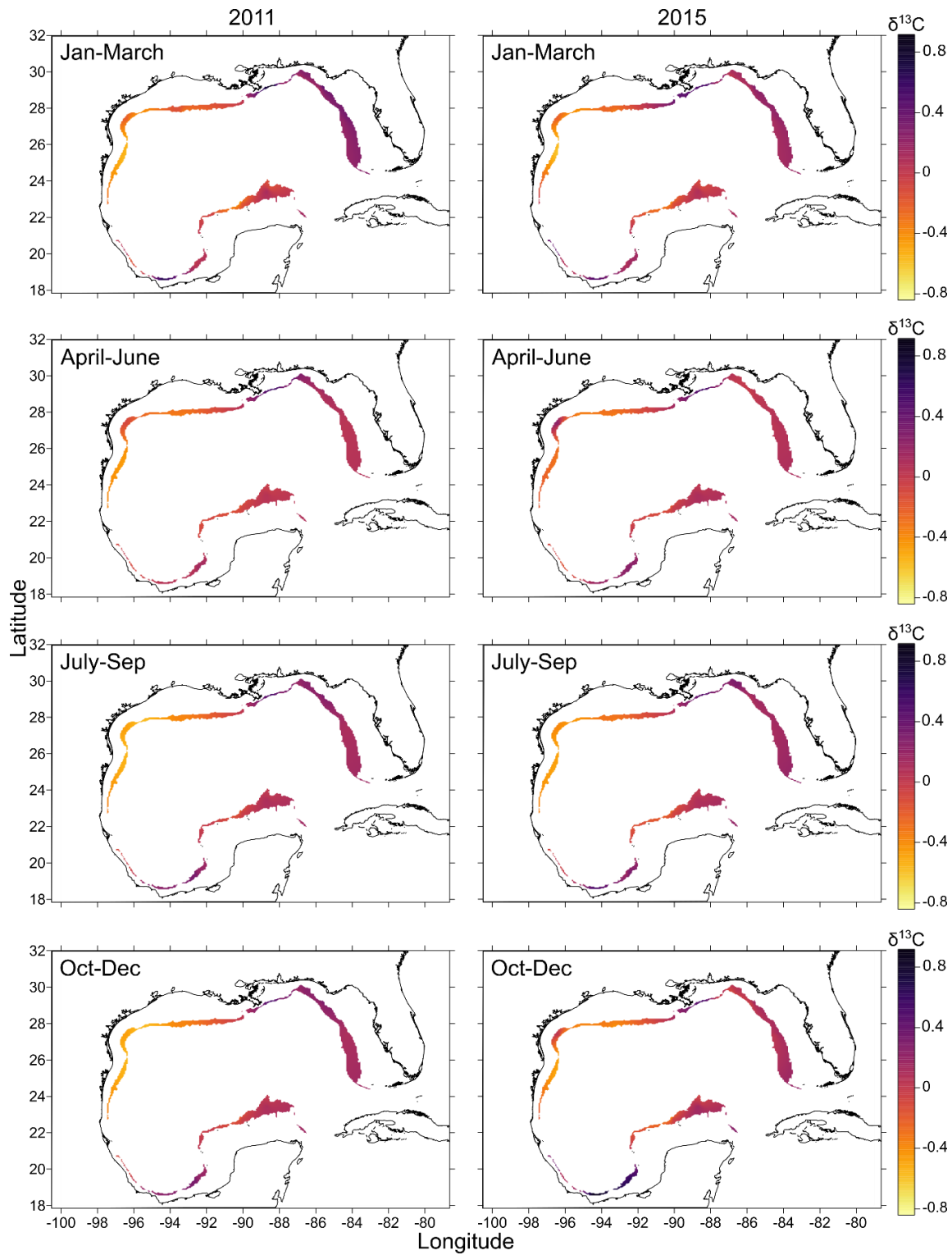
Figure 3.5
Isoscapes created for length-corrected $\delta^{13}C$ values using the model developed with Yellowedge Grouper (Table 3.1) for seasons within a La Niña year (2011) and an El Niño year (2015).
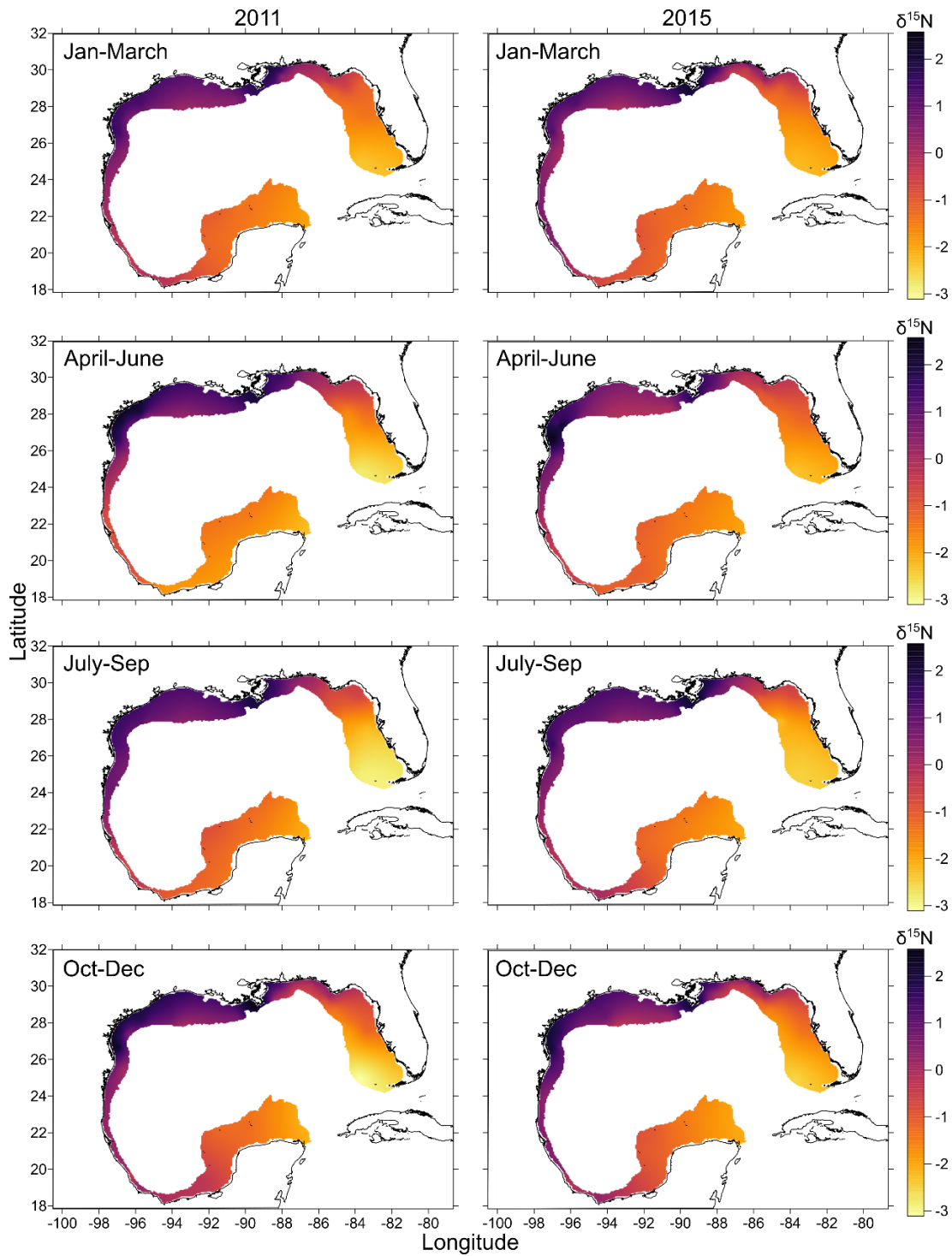
Figure 3.6
Isoscapes created for length-corrected δ^{15}N values using the model developed with Red Snapper
(Table 3.1) for seasons within a La Niña year (2011) and an El Niño year (2015).
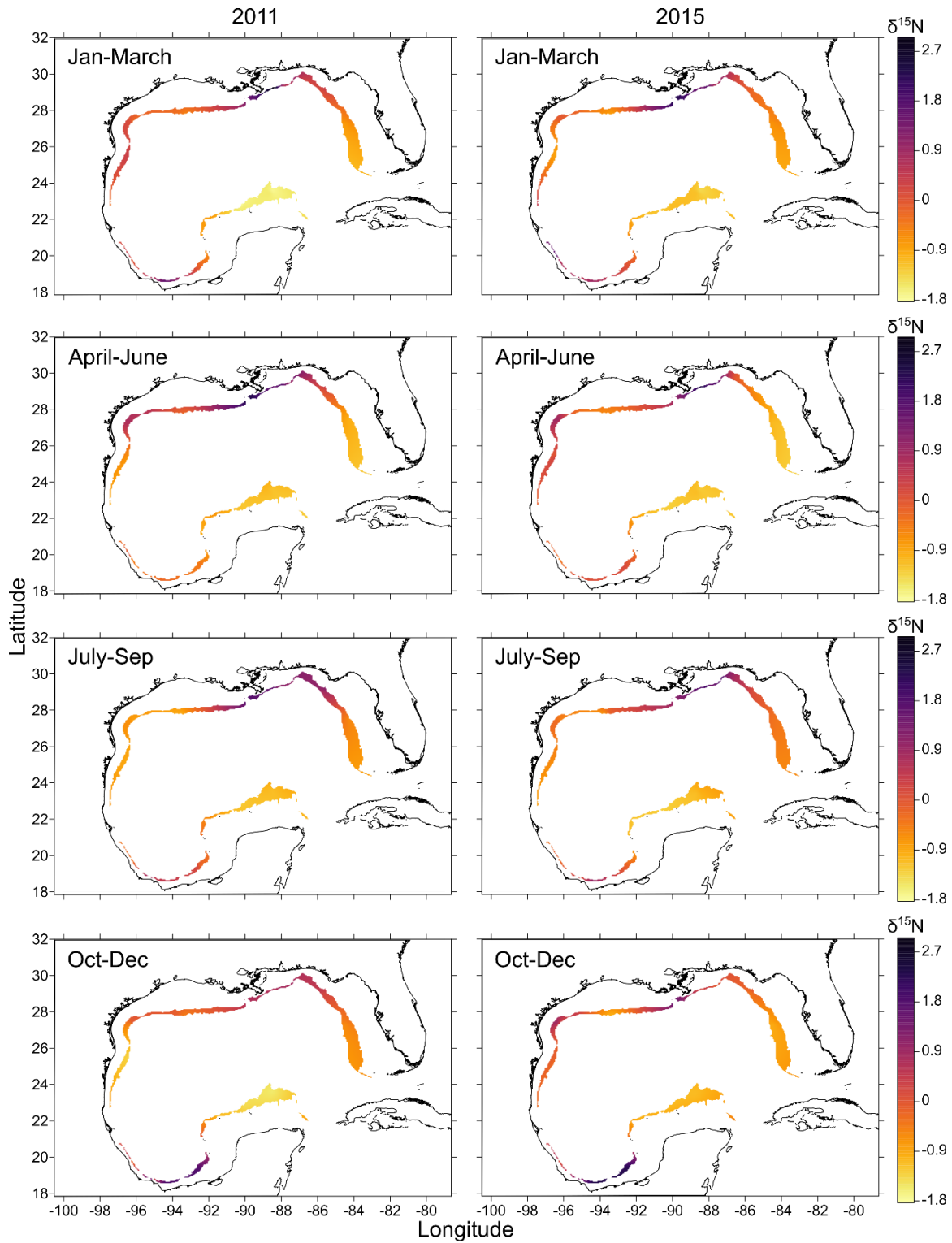
Figure 3.7
Isoscapes created for length-corrected $\delta^{15}N$ values using the model developed with Yellowedge Grouper (Table 3.1) for seasons within a La Niña year (2011) and an El Niño year (2015).

The Yellowedge Grouper $\delta^{13}C$ isoscapes (Figure 3.5) showed very little seasonal or interannual variability. One slight anomaly to the general patterns in the Yellowedge Grouper $\delta^{15}N$ isoscapes was that the area near the Nueces River outflow had slightly higher $\delta^{15}N$ values in the April-June and October-December seasons the El Niño year compared to the La Niña year. A second anomaly was that the October-December season in the El Niño year had higher $\delta^{13}C$ values in near Laguna de Términos than in the La Niña year. Those high $\delta^{13}C$ values were also the highest seen overall in all the Yellowedge Grouper isoscapes.

In the Red Snapper $\delta^{15}N$ model, there was very little seasonal or interannual variability in the overall patterns of change in the Gulf of Mexico other than some slight changes in a few regions (Figure 3.6). The area near the Mississippi River outflow generally had some of the highest $\delta^{15}N$ values in the isoscape. In the April-June and October-December season, the area near the Nueces River outflow had similarly high $\delta^{15}N$ values with an area of relatively lower $\delta^{15}N$ values between the two rivers. In the January-March and July-September seasons, there was not a second high $\delta^{15}N$ value area near the Nueces River outflow, and the relatively lower $\delta^{15}N$ values were more ubiquitous in the entire northwestern Gulf of Mexico. There was some seasonal variability in the $\delta^{13}C$ values at the southwest edge of the West Florida Shelf during the La Niña year (lowering over the course of the year) and in the El Niño year, that same area stayed at the (relatively higher) values depicted in the January-March season.

The Yellowedge Grouper modeled $\delta^{15}N$ isoscapes (Figure 3.7) showed slightly more variability than the modeled $\delta^{13}C$ isoscapes, but the general patterns of increase and decrease were similar among all isoscapes. Seasonally, there were slight differences in the magnitude of $\delta^{15}N$ values in different areas even though general patterns were maintained. First, it appeared that the area near the Nueces River outflow had higher $\delta^{15}N$ values in the April-June season.

Second, the area near Laguna de Términos had higher $\delta^{15}N$ values in the January-March season, and the highest values occurred in the October-December season. Third, the area near the Mississippi River outflow had relatively lower $\delta^{15}N$ values in the October-December season (compared to other seasons), and those relatively high (compared to the surrounding area) values did not extend as far out to the east and west from that region. The only interannual difference among isoscapes was on the Yucatan Peninsula which had lower $\delta^{15}N$ values in the January-March and October-December seasons in the La Niña year whereas the values remained relatively unchanged seasonally in the El Niño year.

3.5 Discussion

3.5.1 Spatial isoscape patterns

The modeled Red Snapper $\delta^{13}C$ isoscapes depicted a pattern of decrease with depth in the northern Gulf of Mexico (indicated in the equation as a negative coefficient on *Depth^2*) and decreasing values closer to the Caribbean in the southern Gulf of Mexico (indicated in the equation as a negative coefficient on *Long* and on *SST*). As was the case with the empirical isoscapes, the depth gradient observed in most areas could be attributed to an increase in productivity nearshore and/or decrease in the importance of benthic primary producers with depth as a result of decreased light availability at depth (Cooper and DeNiro 1989; Muscatine et al. 1989). At a global scale, the $\delta^{13}C$ values of phytoplankton often covary with SST which is usually attributed to SST's effect on growth rates, $[CO_2]$, and rates of CO_2 uptake (Goericke and Fry 1994; Hinga et al. 1994; Gruber et al. 1999; McMahon et al. 2013; Magozzi et al. 2017). However, at global scales, the $\delta^{13}C$ values of phytoplankton generally increase with increased temperature, which is the opposite pattern observed in this dissertation. The $\delta^{13}C$ model also

included *1/PIC*. PIC tends to align with depth/productivity gradients (Acker and Leptoukh 2007) which would suggest it would be redundant with *Depth^2* but, its inclusion suggests it is explaining additional variation, likely through its relationship with lithography (Daniels et al. 2012) and/or its temporal variation.

The Yellowedge Grouper δ^{13}C modeled isoscape depicts a very different pattern from the Red Snapper δ^{13}C modeled isoscape. There was no depth gradient present, most likely because Yellowedge Grouper were captured within a spatially narrower and deeper depth range where benthic primary producers are likely to be less influential. However, *Ln(PAR(z))* was one of the variables included in the Yellowedge Grouper δ^{13}C model which suggests there was some influence from light environment, though it was the least influential of the selected variables based on coefficients. The variable with the largest coefficient was *Ln(Chl)*. Chlorophyll was likely included in the model because of the relationship between productivity and fractionation mentioned above (Popp et al. 1998; Hofmann et al. 2000). Near the edge of the continental shelf, where most Yellowedge Grouper were captured, chlorophyll tends to be lower and less variable than it is near the coastline (Acker and Leptoukh 2007), but the high coefficient on *Chl* suggest that small changes in chlorophyll are associated with relatively large changes in δ^{13}C values. *Ln(Chl)* is most likely the variable that is responsible for the areas of high δ^{13}C values near the Mississippi River outflow and near Laguna de Términos in the modeled isoscape. Both *Ln(Chl)* and *Ln(PAR(z))* have positive coefficients which suggest contradictory processes (areas with high chlorophyll would likely have higher K_d and consequently, lower *Ln(PAR(z))*). It could be that areas of high, variable primary productivity dominate the δ^{13}C patterns but, in areas with lower, less spatially variable productivity (i.e., closer to the Caribbean) the light environment and amount of benthic vs planktonic production is more influential. There is also a pattern of lower

δ^{13}C values in the northwest Gulf of Mexico and medium-high values in the southeast Gulf of Mexico. Rather than having a clear process-based cause in the model equation, this pattern seems to be primarily caused by the positive coefficient on *Long* and the negative coefficient on *Lat^2* which suggests that there are influential variables and processes not included in the statistical model.

The modeled δ^{15}N isoscapes depicted very similar spatial patterns for Red Snapper and Yellowedge Grouper. Overall, δ^{15}N values were lower in oligotrophic areas and higher near areas of freshwater input. This pattern matches that in the empirical isoscapes and has the same explanation regarding the sources of bioavailable nitrogen in these areas. Areas near freshwater input will have high chlorophyll and CDOM which is the likely reason for the inclusion of *Ln(Chl)* in the Red Snapper model and *Ln(CDOM)* in the Yellowedge Grouper model, both with positive coefficients. *Ln(CDOM)* was the only variable included in the Yellowedge Grouper δ^{15}N model whereas the Red Snapper δ^{15}N model also included *Lat*, *Long*, and *PAR*. The inclusion of *Lat* and *Long* suggest there are other variables that account for spatial patterns in Red Snapper δ^{15}N values that were not included in the statistical model. The values for *PAR* are calculated at the surface of the water so they are primarily a function of weather, latitude, and season. Average PAR will decease with latitude, but both *Lat* and *PAR* were selected for the Red Snapper δ^{15}N model which suggests *PAR* was explaining variation in δ^{15}N values not explained by *Lat* (likely temporal variation).

3.5.2 Temporal variability in the isoscapes

Overall, the modeled isoscapes showed very little temporal variability in the general spatial patterns of δ^{13}C and δ^{15}N values in the Gulf of Mexico. One reason for this could be that,

since this dissertation used higher trophic level consumers, any temporal variability was dampened by the relatively long turnover times of fish muscle (Post 2002). Another potential reason the statistical models did not depict high spatial or temporal variation could be that the predictor variables were standardized. Whereas standardizing the variables prevented variables with larger magnitude values from dominating results and allowed for coefficients in the model equations to equate to the relative strength of the relationship between each predictor variable and the explanatory variable, it also decreased the overall variability of each predictor variable (e.g., forced the standard deviation to be 1). Therefore, any seasonal or inter-annual extremes may have been dampened.

Whereas there was little temporal variability overall, the isoscapes were not fully static and the variables selected by the models give some indication for which processes may be influential over time. For Red Snapper $\delta^{13}C$ values, the temporally variable variables included in the model are *1/PIC* and *SST*, and the area that was predicted to experience the most temporal (seasonal) variability is the Campeche Bay and Yucatan Peninsula area. In general, the model predicted higher $\delta^{13}C$ values in the spring and summer than in the fall and winter. PIC did vary temporally (it is generally higher in the winter; Acker and Leptoukh 2007), but it is difficult to determine what affect this has on $\delta^{13}C$ values since the 1/x transformation indicated *PIC* had the largest influence on $\delta^{13}C$ values at *PIC* values nearest to 0 (after standardization). That being said, *SST* was not the likely cause of the higher $\delta^{13}C$ values in spring and summer since it had a negative coefficient in the equation, meaning the warmer summer months would have been associated with lower $\delta^{13}C$ values. This is the opposite pattern expected based on previous studies comparing $\delta^{13}C$ values and SST (Goericke and Fry 1994; Hinga et al. 1994; Gruber et al. 1999; McMahon et al. 2013; Magozzi et al. 2017). Instead, it is possible that SST may have had

an influence on (or been a proxy for) spatial and/or temporal variation in primary producer species composition (Magozzi et al. 2017) which could explain its inclusion in the Red Snapper $\delta^{13}C$ model.

The temporal variability in the $\delta^{15}N$ isoscapes of both species appeared to primarily be related to freshwater inflow. *Ln(CDOM)* was the only variable included in the Yellowedge Grouper $\delta^{15}N$ model which is primarily a combination of organics from terrestrial sources and phytoplankton, both of which will increase with increased freshwater input (Chen et al. 2004; Branco and Kremer 2005). The Red Snapper model included *Ln(Chl)* which is also highly influenced by freshwater input. The $\delta^{15}N$ isoscapes showed the most predicted variability around areas of freshwater input (the Nueces River outflow, the Mississippi River outflow, and, for Yellowedge Grouper, Laguna de Términos). The likely mechanism behind these patterns is the effect of freshwater input on $\delta^{15}N$ values through delivery of nutrients to primary producers and the advection of POM (Mariotti et al. 1984; Kürten et al. 2012).

The Red Snapper $\delta^{15}N$ model also included *PAR* which is likely primarily related to temporal variability (seasonality) rather than spatial variability since there is almost no spatial variability in PAR during summer months (Acker and Leptoukh 2007). In the $\delta^{15}N$ model, *PAR* was most likely explaining variability induced by samples collected in early vs late summer and in different years. *PAR* had a positive coefficient which indicates $\delta^{15}N$ values are higher under higher light conditions. Temporal differences in average surface PAR could have potentially affected $\delta^{15}N$ values through light limitation. It is generally assumed that there is little to no photosynthetic fractionation of nitrogen during the summer months (when these samples were collected) because nitrogen is the limiting factor for photosynthesis and all ambient nitrogen is consumed. However, if PAR was low enough, perhaps due to persistent cloud cover, light could

have been limiting rather than nitrogen which would allow for the photosynthetic fractionation of nitrogen (Altabet 2001; Baker et al. 2011). Under these conditions, lower PAR would have led to increased fractionation of nitrogen and lower primary producer nitrogen values.

3.5.3 Other GOM isoscapes

To my knowledge, there have been four other studies that created isoscapes for the Gulf of Mexico. Radabaugh et al. (2013) created measured isoscapes for $\delta^{13}C$ and $\delta^{15}N$ values for the West Florida Shelf based on fish muscle, and Radabaugh and Peebles (2014) created statistical models for those same data. The models were created using static (latitude, longitude, and depth) and satellite derived variables (SST, POC, PIC, CDOM, Chlorophyll a, K_d, and PAR) as predictor variables. The $\delta^{13}C$ isoscape depicted a pattern of decreasing $\delta^{13}C$ values with depth, which the authors attributed to the effect of light environment on basal resource availability. The $\delta^{13}C$ model the authors created included *SST*, *PAR(z)*, and *Ln(POC)* with *PAR(z)* explaining the most variation and *SST* explaining the least variation. The $\delta^{15}N$ isoscape depicted a pattern of lower $\delta^{15}N$ values near the Caribbean and higher $\delta^{15}N$ values towards the Mississippi River outflow, which the authors attributed to transition from higher $\delta^{15}N$ nitrogen sources in the north (human and livestock waste) and lower $\delta^{15}N$ sources in the south (denitrifying bacteria). The $\delta^{15}N$ model the authors created included *Longitude*, *SST*, and *Ln(POC)* with *Longitude* explaining the most variation and *SST* explaining the least variation.

Vander Zanden et al. (2015) created measured $\delta^{13}C$ and $\delta^{15}N$ isoscapes of potential foraging areas of loggerhead sea turtles, including the eastern Gulf of Mexico, Yucatan peninsula, Cuba, Bahamas, and the east Florida shelf, using the scutes of loggerhead sea turtles for the purpose of assigning individuals to a specific region. Most of the lower $\delta^{13}C$ values were

located towards the middle of the West Florida Shelf and higher δ^{13}C values were located closer to the Caribbean. The authors attribute the higher δ^{13}C values near the Caribbean to a shift to a seagrass dominated ecosystem. There was no apparent δ^{13}C depth gradient. The δ^{15}N isoscape depicted lower δ^{15}N values towards the Caribbean and higher δ^{15}N values towards the Mississippi River outflow in the north and near Laguna de Términos in the south, though the area near the Mississippi River outflow was higher overall than the area near Laguna de Términos. The authors attribute spatial δ^{15}N patterns to shifts in nitrogen sources similar to Radabaugh et al. (2013) and Radabaugh and Peebles (2014).

Le-Alvarado et al. (2021) created measured isoscapes of zooplankton bulk δ^{13}C values, bulk δ^{15}N values, and phenylalanine (a source amino acid) δ^{15}N values in the entire Gulf of Mexico for the purpose of determining the feeding areas and trophic positions of Yellowfin Tuna. The bulk δ^{13}C isoscape has its lowest values in the northwestern Gulf of Mexico and a relative low near Laguna de Términos. The highest δ^{13}C values were near the Florida Keys. The bulk and phenylalanine δ^{15}N isoscapes depicted very similar patterns with the highest δ^{15}N values near the Mississippi River outflow and near the Trinity River outflow on the northern Texas coast with a locally relative high near Laguna de Términos. The authors attribute spatial δ^{15}N patterns to shifts in nitrogen sources similar to the other studies in this section (Radabaugh et al. 2013; Radabaugh and Peebles 2014; Vander Zander et al. 2015).

Previous Gulf of Mexico δ^{15}N isoscapes show strong agreement with each other and with the isoscapes presented in this dissertation, whereas the δ^{13}C isoscapes do not show as high a level of agreement. In every case, δ^{15}N isoscapes depict higher values near areas of freshwater input and lower values near areas of low productivity (tropical areas or, in the case of Le-Alvarado et al. 2021, off the continental shelf). In every case, the authors attribute these spatial

patterns to influxes of animal and human waste nitrogen from rivers and input of diazotroph

nitrogen from nitrogen fixation in oligotrophic areas (Carpenter et al. 1997; Montoya et al. 2002;

Montoya 2007). These patterns appear to be consistent whether the isoscapes are created from

organisms relying on planktonic basal resources (zooplankton; Le-Alvarado et al. 2021),

organisms relying on benthic basal resources (Vander Zanden et al. 2015), or organisms that

likely integrate those two trophic pathways (fish; Radabaugh et al. 2013, Radabaugh and Peebles

2014, and this disertation). Radabaugh et al. (2013) and Radabaugh and Peebles (2014)

documented a strong depth gradient in δ^{13}C values, and a similar depth gradient was found in the

Red Snapper δ^{13}C isoscape of this study. The statistical models created in both cases included an

explanatory variable relating to depth (*Depth* and *PAR(z)* for this dissertation and their study

respectively). However, the δ^{13}C isoscapes of the other studies do not appear to contain depth

gradients (it should be noted that Vander Zanden et al. 2015 mention a δ^{13}C depth gradient but,

when visually examining their isoscape, there is a slight depth gradient in south Florida but not

elsewhere within the Gulf of Mexico). One reason Le-Alvarado et al. (2021) and Vander Zanden

et al. (2015) may not have found depth gradients in δ^{13}C values is that the species used to create

both isoscapes are likely primarily relying on one basal resource. One of the potential reasons for

the decrease in δ^{13}C values with depth that is found in this dissertation's isoscape and the

isoscape of Radabaugh and Peebles 2015 is that fish switch from higher δ^{13}C value benthic basal

resources inshore to lower δ^{13}C value planktonic basal resources near the shelf edge where

deeper waters decrease benthic production (France 1995; Doi et al. 2010). The Le-Alvarado et al.

(2021) δ^{13}C isoscape depicts patterns that are nearly the reverse of the δ^{13}C patterns in the Red

Snapper δ^{13}C isoscape of this study. The authors do not offer an explanation for the spatial

patterns of their δ^{13}C isoscape but one possible explanation for lower zooplankton δ^{13}C values in

114

high productivity areas is that higher productivity areas tend to have phytoplankton with larger cell sizes (Popp et al. 1998) which could allow for larger zooplankton to feed directly on phytoplankton cells and shorten food chains. If the zooplankton collected in high productivity areas were at lower trophic positions on average than those collected in oligotrophic waters, it could explain why their δ^{13}C values were lower (Minagawa and Wada 1984; Post 2002). In this dissertation and in the Radabaugh and Peebles (2015) study, a length correction was applied to δ^{13}C and δ^{15}N values to reduce the effect of spatial differences in trophic position which could explain the different patterns. That being said, trophic fractionation of δ^{13}C values is often very minimal (Fry and Sherr 1989; Peterson and Fry 1987; Vander Zanden and Rasmussen 1999) so it is possible there are other unknown causes of the Le-Alvarado et al. (2021) δ^{13}C patterns.

3.5.4 Limitations and future work

The δ^{13}C and δ^{15}N models created here both depict isoscapes that are relatively consistent over time that could be used for various stable isotope ecology applications in the Gulf of Mexico. However, it is important to note the limitations of these models that should be taken into account for future use. First, while the δ^{15}N model of each species performed moderately well when predicting δ^{15}N values of the other species, the δ^{13}C models of both species performed poorly in that regard. The isoscapes created by the δ^{13}C models also did not depict similar spatial patterns between species which suggests the δ^{13}C isoscapes created here may not be applicable to other species. Another consideration is predicted isoscapes for time periods other than when the data were collected have the implicit assumption that the relationships between the predictor variables and the predicted isotopic ratios do not change over time (e.g., the selected variables and coefficients do not change over time) which may not be the case. A three-month average for

remotes sensing data was used to reflect an assumption of a consistent muscle turnover time of three months, but turnover time likely differs based on the growth rate of the fish, which will change with age and season (Boecklen et al. 2011). The statistical model assumes a static linear relationship between standard length and the isotopic values of the consumer (e.g., trophic position), but there is some evidence that the relationship between diet and consumer isotopic value (trophic discrimination factor) may change based on consumer physiology, consumer type, diet quality, and trophic level (Vanderklift and Ponsard 2003; Caut et al. 2009). The remote sensing products used in the isoscape models only represent surface values, whereas the fish used in this study were primarily benthic-associated thus, much of the unexplained variability in the isotopic models may due to differences between surface and bottom waters. Additionally, remote sensing products are confounded in near-shore waters due to suspended sediment, CDOM in coastal runoff, and bottom interference (Hu et al. 2010) so, the predicted isotopic values for any near-shore samples may be less accurate.

In the future, better predictive Gulf of Mexico isoscape models may be achieved in the following ways. First, particularly for $\delta^{13}C$ values, the spatial and temporal scale of variability of baseline isotopes could be investigated. Both the $\delta^{13}C$ models created here and those in Radabaugh and Peebles (2014) had relatively low predictive power based on their R^2 values. This may be due to the reasons discussed above or it could be that $\delta^{13}C$ baselines have higher spatial or temporal variability that was not measured by these models and introduced a high level of error. Second, additional potential explanatory variables could be introduced into the models to improve fit. In particular, variables explicitly describing freshwater input from various major rivers and variables describing sub-surface water conditions (i.e., sonde data) may be useful. Finally, models could be modified to include traits of individual fish to account for variability in

trophic fractionation and in tissue turnover time. With all the above considerations, the modeled

isoscapes created here may be useful for future stable isotope investigations of trophic level,

basal resource dependence, and animal migration (Graham et al. 2010; Hobson et al. 2010; Olson

et al. 2010).

3.6 Citations

Acker, J. G., and Leptoukh, G. 2007. Online analysis enhances use of NASA earth science

data. *Eos, Transactions American Geophysical Union* 88(2): 14-17.

Allen, G.R., 1985. FAO Species Catalogue. Vol. 6. Snappers of the world. An annotated and

illustrated catalogue of lutjanid species known to date. *FAO Fisheries Synopsis* 125(6):208 p.

Rome: FAO.

Altabet, M. A., Pilskaln, C., Thunell, R., Pride, C., Sigman, D., Chavez, F., and Francois, R.

1999. The nitrogen isotope biogeochemistry of sinking particles from the margin of the Eastern

North Pacific. *Deep Sea Research Part I: Oceanographic Research Papers* 46(4): 655-679.

Altabet, M. A. 2001. Nitrogen isotopic evidence for micronutrient control of fractional NO3−

utilization in the equatorial Pacific. *Limnology and Oceanography* 46(2): 368-380.

Alt-Epping, U., Mil-Homens, M., Hebbeln, D., Abrantes, F., and Schneider, R.R. 2007.

Provenance of organic matter and nutrient conditions on a river- and upwelling influenced shelf:

a case study from the Portuguese Margin. *Marine Geology* 243: 169–179.

Acker, J. G. and Leptoukh, G. 2007. Online analysis enhances use of NASA earth science data. *Eos, Transactions American Geophysical Union* 88(2): 14-17.

Baker, D. M., Kim, K., Andras, J. P., and Sparks, J. P. 2011. Light-mediated 15 N fractionation in Caribbean gorgonian octocorals: implications for pollution monitoring. *Coral Reefs* 30(3): 709-717.

Barnes, C., Jennings, S., and Barry, J. T. 2009. Environmental correlates of large-scale spatial variation in the δ^{13}C of marine animals. *Estuarine, Coastal, and Shelf Science* 81(3): 368-374.

Berrick, S. W., G. Leptoukh, J.D. Farley, and H.L. Rui. 20009. Giovanni: A Web Service Workflow-Based Data Visualization and Analysis System IEEE Transactions on Geoscience and Remote Sensing, 47: 106-113.

Boecklen, W. J., Yarnes, C. T., Cook, B. A., and James, A. C. 2011. On the use of stable isotopes in trophic ecology. *Annual Review of Ecology, Evolution, and Systematics* 42: 411-440.

Bowen, G. J. and J. Revenaugh. 2003. Interpolating the isotopic composition of modern meteoric precipitation. *Water Resources Research* 39:1299.

Bowen, G. J. 2010. Isoscapes: spatial pattern in isotopic biogeochemistry. *Annual Review of Earth and Planetary Sciences* 38: 161-187.

Branco, A. B. and Kremer, J. N. 2005. The relative importance of chlorophyll and colored dissolved organic matter (CDOM) to the prediction of the diffuse attenuation coefficient in shallow estuaries. *Estuaries* 28(5): 643-652.

Buchheister, A., and Latour, R. J. 2010. Turnover and fractionation of carbon and nitrogen stable isotopes in tissues of a migratory coastal predator, summer flounder (*Paralichthys dentatus*). *Canadian Journal of Fisheries and Aquatic Sciences* 67(3): 445-461.

Bump, J. K., Fox-Dobbs, K., Bada, J. L., Koch, P. L., Peterson, R. O., and Vucetich, J. A. 2007. Stable isotopes, ecological integration and environmental change: wolves record atmospheric carbon isotope trend better than tree rings. *Proceedings of the Royal Society B: Biological Sciences* 274(1624): 2471-2480.

Capone, D. G., Bronk, D. A., Mulholland, M. R., and Carpenter, E. J. (Eds.). 2008. Nitrogen in the Marine Environment. Academic Press.

Carpenter, E.J., Harvey, H.R., Fry, B., and Capone, D.G., 1997. Biogeochemical tracers of the marine cyanobacterium Trichodesmium. *Deep Sea Research Part A: Oceanographic Research Papers* 44: 27–38.

Caut, S., Angulo, E. and Courchamp, F. 2009. Variation in discrimination factors (Δ^{15}N and Δ^{13}C): the effect of diet isotopic values and applications for diet reconstruction. *Journal of Applied Ecology* 46: 443-453. doi:10.1111/j.1365-2664.2009.01620.x

Ceia, F. R., Cherel, Y., Paiva, V. H., and Ramos, J. A. 2018. Stable isotope dynamics (δ^{13}C and δ^{15}N) in neritic and oceanic waters of the North Atlantic inferred from GPS-tracked Cory's shearwaters. *Frontiers in Marine Science* 5: 377.

Chen, R.F., Bissett, P., Coble, P., Conmy, R., Gardner, G.B., Moran, M.A., Wang, X., Wells, M.L., Whelan, P. and Zepp, R.G.2004. Chromophoric dissolved organic matter (CDOM) source characterization in the Louisiana Bight. *Marine Chemistry* 89(1-4): 257-272.

Childs, C. R., Rabalais, N. N., Turner, R. E., and Proctor, L. M. 2002. Sediment denitrification in the Gulf of Mexico zone of hypoxia. *Marine Ecology Progress Series* 240: 285-290.

Cifuentes, L. A., Sharp, J. H., and Fogel, M. L. 1988. Stable carbon and nitrogen isotope biogeochemistry in the Delaware estuary. *Limnology and Oceanography* 33(5): 1102-1115.

Cook, R. D., and Weisberg, S. 1982. Residuals and influence in regression. New York: Chapman and Hall.

Cooper, L.W. and DeNiro, M.J. 1989. Stable carbon isotope variability in the seagrass *Posidonia oceanica*: evidence for light intensity effects. *Marine Ecology Progress Series* 50: 225–229.

Cowen, R. K., Lwiza, K. M., Sponaugle, S., Paris, C. B., and Olson, D. B. 2000. Connectivity of marine populations: open or closed? *Science* 287(5454): 857-859.

Craig, M.T. and Hastings, P.A. 2007. A molecular phylogeny of the groupers of the subfamily Epinephelinae (Serranidae) with revised classification of the epinephelini. *Ichthyological Research* 54:1-17.

Craig, M. T., Sadovy de Mitcheson, Y. J., and Heemstra, P. C. 2011. Groupers of the world: a field and market guide. North America: CRC Press/Taylor and Francis Group. 356 p.

Dagg, M. J. and Breed, G. A. 2003. Biological effects of Mississippi River nitrogen on the northern Gulf of Mexico—a review and synthesis. *Journal of Marine Systems* 43(3-4): 133-152.

Daniels, C. J., Tyrrell, T., Poulton, A. J., and Pettit, L. (2012). The influence of lithogenic material on particulate inorganic carbon measurements of coccolithophores in the Bay of Biscay. *Limnology and Oceanography* 57(1): 145-153 doi: 10.4319/lo.2012.57.1.0145.

Dansgaard, W. 1954. The O18-abundance in fresh water. *Geochimica et Cosmochimica Acta 6*(5-6): 241-260.

Dodd, C. K. 1988. Synopsis of the biological data on the loggerhead sea turtle *Caretta caretta* (Linnaeus 1758). Biological Report 88(14). Department of Interior, U.S. Fish and Wild Services, Washington, D.C., USA.

Doi, H., Kikuchi, E., Shikano, S., and Takagi, S. 2010. Differences in nitrogen and carbon stable isotopes between planktonic and benthic microalgae. *Limnology* 11(2): 185-192.

Dutton A, Wilkinson BH, Welker JM, Bowen GJ, Lohmann KC. 2005. Spatial distribution and seasonal variation in 18O/16O of modern precipitation and river water across the conterminous United States. *Hydrological Processes: An International Journal* 19: 4121–46

Eppley, R. W. 1972. Temperature and phytoplankton growth in the sea. *Fisheries Bulletin* 70(4): 1063-1085.

Fox, J. 1997. <u>Applied Regression, Linear Models, and Related Methods</u>. Sage Publications Inc.

Fox, J., and Monette, G. 1992. Generalized collinearity diagnostics. *Journal of the American Statistical Association* 87(417): 178-183.

Fox, J. and Weisberg, S. 2011. <u>An R Companion to Applied Regression, Second edition</u>. Sage Publications Inc.

France, R. L. 1995. Carbon-13 enrichment in benthic compared to planktonic algae: foodweb implications. *Marine Ecology Progress Series* 124: 307-312.

Frimodt, C., 1995. Multilingual illustrated guide to the world's commercial coldwater fish. Fishing News Books, Osney Mead, Oxford, England. 215 p.

Fry, B. 1981. Natural stable carbon isotope tag traces Texas shrimp migrations. *Fishery Bulletin* 79 (2): 337–345.

Fry, B., and Sherr, E. B. 1984. δ^{13}C measurements as indicators of carbon flow in marine and freshwater ecosystems. *Contributions in Marine Science* 27: 13–47.

Gearing, J. N., Gearing, P. J., Rudnick, D. T., Requejo, A. G., and Hutchins, M. J. 1984. Isotopic variability of organic carbon in a phytoplankton-based, temperate estuary. *Geochimica et Cosmochimica Acta* 48(5): 1089-1098.

GMFMC (Gulf of Mexico Fishery Management Council). 2010. Final regulatory amendment to the reef fish fishery management plan to set total allowable catch for Red Snapper. GMFMC, Tampa, Florida.

Goericke, R., and B. Fry. 1994. Variations of marine plankton δ^{13}C with latitude, temperature, and dissolved CO2 in the world ocean. *Global Biogeochemical Cycles* 8:85–90.

Graham, B.S., Koch, P.L., Newsome, S.D., McMahon, K.W., and Aurioles, D., 2010. Using isoscapes to trace the movements and foraging behavior of top predators in oceanic ecosystems. In: West, J.B., Bowen, G.J., Dawson, T.E., and Tu, K.P. (Eds.), Isoscapes: Understanding Movement, Pattern, and Process on Earth through Isotope Mapping. Springer, New York, pp. 299–318.

Gruber, N., Keeling, C. D., Bacastow, R. B., Guenther, P. R., Lueker, T. J., Wahlen, M., Meijer, H.A., Mook, W.G. and Stocker, T.F. 1999. Spatiotemporal patterns of carbon-13 in the global surface oceans and the oceanic Suess effect. *Global Biogeochemical Cycles* 13(2): 307-335.

Hannides, C. C. S., Popp, B. N., Landry, M. R., and Graham, B. S. 2009. Quantitative determination of zooplankton trophic position using amino acid-specific stable nitrogen isotope analysis. *Limnology and Oceanography* 54: 50-61.

Hansson, S., Hobbie, J.E., Elmgren, R., Larsson, U., Fry, B., and Johansson, S., 1997. The stable nitrogen isotope ratio as a marker of food-web interactions and fish migration. *Ecology* 78: 2249–2257.

Hinga, K. R., Arthur, M. A., Pilson, M. E., and Whitaker, D. 1994. Carbon isotope fractionation by marine phytoplankton in culture: the effects of CO_2 concentration, pH, temperature, and species. *Global Biogeochemical Cycles* 8(1): 91-102.

Hobson, K.A., Barnett-Johnson, R., and Cerling, T., 2010. Using isoscapes to track animal migration. In: West, J.B., Bowen, G.J., Dawson, T.E., and Tu, K.P. (Eds.), Isoscapes: Understanding Movement, Pattern, and Process on Earth through Isotope Mapping. Springer, New York, pp. 273–298.

Hofmann, M., D.A. Wolf-Gladrow, T. Takahashi, S.C. Sutherland, K.D. Six, E. Maier-Reimer. 2000. Stable carbon isotope distribution of particulate organic matter in the ocean: a model study. *Marine Chemistry* 72 (2000): 131-150.

Hu, C., Cannizzaro, J., Carder, K. L., Muller-Karger, F. E., and Hardy, R. 2010. Remote detection of Trichodesmium blooms in optically complex coastal waters: Examples with MODIS full-spectral data. *Remote Sensing of Environment* 114(9): 2048-2058.

James, G., Witten, D., Hastie, T., and Tibshirani, R. 2013. An introduction to statistical learning: With applications in R. (Vol. 112, p. 18). New York: springer.

Jennings, S. and K.J. Warr. 2003. Environmental correlates of large-scale spatial variation in the $\delta^{15}N$ of marine animals. *Marine Biology* 142: 1131-1140.

Jones, D. L. 2012. The fathom toolbox for MATLAB: multivariate ecological and oceanographic data analysis. College of Marine Science, University of South Florida, St. Petersburg, FL, USA. Available from: http//seas.marine.usf.edu/~djones/.

Kell, L. T., Dickey-Collas, M., Hintzen, N. T., Nash, R. D., Pilling, G. M., and Roel, B. A. 2009. Lumpers or splitters? Evaluating recovery and management plans for metapopulations of herring. *ICES Journal of Marine Science* 66(8): 1776-1783.

Kendall, C., Silva, S.R., and Kelly, V.J., 2001. Carbon and nitrogen isotopic compositions of particulate organic matter in four large river systems across the United States. *Hydrological Processes* 15: 1301–1346.

Kirk, J. T. 1994. <u>Light and photosynthesis in aquatic ecosystems (2nd edition)</u>. Cambridge University Press. Cambridge.

Kline, Jr, T. C. 1999. Temporal and spatial variability of $^{13}C/^{12}C$ and $^{15}N/^{14}N$ in pelagic biota of Prince William Sound, Alaska. *Canadian Journal of Fisheries and Aquatic Sciences* 56(S1): 94-117.

Kootker, L. M., van Lanen, R. J., Kars, H., and Davies, G. R. 2016. Strontium isoscapes in The Netherlands. Spatial variations in 87Sr/86Sr as a proxy for palaeomobility. *Journal of Archaeological Science: Reports* 6: 1-13.

Kürten, B., Frutos, I., Struck, U., Painting, S. J., Polunin, N. V., and Middelburg, J. J. 2013. Trophodynamics and functional feeding groups of North Sea fauna: a combined stable isotope and fatty acid approach. *Biogeochemistry* 113(1-3): 189-212.

Le-Alvarado, M., Romo-Curiel, A. E., Sosa-Nishizaki, O., Hernández-Sánchez, O., Barbero, L., and Herzka, S. Z. 2021. Yellowfin tuna (*Thunnus albacares*) foraging habitat and trophic position in the Gulf of Mexico based on intrinsic isotope tracers. *PloS One* 16(2): e0246082.

Lohrenz, S. E., Fahnenstiel, G. L., Redalje, D. G., Lang, G. A., Chen, X., and Dagg, M. J. 1997. Variations in primary production of northern Gulf of Mexico continental shelf waters linked to nutrient inputs from the Mississippi River. *Marine Ecology Progress Series* 155: 45-54.

Magozzi, S., Yool, A., Vander Zanden, H. B., Wunder, M. B., and Trueman, C. N. 2017. Using ocean models to predict spatial and temporal variation in marine carbon isotopes. *Ecosphere* 8(5): e01763.

Mariotti, A., Lancelot, C., & Billen, G. 1984. Natural isotopic composition of nitrogen as a tracer of origin for suspended organic matter in the Scheldt estuary. *Geochimica et Cosmochimica Acta* 48(3): 549-555.

McMahon, K. W., Hamady, L. L., and Thorrold, S. R. 2013. A review of ecogeochemistry approaches to estimating movements of marine animals. *Limnology and Oceanography* 58(2): 697-714.

McIntyre, P. B., and Flecker, A. S. 2006. Rapid turnover of tissue nitrogen of primary consumers in tropical freshwaters. *Oecologia* 148(1): 12-21.

Minagawa, M. and Wada, E. 1984. Stepwise enrichment of ^{15}N along food chains: further evidence and the relation between δ^{15}N and animal age. *Geochimica et Cosmochimica Acta* 48(5): 1135-1140.

Monroy-García, C., M. G. Andrade, and J. C. Espinoza. 2002. Análisis de la pesqueria de huachinango (*Lutjanus campechanus*) en el Banco de Campeche. [Analysis of the Red Snapper fishery (*Lutjanus campechanus*) on the Campeche Bank.] *Proceedings of the Gulf and Caribbean Fisheries Institute* 53:507–515.

Montoya, J. P., Carpenter, E. J., and Capone, D. G., 2002. Nitrogen fixation and nitrogen isotope abundances in zooplankton of the oligotrophic North Atlantic. *Limnology and Oceanography* 47: 1617–1628.

Montoya, J. P. 2007. Natural abundance of ^{15}N in marine planktonic ecosystems. In: Michener R and K. Lajtha (eds) Stable isotopes in ecology and environmental science, 2nd ed. Blackwell, Malden, M. A., pp 176–201

Morel, A., Y. Huot, B. Gentili, P.J. Werdell, S.B. Hooker, and B.A. Franz. 2007. Examining the consistency of products derived from various ocean color sensors in open ocean (Case 1) waters in the perspective of a multi-sensor approach. *Remote Sensing Environment* 111: 69-88.

Murawski, S. A., Peebles, E. B., Gracia, A., Tunnell, J. W., and Armenteros, M. 2018. Comparative abundance, species composition, and demographics of continental shelf fish assemblages throughout the Gulf of Mexico. *Marine and Coastal Fisheries* 10(3): 325-346.

Muscatine, L., Porter, J.W., and Kaplan, I.R., 1989. Resource partitioning by reef corals as determined from stable isotope composition. 1. δ^{13}C of zooxanthellae and animal tissue vs depth. *Marine Biolog*y 100: 185–193.

Needoba, J. A., Waser, N. A., Harrison, P. J., and Calvert, S. E. 2003. Nitrogen isotope fractionation in 12 species of marine phytoplankton during growth on nitrate. *Marine Ecology Progress Series* 255: 81-91.

Nelson, J., Chanton, J., Coleman, F., and Koenig, C. 2011. Patterns of stable carbon isotope turnover in gag, Mycteroperca microlepis, an economically important marine piscivore determined with a non-lethal surgical biopsy procedure. *Environmental Biology of Fishes* 90(3): 243-252.

Nerot, C., Lorrain, A., Grall, J., Gillikin, D.P., Munaron, J.M., Le Bris, H., and Paulet, Y.M., 2012. Stable isotope variations in benthic filter feeders across a large depth gradient on the continental shelf. *Estuarine, Coastal and Shelf Science* 96: 228–235.

Olson, R.J., Popp, B.N., Graham, B.S., Lopez-Ibarra, G.A., Galvan-Magana, F., LennertCody, C.E., Bocanegra-Castillo, N., Wallsgrove, N.J., Gier, E., Alatorre-Ramirez, V., Balance, L.T.,

and Fry, B., 2010. Food-web inferences of stable isotope spatial patterns in copepods and yellowfin tuna in the pelagic eastern Pacific Ocean. *Progress in Oceanography* 86: 124–138.

O'Reilly, C.M., Hecky, R.E., Cohen, A.S., and Plisnier, P.D. 2002. Interpreting stable isotopes in food webs: recognizing the role of time averaging at different trophic levels. *Limnology and Oceanography* 47: 306–309.

Patterson, W. F. 2007. A review of movement in Gulf of Mexico red snapper: implications for population structure pp. 221-235. In *Red Snapper Ecology and Fisheries in the US Gulf of Mexico. American Fisheries Society, Symposium* (Vol. 60).

Peterson, B. J., and Fry, B. 1987. Stable isotopes in ecosystem studies. *Annual Review of Ecology and Systematics* 18: 293–320.

Pinnegar, J. K. and Polunin , N. V. C. 1999. Differential fractionation of delta C-13 and delta N-15 among fish tissues: implications for the study of trophic interactions. *Functional Ecology* 13(2): 225-231.

Popp B.N., Laws E.A., Bidigare R.R., Dore J.E., Hanson K.L. and Wakeham S.G. 1998. Effect of phytoplankton cell geometry on carbon isotopic fractionation. *Geochimica et Cosmochimica Acta* 62: 66–77.

Post, D. M. 2002. Using stable isotopes to estimate trophic position: models, methods, and assumptions. *Ecology* 83(3): 703-718.

Quillfeldt, P., Ekschmitt, K., Brickle, P., McGill, R. A., Wolters, V., Dehnhard, N., and Masello, J. F. 2015. Variability of higher trophic level stable isotope data in space and time–a case study in a marine ecosystem. *Rapid Communications in Mass Spectrometry* 29(7): 667-674.

R Core Team. 2020. R: A language and environment for statistical computing. R Foundation for Statistical Computing, Vienna, Austria. URL https://www.R-project.org/

Radabaugh, K. R., Hollander, D. J., and Peebles, E. B. 2013. Seasonal $\delta^{13}C$ and $\delta^{15}N$ isoscapes of fish populations along a continental shelf trophic gradient. *Continental Shelf Research* 68: 112-122.

Radabaugh, K. R., and Peebles, E. B. 2014. Multiple regression models of $\delta^{13}C$ and $\delta^{15}N$ for fish populations in the eastern Gulf of Mexico. *Continental Shelf Research* 84: 158-168.

Radabaugh, K. R., Malkin, E. M., Hollander, D. J., and Peebles, E. B. 2014. Evidence for light-environment control of carbon isotope fractionation by benthic microalgal communities. *Marine Ecology Progress Series* 495: 77-90.

Rau, G. H., Riebesell, U., and Wolf-Gladrow, D. 1997. CO_2aq-dependent photosynthetic ^{13}C fractionation in the ocean: A model versus measurements. *Global Biogeochemical Cycles* 11(2): 267-278.

Rooker, J. R., Stunz, G. W., Holt, S. A., and Minello, T. J. 2010. Population connectivity of red drum in the northern Gulf of Mexico. *Marine Ecology Progress Series* 407: 187-196.

Schloesser, R. W., Rooker, J. R., Louchuoarn, P., Neilson, J. D., and Secord, D. H. 2009. Interdecadal variation in seawater d13C and d18O recorded in fish otoliths. *Limnology and Oceanography* 54(5): 1665-1668.

Smith, C.L., 1997. <u>National Audubon Society field guide to tropical marine fishes of the Caribbean, the Gulf of Mexico, Florida, the Bahamas, and Bermuda</u>. Alfred A. Knopf, Inc., New York. 720 p.

Suits, N. S., Denning, A. S., Berry, J. A., Still, C. J., Kaduk, J., Miller, J. B., and Baker, I. T. 2005. Simulation of carbon isotope discrimination of the terrestrial biosphere. *Global Biogeochemical Cycles* 19(1).

Vanderklift, M. A., and Ponsard, S. 2003. Sources of variation in consumer-diet $\delta15$ N enrichment: a meta-analysis. *Oecologia* 136(2): 169-182.

Vander Zanden, M. J. and Rasmussen, J. B. 1999. Primary consumer δ^{15}N and δ^{13}C and the trophic position of aquatic consumers. *Ecology* 80: 1395–1404.

Vander Zanden, M.J. and Rasmussen, J.B. 2001. Variation in δ^{15}N and δ^{13}C trophic fractionation: implications for aquatic food web studies. *Limnology and Oceanography* 46: 2061–2066.

Vander Zanden, H. B., Tucker, A. D., Hart, K. M., Lamont, M. M., Fujisaki, I., Addison, D. S., Mansfield, K. L., Phillips, K. F. Wunder, M. B., Bowen, G. J., Pajuelo, M., Bolten, A. B., and Bjorndal, K. A. 2015. Determining origin in a migratory marine vertebrate: a novel method to integrate stable isotopes and satellite tracking. *Ecological Applications* 25(2): 320-335.

West, J. B., Bowen, G. J, and Dawson, T. E. 2010. Isoscapes: understanding movement, pattern, and process on Earth through isotope mapping. Springer, New York, New York, USA.

Chapter 4: Demonstration of the use of a Gulf of Mexico isoscapes to determine fish life history using Red Snapper eye lenses

4.1 Chapter Summary

Fish migration patterns are relevant to multiple realms of fisheries ecology and management. One way to infer fish migration is by comparing stable isotopic ratios found in fish eye lenses to spatial patterns in isotopic ratios found in the environment (isoscapes). Fish eye lenses grow in metabolically inert layers (lamina) and can be sectioned (delaminated) in order to provide a full isotopic history of the fish. The eye lenses of eight Red Snapper from around the Gulf of Mexico were delaminated, and each lamina was analyzed for $\delta^{13}C$ and $\delta^{15}N$ values. Regressions were performed between $\delta^{13}C$ values, $\delta^{15}N$ values, and laminar midpoints and measured isotopic life histories (ILHs) were compared visually and numerically with an ILH that was predicted based on a stationary fish that only had isotopic changes due to increasing trophic position (trophic growth). A fish was considered likely to have moved if the regression between $\delta^{13}C$ and $\delta^{15}N$ values had a low R^2 value, if there was little resemblance in the shapes of the $\delta^{13}C$ and $\delta^{15}N$ ILHs, and if the measured IHLs had a high level of deviation from the ILHs predicted based on stationary trophic growth. Based on these criteria, three fish were highly likely to have moved, three fish were likely to have moved, and two fish were not likely to have moved. Deviations from the predicted ILH were compared with isoscapes to infer how movement occurred. Overall, a high level of individual variation was observed. Two fish sampled in the same region displayed

more similar movement histories, suggesting movement patterns may be more similar within a region than between regions.

4.2 Background

Fish may migrate for a variety of reasons including pursuit of higher food availability and/or lower predation risk, ontogenetic habitat requirements, and avoidance of undesirable local conditions (Gallaway et al. 1999; Dingle and Drake 2007; Patterson et al. 2001b; Stanley and Wilson 2004; Gallaway et al. 2009). Understanding the timing, spatial extent, and associated abundances of migrations is useful not only for fisheries management (Hobson et al. 2019), but for quantifying the movement of biomass, nutrients, and energy within and among ecosystems (Deegan 1993).

One means of studying migration is through the use of stable isotopes (Hobson and Norris 2008). Stable isotopes are assimilated into the tissues of organisms and integrate dietary input over the metabolic turnover of the respective tissues. Thus, stable isotopes can provide information about foraging and movement along isotopically distinct habitats (Peterson and Fry 1987; Hobson 1999). An isoscape provides the expected isotopic changes associated with movement across those habitats which can then be compared to data collected from individual organisms. Migration and/or diet switches can be inferred from stable isotopes by comparing tissues with different turnover rates (Tieszen et al. 1983; Hobson 1999), but that method is limited by the turnover times of the respective tissues and does not provide a complete life history. Instead, many stable isotope migration studies obtain longer histories from metabolically inert tissues such as whiskers, dentin in teeth, otoliths, shark vertebrae, and, most commonly in teleost fish, otoliths (Hobson and Sease 1998; Schwarcz et al. 1998; Estrada et al. 2006; Mendes

135

et al. 2007; Cherel et al. 2009). Metabolically inert tissues provide a "snapshot" of dietary isotopes at the time the tissue was created and, in the case of otoliths, provide a biochemical record of an individual's trophic geography throughout of the entire life of the organism (Campana and Neilson 1985; Trueman et al. 2012). Otoliths are primarily composed of crystalline calcium carbonate on a protein matrix. Therefore, while otoliths provide a good isotopic history of C and O, the very low proportion of organic N inhibits the measurement of $\delta^{15}N$ vlaues, which is frequently used to provide information about consumer diet and movement. This is one of the primary reasons fish eye lenses have recently been explored as a potential lifetime record of trophic geography.

4.2.1 Eye lenses

Whereas the use of eye lens stable isotopes is a relatively new technique, early studies show promise for its utility. Eye lenses are largely composed of crystallin protein which is laid down in layers (laminae) as the fish grows and contains ample N for isotopic analysis (Nicol 1989; Horwitz 2003). After each lamina is laid down, the layer undergoes attenuated apoptosis and protein synthesis stops, making the eye lens metabolically inert record of biochemical life history (Nicol 1989; Dahm et al. 2007; Vihtelic 2008; Wallace et al. 2014). The center of the lens is the oldest material, usually representing the late postlarval time period at the earliest (Grainger et al. 1992), and the outermost layer of the lens is material representing the time shortly before the fish died (Nicol 1989). Because the eye lens grows isometrically with the fish, the size and/or age of the fish at the time each lamina was formed can be estimated using statistical analysis of relationship between eye lens size and fish size for a given species (Wallace et al. 2014; Quaeck-Davies et al. 2018). Eye lens $\delta^{15}N$ and $\delta^{13}C$ values are generally depleted compared to that of

muscle tissue, but isotopic differences are low enough that they are likely to be obscured by between-individual variation and analytical error (Quaeck-Davies et al. 2018). This indicates that eye lens stable isotopes have the potential for direct numeric comparison with more commonly collected muscle stable isotope data. The ability to document many lifetime trophic and geographic records is beneficial considering the growing evidence for high levels of individual variation within species populations (Bolnick et al. 2003; Bearhop et al. 2004; Lorrain et al. 2011; Kim et al. 2012; Wallace et al. 2014). In particular, the core and inner layers of the eye lens provide data regarding early life history, such as ontogenetic shifts in diet and habitat, individual resource use specificity, and other aspects of consumer life history which are often difficult to obtain using other methods (i.e., artificial tags).

Eye lenses have been used to elucidate the life history traits of squid (Parry 2003; Hunsicker et al. 2010; Onthank 2013; Meath 2019; Xu et al. 2019) and fish (Wallace et al. 2014; Kurth et al. 2019; Quaeck-Davies et al. 2018; Simpson et al. 2019; Curtis et al. 2020; Vecchio et al. 2021; Vecchio and Peebles 2022). Many studies have focused on feeding chronologies rather than migration, but that may be due to a lack of appropriate isoscapes to compare with eye lens isotopes. Ontogenetic increases in trophic level ("trophic growth"; Curtis et al. 2020; Vecchio et al. 2021) were a commonly observed trend (Parry 2003; Hunsicker et al. 2010; Onthank 2013; Curtis et al. 2020; Vecchio et al. 2021; Vecchio and Peebles 2022). Trophic growth usually documented as a strong correlation between $\delta^{13}C$ values, $\delta^{15}N$ values, and eye lens diameter (Curtis et al. 2020; Vecchio and Peebles 2020). However, it is also becoming clear that many species demonstrate a high level of inter-individual variation in resource use and/or movement (Wallace et al. 2014; Simpson et al. 2019; Xu et al. 2019; Curtis et al. 2020).

One shortcoming of bulk stable isotope analysis is that both movement and changes in diet have the potential to alter the $\delta^{13}C$ and $\delta^{15}N$ values of consumer tissues and it can be difficult to determine which processes resulted in measured isotopic values. This problem can be mitigated by combining stable isotope data with diet or artificial tag data (i.e., Vecchio and Peebles 2022) or by performing compound specific isotope analysis in conjunction with bulk stable isotope analysis (Wallace 2019) in order to refine or confirm the interpretation of results. If these methods are not available, it is possible to interpret bulk stable isotope data by inferring what an isotopic life history (ILH) would look like if the fish had remained stationary (isotopic changes only the result of trophic growth) and compare that visual to the observed ILH. This process can be achieved by either comparing a species of interest to a model species that is known to remain stationary throughout life (Vecchio and Peebles 2020) or by modeling a stationary ILH using the average relationship between $\delta^{13}C$ and $\delta^{15}N$ values and eye lens diameter and treating deviations from that model as the result of movement (Vecchio and Peebles 2022).

4.2.2 Objectives

This study used the latter method to evaluate the ILHs of eight Red Snapper collected from areas around the Gulf of Mexico. These evaluations were intended to demonstrate how to use comparisons between the ILH of a hypothetical stationary fish and the measured ILH from fish eye lenses in conjunction with the isoscapes created in Chapters 2 and 3 and to gain insight into the life history of Red Snapper. Red Snapper ontogenetic habitat use patterns are well studied (Gallaway et al. 2009) but are not very consistent in regard to a particular depth or cardinal direction and some studies document high levels of individual variation (Diamond 2007;

Patterson 2007; Wallace 2019). Methods like those demonstrated here may be particularly useful in inferring the life histories of many individual fish with relatively little cost and effort.

4.3 Methods

4.3.1 Target species

Eye lenses from Red Snapper *(Lutjanus campechanus)* were used to create individual movement histories in conjunction with isoscapes created from muscle from the same species. Red Snapper is a member of the family Lutjanidae (snappers) and is found throughout the Gulf of Mexico in 10-190 m waters (Allen 1985; Smith 1997). Post-larval Red Snapper settle at 16-19 mm TL on low-relief shell, mud, or sand habitat (for a review of Red Snapper habitat use, see Gallaway et al. 2009; also Szedlmayer and Lee 2004). Juvenile (>50 mm TL) move to more complex, low relief habitats. Sub-adults (~20 cm TL) move to mid- or high-relief structures. Red Snapper reach sexual maturity at age 2 (roughly 20-38 cm TL; Goodyear 1995) and recruit to larger reefs. Adults are generally reef-associated (though adults > 4 years are found more and more often on soft bottom habitat) and feed opportunistically mainly on fishes, shrimps, crabs, worms, cephalopods, and some planktonic items, including urochordates and gastropods (Allen 1985; Frimodt 1995; McCawley and Cowan 2007). Red Snapper support both recreational and commercial fisheries when they enter the fishery at age 2. Regulations for the Red Snapper fishery were introduced in 1990 by the National Marine Fisheries service after a 1988 assessment noted they were in decline (Goodyear and Center 1988). The most recent Red Snapper stock assessment found the species was not being overfished (no overfishing) and was not overfished though they note this is due to a change to the definition of minimum stock size threshold compared with the previous assessment (SEDAR 2018).

4.3.2 Eye lens and muscle collection

Dorsal muscle samples and eyes from Red Snapper (n = 126) were obtained from freshly caught fish aboard chartered, commercial fishing vessels (2011) and the R/V *Weatherbird II* (2015 and 2016; Appendix D). The fish collected here are the same as those in Chapters 2 and 3 and eyes were removed and frozen onboard in the same manner as muscle tissue. See Chapter 2, section 2.2 for details on fish collection and muscle stable isotope analysis.

4.3.3 Isotopic analysis

Eight Red Snapper were chosen for individual movement history analysis (Figure 4.1). The eye lenses of these fish were processed using methods similar to those presented in Wallace et al. (2014) and which were a recommended first choice by Quaeck-Davies et al. (2018). Eyes were thawed individually in the lab before dissection. An incision was made to create a flap in the cornea to allow for the removal of the eye lens using forceps. The lens epithelium was removed, the eye lens was placed in a small amount of deionized water under a dissecting microscope, and fine-tip forceps were used to remove successive layers (laminae) of the eye lens (delamination) until the lens core was reached. After each delamination, the deionized water was removed, eye lens diameter (ELD) was measured using an ocular micrometer, and new deionized water was added to the dish. Individual laminae were air dried for one hour to 24 hours as needed and stored separately in vials. Eye lenses from eight Red Snapper were processed containing a total of 128 laminae.
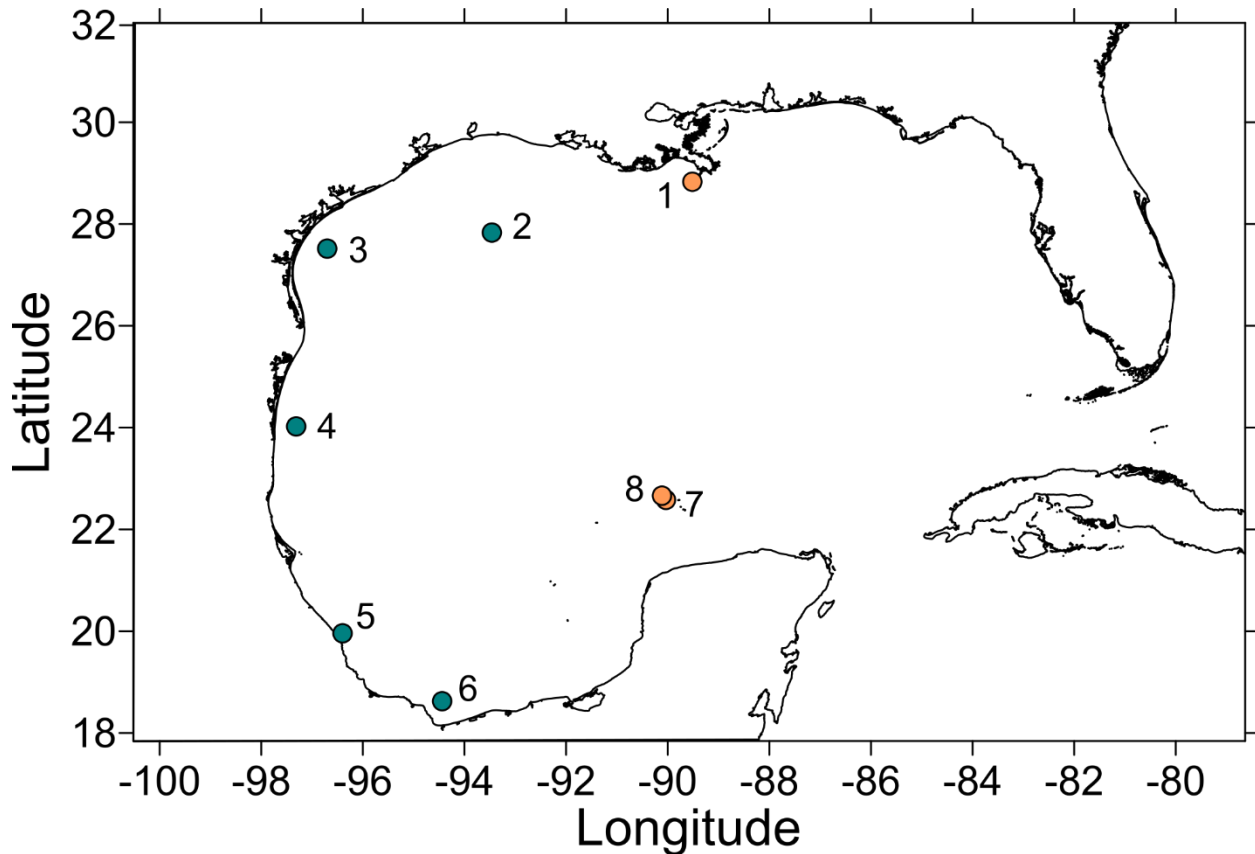
Figure 4.1
A post map of the capture locations of the eight Red Snapper whose eye lenses were analyzed for this study. Points are labeled with fish number. Orange dots represent fish sampled in 2015 and green dots represent fish sampled in 2016.

A dry weight of 150–700 µg of each lamina was placed in tin capsules for combustion and isotopic analysis. $^{13}C/^{12}C$, $^{15}N/^{14}N$, and C:N were measured in replicate using a Carlo-Ebra NA2500 Series II elemental analyzer coupled to a continuous-flow ThermoFinnigan Delta+XL isotope ratio mass spectrometer at the University of South Florida College of Marine Science in St. Petersburg, Florida. The lower limit of quantification was 12 µg C or N. Calibration standards were NIST 8573 ($\delta^{13}C$ value = -26.39 ± 0.09 and $\delta^{15}N$ value = -4.52 ± 0.12) and NIST 8574 L-glutamic acid ($\delta^{13}C$ value = 37.63 ± 0.1 and $\delta^{15}N$ value = 47.57 ± 0.22) standard reference

materials. Results are presented in standard notation (δ, in ‰) relative to international standards

Pee Dee Belemnite (PDB) and air for C and N, respectively:

$$\delta^j X = \left(\frac{(\,^jX/\,^iX)_{sample}}{(\,^jX/\,^iX)_{standard}} - 1 \right) * 1000$$

where X is the element and j and i are each an isotope of X.

4.3.4 Analysis and movement history

Prior to assessment of movement histories, models were created to calculate predicted

$\delta^{13}C$ and $\delta^{15}N$ values based on laminar midpoint. First, ELD of the intact eye lens was regressed

against SL for 45 of the Red Snapper originally sampled in the longlining cruises to verify that

ELD was strongly correlated with SL and can be considered a good proxy for SL. Then, the $\delta^{13}C$

and $\delta^{15}N$ values of the outermost lamina of each lens was regressed against muscle $\delta^{13}C$ and

$\delta^{15}N$ values in order to assess whether eye lens isotopic values are a good proxy for the muscle

isotopic values used to create the isoscapes. Next, ELDs of laminae were converted to laminar

midpoints (LMs), where the midpoint is the lens diameter after lamina removal plus half the

thickness of the removed lamina. Finally, the LMs of the intact eye lenses were regressed against

the measured lens $\delta^{13}C$ and $\delta^{15}N$ values. In essence, this regression equation represented the

relationship between fish size and isotopic values, which can be presumed to be primary the

result of trophic growth (Wallace et al. 2014; Curtis et al. 2020). This regression equation was

used to predict $\delta^{13}C$ and $\delta^{15}N$ values based on the LM of each lamina. The predicted $\delta^{13}C$ and

$\delta^{15}N$ values represented the $\delta^{13}C$ and $\delta^{15}N$ values that would be expected if the fish was not

moving and changes in $\delta^{13}C$ and $\delta^{15}N$ values were due only to trophic growth.

Two statistical measures were used to infer whether a fish had undergone movement. First, deviation scores were calculated by summing the absolute value of the difference between the predicted and measured isotopic value of each lamina for a fish.

$$\delta X \; Deviation \; score = \sum_{i=1}^{n} |predicted \; \delta X - measured \; \delta X|$$

In the above equation, δX is either $\delta^{13}C$ or $\delta^{15}N$ values and n is the number of lamiae for a particular fish. If a fish's total deviation score was relatively low, it was considered an indication that the fish did not move. It should be noted that this metric is vulnerable to baseline offsets so, if a fish was captured in an area with a numerically unusual baseline, it is possible for it to have a high deviation score even if it remained stationary. Second, Spearman rank correlations were performed between laminae $\delta^{13}C$ and $\delta^{15}N$ values within each eye lens (one correlation for each fish). If the *rho* of this correlation was relatively low, it was considered an indication that the fish moved (Vecchio et al. 2021). It should be noted that this metric may be less accurate in areas where $\delta^{13}C$ and $\delta^{15}N$ values are spatially correlated. In these areas, a fish could move, and its *rho* would still be relatively high.

As an additional means of assessment, plots were made of the measured $\delta^{13}C$ and $\delta^{15}N$ ILHs of each fish for for comparison with ILHs predicted based on LM. For fish that were likely to have moved, these plots were compared with capture location and the modeled $\delta^{13}C$ and $\delta^{15}N$ isoscapes to infer movement. The predicted isoscapes were created using data from the time of capture of the fish (the "catchdate" isoscapes seen in Chapter 3). For the methods of isoscape generation, see Chapters 2 and 3. Movement histories were inferred based on the sign (positive or negative) and magnitude of isotopic deviations from the values predicted by the ELD-isotope

regressions and the spatial isotopic patterns seen in the isoscapes near the capture location of

each fish (Figure 4.2). All analysis was performed in R (version 4.0.5, R Core Team 2020).
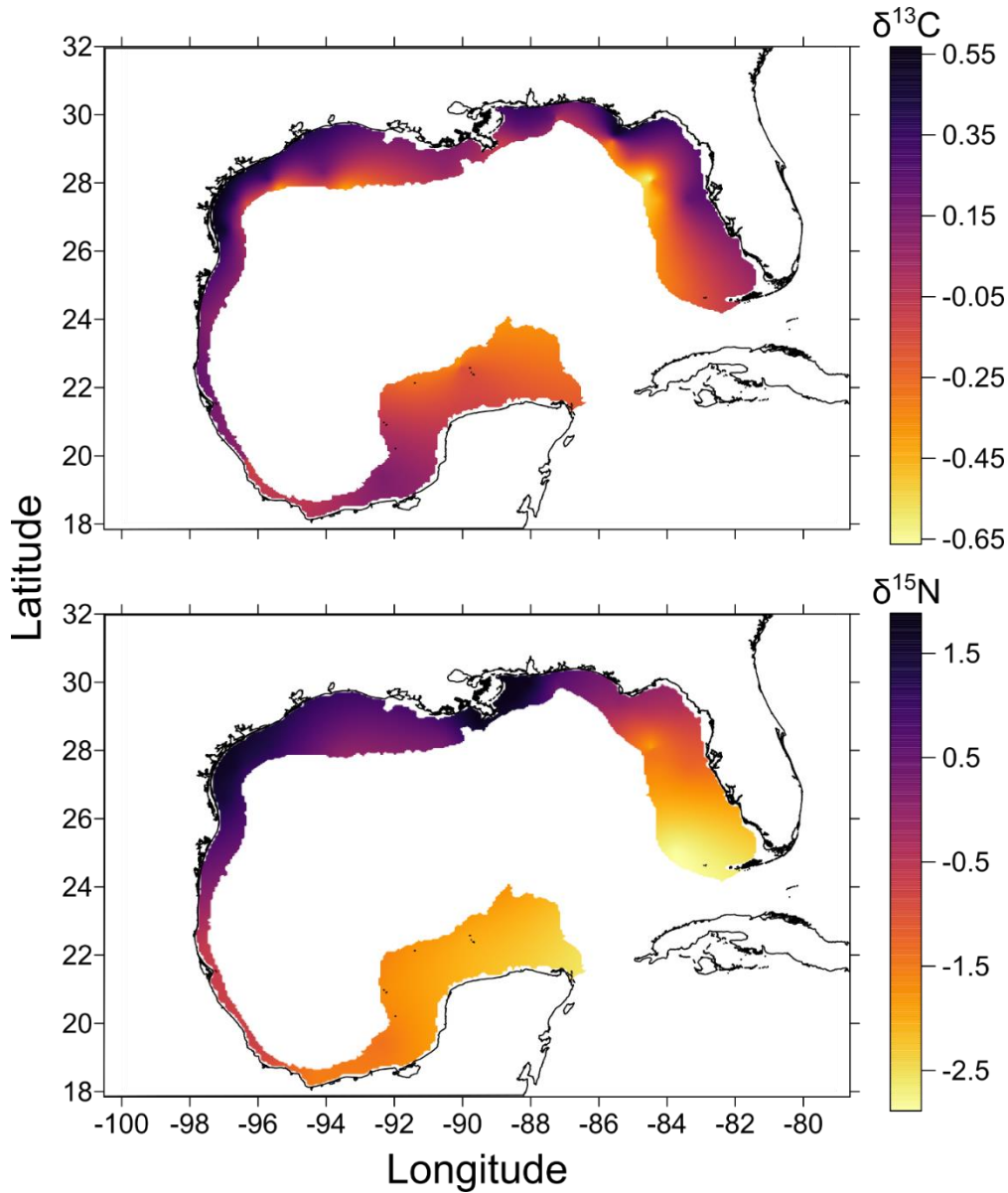
Figure 4.2
Isoscapes of length-corrected $\delta^{13}C$ and $\delta^{15}N$ values created using the multiple regression models created in Chapter 2 and measured static and dynamic predictors from the time of capture all Red Snapper (these are identical to the "catchdate" Red Snapper isoscapes from Chapter 2).

4.4 Results

4.4.1 Eye lenses as isotopic recorders

The first set of analyses of the eye lenses used in this study was to verify their utility as isotopic recorders. A regression between ELD and SL demonstrated that the eye lenses of Red Snapper grow isometrically with fish length and that ELD can be reliably used to predict SL (Figure 4.3). Regressions between the outermost lamina isotopic values and muscle isotopic values (Figure 4.4) indicated that lens δ^{15}N values were a good predictor of muscle δ^{15}N values ($R^2 = 0.85$, $p < 0.01$) whereas lens δ^{13}C values were a somewhat poor predictor of muscle δ^{13}C values ($R^2 = 0.39$, $p = 0.10$). However, it is possible the δ^{13}C R^2 would be higher with a larger sample size ($n = 8$). On average, muscle δ^{13}C values were lower than eye lens δ^{13}C values (with the exception of Fish 3), and muscle δ^{15}N values were higher than eye lens δ^{15}N values (with the exceptions of Fish 6, Fish 7, and Fish 8). The average difference between muscle and eye lens isotopic values was 0.41 ‰ for δ^{13}C values and 0.12 ‰ for δ^{15}N values. Compared to the other fish, Fish 3 appears to be an anomaly where the muscle δ^{13}C values were higher than eye lens δ^{13}C value, and the muscle δ^{15}N values were far higher than eye lens δ^{15}N values (muscle-lens = 1.39).
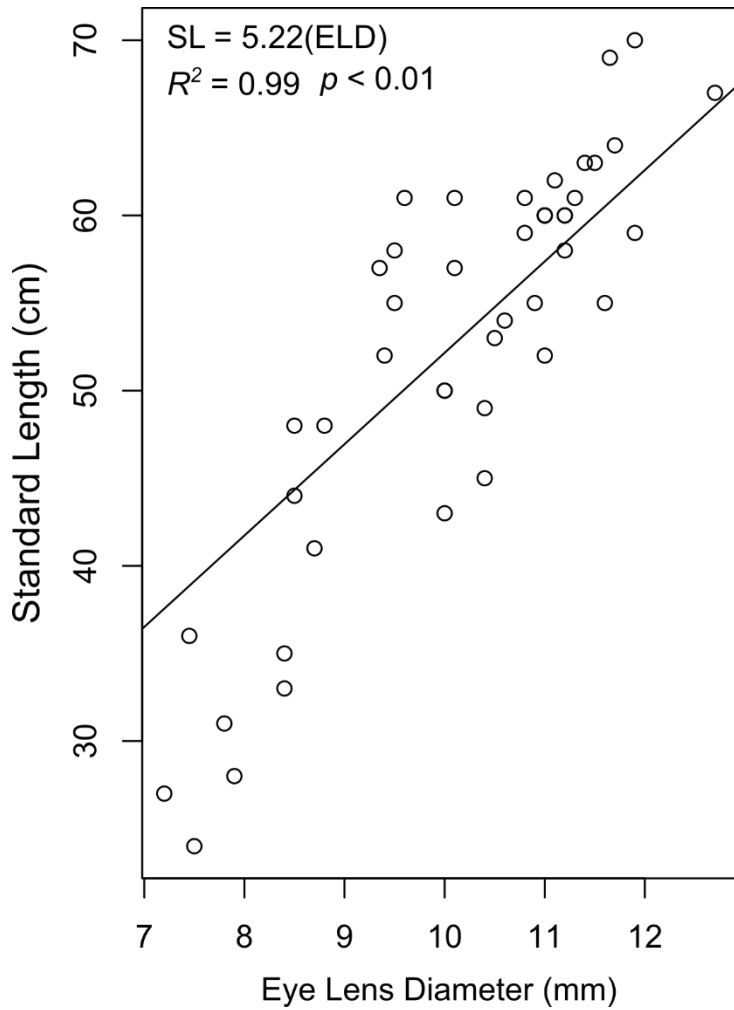
Figure 4.3
The graph of a linear regression of the ELDs and SLs of 45 Red Snapper. Dots are individual fish. The regression analysis included a forced intercept of zero (a fish with a length of zero would have an eye lens with a diameter of zero). The regression equation, R^2, and p-value are presented at the top of the graph.
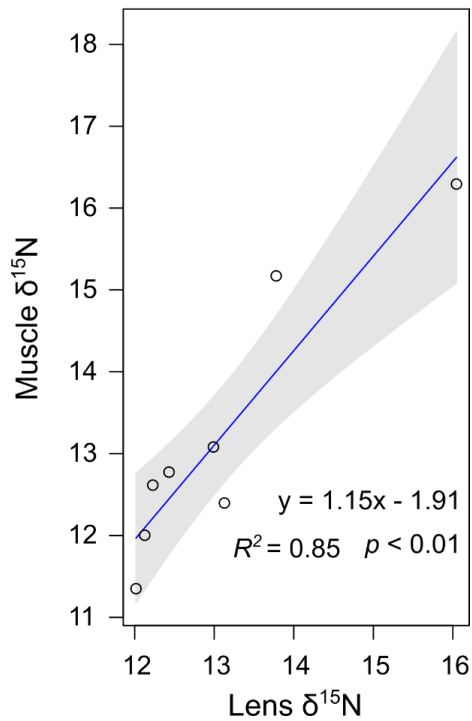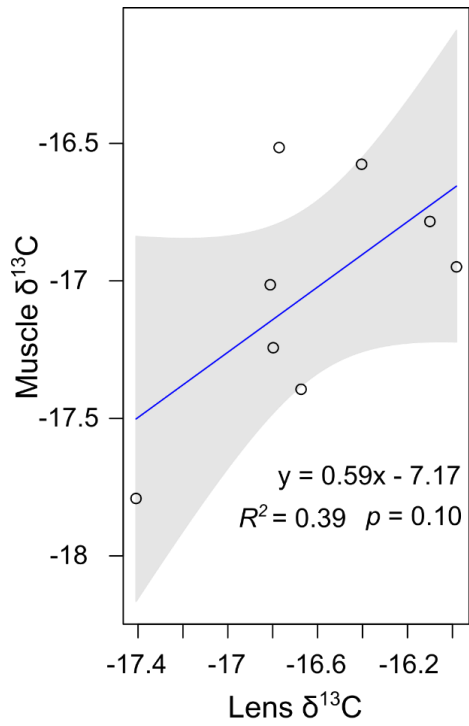
Figure 4.4
Graphs of the linear regressions of $\delta^{13}C$ and $\delta^{15}N$ values measured in outermost eye lens lamina and in the muscle tissue of eight Red Snapper wherein dots are individual fish. The regression equation, R^2, and p-value are presented at the bottom of each graph.

4.4.2 Trophic growth

A total of eight Red Snapper eye lenses were analyzed for $\delta^{13}C$ and $\delta^{15}N$ values. The size of the fish used ranged from 28 to 76 cm (Table 4.1). The number of laminae per eye lens ranged from 14 to 20 with larger eye lenses generally having more laminae. The $\delta^{13}C$ values of the laminae ranged from -21.61 ‰ to -14.34 ‰, and the $\delta^{15}N$ values of the laminae ranged from 5.31 ‰ to 16.20 ‰. The $\delta^{13}C$ standard deviation within a fish ranged from 0.57 ‰ to 1.35 ‰, and the $\delta^{15}N$ values standard deviation within a fish ranged from 1.40 ‰ to 2.55 ‰.

Regression analysis performed between $\delta^{13}C$ values and LM (Figure 4.5), between $\delta^{15}N$ values and LM (Figure 4.5), and between $\delta^{13}C$ and $\delta^{15}N$ values (Figure 4.6) were all significant, though R^2 values were moderate to low. These results suggest that, in general, Red Snapper undergo trophic growth over the course of their lives, but, for most Red Snapper, there are other influences on $\delta^{13}C$ and $\delta^{15}N$ values. Whereas the relationship between $\delta^{13}C$ and $\delta^{15}N$ values was significant at the aggregate level (Figure 4.6), not all individuals had significant correlations between $\delta^{13}C$ and $\delta^{15}N$ values within their eye lens (Table 4.1) level. The *rho* values of the correlations between $\delta^{13}C$ and $\delta^{15}N$ values within eye lenses ranged from 0.33 to 0.77.

Table 4.1

A table of results for individual Red Snapper analyzed for eye lens stable isotopes. The means and standard deviations (STDEV) of the isotopic values refers to the isotopic values of all laminae within a fish. The *rho* and *p*-value columns depict the results of a Spearman rank correlations between $\delta^{13}C$ or $\delta^{15}N$ values within each eye lens. The deviation score columns refer to the summed absolute values of the differences between the $\delta^{13}C$ or $\delta^{15}N$ value predicted by the regression equation using LM (Figure 4.5) and the measured $\delta^{13}C$ or $\delta^{15}N$ value for each lamina.

Fish	Standard Length (cm)	*n* Laminae	Mean $\delta^{13}C$ value	$\delta^{13}C$ STDEV	Mean $\delta^{15}N$ value	$\delta^{15}N$ STDEV	*rho*	*p*-value	$\delta^{13}C$ deviation score	$\delta^{15}N$ deviation score	Total deviation score
1	57	16	-16.92	0.92	14.54	1.55	0.34	0.20	8.41	36.20	44.62
2	57	16	-17.74	0.73	12.47	2.55	0.69	< 0.01	11.65	25.60	37.25
3	58	16	-17.58	0.57	12.98	2.37	0.54	0.03	9.21	22.98	32.20
4	36	14	-17.37	0.91	12.02	2.08	0.77	< 0.01	8.96	15.66	24.62
5	69	20	-16.88	0.66	11.63	1.45	0.44	0.05	6.65	31.00	37.65
6	28	14	-17.69	1.00	12.19	2.18	0.57	0.03	6.47	23.80	30.28
7	58	14	-16.29	1.17	10.28	2.11	0.56	0.04	14.49	21.74	36.22
8	76	18	-16.89	1.35	11.24	1.39	0.33	0.18	10.50	19.86	30.36
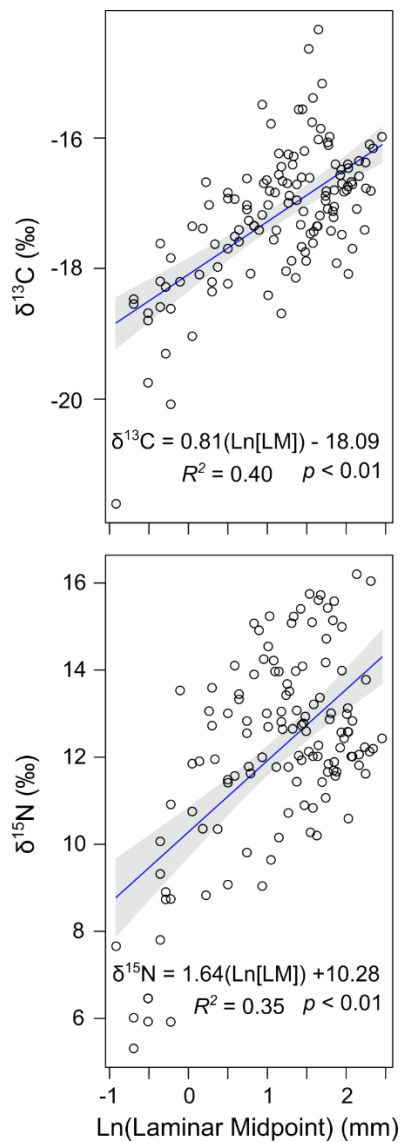
Figure 4.5
A graph of the regressions of the natural log transformed laminar midpoint (measured as the eye lens diameter at half the thickness of the removed lamina) of each lamina and its measured $\delta^{13}C$ or $\delta^{15}N$ value. Dots represent individual laminae (n = 128) of eight Red Snapper. The regression equation, R^2, and p-value are presented at the bottom of each graph.
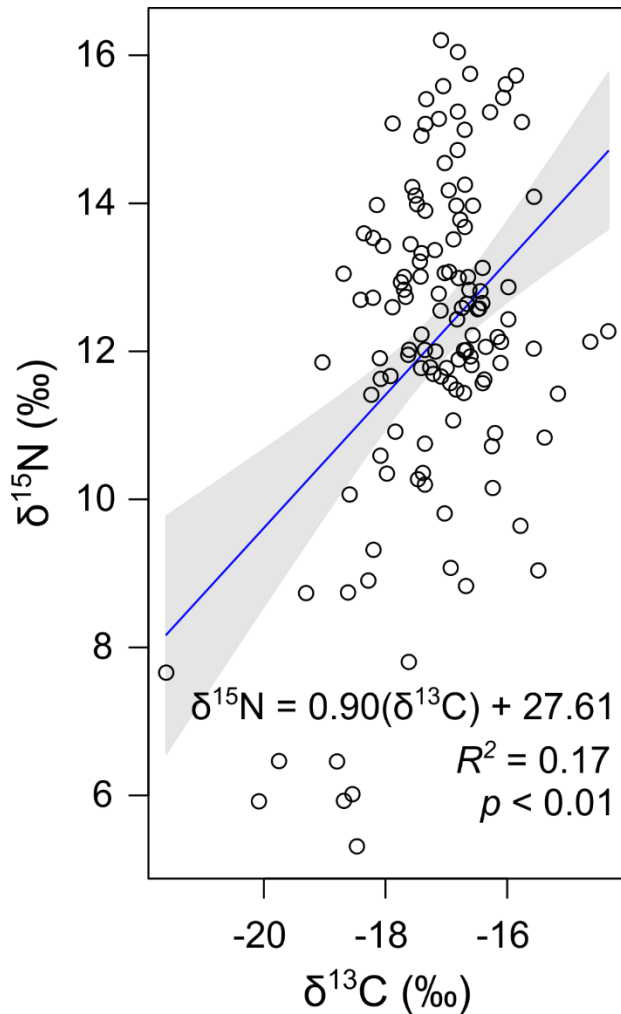
Figure 4.6
A graph depicting the linear regression between the measured $\delta^{13}C$ and $\delta^{15}N$ values of individual laminae when all laminae were aggregated. Dots represent individual laminae (n = 128). Both linear and logarithmic regression were performed. The linear regression had a higher R^2 value and was used for the figure. The equation, R^2, and p-values are written on the graph.

4.4.3 Isotopic life histories

The ILHs of individual Red Snapper depict a few common patterns, but overall, there appears to be a fair amount of individual variation. The life histories of $\delta^{13}C$ and $\delta^{15}N$ values generally showed a logarithmic increase over the lives of individual fish (Figure 4.7 and Figure 4.8), however, many fish also deviate from this pattern. It appears there is generally less convergence of ILHs among fish in $\delta^{15}N$ IHLs than in $\delta^{13}C$ IHLs. Fish 1, Fish 2, Fish 7, and Fish

8 all demonstrate a local peak and subsequent decrease in $\delta^{13}C$ values around a laminar midpoint of 5.5 mm (~ 30 cm SL), and Fish 4 has a smaller local peak around a laminar midpoint of 2.5 mm (15 cm SL) all of which could represent movement or a diet shift. Similarly, Fish 4, Fish 5, and Fish 6 demonstrate a local peak in $\delta^{15}N$ values around a laminar midpoint of 2.5 mm (~15 cm SL), and Fish 2 has a local peak around a laminar midpoint of 5 mm (~25 cm SL). Based on the $\delta^{13}C$ values generally observed in all laminae, it is possible the relatively low initial $\delta^{13}C$ value observed in Fish 8 was a measurement error. The measurement was of the eye lens core which had a mass lower than ideal for isotopic analysis (0.036 mg) which could cause a measurement error. However, there was no indication of measurement error from the IRMS quality control metrics and the concurrent $\delta^{15}N$ value measurement was not anomalous, therefore, for the purposes of this study, the low $\delta^{13}C$ value in Fish 8 will not be treated as an error.

The likelihood a fish moved during its life was inferred through an examination of the $\delta^{13}C$ and $\delta^{15}N$ correlation *rho* values (Table 4.1), deviation scores (Table 4.1), and ILH plots (Figures 4.7-4.11) of each fish. The $\delta^{13}C$ deviation scores for ranged from 6.47 to 14.49, and $\delta^{15}N$ deviation scores ranged from 15.66 to 36.20. The total deviation scores ranged from 24.62 (Fish 4) to 44.62 (Fish 1). When examining the ILH plots, Fish 4, Fish 5, and Fish 6 had very similar shapes to their $\delta^{13}C$ and $\delta^{15}N$ plots, and Fish 1, Fish 7, and Fish 8 had very different shapes to their $\delta^{13}C$ and $\delta^{15}N$ plots (Figure 4.11). If a Fish had a high $\delta^{13}C$ and $\delta^{15}N$ correlation *rho*, a low total deviation score, and a high level of similarity between its $\delta^{13}C$ and $\delta^{15}N$ ILH plots, it was inferred that it likely remained stationary throughout its life. Based on this evaluation, Fish 4 and Fish 6 are the most likely to have remained stationary, and Fish 1 and Fish 8 are the most likely to have moved.
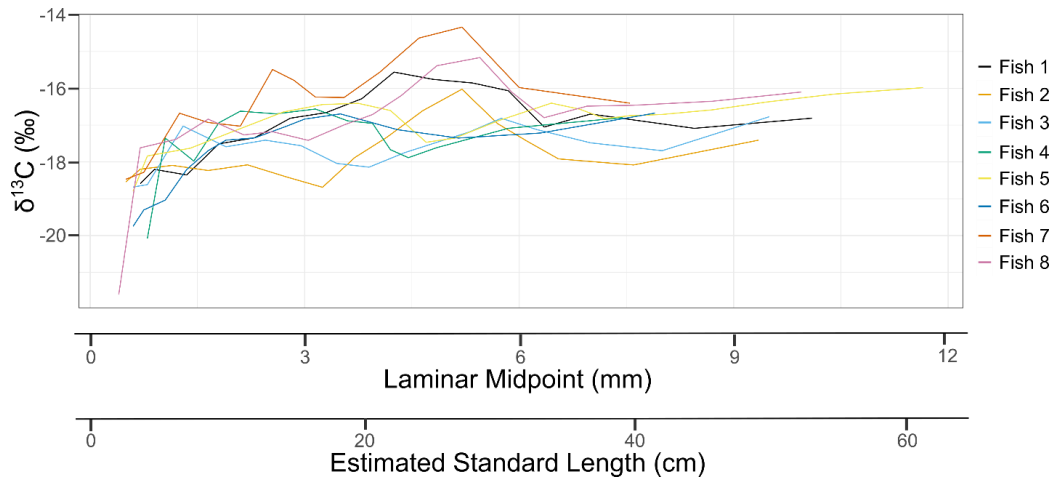
Figure 4.7
A graph of the lifetime history of $\delta^{13}C$ values as recorded in the eye lenses of eight Red Snapper. Each colored line represents the $\delta^{13}C$ ILH of an individual fish. Estimated standard length, which was generated using the equation from Figure 4.3 is shown below laminar midpoint. The number of laminae per fish ranged from 14 to 20.
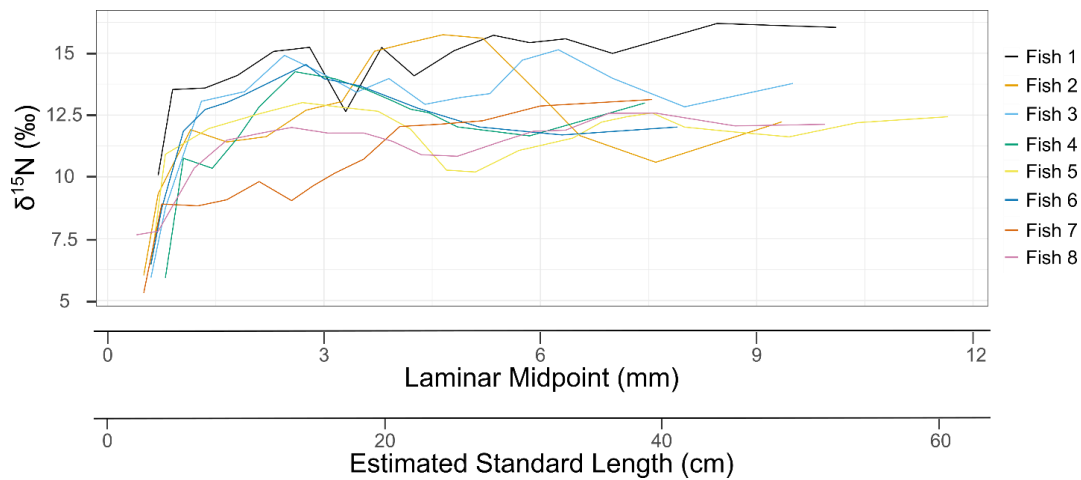
Figure 4.8
A graph of the lifetime history of $\delta^{15}N$ values as recorded in the eye lenses of eight Red Snapper. Each colored line represents the $\delta^{15}N$ ILH of an individual fish. Estimated standard length, which was generated using the equation from Figure 4.3 is shown below laminar midpoint. The number of laminae per fish ranged from 14 to 20.

153
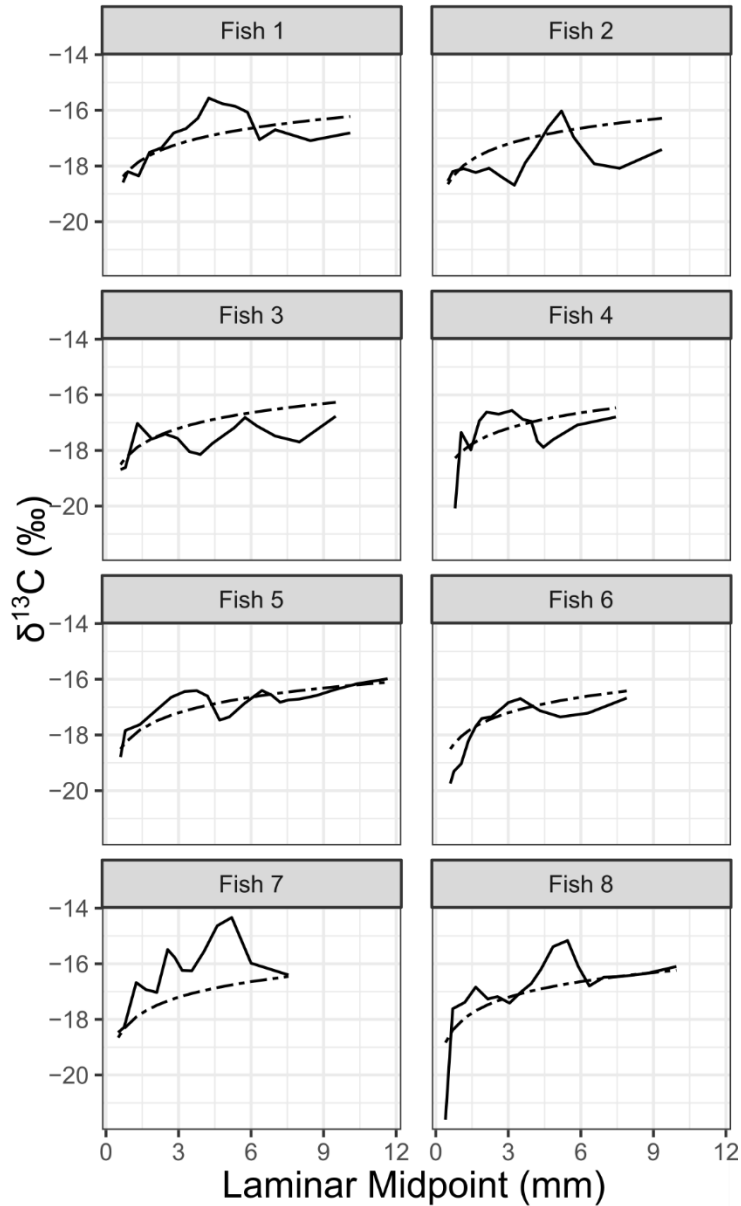
Figure 4.9

Graphs of the predicted and measured $\delta^{13}C$ isotopic lifetime histories of eight Red Snapper. The predicted $\delta^{13}C$ values are represented as a dotted line and were derived from the laminar midpoint of each lamina and the regression equation from Figure 4.5 The measured $\delta^{13}C$ values are represented as a solid line. Deviations of the solid line from the dotted line are presumed to represent movement.
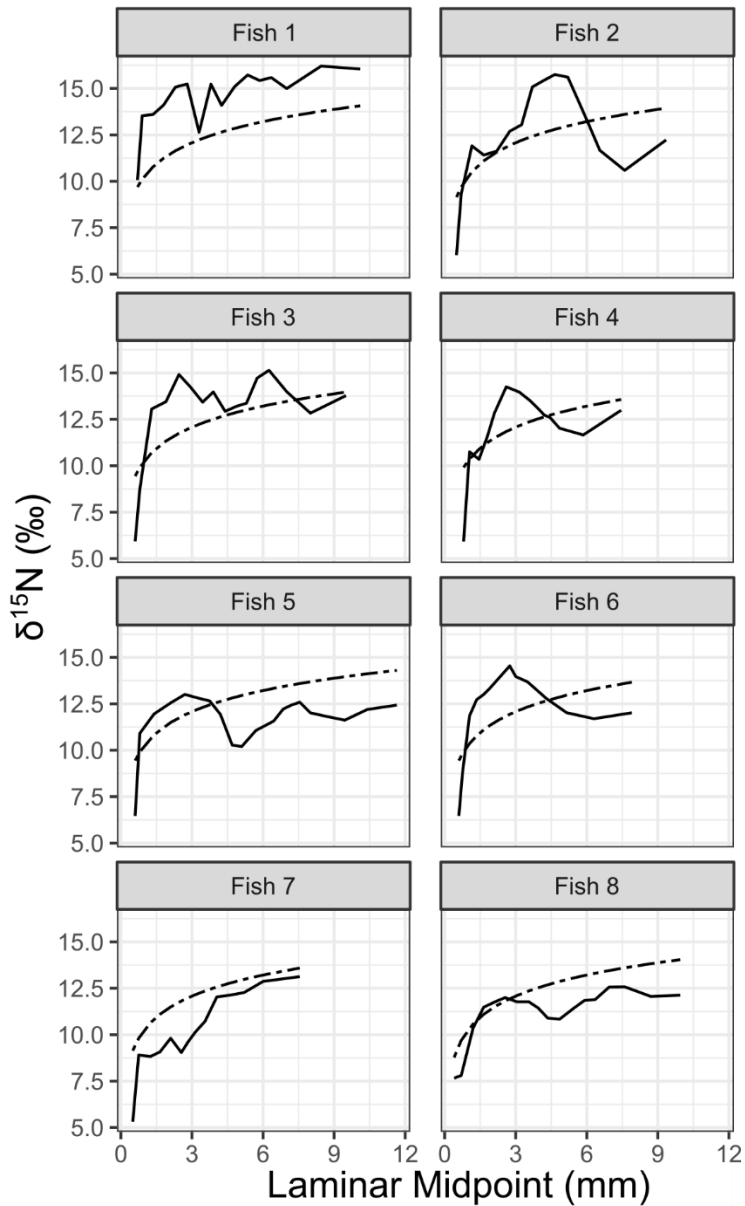
Figure 4.10
Graphs of the predicted and measured δ^{15}N isotopic lifetime histories of eight Red Snapper. The predicted δ^{15}N values are represented as a dotted line and were derived from the laminar midpoint of each lamina and the regression equation from Figure 4.5. The measured δ^{15}N values are represented as a solid line. Deviations of the solid line from the dotted line are presumed to represent movement.
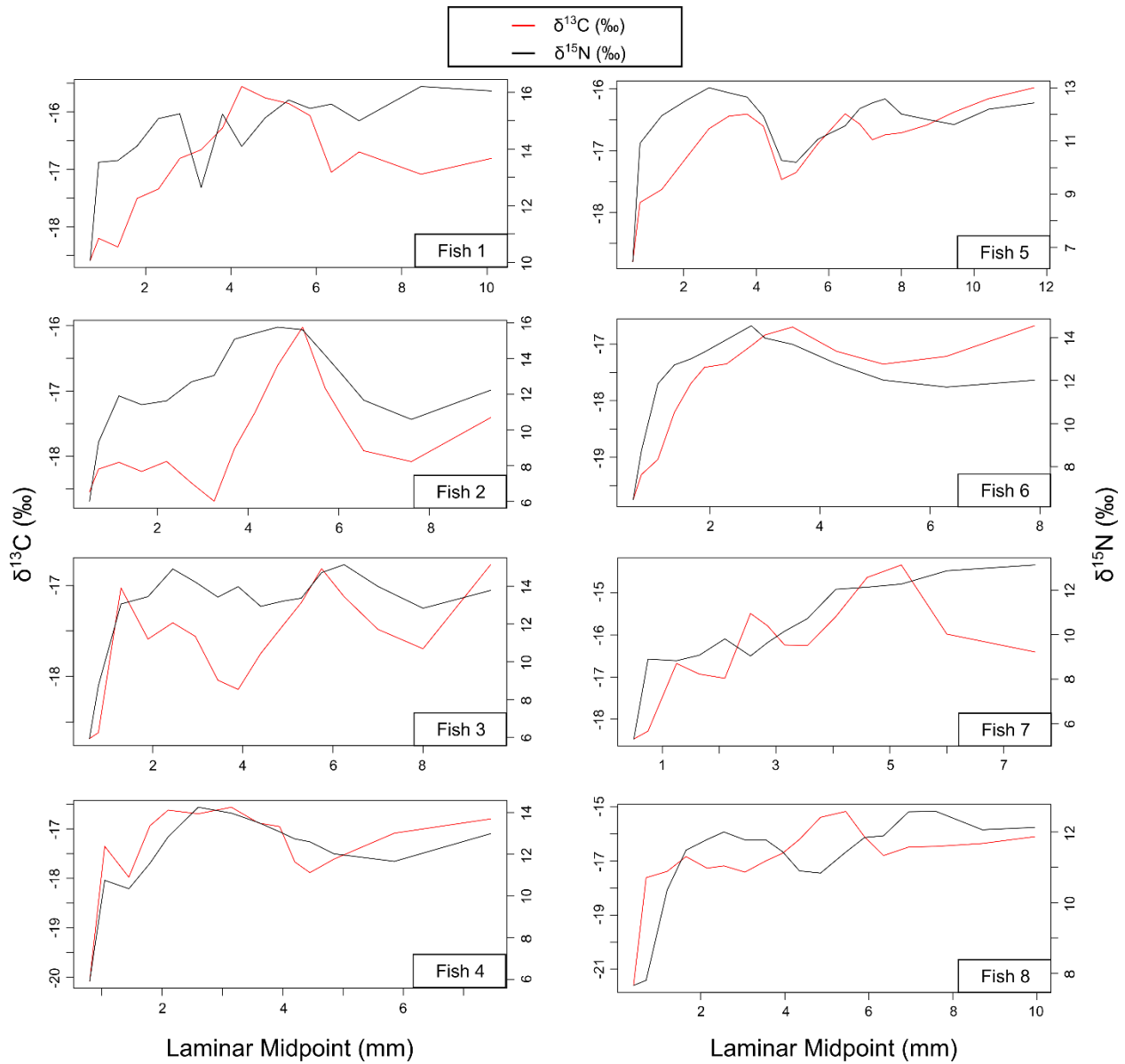
Figure 4.11
Graphs depicting the δ^{13}C and δ^{15}N isotopic life histories measured in the eye lenses of eight Red Snapper. The left y-axis and red lines correspond to the measured δ^{13}C value of each lamina, and the right y-axis and black lines correspond to the measured δ^{15}N value of each lamina. Similar shapes in the δ^{13}C and δ^{15}N lines indicate the fish may have been stationary throughout life.

156

4.5 Discussion

4.5.1 Eye lens and muscle isotopes

The preliminary analyses performed on the eye lenses indicated a weak relationship between eye lens $\delta^{13}C$ values and muscle $\delta^{13}C$ values, wherein muscle $\delta^{13}C$ values were higher on average compared to eye lens $\delta^{13}C$ values. A stronger linear relationship was observed between eye lens $\delta^{15}N$ values and muscle $\delta^{15}N$ values, though the difference between the isotopic values of the muscle and eye lens was less consistent than that of $\delta^{13}C$ values. These results contrast those of Quaeck-Davies et al. (2018) who found that muscle tissue had consistently higher $\delta^{13}C$ and $\delta^{15}N$ values than eye lens tissue, though they noted that the differences were minor enough to be obscured by between-individual variation and analytical error. In the results presented here, the average difference between muscle and eye lens tissue isotopic values was low enough to be considered negligible but, in the case of individual fish (Fish 5 $\delta^{13}C$ values and Fish 3 $\delta^{15}N$ values), the difference could be considered substantial. It is also notable that there was not a strong linear relationship between eye lens and muscle $\delta^{13}C$ values. These results could be due to a fractionation process within the body of Red Snapper that is not consistent between muscle and eye lens tissue, or it could be due to a lag between isotopic values being recorded in muscle and in eye lens laminae. If many of the fish changed their basal resource dependence (Keough et al. 1998; Araujo et al. 2007; Ellis et al. 2014) or moved along a spatial $\delta^{13}C$ gradient, the shift in $\delta^{13}C$ values would be recorded first in the eye lens (which had a lag of 50 days; Granneman 2018), whereas the muscle would be an average of the isotopic environment encountered by the fish over last few months (Buchheister and Latour 2010; Nelson et al. 2011). Even though there is a weaker relationship between bulk muscle and eye lens $\delta^{13}C$ values, the $\delta^{13}C$ isoscape (which was created using Red Snapper muscle) should still be applicable to eye

lens data since that isoscape uses data that were corrected and kriged in order to infer how environmental isotopic conditions would be reflected in Red Snapper without influence from the condition of individual fish.

4.5.2 Trophic growth

The eye lens isotopic histories showed an overall increase in δ^{13}C and δ^{15}N values over the course of the life of most fish. An increase in δ^{13}C and δ^{15}N values with age/size is generally interpreted as trophic growth (i.e., increase in trophic position with size; Curtis et al. 2020; Vecchio et al. 2022). The pattern of increase in the data was logarithmic (i.e., a natural log transformation on regressions between δ^{13}C and δ^{15}N values and LM improved fit over a linear regression), which indicates that δ^{13}C and δ^{15}N values increased logarithmically with the growth of the fish. Patterns associated with trophic growth have been observed in the majority of fish eye lens studies to date (Curtis et al. 2020; Kurth et al. 2019; Quaeck-Davies et al. 2018; Simpson et al. 2019; Wallace 2019; Vecchio et al. 2021; Vecchio and Peebles 2022; Wallace et al. 2014), and diet studies have also documented trophic growth in Red Snapper (Wells et al. 2008). Whereas the isotope-LM regressions were significant, both had moderate to low R^2 values, which indicated trophic growth was not the only influence on δ^{13}C and δ^{15}N values over the course the lifetimes of the sampled Red Snapper. The influence of trophic growth may be obscured by shifts between basal resources and/or by movement across an isotopic gradient, or it could be that shifts in diet are sometimes tied to shifts in habitat rather than fish size (Szedlmayer and Lee 2004; Gallaway et al. 2009).

At the individual level, several fish did not demonstrate a consistent increase in either δ^{13}C or δ^{15}N values with growth, as seen in the individual δ^{13}C and δ^{15}N correlation results and

visually in the IHL plots. Most fish had their highest δ^{13}C values at 20-30 cm rather than at their maximum SL and, three fish (Fish 2, Fish 4, and Fish 6) had their highest δ^{15}N values at a smaller size (10-20 cm) followed by a decrease. In both cases, the patterns seen here likely indicate movement which will be discussed below. A high carbon value earlier in life is similar to the "carbon bump" discussed in Vecchio and Peebles (2022). This pattern is defined as a peak in δ^{13}C values, wherein δ^{13}C values increase faster than δ^{15}N values and then decrease faster than δ^{15}N values (Vecchio and Peebles 2022). By this definition, only Fish 2 would be considered to have a carbon bump and, even though it fits the technical definition, the bump in δ^{13}C values is accompanied by a bump in δ^{15}N values. An accompanying bump in δ^{15}N values is also seen for other fish that had their highest δ^{13}C value earlier in their lives. In Vecchio and Peebles (2022), the carbon bump was attributed to juvenile fish settling in nearshore environments and increasing their dependence on benthic basal resources rather than the more planktonic resources they had relied on earlier in life, followed by movement back to the outer continental shelf at sexual maturity and a switch back to planktonic basal resource dependence. For the fish analyzed in this dissertation, the patterns seen in δ^{13}C and δ^{15}N values do not appear to follow the pattern expected for a "carbon bump", and therefore the results do necessarily not suggest an early life, temporary switch to basal benthic resources in Red Snapper.

4.5.3 Movement

Eye lenses are a relatively new but increasingly used source of organism ILH. A general means of determining movement is to determine what the expected δ^{13}C and δ^{15}N ILH curves would look like if no movement was occurring and assume any deviations are due to movement. Methods for determining potential movement of fish from eye lens isotopes include comparing

159

the eye lens ILH of the species of interest to the eye lens ILH of a species known to be stationary throughout life (Vecchio et al. 2021), performing correlations between δ^{13}C values, δ^{15}N values, and ELD (Vecchio et al. 2021), and comparing the measured eye lens ILH of a fish with a predicted eye lens ILH based on ELD (Vecchio and Peebles 2022). In this dissertation, a combination of the second and third methods was used. The basic principle behind these methods is that, if a fish was stationary throughout its life, δ^{13}C and δ^{15}N values would follow a general logarithmic pattern of trophic growth (Curtis et al. 2020; Vecchio and Peebles 2021) and be highly correlated with ELD and with each other (Vecchio et al. 2021). It should be noted that, while a strong correlation between δ^{13}C and δ^{15}N values is generally indicative of stationary trophic growth (Vecchio et al. 2021), there are several areas in the GOM where δ^{13}C and δ^{15}N values are spatially correlated (i.e., Western GOM), so a moving fish could also have highly correlated δ^{13}C and δ^{15}N values in those areas. For this reason, it is prudent to combine an evaluation of δ^{13}C and δ^{15}N correlations with a numerical (deviation score) and visual comparison of the eye lens ILH and expected logarithmic trophic growth.

Based on the correlation of δ^{13}C and δ^{15}N values and the plots of measured and predicted ILHs, Fish 4 and Fish 6 are the least likely to have moved, Fish 1 is the most likely to have moved, and the other fish sampled likely moved and/or changed diet several times in their lives. These results agree with numerous studies that have documented Red Snapper moving throughout their lives (Patterson et al. 2001a; Addis et al. 2013; Dance and Rooker 2019; Wallace 2019). Red Snapper may move for a variety of reasons including ontogenetic habitat shifts (Gallaway et al. 2009), diet changes (McCawley and Cowan 2007), water temperature (Gallaway et al. 1999), episodic events such as hurricanes and hypoxia (Patterson et al. 2001a; Stanley and Wilson 2004), and other local conditions (Diamond et al. 2007).

Several fish had early life peaks in $\delta^{13}C$ values (Fish 1, Fish 2, Fish 5, and Fish 7) and/or

$\delta^{15}N$ values (Fish 2, Fish 4, Fish 5, and Fish 6) around 10-30 cm SL. Red Snapper reach sexual

maturity at age 2 (roughly 20-38 cm TL; Goodyear 1995) and recruit to larger reefs (Gallaway et

al. 2009). The peaks in $\delta^{13}C$ values seen in the Red Snapper sampled here seem to coincide with

the size at which Red Snapper reach sexual maturity which may indicate that some Red Snapper

either move in the positive direction along a $\delta^{13}C$ gradient or temporarily increase the proportion

of prey derived from a benthic basal resource around sexual maturity. Red Snapper may switch

habitat several times prior to sexual maturity, moving to areas of increasing relief as they

increase in size (Gallaway et al. 2009). The peaks in $\delta^{15}N$ values occurred at a smaller size than

the peaks in $\delta^{13}C$ values and may coincide with one of these earlier movements to habitats of

higher relief. If this is the case, since movement is likely determined by the available habitat

rather than depth, the early-life patterns seen in $\delta^{15}N$ values may depend on the relative direction

of movement required to reach higher relief reefs. In general, the fish sampled displayed a high

level of individual variation in ILHs which suggests Red Snapper may be highly plastic in their

behavior. The ILHs of several of the sampled fish are discussed below to demonstrate how to

interpret eye lens ILHs and to illustrate ecologically interesting cases.

Fish 8 has a relatively weak correlation between $\delta^{13}C$ and $\delta^{15}N$ values yet, looking at the

ILHs, it seems to demonstrate logarithmic trophic growth in the $\delta^{15}N$ graph, though at a lower

$\delta^{15}N$ values than predicted. It could be that Fish 8 was feeding at a lower trophic level than

predicted, or the lower values could reflect that the area Fish 8 was captured which had lower

$\delta^{15}N$ values on the isoscape than any of the other capture locations. The $\delta^{13}C$ life history of Fish

8 does not appear to show stationary trophic growth which could be due to either of two possibly

concurrent reasons. First, it could be that Fish 8 moved around near the area it was caught, but

this was not recorded in the δ^{15}N ILH because there is very little spatial variation in δ^{15}N values in this area compared with δ^{13}C values. Second, it could be that the deviations in the δ^{13}C ILH are due to shifts in basal resource dependence rather than movement. Red Snapper are opportunistic predators that prey on a wide variety of taxa such as fishes, squids, crustaceans, and larger zooplankton (McCawley and Cowan 2007; Ward 2017), so it could be that the jagged shape to most of the δ^{13}C ILHs are at least partially due to haphazard basal resource usage. Fish 7 was captured very close to Fish 8 and has a very similar ILH to that discussed above (though the δ^{13}C ILH is even more jagged than that of Fish 8 and higher than expected) which could indicate fish have less individual variation at the regional level.

Fish 1 was the individual for which movement was most likely to have occurred. The δ^{13}C and δ^{15}N ILHs were very deviant, both from each other and from the ILHs predicted for a stationary fish. The δ^{13}C ILH had a peak at a median size as discussed above followed by an overall decrease in δ^{13}C values. In the isoscape, areas of higher δ^{13}C values than the capture location include near the outflow of the Apalachicola River, near Corpus Cristi, and, to a lesser extent, near the Alabama River outflow. The δ^{15}N ILH of Fish 1 has a somewhat jagged shape that is overall higher than the δ^{15}N values predicted for a stationary fish. Upon visual examination of the δ^{15}N measured and predicted plots, it is clear that the high deviation score of Fish 1 due at least in part to a higher overall baseline located in that area. The jagged shape of the life history could be due to movement towards and away from the West Florida Shelf where δ^{15}N values rapidly decrease. However, δ^{13}C values also decrease in that direction so it would follow that δ^{15}N and δ^{13}C values would be more correlated in that case unless changes in δ^{13}C values due to movement were overwhelmed by changes in δ^{13}C values due to basal resource usage. It also should be noted that Fish 1 was collected in an area that likely experiences higher

162

temporal variability than other areas due to the influence of the Mississippi River, so some of the deviation in the ILH could have been due to changing conditions at a stationary location rather than movement.

Fish 5 is a case where δ^{13}C and δ^{15}N values are moderately correlated, but the life history does not closely follow the predicted logarithmic growth curve. The δ^{15}N ILH had more deviation from the predicted trophic growth curve than the δ^{13}C ILH. The likely reason for this is there is more spatial variation in δ^{15}N values than in δ^{13}C values in the area Fish 5 was captured, so movement would result in larger deviations in δ^{15}N values than in δ^{13}C values. In the isoscape, both δ^{13}C and δ^{15}N values are relatively lower towards Campeche Bay and relatively higher towards mid-Texas. Based on the spatial isotopic patterns and the ILH of observed in the eye lens, it is likely Fish 5 initially settled in an area with low or moderate isotopic values (either off LA, south of Texas, or near the edge of the continental shelf) before rapidly moving closer to Corpus Cristi Bay and finally, gradually moving south to where it was captured. Fish 5 is particularly notable because if it moved in the manner described above, it would have moved over a large area including between the waters of different countries which has implications for both ecology and fisheries. This inferred movement history contrasts the results of Patterson et al. (2007) who found that Red Snapper did not cross the boundary between the US and Mexico and, instead, moved eastward from Texas. However, the Patterson et al. (2007) study was conducted on age 0 fish rather than adults, so the results in this dissertation may not be contradictory to this study.

4.5.4 Caveats

While the methods presented here are potentially useful for assessing the movement and basal resource dependence of fish, there are a few important caveats that should be considered. First, as discussed above, it is often not clear which portions of the patterns in δ^{13}C ILH are due to movement and which portions are due to changes in basal resource dependence, especially for an opportunistic mesopredator like Red Snapper. Second, the regressions used to make the predicted ILHs for a stationary fish were created using only eight fish, most of which were likely not stationary throughout their lives. If a larger sample size of fish is available, a better method would be to split the fish into 'likely moved' and 'likely stationary' categories and only use the later to create the regression location (Vecchio and Peebles 2022). Also, the form of model used to predict trophic growth assumes Red Snapper trophic growth is smooth and uniform, which may or not be the case for individuals or the species as a whole. Compound specific isotopic analysis by Wallace (2019) suggests Red Snapper trophic growth is indeed a relatively smooth curve. Third, the isoscapes that are compared with eye lens life histories were created using muscle and, as shown here, muscle δ^{13}C isotopes may not be very strongly correlated with eye lens isotopes. Fourth, it is important to note that the deviation score measure is vulnerable to baseline offsets (as seen in Fish 1), and the correlations of δ^{13}C and δ^{15}N values are vulnerable to areas with spatially correlated δ^{13}C and δ^{15}N values. Therefore, a high deviation score does not always mean a fish moved, and a low correlation *rho* does not always mean the fish did not move. Ideally, multiple metrics should be considered simultaneously when evaluating fish IHLs. Finally, the isoscapes used in this chapter have the same caveats as stated in previous chapters, the most relevant of which is that the isoscapes were created using fish caught within a single season (summer). The models created in Chapter 3 indicated that there is very little seasonal or

interannual variation in the isoscape, but it is also possible that the model created using only summer data was not adequate to predict the isoscapes in other seasons.

4.5.5 Implications

Whereas this study was primarily conducted to demonstrate the utility and associated methods for using isoscapes and eye lens ILHs to infer movement histories, there are a few results which have intriguing implications for Red Snapper ecology. First, the results of this dissertation support those of other studies that suggest Red Snapper may have a metapopulation structure in the Gulf of Mexico (Patterson 2007; Saillant et al. 2010; Fischer et al. 2004). Verifying the population structure of Red Snapper is important for fisheries management to prevent the depletion of localized subpopulations (Kell et al. 2009). Second, the results of this dissertation suggest a high level of individual variation in the movement behavior of Red Snapper which was also seen in other studies (Diamond et al. 2007; Patterson 2007). This implies that studies of Red Snapper should ideally have large sample sizes to document all potential movement patterns, and that there could be substantial annual variation in the location and densities of Red Snapper as they respond to local conditions (Diamond et al. 2007).

4.5.6 Future applications

The methods outlined here could be useful for a variety of species in a variety of areas, as long as there is adequate spatial isotopic variation. Several modifications could be made to these methods to improve the results and refine the interpretation of eye lens ILHs. First, it may be prudent to split large areas into regions for future studies. Fish located in areas of particularly high or low $\delta^{13}C$ or $\delta^{15}N$ values sometimes had a high overall deviation score due to being

consistently higher or lower than the predicted values that were based on all fish combined.

Second, more studies should be conducted to investigate the relationship between eye lens and muscle stable isotopes, since the results of this dissertation do not agree with those of Quaeck-Davies et al. (2018). Alternatively, isoscapes could be created using eye lens data, so direct comparisons could be made to eye lens ILHs. Third, interpretations of ILHs could be improved and refined by analyzing additional isotopes (i.e., ^{18}O, ^{34}S, ^{2}H). For a pilot study regarding a Gulf of Mexico δ^{18}O isoscape, see Appendix E. Finally, in order to differentiate between deviations caused by trophic or basal resource changes and movement, bulk stable isotope data could be combined with compound specific isotope analysis (Bradley et al. 2015; Wallace 2019). Determining the movement histories of fish has high utility for fisheries management and ecology (Deegan 1993; Hobson et al. 2019). Using eye lens stable isotopes to determine movement history can provide data on under sampled life stages and to get data on many fish with relatively low cost and effort (West et al. 2009).

4.6 Citations

Addis, D. T., Patterson III, W. F., Dance, M. A., and Ingram Jr, G. W. 2013. Implications of reef fish movement from unreported artificial reef sites in the northern Gulf of Mexico. *Fisheries Research* 147: 349-358.

Allen, G.R., 1985. FAO Species Catalogue. Vol. 6. Snappers of the world. An annotated and illustrated catalogue of lutjanid species known to date. *FAO Fisheries Synopsis* 125(6):208 p. Rome: FAO.

Araujo, M. S., D. I. Bolnick, G. Machado, A. A. Giaretta, and S. F. dos Reis. 2007. Using delta C-13 stable isotopes to quantify individual-level diet variation. *Oecologia* 152: 643-654.

Bearhop, S., Adams, C. E., Waldron, S., Fuller, R. A., and MacLeod, H. 2004. Determining trophic niche width: a novel approach using stable isotope analysis. *Journal of Animal Ecology* 73(5): 1007-1012.

Bolnick, D. I., Svanbäck, R., Fordyce, J. A., Yang, L. H., Davis, J. M., Hulsey, C. D., and Forister, M. L. 2003. The ecology of individuals: incidence and implications of individual specialization. *The American Naturalist* 161(1): 1-28.

Bradley, C. J., Wallsgrove, N. J., Choy, C. A., Drazen, J. C., Hetherington, E. D., Hoen, D. K., and Popp, B. N. 2015. Trophic position estimates of marine teleosts using amino acid compound specific isotopic analysis. *Limnology and Oceanography: Methods* 13(9): 476-493.

Buchheister, A., and Latour, R. J. 2010. Turnover and fractionation of carbon and nitrogen stable isotopes in tissues of a migratory coastal predator, summer flounder (*Paralichthys dentatus*). *Canadian Journal of Fisheries and Aquatic Sciences* 67(3): 445-461.

Cailliet, G. M., Radtke, R. L., and Welden, B. A. 1986. Elasmobranch age determination and verification: a review. In *Indo-Pacific Fish Biology: proceedings of the second international conference on Indo-Pacific Fishes* (pp. 345-360). Ichthyological Society of Japan, Tokyo.

Cailliet, G. M. and Goldman, K. J. 2004. Age determination and validation in chondrichthyan fishes. In: Carrier J, Musick JA, Heithaus MR (eds) <u>Biology of sharks and their relatives</u>. CRC Press LLC, Boca Raton, FL, pp 399–447

Campana, S. E. 1984. Microstructural growth patterns in the otoliths of larval and juvenile starry flounder, Platichthys stellatus. *Canadian Journal of Zoology* 62(8): 1507-1512.

Campana, S. E., and Neilson, J. D. 1985. Microstructure of fish otoliths. *Canadian Journal of Fisheries and Aquatic Sciences* 42(5): 1014-1032.

Canseco, J. A., Niklitschek, E. J., and Harrod, C. 2021. Variability in δ^{13}C and δ^{15}N trophic discrimination factors for teleost fishes: a meta-analysis of temperature and dietary effects. *Reviews in Fish Biology and Fisheries* 1-17.

Cherel, Y., Kernaléguen, L., Richard, P., and Guinet, C. 2009. Whisker isotopic signature depicts migration patterns and multi-year intra-and inter-individual foraging strategies in fur seals. *Biology Letters*,5(6): 830-832.

Curtis, J. S., Albins, M. A., Peebles, E. B., and Stallings, C. D. 2020. Stable isotope analysis of eye lenses from invasive lionfish yields record of resource use. *Marine Ecology Progress Series* 637: 181-194.

Dahm, R., Schonthaler, H. B., Soehn, A. S., Van Marle, J., and Vrensen, G. F. 2007. Development and adult morphology of the eye lens in the zebrafish. *Experimental Eye Research* 85(1): 74-89.

Dance, M. A. and Rooker, J. R. 2019. Cross-shelf habitat shifts by red snapper (*Lutjanus campechanus*) in the Gulf of Mexico. *PloS One* 14(3): e0213506.

Deegan, L. A. 1993. Nutrient and energy transport between estuaries and coastal marine ecosystems by fish migration. *Canadian Journal of Fisheries and Aquatic Sciences* 50: 74-79.

Diamond, S. L., Campbell, M. D., Olsen, D., and Wang, Y. 2007. Movers and Stayers: Individual Variability in Site Fidelity and Movements of Red Snapper off Texas. In *American Fisheries Society Symposium* 60: 163-187.

Dingle H. and Drake V.A. 2007. What is migration? *BioScience* 57(2):113-121. doi:10.1641/B570206.

Ellis, G. S., G. Herbert, and D. J. Hollander. 2014. Reconstructing carbon sources in a dynamic estuarine ecosystem using oyster amino acid delta C-13 values from shell and tissue. *Journal of Shellfish Research* 33: 217-225.

Estrada, J. A., Rice, A. N., Natanson, L. J., and Skomal, G. B. 2006. Use of isotopic analysis of vertebrae in reconstructing ontogenetic feeding ecology in white sharks. *Ecology* 87(4): 829-834.

Fischer, A. J., Baker Jr, M. S., and Wilson, C. A. 2004. Red snapper (*Lutjanus campechanus*) demographic structure in the northern Gulf of Mexico based on spatial patterns in growth rates and morphometrics. *Fishery Bulletin* 102(4): 593-603.

Fry, B. 1981. Natural stable carbon isotope tag traces Texas shrimp migrations. *Fishery Bulletin* 79 (2): 337–345.

Gallaway, B. J., Cole, J. G., Meyer, R., and Roscigno, P. 1999. Delineation of essential habitat for juvenile red snapper in the northwestern Gulf of Mexico. *Transactions of the American Fisheries Society* 128(4): 713-726.

Gallaway, B. J., Szedlmayer, S. T., and Gazey, W. J. 2009. A life history review for red snapper in the Gulf of Mexico with an evaluation of the importance of offshore petroleum platforms and other artificial reefs. *Reviews in Fisheries Science* 17(1): 48-67.

Goodyear, C. P., and Center, S. F. 1988. *Recent trends in the red snapper fishery of the Gulf of Mexico*. NOAA, National Marine Fisheries Service, Southeast Fisheries Center, Miami Laboratory, Coastal Resources Division.

Goodyear, C. P. 1995. Red snapper in U.S. waters of the Gulf of Mexico. NOAA, National Marine Fisheries Service, Southeast Fisheries Center, Miami Laboratory, Coastal Resources Division. 171 pp.

Grainger, R. M., Henry, J. J., Saha, M. S., and Servetnick, M. 1992. Recent progress on the mechanisms of embryonic lens formation. *Eye* 6(2): 117-122.

Granneman, J. E. 2018. Evaluation of trace-metal and isotopic records as techniques for tracking lifetime movement patterns in fishes. University of South Florida. Graduate Theses and Dissertations. Retrieved from: https://scholarcommons.usf.edu/etd/7675

Hobson, K. A. and Norris, D. R. 2008. Animal migration: a context for using new techniques and approaches. *Terrestrial Ecology* 2: 1-19.

Hobson, K. A. and Sease, J. L. 1998. Stable isotope analyses of tooth annuli reveal temporal dietary records: an example using Steller sea lions. *Marine Mammal Science* 14(1): 116-129.

Hobson, K. A. 1999. Tracing origins and migration of wildlife using stable isotopes:a review. *Oecologia* 120: 314−326.

Hobson, K. A., Norris, D. R., Kardynal, K. J., and Yohannes, E. 2019. Animal migration: a context for using new techniques and approaches. In <u>Tracking animal migration with stable isotopes</u> (pp. 1-23). Academic Press, London.

Horwitz, J. 2003. Alpha-crystallin. *Experimental Eye Research* 76(2): 145-153.

Hunsicker, M. E., Essington, T. E., Aydin, K. Y., and Ishida, B. 2010. Predatory role of the commander squid Berryteuthis magister in the eastern Bering Sea: insights from stable isotopes and food habits. *Marine Ecology Progress Series* 415: 91-108.

Kell, L. T., Dickey-Collas, M., Hintzen, N. T., Nash, R. D., Pilling, G. M., and Roel, B. A. 2009. Lumpers or splitters? Evaluating recovery and management plans for metapopulations of herring. *ICES Journal of Marine Science* 66(8): 1776-1783.

Keough, J. R., C. A. Hagley, E. Ruzycki, and M. Sierszen. 1998. delta C-13 composition of primary producers and role of detritus in a freshwater coastal ecosystem. *Limnology and Oceanography* 43: 734-740.

Kim, S. L., Tinker, M. T., Estes, J. A., and Koch, P. L. 2012. Ontogenetic and among-individual variation in foraging strategies of northeast Pacific white sharks based on stable isotope analysis. *PLoS One* 7(9): e45068

Kurth, B. Neal. 2016. Trophic Ecology and Habitat Use of Atlantic Tarpon (*Megalops atlanticus*). Masters Thesis. University of South Florida. Retrieved from: https://scholarcommons.usf.edu/etd/6531

Kurth, B. N., Peebles, E. B., and Stallings, C. D. 2019. Atlantic Tarpon (*Megalops atlanticus*) exhibit upper estuarine habitat dependence followed by foraging system fidelity after ontogenetic habitat shifts. *Estuarine, Coastal and Shelf Science* 225: 106248.

172

Lorrain, A., Argüelles, J., Alegre, A., Bertrand, A., Munaron, J. M., Richard, P., and Cherel, Y. 2011. Sequential isotopic signature along gladius highlights contrasted individual foraging strategies of jumbo squid (*Dosidicus gigas*). *PLoS One* 6(7): e22194

McCawley, J. R. and Cowan, J. H. 2007. Seasonal and size specific diet and prey demand of red snapper on Alabama artificial reefs. In *American Fisheries Society Symposium* (Vol. 60, p. 77). American Fisheries Society.

Meath, B., Peebles, E. B., Seibel, B. A., and Judkins, H. 2019. Stable isotopes in the eye lenses of *Doryteuthis plei* (Blainville 1823): Exploring natal origins and migratory patterns in the eastern Gulf of Mexico. *Continental Shelf Research* 174: 76-84.

Mendes, S., Newton, J., Reid, R. J., Zuur, A. F., and Pierce, G. J. 2007. Stable carbon and nitrogen isotope ratio profiling of sperm whale teeth reveals ontogenetic movements and trophic ecology. *Oecologia* 151(4): 605-615.

Minagawa, M. and E. Wada. 1984. Stepwise enrichment of $\delta^{15}N$ along food chains: Further evidence and the relation between $\delta^{15}N$ and animal age. *Geochimica et Cosmochimica Acta* 48(5): 1135-1140.

Murawski, S. A., Peebles, E. B., Gracia, A., Tunnell, J. W., and Armenteros, M. 2018. Comparative abundance, species composition, and demographics of continental shelf fish assemblages throughout the Gulf of Mexico. *Marine and Coastal Fisheries* 10(3): 325-346.

Nelson, J., Chanton, J., Coleman, F., and Koenig, C. 2011. Patterns of stable carbon isotope turnover in gag, *Mycteroperca microlepis*, an economically important marine piscivore determined with a non-lethal surgical biopsy procedure. *Environmental Biology of Fishes* 90(3): 243-252.

Nicol, J. A. C. 1989. The eyes of fishes. Oxford University Press, Oxford. 308pp.

Nielsen, J., Hedeholm, R. B., Heinemeier, J., Bushnell, P. G., Christiansen, J. S., Olsen, J., ... and Steffensen, J. F. 2016. Eye lens radiocarbon reveals centuries of longevity in the Greenland shark (Somniosus microcephalus). *Science* 353(6300): 702-704.

Onthank, K. L. 2013. Exploring the life histories of Cephalopods using stable isotope analysis of an archival tissue. PhD Dissertation, School of Biological Sciences, Washington State University. Retrieved from: https://www.proquest.com/docview/1425317087?pq-origsite=gscholar&fromopenview=true

Parry, M. 2003. The trophic ecology of two Ommastrephid squid species, *Ommastrephes bartramii* and *Shenotheuthis oualaniensis*, in the North Pacific sub-tropical gyre. PhD

Dissertation, Oceanography (Marine Biology), University of Hawaii-Manoa. Retrieved from: https://scholarspace.manoa.hawaii.edu/handle/10125/3068

Patterson III, W. F., Cowan Jr, J. H., Wilson, C. A., and Shipp, R. L. 2001a. Age and growth of red snapper, *Lutjanus campechanus*, from an artificial reef area off Alabama in the northern Gulf of Mexico. *Fishery Bulletin* 99(4): 617-628.

Patterson III, W. F., Watterson, J. C., Shipp, R. L., and Cowan Jr, J. H. 2001b. Movement of tagged red snapper in the northern Gulf of Mexico. *Transactions of the American Fisheries Society* 130(4): 533-545.

Patterson, W.F., III. 2007. A review of Gulf of Mexico red snapper movement studies: Implications for population structure. In W.F. Patterson, III, J.H. Cowan, Jr., D.A. Nieland, and G.R. Gitzhugh, editors. *Population Ecology and Fisheries of U.S. Gulf of Mexico Red Snapper. American Fisheries Society* 60: 221-236. Bethesda, Maryland.

Post, D. M. 2002. Using stable isotopes to estimate trophic position: Models, methods, and assumptions. *Ecology* 83(3): 703-718.

Quaeck-Davies, K., Bendall, V. A., MacKenzie, K. M., Hetherington, S., Newton, J., and Trueman, C. N. 2018. Teleost and elasmobranch eye lenses as a target for life-history stable isotope analyses. *PeerJ* 6: e4883.

R Core Team. 2020. R: A language and environment for statistical computing. R Foundation for Statistical Computing, Vienna, Austria. URL https://www.R-project.org/

Saillant, E., S. C. Bradfield, and J. R. Gold. 2010. Genetic variation and spatial autocorrelation among young-of-the-year red snapper (*Lutjanus campechanus*) in the northern Gulf of Mexico. *ICES Journal of Marine Science* 67(6):1240-1250.

Schwarcz, H. P., Gao, Y., Campana, S., Browne, D., Knyf, M., and Brand, U. 1998. Stable carbon isotope variations in otoliths of Atlantic cod (*Gadus morhua*). *Canadian Journal of Fisheries and Aquatic Sciences* 55(8) 1798-1806.

SEDAR. 2018. SEDAR 52 Stock Assessment Report: Gulf of Mexico Red Snapper. SEDAR, North Charleston, SC. 434p. Available online at: http://sedarweb.org/docs/sar/S52_Final_SAR_v2.pdf.

Simpson, S. J., Sims, D. W., and Trueman, C. N. 2019. Ontogenetic trends in resource partitioning and trophic geography of sympatric skates (Rajidae) inferred from stable isotope composition across eye lenses. *Marine Ecology Progress Series* 624: 103-116.

Smith, C.L., 1997. National Audubon Society field guide to tropical marine fishes of the Caribbean, the Gulf of Mexico, Florida, the Bahamas, and Bermuda. Alfred A. Knopf, Inc., New York. 720 p.

Stanley, D. R. and Wilson, C. A. 2004. Effect of hypoxia on the distribution of fishes associated with a petroleum platform off coastal Louisiana. *North American Journal of Fisheries Management* 24(2): 662-671.

Szedlmayer, S. T. and Lee, J. D. 2004. Diet shifts of juvenile red snapper (*Lutjanus campechanus*) with changes in habitat and fish size. *Fishery Bulletin* 102(2): 366-375.

Tieszen, L. L., Boutton, T. W., Tesdahl, K. G., and Slade, N. A. 1983. Fractionation and turnover of stable carbon isotopes in animal tissues: implications for $\delta^{13}C$ analysis of diet. *Oecologia* 57(1-2): 32-37.

Trueman, C. N., MacKenzie, K. M., and Palmer, M. R. 2012. Identifying migrations in marine fishes through stable-isotope analysis. *Journal of Fish Biology* 81(2): 826-847.

Peterson, B. J. and Fry, B. 1987. Stable isotopes in ecosystem studies. *Annual Review of Ecology and Systematics* 18(1): 293-320.

Post, D. M. 2002. Using stable isotopes to estimate trophic position: models, methods, and assumptions. *Ecology* 83(3): 703-718.

Vecchio, J. L., and Peebles, E. B. 2020. Spawning origins and ontogenetic movements for demersal fishes: An approach using eye-lens stable isotopes. *Estuarine, Coastal and Shelf Science* 246: 107047.

Vecchio, J. L., Ostroff, J. L., and Peebles, E. B. 2021. Isotopic characterization of lifetime movement by two demersal fishes from the northeastern Gulf of Mexico. *Marine Ecology Progress Series* 657: 161-172.

Vecchio, J. L. and Peebles, E. B. 2022. Lifetime-scale ontogenetic movement and diets of red grouper inferred using a combination of instantaneous and archival methods. *Environmental Biology of Fishes* 1-20.

Vihtelic, T. S. 2008. Teleost lens development and degeneration. *International Review of Cell and Molecular Biology* 269: 341-373.

Wallace, A. A., Hollander, D. J., and Peebles, E. B. 2014. Stable isotopes in fish eye lenses as potential recorders of trophic and geographic history. *PloS One* 9(10): e108935.

Wallace, A. A. 2019. Reconstructing Geographic and Trophic Histories of Fish Using Bulk and Compound-Specific Stable Isotopes from Eye Lenses. University of South Florida. Graduate Theses and Dissertations. Retrieved from https://www.proquest.com/dissertations-theses/reconstructing-geographic-trophic-histories-fish/docview/2343285720/se-2?accountid=14745

Ward, C. H. (Ed.). 2017. <u>Habitats and Biota of the Gulf of Mexico: Before the Deepwater Horizon Oil Spill: Volume 2: Fish Resources, Fisheries, Sea Turtles, Avian Resources, Marine Mammals, Diseases and Mortalities</u> (Vol. 2). Springer.

Weisberg, R. H., Zheng, L., and Peebles, E. 2014. Gag grouper larvae pathways on the West Florida Shelf. *Continental Shelf Research* 88: 11-23.

Wells, R. D., Cowan Jr, J. H., and Fry, B. 2008. Feeding ecology of red snapper *Lutjanus campechanus* in the northern Gulf of Mexico. *Marine Ecology Progress Series* 361: 213-225.

West, J. B., Bowen, G. J., Dawson, T. E., and Tu, K. P. (Eds.). 2009. <u>Isoscapes: understanding movement, pattern, and process on Earth through isotope mapping.</u> Springer Science & Business Media, New York. 487 pp.

Wride, M. A. 2011. Lens fibre cell differentiation and organelle loss: many paths lead to clarity. *Philosophical Transactions of the Royal Society B: Biological Sciences* 366(1568): 1219-1233.

Xu, W., Chen, X., Liu, B., Chen, Y., Huan, M., Liu, N., and Lin, J. 2019. Inter-individual variation in trophic history of Dosidicus gigas, as indicated by stable isotopes in eye lenses. *Aquaculture and Fisheries* 4(6): 261-267.

Chapter 5: Conclusions

The objectives of this dissertation were to create isoscapes for the Gulf of Mexico that could be used in various ecological studies and to provide a demonstration of how to use those isoscapes in conjunction with fish eye lenses to infer movement and diet histories for individuals. First, I created empirical isoscapes using the length-corrected δ^{13}C and δ^{15}N values of muscle tissue from two species of reef fish (Red Snapper and Yellowedge Grouper). I described the general spatial patterns in δ^{13}C and δ^{15}N as well as likely ecological explanations for those patterns. I assessed how the isoscapes varied between species and likely reasons for those differences. Next, I developed statistical models for the spatial patterns of δ^{13}C and δ^{15}N using static (latitude, longitude, and depth) and temporally dynamic (satellite products) predictors in order to make the isoscapes temporally dynamic and to further elucidate how ecological processes affected δ^{13}C and δ^{15}N values. I used these models to create predicted isoscapes for different seasons within an El Nino (2015) and a La Nina (2011) year to assess how different environmental conditions would change the isoscapes. I used these isoscapes in one application using Red Snapper eye lens isotopes. I demonstrated a series of techniques to assess whether a particular fish has moved over the course of its life. I developed a metric, called a "deviation score", which indicated how much the isotopic history of a fish deviated from a predicted isotopic life history where no movement occurred. Throughout this work, I showed how isotopic tools can be used to infer regional and organismal ecology. The products and techniques

developed here can be used for a variety of management and ecological purposes within the Gulf of Mexico and could even be modified for global applications.

5.1 Chapter summaries

5.1.1 Chapter 2

Isoscapes of δ^{13}C and δ^{15}N values were created using reef-fish muscle from two species, Red Snapper *(Lutjanus campechanus*; n = 127*)* and Yellowedge Grouper (*Epinephelus flavolimbatus*: n = 99). Fishes were collected on demersal longline research cruises throughout the Gulf of Mexico continental shelf. Muscle samples were dried and homogenized before being analyzed for δ^{13}C and δ^{15}N values using continuous flow mass spectrometry. Mann-Whitney U-Tests were used to determine whether there was a significant difference between the average capture depths and/or isotopic values of the two species. Both species had significant relationships between both δ^{13}C and δ^{15}N values and standard length, indicating both species undergo trophic growth. To remove the effect of spatial differences in trophic position, residuals from isotope-length regressions (length-corrected δ^{13}C and δ^{15}N values) were used in place of unaltered isotopic values for isoscape creation. This was done to prevent so isoscapes would primarily depict spatial differences in baseline isotopic levels relevant to the captured species.

Both δ^{13}C isoscapes produced a general pattern of higher δ^{13}C values near areas of freshwater input which can be attributed to rivers delivering nutrients which allows for higher productivity and, consequently higher δ^{13}C values (Popp et al. 1998; Hofmann et al. 2000). The Red Snapper δ^{13}C isoscape depicted decrease in δ^{13}C values with depth, which could be similarly attributed higher productivity closer to shore and or/ it could be attributed to a decrease in the importance of benthic primary producers with depth (Cooper and DeNiro 1989; Muscatine et al.

1989; Radabaugh et al. 2014). Both δ^{15}N isoscapes depicted a general pattern of higher δ^{15}N values near areas of freshwater input and lower values closer to oligotrophic/Caribbean regions. These patterns are most likely due to rivers delivering bioavailable nitrogen from organic waste sources such as livestock effluent or sewage which has higher δ^{15}N values, whereas, in oligotrophic regions, a larger portion of the bioavailable nitrogen comes from diazotrophic nitrogen fixation which has lower δ^{15}N values (Carpenter et al. 1997; Hansson et al. 1997; Kendall et al. 2001; Montoya et al. 2002; Montoya 2007). The high δ^{15}N values depicted in the northern Gulf of Mexico could be explained by the above processes but, it should be noted, this area experiences seasonal hypoxia and anoxia which allows for denitrification. Denitrification leaves behind high δ^{15}N nitrate which could be a contributing reason for the high δ^{15}N values found in consumers in that area (Altabet et al. 1999; Childs et al. 2002; Granger et al. 2008).

The differences that were observed between species (mostly in the δ^{13}C isoscapes) appear to primarily be a function of the differences in capture locations. For example, Yellowedge Grouper had less isotopic variation than Red Snapper based on the standard deviation of isotopic values. Yellowedge Grouper also had a large portion of its isotopic variation explained by trophic position based on the R^2 values of regressions between standard length and isotopic values. One explanation for these findings is that Yellowedge Grouper exhibit less overall spatial isotopic variability because they were collected from a smaller spatial area that was closer to the open waters of the deep Gulf of Mexico and therefore, a greater proportion of the total isotopic variation was explained by length.

There are a few caveats to consider in regard to these isoscapes. First, the spatial variation depicted here could be due to spatial differences in basal resource dependence of the consumers rather than baseline differences (as may be the case with the δ^{13}C depth gradient).

Second, the methods used here have the implicit assumption that the sampled fish were an adequate representation of local isotopic conditions and had not recently moved to the collection location from an area with differing baseline values. Third, the isoscapes created here may only represent isotopic conditions at the time of the sample collections and there may be temporal variation in baseline $\delta^{13}C$ and $\delta^{15}N$ values.

5.1.2 Chapter 3

While empirical isoscapes like those created in Chapter 2 are useful in many cases, they may only represent a snapshot of time and, if ecological processes influencing isotopic values have temporal variability, it is possible an isoscape will not be static over (Bowen and Revenaugh, 2003). In order to address this issue, I created statistically modeled isoscapes for length-corrected $\delta^{13}C$ and $\delta^{15}N$ values using the muscle tissue of Red Snapper and Yellowedge Grouper (collection and isotopic analysis methods are as described in Chapter 2) and satellite data products. Three-month averages of colored dissolved organic matter (CDOM; m^{-1}), chlorophyll a (Chl; mg/m^3), particulate organic carbon (POC; mg/m^3), particulate inorganic carbon (PIC; mol/m^3), sea surface temperature (SST; °C), surface photosynthetically active radiation (PAR; Einstein/m^2day), and light attenuation at 490 nm [$K_d(490)$; m^{-1}] data were obtained from the Giovanni online database (http://giovanni.gsfc.nasa.gov) for the MODIS-Aqua satellite at 4 km resolution. The three-month time frame was selected to reflect fish muscle turnover time, (McIntyre and Flecker 2006; Buchheister and Latour 2010; Nelson et al. 2011). The light attenuation coefficient of photosynthetically active radiation, $K_d(PAR)$, was calculated from MODIS-Aqua derived light attenuation at 490 nm, $K_d(490)$, using Equation 9 from Morel

et al., 2007. PAR at depth, PAR(z), was calculated using water depth (z), K_d(PAR), and PAR (Kirk 1994).

I combined the remote sensing data were with variables calculated from said data [light attenuation coefficient of photosynthetically active radiation; K_d(PAR) and PAR at depth; PAR(z)] and static spatial data (latitude, longitude, water depth) which were collected at the time of the corresponding muscle collections.. Several possible transformations were evaluated to allow for non-linear relationships between the datasets including, x^2, Ln(x), $1/x$, and $\sqrt{x}$. If any transformation improved the R^2_{adj} of a linear regression between a transformed predictor variable and the δ^{13}C or δ^{15}N data, by 0.01 or greater, the transformed variable was used instead of the original. Finally, the predictor variables were used in multiple regression analysis with δ^{13}C and δ^{15}N wherein variables were selected using forward selection and AIC.

The resultant Red Snapper models were:

LC_ δ^{13}C = -0.198*Depth^2 - 0.178*Long - 0.157*1/PIC - 0.130*SST + 0.015

LC_ δ^{15}N = -0.991*Long + 0.746*Ln(Chl) + 0.724*Lat + 0.272*PAR - 0.016

The resultant Yellowedge Grouper models were:

LC_ δ^{13}C = 0.333*Ln(Chl) + 0.194*Long - 0.162*Lat^2 + 0.157*Ln(PAR(z)) - 0.002

LC_ δ^{15}N = 0.950*Ln(CDOM) + 0.036

For all the above equations, explanatory variables are presented in order of most explained variation to least explained variation. The inclusion of latitude and longitude variables in several models suggest there are additional influential processes that were not captured by the potential predictors included in this study. The δ^{13}C models of both species had lower R^2 values and did not perform as well when the model created using one species was used to predict the isotopic values of the other species.

Isoscapes were created based on predicted δ^{13}C and δ^{15}N values from the multiple regression models above. First, four isoscapes were created using remote sensing data from the collection dates of the original muscle samples. Then, in order to assess the maximum temporal variability that could be expected based on the models, isoscapes were generated based on model predictions using data from each season in an El Niño year (2015) and a La Niña year (2011).

Similar to the empirical isoscapes, the modeled Red Snapper δ^{13}C isoscapes depicted a pattern of decrease with depth in the northern Gulf of Mexico and decreasing values closer to the Caribbean in the southern Gulf of Mexico. The depth gradient is represented in the model by the selection of the depth variable but the ecological reason for the depth gradient is likely due to productivity and/or basal resource dependence. The Red Snapper δ^{13}C model also included SST with a negative coefficient which is the opposite of the relationship between δ^{13}C and SST found at global scales (McMahon et al. 2013). I hypothesized that, in the case of the GOM isoscape, SST is a proxy for phytoplankton species composition wherein smaller phytoplankton are found near oligotrophic tropical regions with high SST. Since smaller phytoplankton tend to have lower δ^{13}C than larger phytoplankton, that would explain the region of lower δ^{13}C near the Caribbean depicted in the isoscape.

The Yellowedge Grouper δ^{13}C modeled isoscape did not depict a depth gradient, most likely because Yellowedge Grouper were captured within a spatially narrower and deeper depth range. Based on the model equations, chlorophyll levels were the most influential variable for Yellowedge Grouper δ^{13}C followed by light levels. Chlorophyll was likely included in the model because higher chlorophyll is associated with higher productivity and higher productivity is associated higher δ^{13}C values in primary producers (Popp et al. 1998; Hofmann et al. 2000). The selection of light levels at depth for the Yellowedge Grouper model may be indicative of basal

185

resource dependence, particularly in areas where chlorophyll is more uniform (most of the shelf edge apart from the northern GOM; Acker and Leptoukh 2007).

The modeled δ^{15}N isoscapes had very similar spatial patterns for both species. Lower δ^{15}N values were depicted near the tropical, oligotrophic Caribbean, and higher δ^{15}N values were depicted near areas of freshwater input. Similar to the empirical isoscapes, this pattern can be explained by the relative influence of bioavailable nitrogen from organic waste and nitrogen fixation in these areas (Carpenter et al. 1997; Hansson et al. 1997; Kendall et al. 2001; Montoya et al. 2002; Montoya 2007).

When isoscapes were created based on the isotopic values predicted by the models for seasons in and El Niño year and a La Niña year, the modeled isoscapes showed very little temporal variability in the general spatial patterns of δ^{13}C and δ^{15}N. It could be that the Gulf of Mexico experiences very little isotopic variation over time however, there are additional explanations for the observed low temporal variability. First, since the models used higher trophic level consumers, temporal variability may be dampened by the relatively long turnover times of fish muscle (Post 2002). Second, since the predictor variables were standardized which decreased the overall variability of each predictor variable (e.g., forced the standard deviation to be 1).

The δ^{13}C and δ^{15}N models created here could be used for various stable isotope ecology applications in the Gulf of Mexico however, there are several limitations of these models that should be noted for future use. First, the δ^{13}C models of both species performed poorly in regard to predicting the δ^{13}C values of the other species and the isoscapes created using the generated models depicted different spatial patterns in δ^{13}C. Therefore, the δ^{13}C models and isoscapes may not be as applicable to other species and studies as the δ^{15}N models and isoscapes. Second, the

statistical models the implicit assumption the ecological processes determining spatial patterns in isotopic values do not change over time which may not be the case. Third, using a three-month average for satellite data assumed a consistent muscle turnover time of three months, but turnover time likely changes based on the growth rate/age of the fish (Boecklen et al. 2011). Third, assessing trophic growth via linear regression assumes a static linear relationship between fish size/age and trophic position, but there is some evidence that trophic discrimination factors may change based on consumer physiology, consumer type, diet quality, and trophic level and fish may not increase their trophic position in a linear fashion (Vanderklift and Ponsard 2003; Caut et al. 2009). Last, the remote sensing products used in the isoscape models captured surface conditions whereas the fish used in this study were primarily benthic-associated, thus much of the unexplained variability in the isotopic models may due to subsurface conditions.

5.1.3 Chapter 4

I used the Red Snapper isoscapes described above in conjunction with stable isotopes from the eye lenses from eight Red Snapper to infer individual movement histories. Red Snapper samples were collected on the same longlining cruises described in Chapter 2. In the lab, I used fine-tip forceps to remove successive layers (laminae) of the eye lens until the lens core was reached measuring the diameter of the eye lens after each removal. I then analyzed each lamina for $\delta^{13}C$ and $\delta^{15}N$ values using continuous flow isotope mass spectrometry.

Linear regressions between $\delta^{13}C$ values, $\delta^{15}N$ values, and eye lens diameter indicated Red Snapper underwent trophic growth, however the moderate to low R^2 values of these regressions indicated trophic growth was not the only influence on $\delta^{13}C$ and $\delta^{15}N$ values within the eye lenses of Red Snapper. At the individual level, most fish demonstrated a general increase in $\delta^{13}C$

187

and δ^{15}N values, but neither always increased from point to point within a fish's isotopic life history and there was a high degree of individual variation in the shape of isotopic life histories.

The regression equations from the above analysis were used to predict δ^{13}C and δ^{15}N values based on the eye lens diameter of each lamina. The predicted δ^{13}C and δ^{15}N values represented the δ^{13}C and δ^{15}N values that would be expected if the fish was stationary and changes in δ^{13}C and δ^{15}N values were due only to trophic growth. Deviation scores were calculated by summing the absolute value of the difference between the predicted and measured isotopic value of each lamina for a fish. If the R^2 value of the regressions between δ^{13}C and δ^{15}N values was low and the deviation scores were high, a fish was considered likely to have moved over its life. Based on these criteria, six of the eight sampled fish were likely to have moved. Differences between the measured and predicted isotopic life histories (IHLs) of each fish were compared to values found in isoscapes to infer how each fish may have moved over its life. In general, the fish sampled displayed a high level of individual variation in ILHs which suggests Red Snapper may be highly plastic in their behavior

There are several caveats to consider when applying the methods described above. First, the δ^{13}C of a consumer may change due to movement along a baseline δ^{13}C gradient or due to changes in basal resource dependence and, it is often not clear which is responsible for the patterns observed in δ^{13}C ILHs. Second, the ILHs predicted for a hypothetical stationary fish were based on regression equations from regression using only eight fish, most of which were likely not stationary throughout their lives. A more accurate predicted ILH could be created using only fish that were likely to be stationary (Vecchio and Peebles 2022). Finally, the isoscapes used in this chapter have the same caveats and considerations as stated in previous chapter summaries.

5.2 My work in context of other studies

Several other δ^{13}C and δ^{15}N isoscapes have been created for the Gulf of Mexico and these show varying levels of agreement with the isoscapes created in this dissertation. Overall, δ^{15}N isoscapes from other studies show a high level of agreement with the isoscapes created for this dissertation and with each other. All these isoscapes depict δ^{15}N values are high near areas of freshwater input and low in oligotrophic regions and these patterns are always attributed to the relative contributions of bioavailable nitrogen from riverine sources and diazotrophic nitrogen fixation (Radabaugh et al. 2013; Radabaugh and Peebles 2014; Vander Zanden et al. 2015; Le-Alvarado et al. 2021). Relatively low δ^{15}N values in the Caribbean Sea are also depicted in isoscapes at a global scale (McMahon et al. 2013). The spatial pattern of δ^{15}N in the Gulf of Mexico appears to be consistent whether the isoscapes are created from organisms relying on planktonic basal resources (zooplankton; Le-Alvarado et al. 2021), organisms relying on benthic basal resources (Vander Zanden et al. 2015), or organisms that likely integrate multiple trophic pathways (fish; Radabaugh et al. 2013, Radabaugh and Peebles 2014, and this dissertation).

There is considerably less agreement among δ^{13}C isoscapes in the Gulf of Mexico. Isoscapes created using fish muscle on the West Florida Shelf depicted a δ^{13}C depth gradient similar to that seen in the Red Snapper δ^{13}C isoscape created in this dissertation, which the authors attributed to the effect of light environment on basal resource availability (Radabaugh et al. 2013; Radabaugh and Peebles 2014). Other Gulf of Mexico δ^{13}C isoscapes did not share this trend. One reason the other isoscapes did not find δ^{13}C depth gradients is that the species used to create both isoscapes are likely only relying on one basal resource whereas the fish used in this dissertation likely integrate multiple basal resources. One possible explanation for the decrease

189

in δ^{13}C values depicted in the isoscapes of this dissertation, is that fish switch from higher δ^{13}C benthic basal resources inshore to lower δ^{13}C planktonic basal resources near the shelf edge (France 1995; Doi et al. 2010). Therefore, it could be that isoscapes that use species that do not have the potential to switch basal resources spatially would not depict a δ^{13}C depth gradient.

The results of this dissertation suggest a different relationship between δ^{13}C and SST than what is commonly observed in other studies. At a global scale, the δ^{13}C values of phytoplankton often covary with SST, which is usually attributed to SST's effect on growth rates, [CO_2], and rates of CO_2 uptake (Goericke and Fry 1994; Hinga et al. 1994; Gruber et al. 1999; McMahon et al. 2013; Magozzi et al. 2017). However, at global scales, the δ^{13}C of phytoplankton generally increases with increased temperature which is the opposite pattern observed in my dissertation. It may be that the inverse relationship between δ^{13}C and SST documented in my dissertation is because SST had an influence on (or was a proxy for) spatial and/or temporal variation in primary producer species composition (Magozzi et al. 2017).

The results from the eye lens analysis in Chapter 4 present a few contrasts to previously published studies. First, the preliminary analyses performed on the eye lenses indicated muscle δ^{13}C values were higher on average compared to eye lens δ^{13}C values, and the difference between the δ^{15}N values of the muscle and eye lens was inconsistent. These results differ from those of a previous study which found that muscle tissue had consistently higher δ^{13}C and δ^{15}N values than eye lens tissue (Quaeck-Davies et al. 2018). Second, based on the widely used δ^{13}C and δ^{15}N tropic discrimination factors of 1 ‰ for δ^{13}C values and 3-3.4 ‰ for δ^{15}N values (Minagawa & Wada 1984; Post 2002), the expected slope for a regression between δ^{13}C and δ^{15}N would be around 3-3.4. However, the slope coefficient for the fish that was inferred to be most likely to have remained stationary was 2.05, which indicated the ratio of the trophic

190

discrimination factors of $\delta^{15}N$ and $\delta^{13}C$ values was close to 2.05. Since Red Snapper are likely to feed at a moderate to high trophic position, this result may align with the work of Hussey et al. (2014) which suggested that the trophic discrimination of $\delta^{15}N$ values decreases at higher trophic positions.

The ILHs observed in Chapter 4 have a few implications for Red Snapper ecology. First, my results support those of other studies that suggest Red Snapper may have a metapopulation structure in the Gulf of Mexico (Patterson 2007; Saillant et al. 2010; Fischer et al. 2004). Verifying whether Gulf of Mexico Red Snapper should be considered a single population or a metapopulation is important for fisheries management to prevent the depletion of localized subpopulations (Kell et al. 2009). My results also suggest a high level of individual variation in the behavior of Red Snapper, even with the small sample size used in my dissertation. Other studies have also found individual variation in Red Snapper and these results suggest that studies of Red Snapper should ideally have large sample sizes to document all potential behavioral patterns. The plastic response of Red Snapper to local conditions could also cause unexpected variation in the location and densities of Red Snapper (Diamond et al. 2007; Patterson 2007).

5.3 Conclusions and future directions

The major findings of this dissertation are as follows. Consumer isoscapes may present differences based on the location and life history differences of different species but, generally, spatial patterns of $\delta^{13}C$ values respond to basal resource dependence and productivity gradients and spatial patterns of $\delta^{15}N$ values respond to the $\delta^{15}N$ values of bioavailable nitrogen (animal waste near areas of freshwater input and diazotrophic fixed nitrogen near the tropics). There is little predicted seasonal or interannual variation in the general spatial patterns of increase and

decrease in $\delta^{13}C$ and $\delta^{15}N$ values though this area requires further study, particularly for $\delta^{13}C$ values. Pairwise regressions among $\delta^{13}C$ values, $\delta^{15}N$ values, and eye lens diameter can be used in conjunction with how a fish's isotopic life history deviates from that predicted based on only trophic growth (deviation score) to assess whether and in what direction a fish moved throughout its life. Red Snapper have a high level of individual variation in their movement and diet histories though there may some convergence in those traits at a regional scale.

In the future, the Gulf of Mexico isoscape models could potentially be improved in the following ways. First, the spatial and temporal scale of variability of baseline isotopes could be investigated, particularly that of $\delta^{13}C$ values. Whereas $\delta^{15}N$ isoscapes appear to be consistent regardless of temporal or spatial scales, the $\delta^{13}C$ isoscapes created here were not very consistent and the $\delta^{13}C$ models had relatively low predictive power. It could be the spatial or temporal variability of $\delta^{13}C$ baselines was not captured in these models and that introduced a high level of error. Second, additional explanatory variables could be evaluated for the multiple regression models to improve fit. Variables explicitly describing freshwater input or organic loading from various major rivers and variables describing sub-surface water conditions (i.e., sonde data) may particularly relevant.

Several modifications could be made to improve the results and refine the interpretation of eye lens isotopic life histories. First, it may be prudent to split large areas into smaller regions for future studies if sample sizes allow. The deviation score metric was vulnerable to baseline offsets, and it is possible that fish located in areas of particularly high or low $\delta^{13}C$ or $\delta^{15}N$ values could have high deviation scores despite remaining stationary. Splitting large areas into regions could lower the influence of baseline offsets and increase the interpretive power of deviation scores. Second, the relationship between the stable isotope values of eye lenses and muscle tissue

192

requires further investigation. The results presented in this dissertation differ from previous studies (Quaeck-Davies et al. 2018) which suggests the relationship between muscle and eye lens stable isotopes may be variable and eye lens data may not be as directly applicable to isoscapes created with muscle tissue. Third, data from other isotopes (i.e., ^{18}O, ^{34}S, ^{2}H) could increase the accuracy of ILH interpretations. Fourth, bulk stable isotope data could be combined with compound specific isotope analysis in order to determine what portions of ILH variability is due trophic or basal resource changes and what portions of variation are due to movement (Bradley et al. 2015; Wallace 2019).

Finally, both isoscape models and eye lens interpretations could be modified to include traits of individual fish to account for variability in trophic fractionation and in tissue turnover time. There is evidence that trophic fractionation is not constant and responds to a variety of factors including consumer physiology, consumer type, diet quality, and trophic level (Vanderklift and Ponsard 2003; Caut et al. 2009). Of particular concern to the interpretation of eye lens isotopes, it is possible that the growth rate at the time of tissue formation may affect the tissue-diet isotopic spacing (Trueman et al. 2005) and/or isotopic incorporation rate. Only one study, to date, has investigated the timing of isotopic incorporation within eye lenses (Granneman 2018). This study found that isotopic incorporation began 16 days after a diet switch however, this study used younger fish (< 1 year) that were experiencing a relatively high growth rate and, it is possible that, for adult fish, isotopic incorporation may not be as rapid. Future studies could investigate these relationships and develop equations that could modify the measured eye lens isotopes based on life stage to better infer location or trophic position. Future investigation of these relationships could also be applied to interpretations based on the growth

seasons of certain species (e.g., the location/diet of the fish during growth seasons may be overrepresented within a lamina).

5.4 Citations

Acker, J. G., and Leptoukh, G. 2007. Online analysis enhances use of NASA earth science data. *Eos, Transactions American Geophysical Union* 88(2): 14-17.

Altabet, M. A., Pilskaln, C., Thunell, R., Pride, C., Sigman, D., Chavez, F., and Francois, R. 1999. The nitrogen isotope biogeochemistry of sinking particles from the margin of the Eastern North Pacific. *Deep Sea Research Part I: Oceanographic Research Papers* 46(4): 655-679.

Alt-Epping, U., Mil-Homens, M., Hebbeln, D., Abrantes, F., and Schneider, R. R. 2007. Provenance of organic matter and nutrient conditions on a river- and upwelling influenced shelf: a case study from the Portuguese Margin. *Marine Geology* 243, 169–179.

Barnes, C., Jennings, S., and Barry, J. T. 2009. Environmental correlates of large-scale spatial variation in the $\delta^{13}C$ of marine animals. *Estuarine, Coastal and Shelf Science* 81(3): 368-374.

Boecklen, W. J., Yarnes, C. T., Cook, B. A., and James, A. C. 2011. On the use of stable isotopes in trophic ecology. *Annual Review of Ecology, Evolution, and Systematics* 42: 411-440.

Bowen, G. J. 2010. Isoscapes: Spatial Pattern in Isotopic Biogeochemistry. *Annual Review of Earth and Planetary Sciences* 38(1): 161-187.

Bowen, G. J. and J. Revenaugh. 2003. Interpolating the isotopic composition of modern meteoric precipitation. *Water Resources Research* 39:1299.

Bradley, C. J., Wallsgrove, N. J., Choy, C. A., Drazen, J. C., Hetherington, E. D., Hoen, D. K., and Popp, B. N. 2015. Trophic position estimates of marine teleosts using amino acid compound specific isotopic analysis. *Limnology and Oceanography: Methods* 13(9): 476-493.

Buchheister, A., and Latour, R. J. 2010. Turnover and fractionation of carbon and nitrogen stable isotopes in tissues of a migratory coastal predator, summer flounder (*Paralichthys dentatus*). *Canadian Journal of Fisheries and Aquatic Sciences* 67(3): 445-461.

Campana, S. E., and Neilson, J. D. 1985. Microstructure of fish otoliths. *Canadian Journal of Fisheries and Aquatic Sciences* 42(5): 1014-1032.

Canseco, J. A., Niklitschek, E. J., and Harrod, C. 2021. Variability in δ^{13}C and δ^{15}N trophic discrimination factors for teleost fishes: a meta-analysis of temperature and dietary effects. *Reviews in Fish Biology and Fisheries* 1-17.

Carpenter, E. J., Harvey, H. R., Fry, B., and Capone, D. G., 1997. Biogeochemical tracers of the marine cyanobacterium Trichodesmium. *Deep Sea Research Part A: Oceanographic Research Papers* 44: 27–38.

Caut, S., Angulo, E. and Courchamp, F. 2009. Variation in discrimination factors (Δ^{15}N and Δ^{13}C): the effect of diet isotopic values and applications for diet reconstruction. *Journal of Applied Ecology* 46: 443-453. doi:10.1111/j.1365-2664.2009.01620.x

Childs, C. R., Rabalais, N. N., Turner, R. E., and Proctor, L. M. 2002. Sediment denitrification in the Gulf of Mexico zone of hypoxia. *Marine Ecology Progress Series* 240: 285-290.

Cifuentes, L. A. 1987. Sources and biogeochemistry of organic matter in the Delaware estuary. Doctoral dissertation, University of Delaware. Retrieved from: https://www.proquest.com/docview/303473515?pq-origsite=gscholar&fromopenview=true

Ceia, F. R., Cherel, Y., Paiva, V. H., and Ramos, J. A. 2018. Stable Isotope Dynamics (δ^{13}C and δ^{15}N) in Neritic and Oceanic Waters of the North Atlantic Inferred From GPS-Tracked Cory's Shearwaters. *Frontiers in Marine Science* 5.

Cooper, L. W. and DeNiro, M. J. 1989. Stable carbon isotope variability in the seagrass *Posidonia oceanica*: evidence for light intensity effects. *Marine Ecology Progress Series* 50: 225–229.

Curtis, J. S., Albins, M. A., Peebles, E. B., and Stallings, C. D. 2020. Stable isotope analysis of eye lenses from invasive lionfish yields record of resource use. *Marine Ecology Progress Series* 637: 181-194.

Dahm, R., Schonthaler, H. B., Soehn, A. S., Van Marle, J., and Vrensen, G. F. 2007. Development and adult morphology of the eye lens in the zebrafish. *Experimental Eye Research* 85(1): 74-89.

Deegan, L. A. 1993. Nutrient and energy transport between estuaries and coastal marine ecosystems by fish migration. *Canadian Journal of Fisheries and Aquatic Sciences* 50: 74-79.

DeNiro, M. J. and Epstein, S. 1978. Influence of diet on the distribution of carbon isotopes in animals. *Geochimica et Cosmochimica Acta* 42(5): 495-506.

Diamond, S. L., Campbell, M. D., Olsen, D., and Wang, Y. 2007. Movers and Stayers: Individual Variability in Site Fidelity and Movements of Red Snapper off Texas. In *American Fisheries Society Symposium* 60: 163-187.

Dingle H. and Drake V.A. 2007. What is migration? *BioScience* 57(2):113-121. doi:10.1641/B570206.

Fischer, A. J., Baker Jr, M. S., and Wilson, C. A. 2004. Red snapper (*Lutjanus campechanus*) demographic structure in the northern Gulf of Mexico based on spatial patterns in growth rates and morphometrics. *Fishery Bulletin* 102(4): 593-603.

France, R. L. 1995. Carbon-13 enrichment in benthic compared to planktonic algae: foodweb implications. *Marine Ecology Progress Series* 124: 307-312.

Fry, B. 1988. Food web structure on Georges Bank from stable C, N, and S isotopic compositions. *Limnology and Oceanography* 33: 1182–1190.

Gallaway, B. J., Szedlmayer, S. T., and Gazey, W. J. 2009. A life history review for red snapper in the Gulf of Mexico with an evaluation of the importance of offshore petroleum platforms and other artificial reefs. *Reviews in Fisheries Science* 17(1): 48-67.

Gearing, J. N., Gearing, P. J., Rudnick, D. T., Requejo, A. G., and Hutchins, M. J. 1984. Isotopic variability of organic carbon in a phytoplankton-based, temperate estuary. *Geochimica et Cosmochimica Acta* 48(5): 1089-1098.

Goericke, R., and B. Fry. 1994. Variations of marine plankton $\delta^{13}C$ with latitude, temperature, and dissolved CO2 in the world ocean. *Global Biogeochemical Cycles* 8:85–90.

Goodyear, C. P. 1995. Red snapper in U.S. waters of the Gulf of Mexico. NOAA, National Marine Fisheries Service, Southeast Fisheries Center, Miami Laboratory, Coastal Resources Division. 171 pp.

Graham, B.S., Koch, P.L., Newsome, S.D., McMahon, K.W., Aurioles, D., 2010. Using isoscapes to trace the movements and foraging behavior of top predators in oceanic ecosystems. In: West, J.B., Bowen, G.J., Dawson, T.E., Tu, K.P. (Eds.), Isoscapes: Understanding

Movement, Pattern, and Process on Earth through Isotope Mapping. Springer, New York, pp. 299–318.

Granger, J., Sigman, D. M., Lehmann, M. F., and Tortell, P. D. 2008. Nitrogen and oxygen isotope fractionation during dissimilatory nitrate reduction by denitrifying bacteria. *Limnology and Oceanography* 53(6): 2533-2545.

Granneman, J. E. 2018. Evaluation of trace-metal and isotopic records as techniques for tracking lifetime movement patterns in fishes. University of South Florida. Graduate Theses and Dissertations. https://scholarcommons.usf.edu/etd/7675

Gruber, N., Keeling, C. D., Bacastow, R. B., Guenther, P. R., Lueker, T. J., Wahlen, M., Meijer, H.A., Mook, W.G. and Stocker, T.F. 1999. Spatiotemporal patterns of carbon-13 in the global surface oceans and the oceanic Suess effect. *Global Biogeochemical Cycles* 13(2): 307-335.

Hannides, C. C. S., Popp, B. N., Landry, M. R., and Graham, B. S. 2009. Quantitative determination of zooplankton trophic position using amino acid-specific stable nitrogen isotope analysis. *Limnology and Oceanography* 54: 50-61.

Hansson, S., Hobbie, J. E., Elmgren, R., Larsson, U., Fry, B., and Johansson, S. 1997. The stable nitrogen isotope ratio as a marker of food-web interactions and fish migration. *Ecology* 78: 2249–2257.

Hinga, K. R., Arthur, M. A., Pilson, M. E., and Whitaker, D. 1994. Carbon isotope fractionation by marine phytoplankton in culture: the effects of CO2 concentration, pH, temperature, and species. *Global Biogeochemical Cycles* 8(1): 91-102.

Hobson, K. A., Barnett-Johnson, R., and Cerling, T. 2010. Using isoscapes to track animal migration. In: West, J.B., Bowen, G.J., Dawson, T.E., Tu, K.P. (Eds.), Isoscapes: Understanding Movement, Pattern, and Process on Earth through Isotope Mapping. Springer, New York, pp. 273–298.

Hobson, K. A., Norris, D. R., Kardynal, K. J., and Yohannes, E. 2019. Animal migration: a context for using new techniques and approaches. In Tracking animal migration with stable isotopes (pp. 1-23). Academic Press, London.

Hofmann, M., Wolf-Gladrow, D. A., Takahashi, T., Sutherland, S. C., Six, K. D., and MaierReimer, E. 2000. Stable carbon isotope distribution of particulate organic matter in the ocean: a model study. *Marine Chemist*ry 72: 131–150.

Horwitz, J. 2003. Alpha-crystallin. *Experimental Eye Research* 76(2): 145-153.

Hunsicker, M. E., Essington, T. E., Aydin, K. Y., and Ishida, B. 2010. Predatory role of the commander squid Berryteuthis magister in the eastern Bering Sea: insights from stable isotopes and food habits. *Marine Ecology Progress Series* 415: 91-108.

Hussey, N. E., MacNeil, M. A., McMeans, B. C., Olin, J. A., Dudley, S. F., Cliff, G., Wintner, S. P., Fennessy, S. T. and Fisk, A. T. 2014. Rescaling the trophic structure of marine food webs. *Ecology Letters* 17(2): 239-250.

Jennings, S. and K.J. Warr. 2003. Environmental correlates of large-scale spatial variation in the δ^{15}N of marine animals. *Marine Biology* 142: 1131-1140.

Kell, L. T., Dickey-Collas, M., Hintzen, N. T., Nash, R. D., Pilling, G. M., and Roel, B. A. 2009. Lumpers or splitters? Evaluating recovery and management plans for metapopulations of herring. *ICES Journal of Marine Science* 66(8): 1776-1783.

Kendall, C., Silva, S. R., and Kelly, V. J., 2001. Carbon and nitrogen isotopic compositions of particulate organic matter in four large river systems across the United States. *Hydrological Processes* 15: 1301–1346.

Kline, Jr, T. C. 1999. Temporal and spatial variability of ^{13}C/^{12}C and ^{15}N/^{14}N in pelagic biota of Prince William Sound, Alaska. *Canadian Journal of Fisheries and Aquatic Sciences* 56(S1): 94-117.

Kürten, B., Frutos, I., Struck, U., Painting, S. J., Polunin, N. V., and Middelburg, J. J. 2013. Trophodynamics and functional feeding groups of North Sea fauna: a combined stable isotope and fatty acid approach. *Biogeochemistry* 113(1-3): 189-212.

Kurth, B. N., Peebles, E. B., and Stallings, C. D. 2019. Atlantic Tarpon (*Megalops atlanticus*) exhibit upper estuarine habitat dependence followed by foraging system fidelity after ontogenetic habitat shifts. *Estuarine, Coastal and Shelf Science* 225: 106248.

Laws, E. A., Popp, B. N., Bidigare, R. R., Kennicutt, M. C., and Macko, S. A.,1995. Dependence of phytoplankton carbon isotopic composition on growth rate and [CO_2]aq: Theoretical considerations and experimental results. *Geochimica et Cosmochimica Acta* 59: 1131–1138.

Le-Alvarado, M., Romo-Curiel, A. E., Sosa-Nishizaki, O., Hernández-Sánchez, O., Barbero, L., and Herzka, S. Z. 2021. Yellowfin tuna (*Thunnus albacares*) foraging habitat and trophic position in the Gulf of Mexico based on intrinsic isotope tracers. *PloS One* 16(2): e0246082.

Magozzi, S., Yool, A., Vander Zanden, H. B., Wunder, M. B., and Trueman, C. N. 2017. Using ocean models to predict spatial and temporal variation in marine carbon isotopes. *Ecosphere* 8(5): e01763.

Mariotti, A., Lancelot, C., & Billen, G. 1984. Natural isotopic composition of nitrogen as a tracer of origin for suspended organic matter in the Scheldt estuary. *Geochimica et Cosmochimica Acta* 48(3): 549-555.

McIntyre, P. B., and Flecker, A. S. 2006. Rapid turnover of tissue nitrogen of primary consumers in tropical freshwaters. *Oecologia* 148(1): 12-21.

McMahon, K.W., Hamady, L.L., and Thorrold, S.R. 2013. A review of ecogeochemistry approaches to estimating movements of marine animals. *Limnology and Oceanography* 58(2): 697–714.

Meath, B., Peebles, E. B., Seibel, B. A., and Judkins, H. 2019. Stable isotopes in the eye lenses of *Doryteuthis plei* (Blainville 1823): Exploring natal origins and migratory patterns in the eastern Gulf of Mexico. *Continental Shelf Research* 174: 76-84.

Minagawa, M. and Wada, E. 1984. Stepwise enrichment of $\delta^{15}N$ along food chains: Further evidence and the relation between $\delta^{15}N$ and animal age. *Geochimica et Cosmochimica Acta* 48(5): 1135-1140.

Montoya, J.P. 2007. Natural abundance of $\delta^{15}N$ in marine planktonic ecosystems. In: Michener, R. and Lajtha, K. (Eds.), Stable Isotopes in Ecology and Environmental Science, second ed. Blackwell Publishing, Malden, Massachusetts, pp. 176–201.

Montoya, J.P., Carpenter, E.J., and Capone, D.G. 2002. Nitrogen fixation and nitrogen isotope abundances in zooplankton of the oligotrophic North Atlantic. *Limnology and Oceanography* 47: 1617–1628.

Muscatine, L., Porter, J.W., and Kaplan, I.R. 1989. Resource partitioning by reef corals as determined from stable isotope composition. 1. $\delta^{13}C$ of zooxanthellae and animal tissue vs depth. *Marine Biolog*y 100: 185–193.

Nelson, J., Chanton, J., Coleman, F., and Koenig, C. 2011. Patterns of stable carbon isotope turnover in gag, Mycteroperca microlepis, an economically important marine piscivore determined with a non-lethal surgical biopsy procedure. *Environmental Biology of Fishes* 90(3): 243-252.

Nerot, C., Lorrain, A., Grall, J., Gillikin, D. P., Munaron, J. M., Le Bris, H., and Paulet, Y. M. 2012. Stable isotope variations in benthic filter feeders across a large depth gradient on the continental shelf. *Estuarine, Coastal and Shelf Science* 96: 228–235.

Nicol, J. A. C. 1989. The eyes of fishes. Oxford University Press, Oxford. 308pp.

Olson, R. J., Popp, B. N., Graham, B. S., Lopez-Ibarra, G. A., Galvan-Magana, F., LennertCody, C. E., Bocanegra-Castillo, N., Wallsgrove, N. J., Gier, E., Alatorre-Ramirez, V., Balance, L.T., Fry, B. 2010. Food-web inferences of stable isotope spatial patterns in copepods and yellowfin tuna in the pelagic eastern Pacific Ocean. *Progress in Oceanography* 86: 124–138.

Onthank, K. L. 2013. Exploring the life histories of Cephalopods using stable isotope analysis of an archival tissue. PhD Dissertation, School of Biological Sciences, Washington State University. Retrieved from: https://www.proquest.com/docview/1425317087?pq-origsite=gscholar&fromopenview=true

Parry, M. 2003. The trophic ecology of two Ommastrephid squid species, *Ommastrephes bartramii* and *Shenotheuthis oualaniensis*, in the North Pacific sub-tropical gyre. PhD Dissertation, Oceanography (Marine Biology), University of Hawaii-Manoa. Retrieved from: https://scholarspace.manoa.hawaii.edu/handle/10125/3068

Patterson, W.F., III. 2007. A review of Gulf of Mexico red snapper movement studies: Implications for population structure. In W.F. Patterson, III, J.H. Cowan, Jr., D.A. Nieland, and G.R. Gitzhugh, editors. *Population Ecology and Fisheries of U.S. Gulf of Mexico Red Snapper. American Fisheries Society* 60: 221-236. Bethesda, Maryland.

Peterson, B. J. and Fry, B. 1987. Stable isotopes in ecosystem studies. *Annual Review of Ecology and Systematics* 18(1): 293-320.

Pinnegar, J. K. and Polunin, N. V. C. 1999. Differential fractionation of delta C-13 and delta N-15 among fish tissues: implications for the study of trophic interactions. *Functional Ecology* 13(2): 225-231.

Popp, B. N., Laws, E. A., Bidigare, R. R., Dore, J. E., Hanson, K. L., and Wakeham, S. G. 1998. Effect of phytoplankton cell geometry on carbon isotopic fractionation. *Geochimica et Cosmochimica Acta* 62(1): 69-77.

Post, D. M. 2002. Using stable isotopes to estimate trophic position: Models, methods, and assumptions. *Ecology* 83(3): 703-718.

Quaeck-Davies, K., Bendall, V. A., MacKenzie, K. M., Hetherington, S., Newton, J., and Trueman, C. N. 2018. Teleost and elasmobranch eye lenses as a target for life-history stable isotope analyses. *PeerJ* 6: e4883.

Quillfeldt, P., Ekschmitt, K., Brickle, P., McGill, R. A., Wolters, V., Dehnhard, N., and Masello, J. F. 2015. Variability of higher trophic level stable isotope data in space and time – a case study in a marine ecosystem. *Rapid Communications in Mass Spectrometry* 29(7): 667-674.

Radabaugh, K. R., Hollander, D. J. and Peebles, E. B. 2013. Seasonal $\delta^{13}C$ and $\delta^{15}N$ isoscapes of fish populations along a continental shelf trophic gradient. *Continental Shelf Research* 68: 112-122.

Radabaugh, K. R., and Peebles, E. B. 2014. Multiple regression models of $\delta^{13}C$ and $\delta^{15}N$ for fish populations in the eastern Gulf of Mexico. *Continental Shelf Research* 84: 158-168.

Radabaugh, K. R., Malkin, E. M., Hollander, D. J., and Peebles, E. B. 2014. Evidence for light-environment control of carbon isotope fractionation by benthic microalgal communities. *Marine Ecology Progress Series* 495: 77-90.

Rau, G. H., Riebesell, U., and Wolf-Gladrow, D. 1996. A model of photosynthetic ^{13}C fractionation by marine phytoplankton based on diffusive molecular CO_2 uptake. *Marine Ecology Progress Series* 133: 275-285.

Rooker, J. R., Stunz, G. W., Holt, S. A., and Minello, T. J. 2010. Population connectivity of red drum in the northern Gulf of Mexico. *Marine Ecology Progress Series* 407: 187-196.

Saillant, E., S. C. Bradfield, and J. R. Gold. 2010. Genetic variation and spatial autocorrelation among young-of-the-year red snapper (*Lutjanus campechanus*) in the northern Gulf of Mexico. *ICES Journal of Marine Science* 67(6):1240-1250.

Schloesser, R. W., Rooker, J. R., Louchuoarn, P., Neilson, J. D., and Secord, D. H. 2009. Interdecadal variation in seawater $\delta^{13}C$ and $\delta^{18}O$ recorded in fish otoliths. *Limnology and Oceanography* 54(5): 1665-1668.

Simpson, S. J., Sims, D. W., and Trueman, C. N. 2019. Ontogenetic trends in resource partitioning and trophic geography of sympatric skates (Rajidae) inferred from stable isotope composition across eye lenses. *Marine Ecology Progress Series* 624: 103-116.

Szedlmayer, S. T. and Lee, J. D. 2004. Diet shifts of juvenile red snapper (*Lutjanus campechanus*) with changes in habitat and fish size. *Fishery Bulletin* 102(2): 366-375.

Trueman, C. N., McGill, R. A., and Guyard, P. H. 2005. The effect of growth rate on tissue-diet isotopic spacing in rapidly growing animals. An experimental study with Atlantic salmon (*Salmo salar*). *Rapid Communications in Mass Spectrometry* 19(22): 3239-3247.

Trueman, C. N., MacKenzie, K. M., and Palmer, M. R. 2012. Identifying migrations in marine fishes through stable-isotope analysis. *Journal of Fish Biology* 81(2): 826-847.

Vanderklift, M. A., and Ponsard, S. 2003. Sources of variation in consumer-diet δ15 N enrichment: a meta-analysis. *Oecologia* 136(2): 169-182.

Vander Zanden, M. J. and Rasmussen, J. B. 2001. Variation in $\delta^{15}N$ and $\delta^{13}C$ trophic fractionation: implications for aquatic food web studies. *Limnology and Oceanography* 46, 2061–2066.

Vander Zanden, H. B., Tucker, A. D., Hart, K. M., Lamont, M. M., Fujisaki, I., Addison, D. S., ... and Bjorndal, K. A. 2015. Determining origin in a migratory marine vertebrate: a novel method to integrate stable isotopes and satellite tracking. *Ecological Applications* 25(2): 320-335.

Vecchio, J. L., and Peebles, E. B. 2020. Spawning origins and ontogenetic movements for demersal fishes: An approach using eye-lens stable isotopes. *Estuarine, Coastal and Shelf Science* 246: 107047.

Vecchio, J. L., Ostroff, J. L., and Peebles, E. B. 2021. Isotopic characterization of lifetime movement by two demersal fishes from the northeastern Gulf of Mexico. *Marine Ecology Progress Series* 657: 161-172.

Vecchio, J. L. and Peebles, E. B. 2022. Lifetime-scale ontogenetic movement and diets of red grouper inferred using a combination of instantaneous and archival methods. *Environmental Biology of Fishes* 1-20.

Vihtelic, T. S. 2008. Teleost lens development and degeneration. *International Review of Cell and Molecular Biology* 269: 341-373.

Wallace, A. A., Hollander, D. J. and Peebles, E. B. 2014. Stable isotopes in fish eye lenses as potential recorders of trophic and geographic history. *PLOS One* 9(10): e108935 DOI: 10.1371/journal.pone.0108935

West, J. B., Bowen, G. J., Dawson, T. E., and Tu, K. P. (Eds.). 2009. <u>Isoscapes: understanding movement, pattern, and process on Earth through isotope mapping.</u> Springer Science & Business Media, New York. 487 pp.

Wride, M. A. 2011. Lens fibre cell differentiation and organelle loss: many paths lead to clarity. *Philosophical Transactions of the Royal Society B: Biological Sciences* 366(1568): 1219-1233.

Xu, W., Chen, X., Liu, B., Chen, Y., Huan, M., Liu, N., and Lin, J. 2019. Inter-individual variation in trophic history of *Dosidicus gigas*, as indicated by stable isotopes in eye lenses. *Aquaculture and Fisheries* 4(6): 261-267.

Appendix A: Pilot study of growth rate effect on trophic discrimination factor using Common Snook (*Centropomus undecimalis*) fin clips

A.1. Background

The idea of animals interacting in a food web goes back as far as the 1920's (Elton 1927). The introduction of this concept was important for a number of reasons, not least of which is the implication that species do not exist in isolation and therefore should not be managed in the same way as isolated resources. The food web concept was later updated by the theory of trophic dynamics (Lindeman 1942), which included the definition of discrete trophic levels representing how far up the food chain an animal was from a primary producer. However, trophic levels do not capture the real-world complexity of individuals feeding on any number of food sources, each with their own different respective places in the food web. Therefore, "trophic position" is a more accurate measure to use when describing measured trophic relationships. As opposed to the discrete numbers that represent trophic level, trophic position is a quantitative, continuous measure of the hierarchical position of a given species in the food web (Vander Zanden and Rasmussen 1996).

The application of food webs and trophic positions to ecology allowed for a number of insights including the length of food chains (Vander Zanden et al. 1999a), the role of bottom up or top down forcing in community structure (Menge and Sutherland 1976), levels of omnivory (Thompson et al. 2007), and the presence of trophic cascades (Bascompte et al. 2005). In terms of resource management and conservation, these concepts provide a quantitative metric to

measure the effects of fishing, (Pauly et al. 1998; Branch et al., 2010), altered trophic linkages (Vander Zanden et al. 1999b), and species removal (Myers et al. 2007). Trophic position may be calculated from stomach contents, whereby an aggregate trophic position is calculated for the consumer based on the proportions of broad prey groups. However, this method is biased towards more recent meals and more refractory prey items which may create an incomplete or incorrect picture of trophic position and food web dynamics. A method that is becoming more common, in conjunction with or as an alternative to stomach content analysis, is a calculation of trophic position using nitrogen stable isotope analysis (Hobson and Welch 1992; Post 2002).

A.1.1 Trophic discrimination factors

In order to calculate a trophic position using $\delta^{15}N$ values, first a $\delta^{15}N$ value for the basal resource must be known. This can be achieved through compound specific isotope analysis (Chikaraishi et al. 2014), applying a priori knowledge about the species' diet, or by using a $\delta^{13}C$ mixing model (Post 2000). Once the $\delta^{15}N_{consumer-basal}$ value is known, it can be divided by a trophic discrimination factor (TDF) in order to calculate the trophic position (Hobson and Welch 1992; Post 2002). Trophic discrimination factors, sometimes referred to as trophic enrichment factors, are a quantity reflecting the isotopic enrichment accompanying an increase in trophic level ($\Delta^{13}C$ and $\Delta^{15}N$ for carbon and nitrogen, respectively; DeNiro and Epstein 1981; Minagawa and Wada 1984; Post 2002; Chikaraishi et al. 2007). An accurate estimate of trophic position requires an accurate TDF estimate (Post 2002).

Reported TDFs range from -8.79 to 6.1 ‰ for $\Delta^{13}C$, and -3.22 to 9.2 ‰ for $\Delta^{15}N$ (Caut et al. 2009) but, generally, a fixed value of 1.0 ‰ per trophic level for bulk $\delta^{13}C$ values and 3.4‰ per trophic level for bulk $\delta^{15}N$ values are used in food web studies (Minagawa and Wada

1984; Post 2002). While using these fixed values may be adequate in some cases, there is evidence that TDFs are not constant and respond to a variety of factors including consumer physiology, consumer type, diet quality, and trophic level (Vanderklift and Ponsard 2003; Caut et al. 2009). Both the calculation of trophic position and the creation of food webs using mixing models are highly sensitive to inaccuracies in TDF (Bond and Diamond 2011; Caut et al. 2009; Ben-David and Schell 2001). In fact, the accuracy of the TDF is often cited as the weakest link in the use of stable isotopes for food web studies (Phillips and Koch 2002; Gannes et al. 1997; Wolf et al. 2009). Understanding the mechanisms that cause changes in TDFs within individuals over time, among members of a species, or among species is necessary in order to use the correct TDF in the application of stable isotopes in food webs.

A.1.2 Variation in TDFs

One of the oldest theories for the cause behind trophic fractionation was the excretion of isotopically light nitrogen by the consumer, leaving a heavier ratio of nitrogen in the consumer's tissues (Minagawa and Wada 1984). It follows that taxa with different excretion mechanisms may have differences in the associated fractionation. It has been shown that ureotelic organisms and uricotelic organisms yielded significantly higher trophic enrichment than ammonotelic organisms, guanicotelic organisms, and organisms excreting mainly amino acids (Vanderklift and Ponsard 2003). The difference in fractionation is hypothesized to be the result of the additional biochemical reactions required to synthesize urea or uric acid from ammonia. The additional reactions may involve additional fractionation which would result in urea and uric acid being isotopically lighter than ammonia, all other things being equal (Rieutord 1999;

Vanderklift and Ponsard 2003). For example, one might expect most marine fishes (ammonotelic) to display less trophic enrichment than elasmobranchs (ureotelic).

Diet can create differences in trophic discrimination among individuals within a species or even within an individual over time. One of the first published instances of the effect of diet on trophic discrimination was documented as an increased trophic enrichment in bird species associated with fasting, both in a controlled experiment and in the field during egg laying and incubation (Hobson and Clark 1993). It was hypothesized that under conditions of nutritional stress, more nitrogenous compounds are derived from catabolism for protein synthesis. Since this source of nitrogen has already been enriched, the catabolism would "double enrich" the synthesized protein leading to an increase in trophic fractionation. The quality of diet (often measured as protein content or C:N) can similarly affect trophic fractionation through nutritional stress. An increase in $\Delta^{15}N$ with lower diet quality has been found in copepods (Trochine et al., 2019), anomopod crustaceans (Adams and Sterner 2000), fish (Bowes et al. 2014), mammals and birds (Robbins et al. 2005), and in meta-analysis (Vanderklift and Ponsard 2003; McMahon and McCarthy 2016). In a few studies (Adams and Sterner 2000; Trochine et al. 2019), results indicated that nutritional stress from decreased diet quality may have a greater effect on trophic fractionation than fasting. It was hypothesized that when an animal is fasting, its tissues initially increase $\delta^{15}N$ values as it breaks down proteins into amino acids and then keto acids, each transamination resulting in nitrogen isotope discrimination (Scrimgeour et al. 1995). But, after a time, the animal stops breaking down proteins and switches to lipids as an energy source instead and the associated increase in $\delta^{15}N$ values stops (Castellini and Rea 1992; Cherel et al. 1988). Therefore, while starvation is a state of enhanced nutritional stress compared to a consistent intake of a lower quality diet, a low-quality diet may result in ongoing "double enrichment" and

may be associated with greater trophic fractionation. However, other studies have found either the opposite relationship (Doi et al. 2011; Tamelander et al. 2006; Oelbermann and Scheu 2002) or a null result (Aberle and Malzahn 2007; Aguilar et al. 2014; Robbins et al. 2005) which suggests the effect of nutritional stress may be dependent on the species being studied.

Another source of variability in trophic discrimination is the $\delta^{15}N$ values of the food source. There is evidence that $\Delta^{15}N$ decreases as $\delta^{15}N$ values (trophic position) increases (Caut et al. 2008; Caut et al. 2009; Germain et al. 2013; Hussey et al. 2014). To my knowledge, there is no proposed mechanism for this decreasing fractionation. It is possible that, if fractionation affects a proportion of the nitrogen rather than a set value, there is less and less ^{14}N left as trophic postion increases and so there is less ^{14}N available as an option for excretion or other fractionation processes. Regardless, it appears this effect occurs within bulk tissues (Caut et al. 2008; Caut et al. 2009; Hussey et al. 2014), as well as amino acids (Germain et al. 2013). The pattern of decreasing $\Delta^{15}N$ with increasing trophic position has many important implications including a likelihood that the lengths of many food chains have been underestimated.

A.1.3 TDFs and growth rate

Previously published mechanisms for variability in trophic discrimination could imply that the growth rate of an organism may play a role in determining trophic discrimination. First, since the mortality of fishes tends to decrease as their size increases (Houde 1987), juvenile fish may be increasing the proportion of nitrogenous compounds derived from catabolism in order to maximize their protein synthesis capabilities and therefore maximize their growth rate. If this is the case, faster growth rates would be associated with increased trophic fractionation. However, if food is not as limiting (as were the conditions for this study), then fish may not rely on the

slower catabolism, transamination, and deamination processes and instead use the amino acids and proteins of their food unaltered. If this is the case, faster growth rates would be associated with decreased trophic fractionation. Another consideration is N use efficiency which may change either ontogenetically and/or in connection with growth rate.

There are a few studies that have found differences in trophic discrimination with age, life stage, or body size (Roth and Hobson, 2000; Vander Zanden et al. 2012; Villamarín et al. 2018). These observed differences may be related to changes in growth rate since most organisms have an inverse relationship between growth rate and age/life stage/body size (West et al. 2001), but, to my knowledge, there had only been one paper that has specifically investigated the effect of individual growth rate on trophic discrimination factor in a controlled setting. Trueman et al. (2006) conducted a controlled feeding experiment with Atlantic salmon, *Salmo salar*, and compared individual growth rate to muscle, liver, and hind gut contents $\delta^{13}C$ and $\delta^{15}N$ values. They found fish with faster growth rates exhibited significantly lower $\delta^{15}N$ trophic discrimination in muscle tissue and no significant relationships between growth rate and trophic discrimination for liver $\delta^{15}N$ values or muscle or liver $\delta^{13}C$ values. The authors attributed the differences in trophic discrimination to variation in N use efficiency, suggesting that increasing growth rate is accompanied by increasing N use efficiency and a decrease in *de novo* amino acid synthesis. They further suggest that the lack of significant change in trophic discrimination in liver tissue may be because liver tissue contains a greater proportion of essential amino acids relative to amino acids that are potentially synthesized *de novo*, so changes in N use efficiency have a reduced effect. They propose two mechanisms for growth rate related changes in N use efficiency; either individuals with higher food intake rates have greater N use efficiency, or genetic variation in N use efficiency leads to variation in individual growth rates. Other studies

have found the opposite pattern (Rother and Hobson 2000), or a null result (Ponsard and Averbuch 1999) which is one reason the relationship between TDFs and growth rate merits further investigation.

A.1.4 Objectives

The objective of this study was to determine what, if any, effect the growth rate of fish has on trophic discrimination factor. Such a relationship would have implications for trophic and migration studies using stable isotopes. When inferring migration over time, changes in trophic position and their associated effect on $\delta^{13}C$ and $\delta^{15}N$ values are often calculated or inferred so that the remaining changes to $\delta^{13}C$ and $\delta^{15}N$ values can be said to be due to movement. Most often, this is done using fixed trophic discrimination factors but, if more accurate, dynamic trophic discrimination factors could be used instead, it could increase the accuracy of the calculated movement.

A.2 Methods

A.2.1 Sample collection

Juvenile Common Snook (*Centropomus undecimalis*) fin clips and fish feed were obtained from Mote Aquaculture Park in Sarasota, Florida. The fish were hatched and reared as a single cohort in a controlled tank environment and fed the same food throughout. Thirty fish were selected haphazardly from the cohort, representing the full size range of the cohort. Standard length (SL), fork length (FL), total length (TL), and weight in grams were measured for each fish and a dorsal fin clip was collected and frozen. Since all fish were growing for the same

amount of time, the largest fish had the fastest average growth rate, and the smallest fish had the slowest average growth rate.

A.2.2 Isotopic analysis

In the lab, fin clip samples and fish feed were dried at 55°C for a minimum of 48 hours. A dry weight of 300–600 µg of material was placed in tin capsules for combustion and isotopic analysis. $^{13}C/^{12}C$, $^{15}N/^{14}N$, and C:N measured in replicate using a Carlo-Ebra NA2500 Series II elemental analyzer coupled to a continuous-flow ThermoFinnigan Delta Plus XL isotope ratio mass spectrometer at the University of South Florida College of Marine Science in St. Petersburg, Florida. Calibration standards were NIST 8573 and NIST 8574 L-glutamic acid standard reference materials. Results are presented in standard notation (δ, in ‰) relative to international standards Pee Dee Belemnite (PDB) and air:

$$\delta^j X = \left(\frac{(^jX/\,^iX)_{sample}}{(^jX/\,^iX)_{standard}} - 1 \right) * 1000$$

where *X* is the element and *j* and *i* are each an isotope of *X*.

A.2.3 Statistical analysis

First, a regression was performed between the $\delta^{13}C$ and $\delta^{15}N$ values of all fin clip samples to test the hypothesis that TDFs were constant among individuals. If TDFs were constant among individuals, there would be a strong correlation between $\delta^{13}C$ and $\delta^{15}N$ values. Based on the results of this regression, two samples were eliminated due to anomalous $\delta^{15}N$ values that could have been the result of measurement error or contamination. The $\delta^{13}C$ and $\delta^{15}N$ values of the feed were subtracted from the $\delta^{13}C$ and $\delta^{15}N$ values of the fin clips to calculate $\delta^{13}C$ and $\delta^{15}N$

TDFs. Each variable was tested for normality using Shapiro-Wilk test. All variables were normal except for $\delta^{15}N$ values and, subsequently, $\delta^{15}N$ TDF. However, the linear regressions involving $\delta^{15}N$ values and $\delta^{15}N$ TDF had normally distributed residuals, so assumptions of linear regression were not violated. Linear regressions were performed between $\delta^{13}C$ and $\delta^{15}N$ TDFs, indicators of growth rate (SL, FL, TL, and weight), and C:N to assess whether there was a significant relationship between growth rate and TDF values and whether the C:N ratio of the samples may have influences results. All analyses were performed in R (version 4.0.5, R Core Team 2020).

A.3 Results

A total of 30 juvenile Common Snook fin clips were analyzed for $\delta^{13}C$ and $\delta^{15}N$ values. The size range for the juveniles was 7.8 to 13.4 cm SL with an average SL of 10.3 cm. The weights of the juveniles ranged from 7.99 to 36.65 g with an average weight of 17.42 g. The $\delta^{13}C$ values of the fin clips ranged from -20.41 to -19.54 ‰ with an average of -20.05 ‰ and a standard deviation of 0.20 ‰ (Table A.1). The $\delta^{15}N$ values of the fin clips ranged from 8.07 to 11.74 ‰ with an average of 9.91 ‰ and a standard deviation of 0.66 ‰. The mean isotopic values of the food were -23.39 and 4.48 ‰ for $\delta^{13}C$ and $\delta^{15}N$ respectively, which were subtracted from each of the fin clips to determine TDF values. The full dataset can be seen in Table A.1.

If feed did not change and isotopic TDFs were constant, $\delta^{13}C$ and $\delta^{15}N$ values would be highly correlated. However, while regressions between $\delta^{13}C$ and $\delta^{15}N$ values were significant, R^2 values were below 0.3. This was an indicator that TDFs were not identical among fish. Based on the results of an initial $\delta^{13}C$ and $\delta^{15}N$ regression (Figure A.1a) with all fin clips, two samples that

appeared to have anomalous δ^{15}N values (highest and lowest points on Figure A.1a) were removed from further analysis. The fit of the regression line was improved after the removal of those samples (Figure A.1b), but the R^2 remained below 0.3.
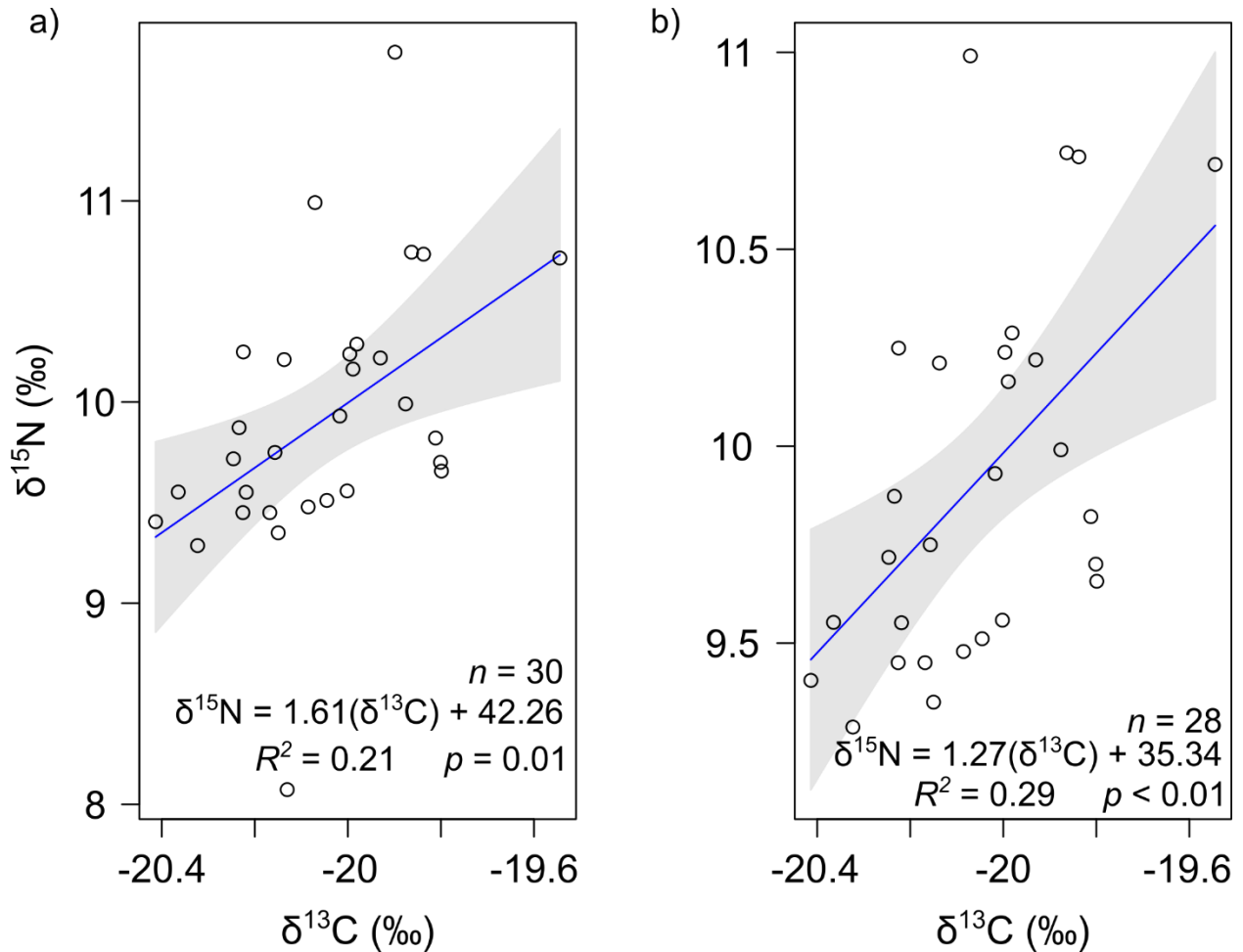
Figure A.1
Results of linear regression between δ^{13}C and δ^{15}N values with all fin clips (a) and with two outlier samples removed (b). Sample size (*n*), regression equations, R^2 values, and *p*-values are displayed on each plot. Shaded area represents standard error.

There does not appear to be a strong relationship between any indicators of growth rate and δ^{13}C TDF. None of the regressions were significant and all had R^2 values at or below 0.01 (Figure A.2 a-d). Of the regressions performed, the strongest was with C:N (Figure A.2e), which

may indicate the relative fat content of the fin clips was the best predictor of $\delta^{13}C$ values. The average C:N ratio among all samples was 4.38 whereas 3.5 is the accepted ratio above which a lipid correction should be performed (Post et al. 2007). It is possible that if the samples were lipid corrected, there would be a stronger relationship between $\delta^{13}C$ TDF and the growth rate indicators.

The linear regression results between $\delta^{15}N$ TDF and indicators of growth rate indicate a stronger relationship between $\delta^{15}N$ TDF and growth rate than $\delta^{13}C$ TDF and growth rate (A.3 a-d). These results agree with those of Trueman et al. (2006). The length- $\delta^{15}N$ TDF regressions collectively had a slope of roughly -0.14 indicating that if a fish had achieved an extra 1 cm of growth up until that point, its $\delta^{15}N$ TDF would be roughly 0.14 ‰ lower. The strongest relationship was between $\delta^{15}N$ TDF and weight where the slope was -0.04 indicating that for every 1 g of extra growth, the $\delta^{15}N$ TDF would be 0.04 ‰ lower. That being said, all regressions had R^2 values below 0.3, which indicates these relationships are not particularly strong and the slopes indicate that there has to be a somewhat substantial difference in growth rate in order to have a noteworthy effect on $\delta^{15}N$ TDF. There was not a strong relationship between $\delta^{15}N$ TDF and C:N, which indicates that the relative lipid content of samples was not a cause of the unexplained variation in $\delta^{15}N$ TDF values. Based on the apparent weak to non-existent relationship between $\delta^{13}C$ and $\delta^{15}N$ TDFs and growth rate, this research was not pursued further for the purposes of this dissertation however, the results presented here did indicate that there was a significant relationship between growth rate and $\delta^{15}N$ TDF which could merit further investigation in another study.
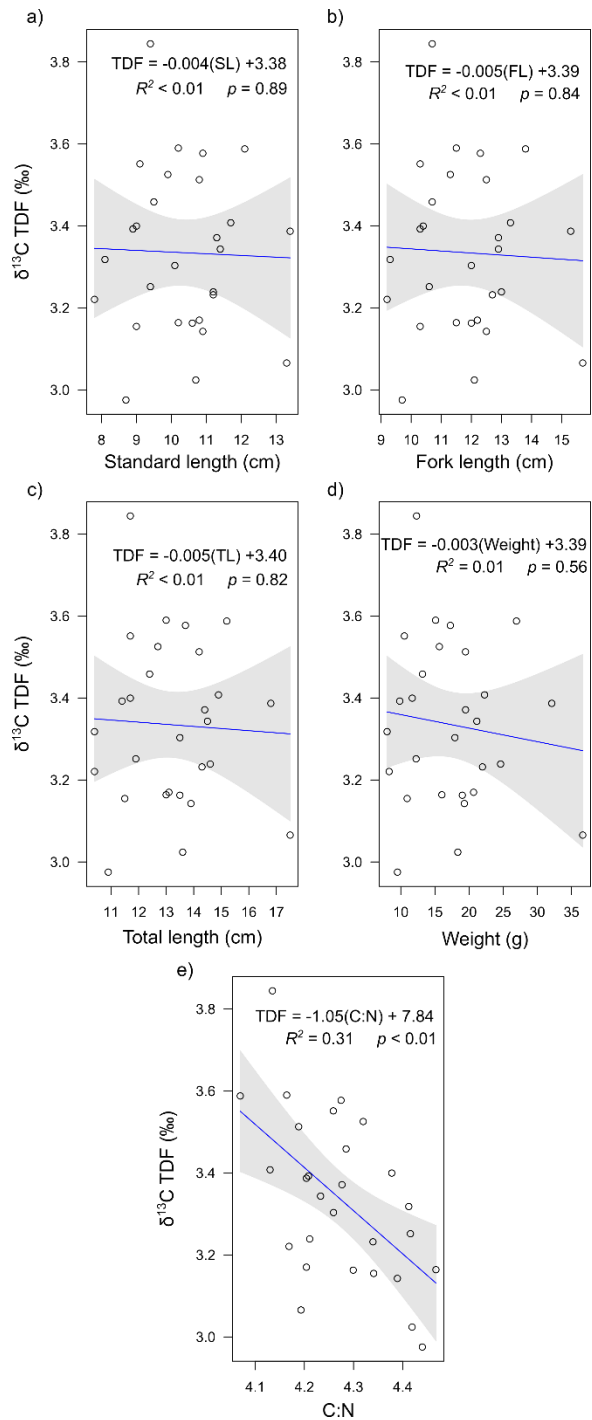
Figure A.2
The results of regressions between δ^{13}C TDF, growth rate indicators [standard length (a), fork length (b), total length (c), weight (d)] and C:N ratios (e). Regression equations, R^2 values, and *p*-values are displayed on each plot. Shaded area represents standard error.
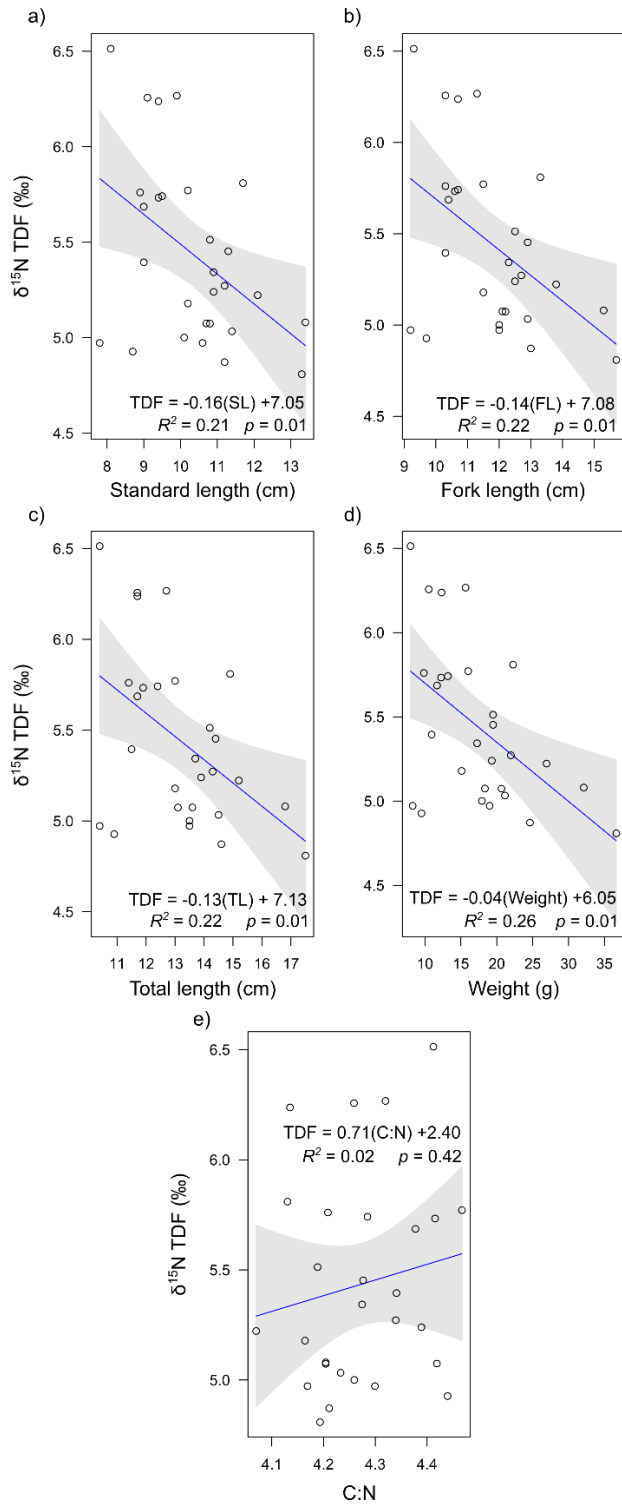
Figure A.3

The results of regressions between $\delta^{15}N$ TDF, growth rate indicators [standard length (a), fork length (b), total length (c), weight (d)] and C:N ratios (e). Regression equations, R^2 values, and *p*-values are displayed on each plot. Shaded area represents standard error.

222

Table A.1
The full dataset used in the Appendix A pilot study. Mean, maximum, minimum, and standard deviation values for each variable are presented at the bottom of the table. Note, Fish 4 and Fish 6 were removed based on the results of the δ^{13}C and δ^{15}N regression based on anomalous δ^{15}N values.

Fish number	SL (cm)	FL (cm)	TL (cm)	Weight (g)	δ^{13}C value (‰)	δ^{15}N value (‰)	C:N	δ^{13}C TDF (‰)	δ^{15}N TDF (‰)
2	12.1	13.8	15.2	26.94	-19.80	9.70	4.07	3.59	5.22
4	9.9	11.3	12.6	14.06	-20.13	8.07	4.20	3.26	3.60
5	10.7	12.1	13.6	18.35	-20.36	9.55	4.42	3.02	5.07
6	10.6	12	13.6	17.93	-19.90	11.74	4.40	3.49	7.26
7	13.3	15.7	17.5	36.65	-20.32	9.29	4.19	3.07	4.81
8	11.2	13	14.6	24.62	-20.15	9.35	4.21	3.24	4.87
9	8.7	9.7	10.9	9.51	-20.41	9.41	4.44	2.98	4.93
10	10.2	11.5	13	16.02	-20.22	10.25	4.47	3.16	5.77
11	8.1	9.3	10.4	7.99	-20.07	10.99	4.41	3.32	6.51
13	9.5	10.7	12.4	13.18	-19.93	10.22	4.28	3.46	5.74
14	11.2	12.7	14.3	21.96	-20.16	9.75	4.34	3.23	5.27
15	7.8	9.2	10.4	8.29	-20.17	9.45	4.17	3.22	4.97
16	11.7	13.3	14.9	22.27	-19.98	10.29	4.13	3.41	5.81
17	13.4	15.3	16.8	32.12	-20.00	9.56	4.20	3.39	5.08
18	10.8	12.5	14.2	19.48	-19.88	9.99	4.19	3.51	5.51
19	9	10.3	11.5	10.93	-20.23	9.87	4.34	3.15	5.39
20	10.9	12.5	13.9	19.31	-20.25	9.72	4.39	3.14	5.24
21	8.9	10.3	11.4	9.85	-20.00	10.24	4.21	3.39	5.76
22	10.8	12.2	13.1	20.66	-20.22	9.55	4.20	3.17	5.07
23	10.1	12	13.5	17.93	-20.09	9.48	4.26	3.30	5.00
24	10.6	12	13.5	19.01	-20.23	9.45	4.30	3.16	4.97
26	11.3	12.9	14.4	19.49	-20.02	9.93	4.28	3.37	5.45
27	9.4	10.7	11.7	12.31	-19.54	10.72	4.14	3.84	6.24

Table A.1 (Continued)

Fish number	SL (cm)	FL (cm)	TL (cm)	Weight (g)	$\delta^{13}C$ value (‰)	$\delta^{15}N$ value (‰)	C:N	$\delta^{13}C$ TDF (‰)	$\delta^{15}N$ TDF (‰)
28	10.2	11.5	13	15.10	-19.80	9.66	4.16	3.59	5.18
29	9.1	10.3	11.7	10.53	-19.84	10.73	4.26	3.55	6.26
30	9	10.4	11.7	11.68	-19.99	10.16	4.38	3.40	5.69
31	11.4	12.9	14.5	21.14	-20.05	9.51	4.23	3.34	5.03
32	9.4	10.6	11.9	12.24	-20.14	10.21	4.42	3.25	5.73
33	9.9	11.3	12.7	15.65	-19.86	10.74	4.32	3.53	6.27
34	10.9	12.3	13.7	17.26	-19.81	9.82	4.27	3.58	5.34
Mean	10.34	11.81	13.22	17.42	-20.05	9.91	4.28	3.34	5.44
Maximum	13.40	15.70	17.50	36.65	-19.54	11.74	4.47	3.84	7.26
Minimum	7.80	9.20	10.40	7.99	-20.41	8.07	4.07	2.98	3.60
Standard Deviation	1.34	1.56	1.70	6.75	0.20	0.66	0.11	0.20	0.66

A.4 Citations

Aberle, N., and Malzahn, A. M. 2007. Interspecific and nutrient-dependent variations in stable isotope fractionation: experimental studies simulating pelagic multitrophic systems. *Oecologia* 154(2): 291-303.

Aguilar, A., Giménez, J., Gómez–Campos, E., Cardona, L., and Borrell, A. 2014. δ^{15}N value does not reflect fasting in mysticetes. *PLoS One* 9(3): e92288.

Bascompte, J., Melián, C. J., and Sala, E. 2005. Interaction strength combinations and the overfishing of a marine food web. *Proceedings of the National Academy of Sciences* 102(15): 5443-5447.

Ben-David, M., and Schell, D. M. 2001. Mixing models in analyses of diet using multiple stable isotopes: a response. *Oecologia* 127(2) 180-184.

Bond, A. L., and Diamond, A. W. 2011. Recent Bayesian stable-isotope mixing models are highly sensitive to variation in discrimination factors. *Ecological Applications* 21(4): 1017-1023.

Bowes, R. E., Lafferty, M. H., and Thorp, J. H. 2014. Less means more: nutrient stress leads to higher δ^{15}N ratios in fish. *Freshwater Biology* 59(9): 1926-1931.

Branch, T. A., Watson, R., Fulton, E. A., Jennings, S., McGilliard, C. R., Pablico, G. T., ... & Tracey, S. R. 2010. The trophic fingerprint of marine fisheries. *Nature* 468(7322): 431-435.

Castellini, M. A., and Rea, L. D. 1992. The biochemistry of natural fasting at its limits. *Experientia* 48(6): 575-582.

Caut, S., Angulo, E., and Courchamp, F. 2008. Discrimination factors (Δ^{15}N and Δ^{13}C) in an omnivorous consumer: effect of diet isotopic ratio. *Functional Ecology* 22(2): 255-263.

Caut, S., Angulo, E. and Courchamp, F. 2009. Variation in discrimination factors (Δ^{15}N and Δ^{13}C): the effect of diet isotopic values and applications for diet reconstruction. *Journal of Applied Ecology* 46: 443-453. doi:10.1111/j.1365-2664.2009.01620.x

Cherel, Y., Robin, J. P., and Maho, Y. L. 1988. Physiology and biochemistry of long-term fasting in birds. *Canadian Journal of Zoology* 66(1): 159-166.

Chikaraishi, Y., Kashiyama, Y., Ogawa, N. O., Kitazato, H., and Ohkouchi, N. 2007. Metabolic control of nitrogen isotope composition of amino acids in macroalgae and gastropods: implications for aquatic food web studies. *Marine Ecology Progress Series* 342: 85-90.

Chikaraishi, Y., Steffan, S. A., Ogawa, N. O., Ishikawa, N. F., Sasaki, Y., Tsuchiya, M., and Ohkouchi, N. 2014. High-resolution food webs based on nitrogen isotopic composition of amino acids. *Ecology and Evolution* 4(12): 2423-2449.

DeNiro, M. J., and Epstein, S. 1978. Influence of diet on the distribution of carbon isotopes in animals. *Geochimica et Cosmochimica Acta* 42(5): 495-506.

Doi, H., Chang, K. H., and Nakano, S. I. 2011. Nitrogen and carbon isotope fractionations of zooplankton consumers in ponds: potential effects of seston C: N stoichiometry. *Marine and Freshwater Research* 62(1): 66-71.

Elton, C. 1927. Animal Ecology. Sidgwick and Jackson, London.

Focken, U. 2001. Stable isotopes in animal ecology: the effect of ration size on the trophic shift of C and N isotopes between feed and carcass. *Isotopes in Environmental and Health Studies* 37(3): 199-211.

Gannes, L. Z., O'Brien, D. M., and Del Rio, C. M. 1997. Stable isotopes in animal ecology: assumptions, caveats, and a call for more laboratory experiments. *Ecology* 78(4): 1271-1276.

Germain, L. R., Koch, P. L., Harvey, J., and McCarthy, M. D. 2013. Nitrogen isotope fractionation in amino acids from harbor seals: implications for compound-specific trophic position calculations. *Marine Ecology Progress Series* 482: 265-277.

Hobson, K. A., and Welch, H. E. 1992. Determination of trophic relationships within a high Arctic marine food web using $\delta^{13}C$ and $\delta^{15}N$ analysis. *Marine Ecology Progress Series* 84: 9-18.

Hobson, K. A., Alisauskas, R. T., and Clark, R. G. 1993. Stable-nitrogen isotope enrichment in avian tissues due to fasting and nutritional stress: implications for isotopic analyses of diet. *The Condor* 95(2) 388-394.

Houde, E. D., and Hoyt, R. 1987. Fish early life dynamics and recruitment variability. *American Fisheries Society Symposium* 2*: 17–29.*

Hussey, N. E., MacNeil, M. A., McMeans, B. C., Olin, J. A., Dudley, S. F., Cliff, G., ... and Fisk, A. T. 2014. Rescaling the trophic structure of marine food webs. *Ecology Letters* 17(2): 239-250.

Kawakami, T., Saito, T., Nishida, K., Yamakawa, T., and Otake, T. 2019. Relationships between growth traits and scale stable isotopes (δ^{13}C, δ^{15}N) of adult chum salmon *Oncorhynchus keta* in Hokkaido, Japan. *Journal of Applied Ichthyology* 35(2): 570-575.

Lindeman, R. L. 1942. The trophic-dynamic aspect of ecology. *Ecology* 23(4): 399-417.

McMahon, K. W., and McCarthy, M. D. 2016. Embracing variability in amino acid δ^{15}N fractionation: mechanisms, implications, and applications for trophic ecology. *Ecosphere* 7(12): e01511.

Menge, B. A., and Sutherland, J. P. 1976. Species diversity gradients: synthesis of the roles of predation, competition, and temporal heterogeneity. *The American Naturalist* 110(973): 351-369.

Minagawa, M., and Wada, E. 1984. Stepwise enrichment of ^{15}N along food chains: further evidence and the relation between δ^{15}N and animal age. *Geochimica et Cosmochimica Acta* 48(5): 1135-1140.

Myers, R. A., Baum, J. K., Shepherd, T. D., Powers, S. P., and Peterson, C. H. 2007. Cascading effects of the loss of apex predatory sharks from a coastal ocean. *Science* 315(5820): 1846-1850.

Oelbermann, K., and Scheu, S. 2002. Stable isotope enrichment (δ^{15}N and δ^{13}C) in a generalist predator (*Pardosa lugubris*, Araneae: Lycosidae): effects of prey quality. *Oecologia* 130(3): 337-344.

Pauly, D., Christensen, V., Dalsgaard, J., Froese, R., and Torres, F. 1998. Fishing down marine food webs. *Science* 279(5352): 860-863.

Phillips, D. L., and Koch, P. L. 2002. Incorporating concentration dependence in stable isotope mixing models. *Oecologia* 130(1): 114-125.

Ponsard, S., and Averbuch, P. 1999. Should growing and adult animals fed on the same diet show different δ^{15}N values?. *Rapid Communications in Mass Spectrometry* 13(13): 1305-1310.

Post, D. M., Pace, M. L., and Hairston, N. G. 2000. Ecosystem size determines food-chain length in lakes. *Nature* 405(6790): 1047-1049.

Post, D. M., Layman, C. A., Arrington, D. A., Takimoto, G., Quattrochi, J., & Montana, C. G. 2007. Getting to the fat of the matter: models, methods and assumptions for dealing with lipids in stable isotope analyses. *Oecologia* 152(1): 179-189.

Post, D. M. 2002. Using stable isotopes to estimate trophic position: models, methods, and assumptions. *Ecology* 83(3): 703-718.

R Core Team. 2020. R: A language and environment for statistical computing. R Foundation for Statistical Computing, Vienna, Austria. URL https://www.R-project.org/

Rieutord, M. 1999. Physiologie animale, vol 2. Les grandes fonctions. Masson, Paris.

Robbins, C. T., Felicetti, L. A., and Sponheimer, M. 2005. The effect of dietary protein quality on nitrogen isotope discrimination in mammals and birds. *Oecologia* 144(4): 534-540.

Scrimgeour, C. M., Gordon, S. C., Handley, L. L., and Woodford, J. A. T. 1995. Trophic levels and anomalous $\delta^{15}N$ of insects on raspberry (*Rubus idaeus L.*). *Isotopes in Environmental and Health Studies* 31(1): 107-115.

Tamelander, T., Søreide, J. E., Hop, H., and Carroll, M. L. 2006. Fractionation of stable isotopes in the Arctic marine copepod Calanus glacialis: Effects on the isotopic composition of marine particulate organic matter. *Journal of Experimental Marine Biology and Ecology* 333(2): 231-240.

Thompson, R. M., Hemberg, M., Starzomski, B. M., and Shurin, J. B. 2007. Trophic levels and trophic tangles: the prevalence of omnivory in real food webs. *Ecology* 88(3): 612-617

Trochine, C., Villanueva, V. D., Balseiro, E., and Modenutti, B. 2019. Nutritional stress by means of high C: N ratios in the diet and starvation affects nitrogen isotope ratios and trophic fractionation of omnivorous copepods. *Oecologia* 190(3): 547-557.

Trueman, C.N., McGill, R.A.R. and Guyard, P.H. 2005. The effect of growth rate on tissue-diet isotopic spacing in rapidly growing animals. An experimental study with Atlantic salmon (*Salmo salar*). *Rapid Communications in Mass Spectrometry* 19: 3239-3247. doi:10.1002/rcm.2199

Vanderklift, M. A., and Ponsard, S. 2003. Sources of variation in consumer-diet δ 15 N enrichment: a meta-analysis. *Oecologia* 136(2): 169-182.

Vander Zanden, H. B., Bjorndal, K. A., Mustin, W., Ponciano, J. M., & Bolten, A. B. 2012. Inherent variation in stable isotope values and discrimination factors in two life stages of green turtles. *Physiological and Biochemical Zoology* 85(5): 431-441.

Vander Zanden, M. J., and Rasmussen, J. B. 1996. A trophic position model of pelagic food webs: impact on contaminant bioaccumulation in lake trout. *Ecological Monographs* 66(4): 451-477.

Vander Zanden, M. J., Shuter, B. J., Lester, N., and Rasmussen, J. B. 1999a. Patterns of food chain length in lakes: a stable isotope study. *The American Naturalist* 154(4): 406-416.

Vander Zanden, M. J., Casselman, J. M., and Rasmussen, J. B. 1999b. Stable isotope evidence for the food web consequences of species invasions in lakes. *Nature* 401(6752): 464-467.

Villamarín, F., Jardine, T. D., Bunn, S. E., Marioni, B., and Magnusson, W. E. 2018. Body size is more important than diet in determining stable-isotope estimates of trophic position in crocodilians. *Scientific Reports* 8(1): 1-11.

West, G., Brown, J. and Enquist, B. 2001. A general model for ontogenetic growth. *Nature* 413: 628–631. https://doi.org/10.1038/35098076

Wolf, N., Carleton, S. A., and Martínez del Rio, C. 2009. Ten years of experimental animal isotopic ecology. *Functional Ecology* 23(1): 17-26.

Appendix B: Tables of adjusted R^2 values used for variable transformation selection

This appendix contains tables of adjusted R^2 values (R^2_{adj}) for the linear regression of individual predictor variables with potential transformations and measured length-corrected $\delta^{13}C$ or $\delta^{15}N$ values. Each variable was transformed (if applicable) and then standardized before linear regression. Asterisks indicate which transformation (if any) was used on the predictor variable in the creation of the multiple regression models. Transformations were used if the R^2_{adj} was at least 0.01 greater than the R^2_{adj} of the regression with the untransformed variable. Transformed or untransformed variables were then standardized and used in the multiple regression analysis in Chapter 3.

Table B.1
R^2_{adj} from linear regressions with Red Snapper length-corrected $\delta^{13}C$ values.

	x	$Ln(x)$	x^2	$1/x$	$\sqrt{x}$
CDOM	0.005	0.076	<0.001	0.123*	0.029
Chl	0.006	0.076	<0.001	0.133*	0.027
Depth	0.154	0.112	0.166*	0.058	0.136
K_d(PAR)	0.010	0.049	<0.001	0.096*	0.026
Lat	0.002*	0.001	0.002	0.001	0.001
Long	0.013*	0.014	0.013	0.014	0.014
PAR	0.066	0.068	0.064*	0.069	0.067
PAR(z)	0.009*	0.001	<0.001	0.002	0.015
PIC	0.004	0.083	<0.001	0.147*	0.023
POC	0.032	0.082	0.008	0.117*	0.055
SST	0.004*	0.004	0.005	0.003	0.004

Table B.2
R^2_{adj} from linear regressions with Red Snapper length-corrected $\delta^{15}N$ values.

	x	Ln(x)	x^2	$1/x$	$\sqrt{x}$
CDOM	0.211	0.554	0.081	0.574*	0.391
Chl	0.315	0.539*	0.215	0.511	0.419
Depth	0.147	0.107	0.158*	0.058	0.130
K_d(PAR)	0.346	0.478	0.244	0.530*	0.414
Lat	0.275*	0.268	0.280	0.258	0.271
Long	0.064*	0.067	0.062	0.070	0.065
PAR	0.009*	0.009	0.008	0.010	0.009
PAR(z)	0.045	0.196*	0.035	0.087	0.072
PIC	0.235*	0.154	0.183	0.053	0.229
POC	0.430	0.517*	0.339	0.508	0.481
SST	0.027*	0.028	0.026	0.029	0.028

Table B.3
R^2_{adj} values from linear regressions with Yellowedge Grouper length-corrected $\delta^{13}C$ values.

	x	Ln(x)	x^2	$1/x$	$\sqrt{x}$
CDOM	0.280*	0.209	0.260	0.100	0.256
Chl	0.208	0.278*	0.103	0.153	0.266
Depth	0.144*	0.134	0.138	0.100	0.142
K_d(PAR)	0.247	0.260	0.192	0.219	0.261*
Lat	0.045	0.035	0.057*	0.026	0.040
Long	0.310*	0.307	0.314	0.302	0.308
PAR	0.182*	0.187	0.176	0.191	0.184
PAR(z)	0.040	0.078*	0.040	0.005	0.038
PIC	0.198	0.167	0.143	0.060	0.217*
POC	0.298*	0.281	0.253	0.196	0.300
SST	0.160	0.148	0.172*	0.137	0.154

Table B.4
R^2_{adj} values from linear regressions with Yellowedge Grouper length-corrected $\delta^{15}N$ values.

	x	$Ln(x)$	x^2	$1/x$	$\sqrt{x}$
CDOM	0.681	0.767*	0.500	0.658	0.749
Chl	0.485	0.706*	0.306	0.680	0.607
Depth	0.013	<0.001	0.034*	0.021	0.004
K_d(PAR)	0.608	0.697	0.481	0.713*	0.660
Lat	0.417	0.383	0.449*	0.349	0.400
Long	0.069*	0.069	0.068	0.069	0.069
PAR	<0.001*	<0.001	0.001	<0.001	<0.001
PAR(z)	0.082	0.393*	0.080	0.034	0.103
PIC	0.249*	0.166	0.250	0.065	0.234
POC	0.658	0.724*	0.558	0.698	0.699
SST	0.028*	0.026	0.031	0.023	0.027

Appendix C: Summary data for predicted values used in temporal variability isoscapes

Table C.1
A table of the maxima (Max), minima (Min), means, and standard deviations (Stdev) of length-corrected δ^{13}C and δ^{15}N values, including those predicted for seasons within La Niña (2011) and El Niño (2015) years. Values were either measured in the muscle tissue of the respective species or predicted based on the statistical models created in Chapter 3 (Table 3.1). The values from the "Catchdate" rows were predicted for the time period each respective station was sampled.

	Red Snapper				**Yellowedge Grouper**			
	Max	**Min**	**Mean**	**Stdev**	**Max**	**Min**	**Mean**	**Stdev**
Measured δ^{13}C values	0.96	-1.04	0.01	0.42	0.58	-0.65	<0.01	0.31
Measured δ^{15}N values	2.35	-3.16	-0.02	1.36	2.40	-1.86	0.04	1.08
Catchdate δ^{13}C values	0.41	-0.59	0.01	0.22	0.53	-0.54	<0.01	0.25
Jan – Mar 2011 δ^{13}C values	0.43	-0.91	0.01	0.29	0.92	-0.69	<0.01	0.34
Apr – Jun 2011 δ^{13}C values	0.50	-0.71	0.01	0.31	0.58	-0.51	<0.01	0.26
July – Sep 2011 δ^{13}C values	0.45	-0.67	0.01	0.23	0.55	-0.61	<0.01	0.32
Oct – Dec 2011 δ^{13}C values	0.41	-0.83	0.01	0.30	0.88	-0.84	<0.01	0.37
Jan – Mar 2015 δ^{13}C values	0.39	-1.03	0.01	0.34	0.58	-0.67	<0.01	0.32
Apr – Jun 2015 δ^{13}C values	0.44	-0.71	0.01	0.29	0.56	-0.39	<0.01	0.23
July – Sep 2015 δ^{13}C values	0.55	-0.72	0.01	0.27	0.54	-0.58	<0.01	0.29
Oct – Dec 2015 δ^{13}C values	0.43	-0.96	0.01	0.31	0.87	-0.66	<0.01	0.34
Catchdate δ^{15}N values	1.81	-2.88	-0.02	1.28	1.97	-1.40	0.04	0.95
Jan – Mar 2011 δ^{15}N values	1.83	-2.36	-0.02	1.06	2.95	-1.83	0.04	0.95
Apr – Jun 2011 δ^{15}N values	2.09	-2.80	-0.02	1.29	2.44	-1.25	0.04	0.95
July – Sep 2011 δ^{15}N values	2.06	-2.86	-0.02	1.21	1.80	-1.30	0.04	0.95
Oct – Dec 2011 δ^{15}N values	2.58	-3.11	-0.02	1.16	1.85	-1.57	0.04	0.95
Jan – Mar 2015 δ^{15}N values	2.17	-2.23	-0.02	1.05	2.43	-1.42	0.04	0.95
Apr – Jun 2015 δ^{15}N values	2.52	-2.32	-0.02	1.15	2.38	-1.34	0.04	0.95
July – Sep 2015 δ^{15}N values	2.12	-2.50	-0.02	1.24	1.95	-1.36	0.04	0.95
Oct – Dec 2015 δ^{15}N values	2.06	-2.54	-0.02	1.15	2.32	-1.12	0.04	0.95

Appendix D: Metadata for research cruises including eye lens samples

Table D.1

Metadata for the research cruises from which the muscle and eye lens samples were obtained. The regions include the West Florida Shelf (WFS), the northern Gulf of Mexico (NG), the western Gulf of Mexico (WG), Campeche Bay, Mexico (CB), and the Yucatan Peninsula, Mexico (YP). The number of Red Snapper (n) refers to the number of Red Snapper caught during each cruise. The muscle and eye lens samples columns refer to how many muscle or eye lens samples were used respectively. Note: eyes were not sampled in 2011.

Year	Vessel	Region	n	Muscle samples	Eye samples
2011	F/V *Sea Fox*	WFS	16	5	0
2011	F/V *Brandy*	WFS	86	23	0
2011	F/V *Pisces*	WFS, NG	475	34	0
2015	R/V *Weatherbird II*	WFS, NG, CB, YP	133	23	3
2016	R/V *Weatherbird II*	NG, WG, CB, YP	347	38	5

Appendix E: Oxygen isoscape of Gulf of Mexico continental shelf using Red Snapper muscle

E.1 Background

E.1.1 Spatial trends in $\delta^{18}O$ values

  Whereas carbon and nitrogen are perhaps the elements used most frequently for food web studies and are also often the preferred elements for migrations studies as well, oxygen has long been used in paleoceanographic studies (Hoefs 2004) and is also used in studies of modern ecosystems (Vander Zanden et al. 2016). Environmental values of $\delta^{18}O$ are primarily driven by hydrologic processes, namely evaporation and precipitation. Evaporation preferentially removes ^{16}O from the oceans and precipitation preferentially adds ^{18}O because of equilibrium fractionation processes (Gat 1996). Because of these processes, a few major patterns emerge. First, $\delta^{18}O$ values tend to be highly correlated with salinity. Ocean regions such as the Mediterranean Sea experience high rates of evaporation and consequently have higher salinity and $\delta^{18}O$ values (Bowen 2010), whereas areas receiving high amounts of freshwater input from precipitation or other sources have lower salinity and $\delta^{18}O$ values (Campana 1999; LeGrande and Schmidt 2006). An exception to this rule is in areas where a high volume of sea ice is being formed. Sea ice preferentially incorporates ^{18}O and excludes salt, and, in these areas, there may be seasonal changes in the $\delta^{18}O$–salinity relationship (Craig and Gordon 1965; Pfirman et al. 2004; LeGrande and Schmidt 2006). A second trend is that of decreasing $\delta^{18}O$ values toward the poles due to Raleigh distillation, wherein ^{18}O is preferentially "rained out" of air masses as they

move away from the equator, leaving only relatively low $\delta^{18}O$ values when the air masses reach the poles (Hoefs 2004). Last, the fractionation of oxygen isotopes is affected by temperature though the effect is relatively small (~0.2 ‰ per °C) and is often overwhelmed by the processes mentioned above (Fry 2006). There is evidence that seasonal extremes can influence time-averaged spatial patterns of precipitation $\delta^{18}O$ values (van der Veer et al. 2009) which would, in turn, affect ocean $\delta^{18}O$ values. Since these relationships are relatively well-understood and predictable, $\delta^{18}O$ values in water can provide key information on water origins (e.g., local precipitation, ground water), climate (ambient temperatures during condensation and precipitation), and the degree of evapotranspiration, and global $\delta^{18}O$ isoscapes can be modeled with good accuracy (Clark and Fritz 1997; LeGrande and Schmidt 2006).

E.1.2 $\delta^{18}O$ isoscapes

Documentation of spatial variation in $\delta^{18}O$ values goes back as far as the 1950's (Dansgaard 1954) and, in the 1960's, relationships between spatial patterns of $\delta^{18}O$ values and precipitation, evaporation, and salinity were described (Craig and Gordon 1965). Whereas the primary focus for oxygen isoscapes and related migration studies has been on terrestrial/freshwater environments (i.e., Bowen 2010), several global seawater oxygen isoscapes have been created based on these same relationships. In 2006, LeGrande and Schmidt created an oxygen isoscape using data from the Schmidt (1999) database. The isoscape was created with empirically measured $\delta^{18}O$ values and a combination of nearby datapoints, and $\delta^{18}O$ values modeled from climatological salinity and the regional $\delta^{18}O$–salinity relationship were used to smooth between points and fill in data-poor areas. They note that the $\delta^{18}O$–salinity slope is greatest at mid-latitudes and high northern latitudes and shallowest at low latitudes and the

Southern Ocean due to the δ^{18}O values of freshwater end members. For instance, near the equator, the majority of water exchanged between the ocean and atmosphere remains in the region, meaning the difference in δ^{18}O values between freshwater endmembers and evaporate is very small. Another isoscape was created using the same dataset (though with more datapoints as it was created years later) by McMahon et al. (2013). Unlike LeGrande and Schmidt (2006), McMahon et al. (2013) only used measured δ^{18}O values and interpolated between them rather than smoothing with modeled δ^{18}O data. However, they do mention a model for δ^{18}O values by Benway and Mix (2004) which uses evaporation, precipitation, advection, and river run off in a mass balance equation. They also note a few areas where the negative relationship between δ^{18}O values and latitude to not hold true namely, the east and west coasts of the United States. On the waters off the west coast, the California Current brings isotopically light polar waters much further south than they would normally be found, and off the east coast, the Gulf Stream brings isotopically heavy tropical waters much further north than they would normally be found. Their isoscape also depicts the plumes of isotopically light water from major rivers such as Amazon and the Orinoco in the tropics and the MacKenzie and Ob in the Arctic.

An important consideration when evaluating δ^{18}O isoscapes is potential temporal variability. Temporal variation has been measured in meteoric, surface, and ground water and that variability is spatially heterogeneous (Kendall and Coplen 2001; Bowen 2008). Freshwater temporal variability can subsequently create temporal variability in an ocean isoscape through precipitation and riverine input. In regard to riverine input, temporal variability could also be introduced through changes in river management (e.g., dams, irrigation return, diversions for agricultural, and urban use) on an intra- or inter-annual scale (Kendall and Coplen 2001). Rooker et al. (2008) found significant inter-annual variability in tuna otolith δ^{18}O values from the

Atlantic Ocean, but they also documented high success (87 %) in assigning natal locations to fish when year classes were pooled. Rooker et al., (2010) found very similar results working with Red Drum in estuaries within the Gulf of Mexico. This suggests that temporal variation may not overwhelm spatial patterns in oxygen isotopes but, accounting for or removing temporal variation (i.e., when fish year classes were analyzed separately) can improve results.

E.1.3 $\delta^{18}O$ values in the Gulf of Mexico

Global isoscapes indicate that there is very little variability in $\delta^{18}O$ values within the Gulf of Mexico except, perhaps, a slight decrease with latitude (LeGrande and Schmidt 2006; McMahon et al. 2013). However, these isoscapes do not appear to have much data coverage for the Gulf of Mexico and the spatial scale for these isoscapes is so large that variation on the scale of the Gulf of Mexico may not be captured. It is likely $\delta^{18}O$ values decrease from south to north in the Gulf of Mexico due to evaporation/precipitation conditions and Raleigh distillation but, there are other processes that are likely to affect $\delta^{18}O$ values at a regional scale.

Many rivers enter the Gulf of Mexico, transporting isotopic values from their watersheds to be mixed with ocean waters. Bowen (2010) created an oxygen isoscape of America's river waters using a model by Dutton et al. (2005) and data from Kendall and Coplen (2001). This isoscape indicates that most rivers leading into the Gulf of Mexico will have $\delta^{18}O$ values ranging from 0 to -6 ‰ but the Mississippi River will be a combination of waters ranging from -2 to -20 ‰, so the Mississippi River plume at the northern end of the Gulf of Mexico may have a lighter isotopic value than other riverine input. This may also mean that the waters in the northern Gulf of Mexico have lighter $\delta^{18}O$ values than would be predicted based purely on latitude or salinity (as would be the case with global isoscapes), and the latitudinal gradient may be steeper than the

one seen in global isoscapes. The Mississippi River plume generally flows west past Louisiana, sometimes reaching as far as Texas (Justić et al. 1995), which could potentially create an east-west gradient as Mississippi River water mixes with isotopically heaver ocean water. On the east side of the Mississippi River, Mobile River puts a substantial volume of freshwater into the Gulf of Mexico but, based on the isoscape by Bowen (2010) the freshwater from Mobile River should be isotopically heavier than Mississippi River water (though still lighter than ocean water). The interaction of these two freshwater sources and ocean water could potentially create another gradient to the east of the Mississippi River or, perhaps, a less linear spatial pattern. The Grijalva–Usumacinta River flows into the south end of Campeche Bay and is transported north-west towards Texas (Zavala-Hidalgo et al. 2003). This could potentially create another gradient between the river and ocean waters going north. The shape of rivers will also influence their isotopic values through evaporative dynamics (e.g., shallower, slower moving rivers will experience more evaporation than deep, fast rivers) and saltwater intrusion. This effect has been observed in otolith $\delta^{18}O$ values from Red Drum in estuaries in the western Gulf of Mexico, wherein $\delta^{18}O$ values were higher in estuaries with higher salinity (higher evaporation and/or saltwater intrusion; Rooker et al. (2010)).

Oxygen has an excellent potential as a natural tag in migration studies because $\delta^{18}O$ values in aquatic organism tissues are primarily determined by water $\delta^{18}O$ values rather than diet/trophic interactions (Ehleringer et al. 2008; Wang et al. 2009; Nielson and Bowen 2010; Soto et al. 2013; Schilder et al. 2015; Vander Zanden et al. 2016; Coulter et al. 2017; Camin et al. 2018). One reason for this relationship may be that most oxygen in biomolecules is found within functional groups and, therefore, oxygen does not experience as much atomic routing compared with other isotopes (Vander Zanden et al. 2016). Most of oxygen isotope work in fish

242

has been conducted using otoliths. According to the work of Thorrold et al. (1997), otoliths are deposited close to equilibrium with the ambient water, with a small but significant fractionation factor due to temperature $[1000\text{In}(\Delta^{18}\text{O}) = 18.56(10^3\,\text{T K}^{-1}) - 32.54)]$. Several studies have found that muscle $\delta^{18}\text{O}$ values are also highly reliant on water $\delta^{18}\text{O}$ values (Turchini et al. 2009; Soto et al. 2013; Coulter et al. 2017; Camin et al. 2019). There is evidence that other tissues may be affected by temperature-controlled fractionation similar to otoliths (Schilder et al. 2015), but not much research has been conducted exploring this effect. Food, physiological factors (i.e., growth rate), and dissolved oxygen $\delta^{18}\text{O}$ values likely have an influence on aquatic animal tissue $\delta^{18}\text{O}$ values (Darnaude et al. 2014; Vander Zanden et al. 2016; Coulter et al. 2017), but given that water $\delta^{18}\text{O}$ values can account for over 80 % of the tissue $\delta^{18}\text{O}$ values (Soto et al. 2013), it seems unlikely that effects from food, physiological factors, or dissolved oxygen would overwhelm the influence of water isotopic values.

E.1.4 $\delta^{18}O$ values in organism studies

Spatial oxygen isotope patters and preserved oxygen isotopes in organism tissues have allowed for oxygen isotopes to be used in a multitude of migration studies. Many of those studies are terrestrial (Hobson and Wassenaar 2008), but the use of oxygen isotopes for migration studies is becoming more common in aquatic studies as well. As mentioned previously, most aquatic studies are conducted using oxygen in otoliths, which provide a complete environmental history for individual fish. Early studies demonstrated that otolith stable carbon and oxygen could be used to differentiate between coastal marine, estuarine, river, and lake environments throughout the life cycle of New Zealand common smelt (Nelson et al. 1989). A subsequent study noted the utility of otolith oxygen isotopes for obtaining information about the larval

phases of fishes (Meyer-Rochiw et al. 1992). Since those early studies, otolith cores have been used to identify larval/juvenile habitat for both freshwater (Dufour et al., 2008; Zeigler and Whitledge 2010; Norman and Whitledge 2015) and marine species (Rooker et al. 2001; Thorrold et al. 2001; Dorval et al. 2005; Rooker et al. 2008). In the Gulf of Mexico, Red Snapper otolith stable isotopes and elemental ratios were used to distinguish six nursery habitats around the Gulf (Sluis et al.2012), and those established nursery chemical characteristics were then used to infer population connectivity for Red Snapper caught around the Gulf (Sluis et al.2015). Whereas those studies used both stable isotopes and elemental ratios, another study was able to distinguish between Gulf of Mexico estuaries as natal habitat using only stable isotopes (Rooker et al. 2010). A classification success of over 80 % was achieved for each year class studied, and it was noted that models containing only oxygen performed better than models containing only carbon. These results indicate, at least for Gulf of Mexico estuaries, oxygen may be more suited to geographic studies than carbon. Otolith stable isotopes have also been used to create environmental histories for fish, especially salinity and temperature histories (Kerr et al. 2007; Darnaude et al. 2014) which may, in turn, be used to infer geographic movement.

Geographic studies using stable oxygen isotopes in fish muscle are much less common, most likely because, unlike otoliths, fish muscle does not provide a lifelong environmental record. The main application for these types of studies appears to be tracing the origin of market fish fillets. Turchini et al. (2009) set out to find the best methods to discriminate between Murray cod from different farms. They found that stable isotopes were more effective than fatty acid and tissue proximate compositions or morphological parameters. They further found that C and N were most useful for discriminating feed types, and that O could be used to link fish to a specific water source. Camin et al. (2019) used H, C, O, N, and S stable isotopes in Italian rainbow trout

investigate the ability of stable isotopes to trace trout fillets back to farms in one of two northern Italian regions. After determining the relationships between the various stable isotopes and either feed type or tank water $\delta^{18}O$ values, they were able to assign geographic origins of fillets with 91% accuracy.

E.1.5 Objectives

The objective of this study was to assess the spatial patterns of $\delta^{18}O$ values in the Gulf of Mexico for possible future use in migration studies. Previous studies indicated there is ample variability in the Gulf of Mexico and that variability would be preserved in fish tissues. Other studies indicated that the $\delta^{18}O$ values of seawater are transferred into fish tissues with no trophic fractionation which makes its interpretation less complicated than that of $\delta^{13}C$ or $\delta^{15}N$ values. If migration studies can use direct isotopic measurements, there is the potential for the ability to resolve differences between freshwater input sources that have $\delta^{18}O$ values that are both lighter than seawater $\delta^{18}O$ values but not equal to each other (i.e., Mississippi river and the Grijalva–Usumacinta River). Of particular relevance to this dissertation, robust prediction of water $\delta^{18}O$ values at different times of year could be used to create temperature-dependent fractionation equations, and these equations could be used to infer thermal histories of individuals using otoliths or eye lenses (Storm-suke et al., 2007; Dufour et al., 2008). Since eye lenses do not have clear demarcations of time increments, it would be very useful to detect an annual temperature cycle in the $\delta^{18}O$ values in eye lenses. Regardless of the temperature fractionation effect, a Gulf of Mexico oxygen isoscape has potential uses for ecology around the Gulf and could be used to resolve migration ambiguities from other isoscapes.

E.2.1 Sample collection and isotopic analysis

Red Snapper muscle samples were collected on longlining cruises in the Gulf of Mexico in the years 2015 and 2016 (Figure E.1a). These were same muscle samples used in Chapters 2 and 3. See Chapter 2 for a full description of sample collection and δ^{13}C and δ^{15}N analysis methods.

Thirty Red Snapper muscle samples were analyzed for δ^{18}O values at the Stable Isotope Core Laboratory at Washington State University. Samples were converted to CO gas with a pyrolysis elemental analyzer (TC/EA, ThermoFinnigan) with a GC column. The gas was then analyzed with a continuous flow isotope ratio mass spectrometer (Delta Plus XP, ThermoFinnigan). Results were presented in standard notation (δ, in ‰) relative to international standard VSMOW:

$$\delta^j X = \left(\frac{(^jX/\ ^iX)_{sample}}{(^jX/\ ^iX)_{standard}} - 1 \right) * 1000$$

where *X* is the element and *j* and *i* are each an isotope of *X*. Results were normalized on scale such that the oxygen value of SLAP (Standard Light Antarctic Precipitation) was -55.5 ‰. The 2-sigma uncertainty of oxygen isotopic results was 0.4 ‰.
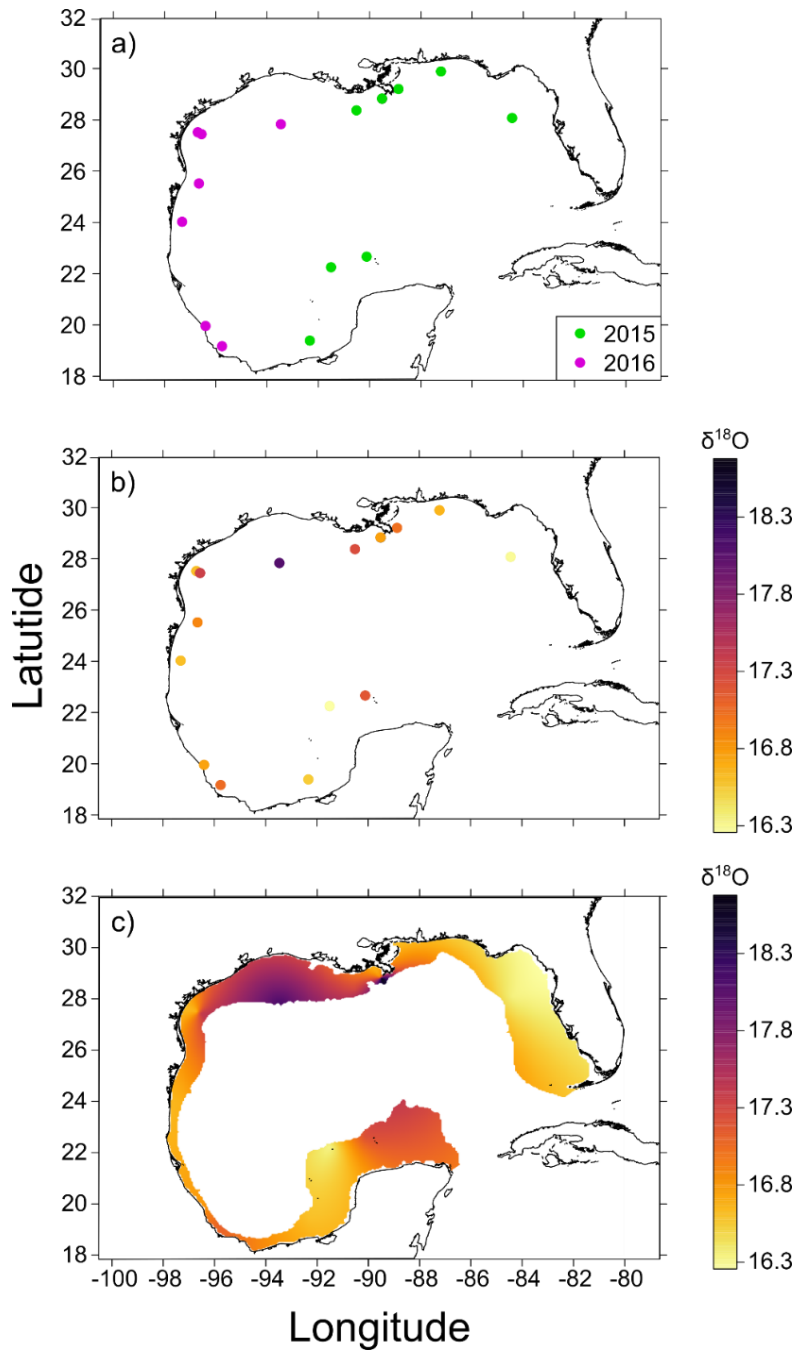
Figure E.1

Maps of the capture locations and years of capture (a), $\delta^{18}O$ values by station (b), and a kriged isoscape based on the measured $\delta^{18}O$ values (c). On map (a), green points were sampled in 2015 and purple points were sampled in 2016. The values in (b) are station averages.

E.2.2 Statistical analysis

First, the δ^{18}O values, SL, δ^{13}C values, and δ^{15}N values of the samples were tested for normality using the Shapiro-Wilk test. In order to assess if δ^{18}O values undergo trophic fractionation, linear regressions were performed between δ^{18}O values and SL, δ^{13}C values, and δ^{15}N values, all typically assumed to increase with trophic position (Post 2002). Spearman rank correlations were performed between δ^{18}O values and the potential predictor variables used in Chapter 3 to assess which might have been influential to δ^{18}O values. The potential predictor variables included colored dissolved organic matter (*CDOM*), chlorophyll a concentration (*Chl a*), the average depth of the trawl (*Depth*), light attenuation of photosynthetically active radiation [*Kd(PAR)*], latitude, longitude, photosynthetically active radiation (*PAR*), particulate inorganic carbon (*PIC*), particulate organic carbon (*POC*), and sea surface temperature (*SST*). All analyses were performed in R (version 4.0.5, R Core Team 2020).

E.3 Results

A total of 30 Red Snapper muscle samples were analyzed for δ^{18}O values. The measured δ^{18}O values ranged from 15.82 to 19.39 ‰ with an average of 17.21 ‰ and a standard deviation of 0.91 ‰ (Table E.2). Trophic fractionation of δ^{18}O values has not been documented in previous studies (Ehleringer et al. 2008; Wang et al. 2009; Nielson and Bowen 2010; Soto et al. 2013; Schilder et al. 2015; Vander Zanden et al. 2016; Coulter et al. 2017; Camin et al. 2018). There was neither a substantial nor significant relationship between δ^{18}O values and SL (Figure E.2a) nor between δ^{18}O and δ^{15}N values (Figure E.2c), which indicated δ^{18}O values were not influenced by trophic growth. It should be noted that δ^{15}N values were not normally distributed in these samples, and that the regression between δ^{15}N and δ^{18}O values did not have normally

distributed residuals. Therefore, the assumptions of linear regression were violated. However, the results of the linear regression were not marginal and, a visual examination of the data did not indicate the conclusion that there was no significant relationship between $\delta^{18}O$ and $\delta^{15}N$ values was incorrect. There was a significant but insubstantial negative relationship between $\delta^{18}O$ and $\delta^{13}C$ values (Figure E.2b) which suggests $\delta^{18}O$ and $\delta^{13}C$ values may be influenced similar ecological processes.
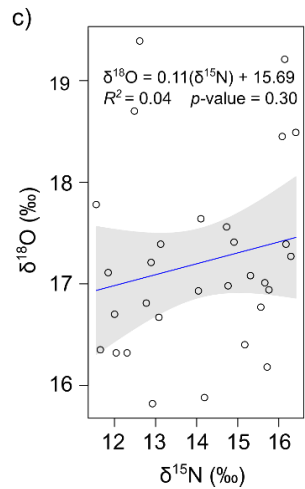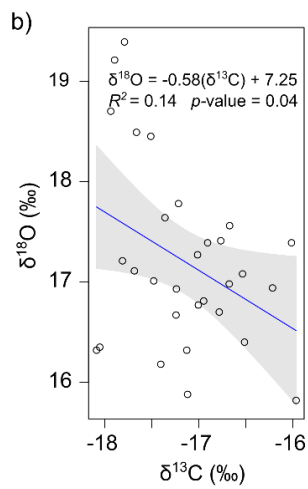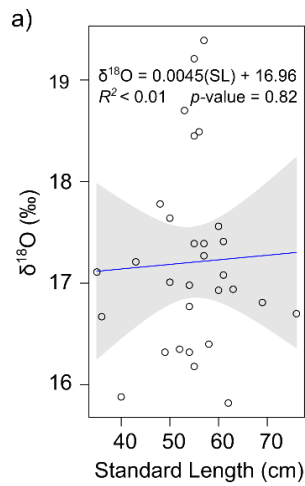
Figure E.2
Graphs for the results of regressions between $\delta^{18}O$ values and SL (a), $\delta^{13}C$ values (b), and $\delta^{15}N$ values(c). The equations, R^2 values, and *p*-values are displayed on each plot. The shaded area represents standard error.

While the kriged isoscape depicts some spatial patterns (Figure E.1c), many of these are based on anomalous high or low values, and there was sometimes a high level of within-station variability. For example, the isoscape would suggest there is an area of high $\delta^{18}O$ values off the coast of Louisiana. However, that pattern is mostly the result of the highest measured value (19.39 ‰) being measured at that location, and the other values measured at that location (18.7 and 16.32 ‰) do not suggest this area commonly has particularly high $\delta^{18}O$ values. Similarly, the area of low $\delta^{18}O$ values off Florida was based off a single measurement of 16.35 ‰. The plot of $\delta^{18}O$ values by station (Figure E.1b) often depicts stations with higher values very close to stations with lower values, which suggests many spatial patterns may not be consistent. There does appear to be a somewhat consistent gradient from the high value off Louisiana to lower values east and west of that location.

The relationship between $\delta^{18}O$ values and the potential predictors of spatial isotopic variation used in Chapter 3 was tested via Spearman rank correlations (Table E.1). None of the potential predictors had a significant correlation with $\delta^{18}O$ values. The predictor that had the strongest relationship was *PIC* (*rho* = 0.49, *p* = 0.05). This correlation along with the significant regression between $\delta^{18}O$ and $\delta^{13}C$ values suggest that there may be fractionation of $\delta^{18}O$ and $\delta^{13}C$ values associated with the creation of PIC (primarily calcium carbonate) which may merit investigation. Overall, the results of these correlations do not indicate there are strong relationships between $\delta^{18}O$ values and the predictors used in this dissertation on the continental shelf of the Gulf of Mexico. In conclusion, I decided not to expand on this pilot study for the purposes of my dissertation, but there may be indications that there is a spatial gradient present in the northern Gulf of Mexico that could be investigated in future studies.

Table E.1

A table of the *rho*s and *p*-values for Spearman rank correlations between $\delta^{18}O$ values and potential predictors of spatial isotopic variation. The potential predictors are colored dissolved organic matter (*CDOM*), chlorophyll a concentration (*Chl a*), the average depth of the trawl (*Depth*), light attenuation of photosynthetically active radiation [*Kd(PAR)*], latitude, longitude, photosynthetically active radiation (*PAR*), particulate inorganic carbon (*PIC*), particulate organic carbon (*POC*), and sea surface temperature (*SST*). All potential predictors except *Depth*, *Lat*, and *Long* were 3-month average values for the location from the MODIS-Aqua satellite (see Chapter 3 for details).

	rho	*p*
CDOM	0.40	0.12
Chl a	0.40	0.12
Depth	0.08	0.77
Kd(PAR)	0.37	0.16
Latitude	0.24	0.36
Longitude	0.02	0.94
PAR	-0.25	0.36
PIC	0.49	0.05
POC	0.38	0.14
SST	0.17	0.53

Table E.2
The full dataset used in the Appendix E pilot study. The "Year" column refers to the year of collection for the muscle tissue. The "SL" column is standard length in cm. The potential predictors are colored dissolved organic matter (*CDOM*), chlorophyll a concentration (*Chl a*), the average depth of the trawl (*Depth*), light attenuation of photosynthetically active radiation [*Kd(PAR)*], latitude, longitude, photosynthetically active radiation (*PAR*), particulate inorganic carbon (*PIC*), particulate organic carbon (*POC*), and sea surface temperature (*SST*). All potential predictors except *Depth*, *Lat*, and *Long* were 3-month average values for the location from the MODIS-Aqua satellite (see Chapter 3 for details).

Sample ID	Station ID	Latitude	Longitude	Year	SL (cm)	*Depth (m)*	δ^{15}N value	δ^{13}C value	δ^{18}O value
1547063	47	28.37	-90.51	2015	43	50.84	12.89	-17.81	17.21
1547069	47	28.37	-90.51	2015	50	50.84	14.10	-17.36	17.64
1547076	47	28.37	-90.51	2015	61	50.84	15.31	-16.54	17.08
150440019	440	28.07	-84.44	2015	52	64.62	11.66	-18.05	16.35
150840005	840	29.89	-87.22	2015	60	75.51	14.73	-16.67	17.56
150840007	840	29.89	-87.22	2015	40	75.51	14.19	-17.12	15.88
151040058	1040	29.20	-88.87	2015	57	57.36	16.17	-16.91	17.39
151040078	1040	29.20	-88.87	2015	54	57.36	15.56	-17.01	16.77
141240003	1240	28.83	-89.51	2014	56	62.21	16.41	-17.66	18.49
141240004	1240	28.83	-89.51	2014	55	62.21	16.08	-17.51	18.45
141240011	1240	28.83	-89.51	2014	55	62.21	16.14	-17.90	19.21
151240041	1240	28.83	-89.51	2015	50	59.85	15.66	-17.48	17.01
151240046	1240	28.83	-89.51	2015	57	59.85	16.29	-17.01	17.27
151240064	1240	28.83	-89.51	2015	55	59.85	15.72	-17.41	16.18
162080003	2080	27.83	-93.46	2016	49	138.50	12.04	-18.09	16.32
162080007	2080	27.83	-93.46	2016	53	138.50	12.49	-17.94	18.70
162080012	2080	27.83	-93.46	2016	57	138.50	12.62	-17.79	19.39
162220003	2220	27.52	-96.70	2016	58	47.13	15.17	-16.52	16.40
162220006	2220	27.52	-96.70	2016	63	47.13	15.76	-16.22	16.94
162240008	2240	27.44	-96.55	2016	61	76.50	14.91	-16.77	17.41

Table E.2 (Continued)

Sample ID	Station ID	Latitude	Longitude	Year	SL (cm)	*Depth (m)*	$\delta^{15}N$ value	$\delta^{13}C$ value	$\delta^{18}O$ value
162440010	2440	25.52	-96.66	2016	60	76.23	14.04	-17.24	16.93
162440011	2440	25.52	-96.66	2016	54	76.23	14.76	-16.68	16.98
162540026	2540	24.02	-97.31	2016	36	90.54	13.08	-17.24	16.67
162740001	2740	19.96	-96.40	2016	69	90.32	12.77	-16.95	16.81
162840001	2840	19.17	-95.76	2016	35	121.04	11.85	-17.69	17.11
153360003	3360	22.25	-91.50	2015	54	114.30	12.31	-17.13	16.32
153460012	3460	22.66	-90.11	2015	48	114.22	11.56	-17.22	17.78
153460015	3460	22.66	-90.11	2015	76	114.22	12.00	-16.78	16.70
154602002	4602	19.39	-92.33	2015	55	63.09	13.13	-16.02	17.39
154602012	4602	19.39	-92.33	2015	62	63.09	12.92	-15.97	15.82

E.4 Citations

Benway, H.M. and Mix, A. 2004. Oxygen isotopes, upper-ocean salinity, and precipitation in the eastern tropical Pacific. *Earth and Planetary Science Letters* 224: 493–507.

Bowen, G. J. 2008. Spatial analysis of the intra-annual variation of precipitation isotope ratios and its climatological corollaries. *Journal of Geophysical Research: Atmospheres* 113: D05113.

Bowen, G. J. 2010. Isoscapes: spatial pattern in isotopic biogeochemistry. *Annual Review of Earth and Planetary Sciences* 38: 161-187.

Camin, F., Perini, M., Bontempo, L., Galeotti, M., Tibaldi, E., and Piasentier, E. 2018. Stable isotope ratios of H, C, O, N and S for the geographical traceability of Italian rainbow trout (*Oncorhynchus mykiss*). *Food Chemistry* 267: 288-295.

Campana, S. E. 1999. Chemistry and composition of fish otoliths: pathways, mechanisms and applications. *Marine Ecology Progress Series* 188: 263-297.

Clark, I. D., and Fritz, P. 1997. Environmental Isotopes in Hydrogeology. CRC Press, London.

Coplen, T. B., and Qi, H. 2012. USGS42 and USGS43: human-hair stable hydrogen and oxygen isotopic reference materials and analytical methods for forensic science and implications for published measurement results. *Forensic Science International* 214(1-3): 135-141.

Coulter, D. P., Bowen, G. J., and Höök, T. O. 2017. Influence of diet and ambient water on hydrogen and oxygen stable isotope ratios in fish tissue: patterns within and among tissues and relationships with growth rates. *Hydrobiologia* 799(1): 111-121.

Craig, H., and Gordon, L. I. 1965. Deuterium and oxygen 18 variations in the ocean and the marine atmosphere, in Stable Isotopes in Oceanographic Studies and Paleotemperatures, edited by E. Tongiorgi, Laboratorio di geologia nucleare, Spoleto, Italy. pp. 9–130.

Dansgaard, W. 1954. The O^{18}-abundance in fresh water. *Geochimica et Cosmochimica Acta* 6(5-6): 241-260.

Darnaude, A. M., Sturrock, A., Trueman, C. N., Mouillot, D., Campana, S. E., and Hunter, E. 2014. Listening in on the past: What can otolith $\delta^{18}O$ values really tell us about the environmental history of fishes?. *PloS One* 9(10): e108539.

Dorval, E., Jones, C. M., Hannigan, R., and van Montfrans, J. 2005. Can otolith chemistry be used for identifying essential seagrass habitats for juvenile spotted seatrout, *Cynoscion nebulosus*, in Chesapeake Bay?. *Marine and Freshwater Research* 56(5): 645-653.

Dorval, E., Jones, C. M., Hannigan, R., and Montfrans, J. V. 2007. Relating otolith chemistry to surface water chemistry in a coastal plain estuary. *Canadian Journal of Fisheries and Aquatic Sciences*, 64(3): 411-424.

Dufour, E., Höök, T. O., Patterson, W. P., and Rutherford, E. S. 2008. High-resolution isotope analysis of young alewife *Alosa pseudoharengus* otoliths: assessment of temporal resolution and reconstruction of habitat occupancy and thermal history. *Journal of Fish Biology* 73(10): 2434-2451.

Dutton, A., Wilkinson, B. H., Welker, J. M., Bowen, G. J., and Lohmann, K. C. 2005. Spatial distribution and seasonal variation in $^{18}O/^{16}O$ of modern precipitation and river water across the conterminous USA. *Hydrological Processes: An International Journal* 19(20): 4121-4146.

Ehleringer, J. R., Bowen, G. J., Chesson, L. A., West, A. G., Podlesak, D. W., and Cerling, T. E. 2008. Hydrogen and oxygen isotope ratios in human hair are related to geography. *Proceedings of the National Academy of Sciences* 105(8): 2788-2793.

Fry, B. 2006. Stable isotope ecology. Springer, New York.

Gat, J.R. 1996. Oxygen and hydrogen isotopes in the hydrologic cycle. *Annual Review of Earth and Planetary Science* 24: 225–262.

Gillanders, B. M. 2002. Temporal and spatial variability in elemental composition of otoliths: implications for determining stock identity and connectivity of populations. *Canadian Journal of Fisheries and Aquatic Sciences* 59(4): 669-679.

Hobson, K.A. and Wassenaar, L.I. 2008. Tracking animal migration with stable isotopes. Academic Press, Elsevier, Oxford.

Hoefs, J. 2004. Stable Isotope Geochemistry. Springer-Verlag, New York.

Justić, D., Rabalais, N. N., Turner, R. E., and Dortch, Q. 1995. Changes in nutrient structure of river-dominated coastal waters: stoichiometric nutrient balance and its consequences. *Estuarine, Coastal and Shelf Science* 40(3): 339-356.

Kendall, C., and Coplen, T. B. 2001. Distribution of oxygen-18 and deuterium in river waters across the United States. *Hydrological Processes* 15(7): 1363-1393.

Kerr, L. A., Secor, D. H., & Kraus, R. T. 2007. Stable isotope (δ^{13}C and δ^{18}O) and Sr/Ca composition of otoliths as proxies for environmental salinity experienced by an estuarine fish. *Marine Ecology Progress Series* 349 245-253.

LeGrande, A. N., and Schmidt, G. A. 2006. Global gridded data set of the oxygen isotopic composition in seawater. *Geophysical Research Letters* 33: L12604.

McMahon, K. W., Hamady, L. L., and Thorrold, S. R. 2013. Ocean ecogeochemistry: a review. *Oceanography and Marine Biology: An Annual Review* 51: 327-374.

Meyer-Rochow, V. B., Cook, I., and Hendy, C. H. 1992. How to obtain clues from the otoliths of an adult fish about the aquatic environment it has been in as a larva. *Comparative Biochemistry and Physiology Part A: Physiology* 103(2): 333-335.

Nielson, K. E., and Bowen, G. J. 2010. Hydrogen and oxygen in brine shrimp chitin reflect environmental water and dietary isotopic composition. *Geochimica et Cosmochimica Acta* 74(6): 1812-1822.

Nelson, C. S., Northcote, T. G., and Hendy, C. H. 1989. Potential use of oxygen and carbon isotopic composition of otoliths to identify migratory and non-migratory stocks of the New Zealand common smelt: A pilot study. *New Zealand Journal of Marine and Freshwater Research* 23(3): 337-344.

Norman, J. D., and Whitledge, G. W. (2015). Recruitment sources of invasive Bighead carp (*Hypopthalmichthys nobilis*) and Silver carp *(H. molitrix)* inhabiting the Illinois River. *Biological invasions* 17(10): 2999-3014.

Pfirman, S., Haxby, W., Eicken, H., Jeffries, M., and Bauch, D. 2004. Drifting Arctic sea ice archives changes in ocean surface conditions. *Geophysical Research Letters* 31: L19401.

Post, D. M. 2002. Using stable isotopes to estimate trophic position: models, methods, and assumptions. *Ecology* 83(3): 703-718.

Qi, H., Coplen, T. B., and Wassenaar, L. I. 2011. Improved online $\delta^{18}O$ measurements of nitrogen-and sulfur-bearing organic materials and a proposed analytical protocol. *Rapid Communications in Mass Spectrometry* 25(14): 2049-2058.

Rooker, J. R., Secor, D. H., Zdanowicz, V. S., and Itoh, T. 2001. Discrimination of northern bluefin tuna from nursery areas in the Pacific Ocean using otolith chemistry. *Marine Ecology Progress Series* 218: 275-282.

Rooker, J. R., Secor, D. H., DeMetrio, G., Kaufman, A. J., Ríos, A. B., and Ticina, V. 2008. Evidence of trans-Atlantic movement and natal homing of bluefin tuna from stable isotopes in otoliths. *Marine Ecology Progress Series* 368: 231-239.

Rooker, J. R., Stunz, G. W., Holt, S. A., and Minello, T. J. 2010. Population connectivity of red drum in the northern Gulf of Mexico. *Marine Ecology Progress Series* 407: 187-196.

Schilder, J., Tellenbach, C., Möst, M., Spaak, P., Van Hardenbroek, M., Wooller, M. J., and Heiri, O. 2015. The stable isotopic composition of *Daphnia ephippia* reflects changes in $\delta^{18}O$ and $\delta^{18}O$ values of food and water. *Biogeosciences* 12(12): 3819-3830.

Schmidt, G. A., G. R. Bigg, and Rohling, E. J. 1999, Global Seawater Oxygen-18 Database, http://data.giss.nasa.gov/o18data/, NASA Goddard Inst. of Space Sci., New York, N. Y.

Sluis, M.Z., Barnett, B.K., Patterson, W.F., III, Cowan, J.H., Jr. and Shiller, A.M. 2012. Discrimination of Juvenile Red Snapper Otolith Chemical Signatures from Gulf of Mexico Nursery Regions. *Marine and Coastal Fisheries* 4: 587-598. doi:10.1080/19425120.2012.703163.

Sluis, M.Z., Barnett, B.K., Patterson, W.F., III, Cowan, J.H., Jr. and Shiller, A.M. 2015. Application of Otolith Chemical Signatures to Estimate Population Connectivity of Red Snapper in the Western Gulf of Mexico. *Marine and Coastal Fisheries* 7: 483-496. doi:10.1080/19425120.2015.1088492.

Soto, D. X., Wassenaar, L. I., and Hobson, K. A. 2013. Stable hydrogen and oxygen isotopes in aquatic food webs are tracers of diet and provenance. *Functional Ecology* 27(2): 535-543.

Storm-Suke, A., Dempson, J. B., Reist, J. D., and Power, M. 2007. A field-derived oxygen isotope fractionation equation for Salvelinus species. *Rapid Communications in Mass Spectrometry* 21(24): 4109-4116.

Thorrold, S. R., Campana, S. E., Jones, C. M., and Swart, P. K. 1997. Factors determining $\delta^{13}C$ and $\delta^{18}O$ fractionation in aragonitic otoliths of marine fish. *Geochimica et Cosmochimica Acta* 61(14): 2909-2919.

Thorrold, S. R., Latkoczy, C., Swart, P. K., and Jones, C. M. 2001. Natal homing in a marine fish metapopulation. *Science* 291(5502): 297-299.

Turchini, G. M., Quinn, G. P., Jones, P. L., Palmeri, G., and Gooley, G. 2009. Traceability and discrimination among differently farmed fish: a case study on Australian Murray cod. *Journal of Agricultural and Food Chemistry* 57(1): 274-281.

Van der Veer, G., Voerkelius, S., Lorentz, G., Heiss, G., and Hoogewerff, J. A. 2009. Spatial interpolation of the deuterium and oxygen-18 composition of global precipitation using temperature as ancillary variable. *Journal of Geochemical Exploration* 101(2): 175-184.

Vander Zanden, H. B., Soto, D. X., Bowen, G. J., and Hobson, K. A. 2016. Expanding the isotopic toolbox: applications of hydrogen and oxygen stable isotope ratios to food web studies. *Frontiers in Ecology and Evolution* 4: 20.

Wang, Y. V., O'brien, D. M., Jenson, J., Francis, D., and Wooller, M. J. 2009. The influence of diet and water on the stable oxygen and hydrogen isotope composition of Chironomidae (Diptera) with paleoecological implications. *Oecologia* 160(2): 225-233.

Zavala-Hidalgo, J., Morey, S. L., and O'Brien, J. J. 2003. Seasonal circulation on the western shelf of the Gulf of Mexico using a high-resolution numerical model. *Journal of Geophysical Research: Oceans* 108: 3389, doi:10.1029/2003JC001879, C12

Zeigler, J. M., and Whitledge, G. W. 2010. Assessment of otolith chemistry for identifying source environment of fishes in the lower Illinois River, Illinois. *Hydrobiologia* 638(1): 109-119.